Cytokine Signaling in Cardiac Development and Hypertensive Cardiovascular Remodeling

Inaugural-Dissertation
to obtain the academic degree
Doctor rerum naturalium (Dr. rer. nat.)
submitted to the Department of Biology, Chemistry, Pharmacy
of Freie Universität Berlin

by

Dilem Ceren APAYDIN

2022

I hereby declare that this dissertation was written and prepared by me independently. Furthermore, no sources and aids other than those indicated have been used. The intellectual property of other authors has been marked accordingly. I also declare that I have not applied for an examination procedure at any other institution and that I have not submitted the dissertation in this or any other form to any other faculty as a dissertation.

This work was conducted from October 2017 until August 2022 at Max Delbruck Center for Molecular Medicine in the Helmholtz Association (MDC) in Berlin under the supervision of Dr. Suphansa Sawamiphak.

1st Reviewer: Dr. Suphansa Sawamiphak

2nd Reviewer: Prof. Dr. Sigmar Stricker

date of defense: 20.01.2023

Table of Contents

Abstract

Cardiac development and remodeling are complex biological processes, including a series of crucial events. These events are controlled and influenced by not only cardiac cells but also inter-organ crosstalk. For example, extra-cardiac organ systems, i.e., central nervous, neuroendocrine, and immune systems, are critical regulators of cardiovascular physiology. Homeostatic disruption of these organ systems in a condition like stress and sodium retention can tip off the pathogenesis of the cardiovascular system. In such settings, the immune system becomes the mediator between different systems. Since cytokines, acting as molecular messengers, shape the immune response, they take center stage in the signaling crosstalk. Stress experienced in early life is known to modify the fetal/postnatal cytokine network, thereby immune response resulting in a disruption in the balance of signaling crosstalk. Indeed, aberrant fetal/neonatal immune activity is associated with the development of cardiovascular disease, including heart failure, in later life. In addition, inflammatory cytokines, secreted from dysregulated immune cells in response to sodium and water imbalance causing increased blood pressure, are the critical determinants driving the progression of hypertension to severe cardiovascular disease and end-organ damage like heart failure. Heart failure is mainly the end stage of pathologic conditions which progress over time and is a major cause of cardiovascular morbidity and mortality due to a lack of efficient therapies. Hence, it is vital to consolidate our understanding of the mechanisms behind the transition from pathological conditions to severe disease. This study reveals that cytokine signaling, i.e., IL4 and IFNγ is a critical player in not only cardiac development but also pathological cardiovascular remodeling in response to stress and hypertensive stimuli. These insights might prove to be valuable as novel intervention checkpoints for future therapeutic approaches to cardiovascular diseases.

In my first project, we gained more insights into how early life stress governs cardiovascular outcomes in adulthood. Our data propose that reduced mitotic activity in cardiomyocytes and subsequent adverse cardiac remodeling due to prolonged exposure to stress early in life might be a causative factor in the transition to cardiovascular disease later in life. We identified novel crosstalk between GR and IL4 signaling through competing for STAT3, which governs a fine balance of cardiomyocyte mitotic activity in the presence of stress factors as well as physiological development of the heart. In this manner, IL4 seems to play an essential role in the prevention of pathological cardiac remodeling upon stress through

competitive activation of STAT3. Finally, this report highlights the potency of STAT3 for targeted interventions to prevent or rescue the cell-cycle exit occurring due to early life stress experience, thereby reducing the risk of cardiovascular disease events later in life.

Hypertension, defined as increased blood pressure, is a prominent risk factor for heart failure. However, its pathogenesis could not be well-characterized due to its multifactorial nature, and there is an urgent need for efficient therapeutic interventions due to inefficient treatment approaches currently used to control hypertension. In my second project, we modified an ion-poor treatment approach, which was previously shown to acutely induce RAS-dependent sodium uptake to establish a novel zebrafish model of ion imbalance. Our model exhibited RAS activation, induction of systemic inflammation, arterial hypertension, cerebrovascular regression, cardiomyocyte hypertrophy, and diastolic dysfunction, mimicking not only key facets of hypertension but also its progression into heart failure observed in humans and animal models. We further investigated the responses to ion-poor mediated hypertensive stimuli over time. Ion-poor treated larvae showed progressive activation of RAS prior to gradual elevation of pro-inflammatory cytokines *IFNg* and *IL1b*, indicating that RAS-induced systemic inflammation might contribute to further cardiovascular remodeling. Additionally, we discovered an altered macrophage transcriptional program characterized by downregulation of gene expression involved in innate immunity and vasculo/neuroprotective function. Importantly, blocking of IFNγ signaling with the administration of an anti-IFNγ antibody was sufficient to rescue, at least partially, cerebrovascular regression, arterial hypertension, and dysregulation of macrophage homeostatic function. Taken together, utilizing this zebrafish model, we provided better mechanistic insights into the cascade of events involved in the pathogenesis of hypertension. These findings highlight the importance of the balance in macrophage homeostatic functions, such as maintaining cell survival as well as modulating the vascular structure and neural activity, for the development of new immune-targeted therapies for hypertension. Finally, this study provides insight into one such potential immune-targeted therapy strategy, IFNγ signaling, to ameliorate the progression of hypertension.

Zusammenfassung

Die Entwicklung und der Umbau des Herzens sind komplexe biologische Prozesse, die eine Reihe von wichtigen Prozessen umfassen. Diese Prozesse werden nicht nur von den Herzzellen kontrolliert und beeinflusst, sondern auch von den Organen, die miteinander in Wechselwirkung stehen. So sind beispielsweise extrakardiale Organsysteme, d. h. das zentrale Nervensystem, das Neuroendokrine System und das Immunsystem, entscheidende Regulatoren der kardiovaskulären Physiologie. Eine homöostatische Störung dieser Organsysteme unter Bedingungen wie Stress und Natriumretention kann die Pathogenese des kardiovaskulären Systems initiieren. In solchen Situationen wird das Immunsystem zum Vermittler zwischen den verschiedenen Systemen, und da Zytokine als molekulare Botenstoffe die Immunantwort steuern, stehen sie im Mittelpunkt des Signalübergangs. Es ist bekannt, dass frühkindlicher Stress das fötale/postnatale Zytokinnetzwerk und damit die Immunantwort verändert, was zu einer Störung des Gleichgewichts des Signal-Crosstalks führt. Tatsächlich wird eine abweichende fetale/neonatale Immunaktivität mit der Entwicklung von Herz-Kreislauf-Erkrankungen, einschließlich Herzinsuffizienz, im späteren Leben in Verbindung gebracht. Darüber hinaus sind Inflammationszytokine, die von dysregulierten Immunzellen als Reaktion auf ein Natrium- und Wasserungleichgewicht, das zu einem erhöhten Blutdruck führt, ausgeschüttet werden, die entscheidenden Faktoren, die das Fortschreiten von Bluthochdruck zu schweren Herz-Kreislauf-Erkrankungen und Endorganschäden wie Herzinsuffizienz fördern. Die Herzinsuffizienz ist vor allem das Endstadium pathologischer Zustände, die im Laufe der Zeit fortschreiten und aufgrund des Mangels an wirksamen Therapien eine der Hauptursachen für kardiovaskuläre Morbidität und Mortalität darstellen. Daher ist es von entscheidender Bedeutung, unser Verständnis der Mechanismen zu vertiefen, die hinter dem Übergang von pathologischen Zuständen wie Stress und Bluthochdruck zu einer schweren Erkrankung stehen. Diese Studie zeigt, dass die Signalisierung von Zytokinen, d. h. IL4 und IFNγ, nicht nur bei der Herzentwicklung, sondern auch beim pathologischen kardiovaskulären Umbau als Reaktion auf Stress- und Bluthochdruckreize eine entscheidende Rolle spielt. Diese Erkenntnisse könnten sich als neuartige Kontrollpunkte für künftige therapeutische Ansätze zur Behandlung von Herz-Kreislauf-Erkrankungen als wertvoll erweisen.

In meinem ersten Projekt haben wir weitere Erkenntnisse darüber gesammelt, wie frühkindlicher Stress die kardiovaskulären Erkrankungen im Erwachsenenalter beeinflusst.

Unsere Daten deuten darauf hin, dass eine verringerte mitotische Aktivität in den Kardiomyozyten und ein schädlicher kardialer Umbau aufgrund von langanhaltendem Stress im frühen Leben ein ursächlicher Faktor für den Übergang zu Herz-Kreislauf-Erkrankungen im späteren Leben sein könnte. Wir haben eine neuartige Wechselwirkung zwischen GR- und IL4-Signalen durch die Konkurrenz um STAT3 identifiziert, dass ein feines Gleichgewicht der mitotischen Aktivität der Kardiomyozyten in Präsenz von Stressfaktoren sowie der physiologischen Entwicklung des Herzens steuert. Auf diese Weise scheint IL4 durch die konkurrierende Aktivierung von STAT3 eine wesentliche Rolle bei der Verhinderung von pathologischem kardialem Umbau bei Stress zu spielen. Schließlich unterstreicht dieser Bericht das Potenzial von STAT3 für spezifische Interventionen zur Verhinderung oder Rettung des Zellzyklusausstiegs, der durch frühe Stresserfahrungen im Leben entsteht, und damit zur Reduzierung des Risikos von Herz-Kreislauf-Erkrankungen im späteren Leben.

Bluthochdruck, ist ein wichtiger Risikofaktor für Herzinsuffizienz. Allerdings konnte die Pathogenese aufgrund ihrer multifaktoriellen Natur nicht gut charakterisiert werden, und es besteht ein dringender Bedarf an effizienten therapeutischen Interventionen aufgrund der ineffizienten Therapieansätze, die derzeit zur Kontrolle des Bluthochdrucks verwendet werden. In meinem zweiten Projekt haben wir einen ionenarmen Behandlungsansatz modifiziert, von dem zuvor gezeigt wurde, dass er die RAS-abhängige Natriumaufnahme akut induziert, um ein neuartiges Zebrafischmodell des Ionen-Ungleichgewichts zu etablieren. Unser Modell zeigte eine RAS-Aktivierung, die Induktion einer systemischen Inflammation, eine arterielle Bluthochdruck, eine zerebrovaskuläre Regression, eine Hypertrophie der Kardiomyozyten und eine diastolische Dysfunktion und ahmte damit nicht nur die wichtigsten Aspekte des Bluthochdrucks, sondern auch dessen Fortschreiten bis hin zur Herzinsuffizienz nach, wie sie bei Menschen und Tiermodellen beobachtet wird. Darüber hinaus untersuchten wir die Reaktionen auf durch Ionenmangel vermittelte blutdrucksteigernde Faktoren im Zeitverlauf. Mit Ionenmangel behandelte Larven zeigten eine schrittweise Aktivierung des RAS, bevor es zu einem allmählichen Anstieg der proinflammatorischen Zytokine *IFNg* und *IL1b* kam, was darauf hindeutet, dass die durch das RAS ausgelöste systemische Inflammation zum weiteren kardiovaskulären Umbau beitragen könnte. Darüber hinaus entdeckten wir ein verändertes Transkriptionsprogramm der Makrophagen, das durch eine Herunterregulierung der Genexpression gekennzeichnet ist, die an der angeborenen Immunität und der vaskulären/neuroprotektiven Funktion beteiligt sind. Wichtig ist, dass die Blockierung der

IFNγ-Signalübertragung durch die Anwendung eines Anti-IFNγ-Antikörpers ausreicht, um die zerebrovaskuläre Regression, die arterielle Druckerhöhung und die Dysregulation der homöostatischen Funktion der Makrophagen zumindest teilweise zu verhindern. Insgesamt konnten wir mit Hilfe dieses Zebrafischmodells bessere mechanistische Einblicke in die Kaskade von Ereignissen gewinnen, die an der Entwicklung von Bluthochdruck beteiligt sind. Diese Ergebnisse unterstreichen die Bedeutung des Gleichgewichts der homöostatischen Funktionen von Makrophagen, wie z. B. die Aufrechterhaltung des Zellüberlebens sowie die Modulation der Gefäßstruktur und der neuronalen Aktivität, für die Entwicklung neuer, auf das Immunsystem abzielender Therapien gegen Bluthochdruck. Schließlich bietet diese Studie einen Einblick in eine solche potenzielle immunologische Therapiestrategie, die IFNγ-Signalisierung, um das Fortschreiten des Bluthochdrucks zu mildern.

1 Introduction

1.1 Cardiac Development

The heart is one of the first organs to develop and function during embryogenesis in order to provide blood and oxygen throughout the embryo. During gastrulation, a hallow cluster of cells called blastula is reorganized into three germ layers of the embryo: dorsal ectoderm, ventral endoderm, and mesoderm layer, which will ultimately differentiate into all tissues and organs in the body. The cardiac progenitor cells arise from the mesoderm in the vertebrates (Srivastava & Olson, 2000; Zaffran & Frasch, 2002). A mature heart is composed of three main layers: the inner endocardium, middle myocardium, and outer epicardium **(Fig. 1.1)**. (Arackal & Alsayouri, 2020). The cellular crosstalk between these layers is crucial for the orchestration of proper myocardial growth and function, and it is an evolutionarily conserved mechanism (Poon & Brand, 2013).

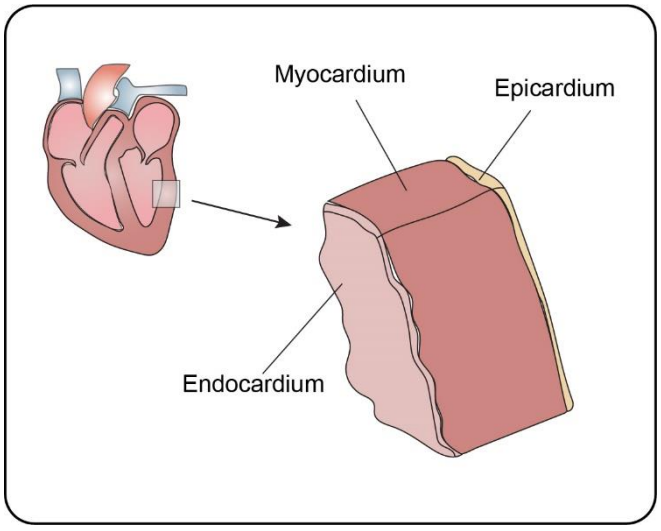

Figure 1.1 The layers of the cardiac wall. White circles indicate the cardiac wall where the layers of the heart are shown. The innermost layer of the heart, the endocardium, is comprised of endothelial cells. The myocardium, the middle layer of the heart wall, contains cardiac muscle cells responsible for contractile force to pump the heart. The outermost layer of the heart, the epicardium, is composed primarily of connective tissue and fat.

The four-chambered mammalian heart has two ventricles and two atria separating the systemic and pulmonary circulations. In contrast, the zebrafish possesses a two-chambered heart with one ventricle and one atrium and, consequently, one single systemic circulation. However, the key steps of heart development are highly conserved among species, and zebrafish heart development undergoes similar cellular and molecular stages as other vertebrates (Xia et al., 2020). The development of the heart begins with the assembly of the cardiac progenitor cells in the lateral marginal zone of the blastula at 5 hours post fertilization

(hpf). This is followed by the gastrulation stages of embryonic development, which results in the origination of primary germ layers: ectoderm, mesoderm, and endoderm, as in mammalians. The cardiac progenitor cells migrate toward the midline of the embryo during gastrulation and fuse into a disk with endocardial cells at approximately 15 hpf, resulting in a cardiac cone formation. The cardiac cone then elongates into a linear heart tube which is composed of myocytes located at the outer layer and endocardial cells in the inner layer. Rhythmic contraction of the linear heart tube starts at around 24 hpf. At around 48 hpf, the cardiac valve is now fully formed, and the heart is looped to form two chambers: the right-sided ventricle and left-sided atrium. The proliferation of cardiomyocytes substantially increases after 48 hpf. (Staudt & Stainier, 2012; Xia et al., 2020). By 72 hpf, developing ventricle stereotypes cardiac trabeculae, which are highly organized myocardial projections to thicken the ventricular wall. To form trabeculae, cardiomyocytes delaminate from the ventricular wall and expand into the ventricular lumen **(Fig. 1.2)**, enabling increase of the myocardial surface to provide sufficient blood oxygenation and contractile force (J. Liu et al., 2010).

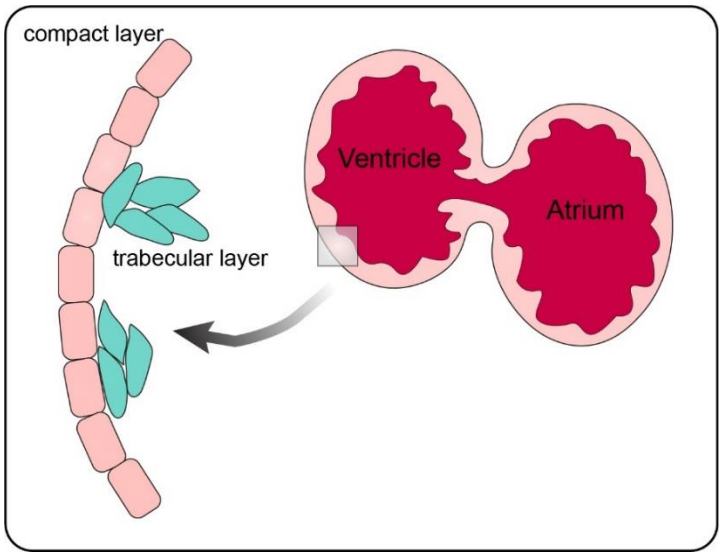

Figure 1.2. Cardiac trabeculation in zebrafish larvae. The ventricular layer is initially formed as a monolayer in the embryonic zebrafish heart. Cardiomyocyte proliferation leads to cellular crowding and tension heterogeneity. A subset of cardiomyocytes with higher tension delaminates from the compact layer (pink) to seed the trabecular layer (blue).

During the early developmental stage, the wall of the linear heart tube is composed of only the myocardium and endocardium in zebrafish, and the epicardium develops from an extra-cardiac cell population. Pro-epicardium becomes morphologically distinguishable around the ventral wall of the heart at 48 hpf and expands over the outside of the myocardial layer to form epicardium at about 72 hpf. In adult zebrafish, epicardium covers the entirety of the surface of the heart (Brown et al., 2016). It was shown that epicardium and endocardium

provide morphogenic and mitogenic signals which play critical roles not only in cardiac development but also in cardiac regeneration in response to injury (Bornhorst & Abdelilah-Seyfried, 2021; Kikuchi, Gupta, et al., 2011; Kikuchi, Holdway, et al., 2011; Quijada et al., 2020).

Cardiac development is a complex multistep process that relies on an intricate orchestration of various cell-autonomous and non-autonomous events to support fine-tuned sequential morphological changes. This time and space-sensitive coordination of the distinct cardiac development processes requires diverse signals and inter-organ crosstalk. (MacGrogan et al., 2018; Solloway & Harvey, 2003). There are various signaling molecules that are well-known regulators of progenitor cell differentiation and proliferation during development; such as retinoic acid, Wnt, bone morphogenic protein (BMP), fibroblast growth factor, Hedgehog, Nodal, and Notch (Staudt & Stainier, 2012). Deregulation of these molecular mechanisms and cellular communications underlies pathological cardiac remodeling progression into cardiovascular diseases.

1.2 Cardiac Remodeling

Cardiac remodeling is a complex process of structural and functional alterations in the heart in response to physiological or pathological stimuli, which increases cardiac output demand. To better adapt itself to the current demand, the heart undergoes molecular, cellular, and interstitial changes identified clinically by changes in the size, mass (hypertrophy and atrophy), geometry (wall thickness and heart shape), and function (Gjesdal et al., 2011). This process is contributed by several cardiac resident and recruited cells, including cardiomyocytes, endothelial cells, fibroblasts, pericytes, and immune cells (González et al., 2018).

During growth, pregnancy, or exercise, the heart undergoes physiological remodeling in response to stimuli, including mechanical forces and growth hormones (Maillet et al., 2013). These stimuli promote myocardium growth by cardiac mass increase (cardiomyocyte size and number) to normalize the wall tension without leading to cardiomyocyte loss or fibrosis (I. Shimizu & Minamino, 2016). Notably, this process includes fine-tuned, highly orchestrated beneficial adaptations, which are reversible once stimuli fade (Maillet et al., 2013). Cardiac remodeling in pathological conditions, similar to physiological ones, exerts compensatory effects to temporarily protect the heart from ventricular wall stress and preserve cardiac

function. However, these effects confer only short-term benefits to the heart. In the presence of persistent pathological stimuli, these initial adaptive alterations transit to maladaptive cardiac remodeling. This is mostly an irreversible process. (I. Shimizu & Minamino, 2016; Van Berlo et al., 2013).

Depending on pathological conditions, maladaptive cardiac remodeling is often accompanied by cell death, hypertrophy, cardiac dysfunction, fibrosis, inflammation, and aberrant gene expression (González et al., 2018). These comorbidities subsequently contribute to the development of several cardiovascular diseases, such as ischemic heart disease, myocardial infarction, and coronary artery disease, which are common causes of heart failure (HF).

1.3 Heart Failure

The term "cardiovascular disease" is used to describe a wide variety of illnesses that limit the heart's capacity to fill with or pump out blood. If the underlying conditions are not treated in time, their limitation of heart function may eventually precede HF. Therefore, HF has been identified as an epidemic and is a staggering clinical and public health concern associated with substantial mortality, morbidity, and healthcare costs (Roger, 2013).

The ejection fraction (EF) is a measure used to quantify the capacity of the heart to pump blood. Depending on EF, HF is classified as reduced EF (HFrEF) or preserved EF (HFpEF). HFrEF, also known as systolic HF, is accompanied by poor contraction ability, causing reduced EF. HFpEF (diastolic HF), in contrast to HFrEF, is characterized by poor mechanical relaxation and filling, increased ventricle stiffness, and, consequently, a higher filling pressure as a result of pressure overload (Roger, 2013; Tanai & Frantz, 2016). The most prevalent underlying reasons for HFpEF are chronic comorbidities, including hypertension, type 2 diabetes, obesity, and renal disease, whereas systolic HF is often preceded by ischemic heart disease, cardiomyopathies, and heart valve disorder (Pfeffer et al., 2019; Tanai & Frantz, 2016).

Numerous efforts have been devoted to studying the pathogenesis of HF, which has resulted in the development of useful therapies for HFrEF, such as β blockers and RAS inhibitors. However, despite extensive research, effective treatments for HFpEF have not yet been identified. Normal EF, diverse pathophysiologies, and more comorbidities in HFpEF

make its diagnosis and treatment more challenging than in HFrEF (Rossignol et al., 2019; Tanai & Frantz, 2016)

In spite of the variations that exist between HFrEF and HFpEF, it has been demonstrated that both types of HF have a link between inflammation and unfavorable cardiovascular outcomes (Dick & Epelman, 2016). Pathological conditions, such as stress, sodium retention, high blood pressure, etc., are known to trigger cardiovascular programming and culminate in HF. Nevertheless, how these factors leading to adverse cardiac remodeling patterns in individuals affect the progression of HF remains to be elucidated.

1.4 Early Life Stress

The survival of complex organisms relies on maintaining an intricate dynamic equilibrium, which is continuously tested by intrinsic or extrinsic adverse forces called stressors that can be real or perceived. The state of disequilibrium in which homeostasis is threatened was defined as *stress*. To re-establish the balance, stress is counteracted by a complex series of physical or behavioral adaptations (Chrousos & Gold, 1992). While this stress response is vital for the survival of the organism, the persistence of stressors, depending on several factors such as severity or duration, can culminate in mental, physical, and pathological conditions associated with several diseases. Exposure to stress during 'critical periods' of development was suggested as one of the major issues in the development of stress-related disorders (Chrousos, 2009).

Stress experienced in early life is also a well-known underlying factor of pathological cardiovascular alterations (Effects of Stress on the Development and Progression of Cardiovascular Disease, 2018). Childhood adversities, including physical or sexual abuse, neglect, and household dysfunction, were associated with an increased risk of cardiovascular disease later in life (Dong et al., 2004; Felitti et al., 1998; Murphy et al., 2017; Su et al., 2015). Some retrospective and prospective studies, for example, showed a linear trend between the dose of adversities experienced in childhood and subsequent risk of ischemic heart disease (Dong et al., 2004; Felitti et al., 1998), myocardial infarction (Rich-Edwards et al., 2012), and stroke (Felitti et al., 1998; Rich-Edwards et al., 2012). In addition, childhood traumatic experiences were reported to be correlated with hypertension occurrence, which is a major risk factor for cardiovascular disease, in adults (Alastalo et al., 2013; Danese et al., 2007; Su et al.,

2014). Moreover, childhood maltreatment was linked to chronic inflammation in adulthood (Danese et al., 2007; Hostinar et al., 2015), suggesting possible role of inflammation as an underlying cause of early life stress-driven cardiovascular pathologies later in life.

Stressful maternal life, as well as anxiety or depression symptoms during pregnancy, were associated with altered fetal immunity (Martinez et al., 2022; O'Connor et al., 2013). For instance, elevated pro-inflammatory cytokines were reported in response to acute stress in humans (Steptoe et al., 2007). A positive correlation between a higher interferon γ / interleukin 4 (IFNγ/IL4) ratio and depressive symptoms was detected in women at mid-pregnancy (Karlsson et al., 2017). Furthermore, elevated levels of T helper (Th) 1 cytokines such as TNFα and Th2 cytokines such as IL6, which are often associated with hypertension, were reported in pregnant women with depression and anxiety symptoms (Cassidy-Bushrow et al., 2012; Christian et al., 2009). On top of that, it is known that some maternal cytokines can pass through the placenta, resulting in abnormal fetal development and adverse health outcomes associated with cardiovascular disease (Glover, 2015; Zaretsky et al., 2004).

All in all, emerging evidence suggests that stress experienced in early life contributes to the development of cardiovascular disease in adulthood.

1.5 Glucocorticoids

The stress response is highly conserved in vertebrates and regulated by a well-organized interconnected network of processes, including various hormones, signaling pathways, and inter-organ crosstalk (Godoy et al., 2018). In this network, Glucocorticoids (GCs) are the central players orchestrating the stress response (Chrousos & Gold, 1992). GCs are a group of corticosteroids, a class of steroid hormones synthesized from a cholesterol precursor in a series of enzymatic processes termed steroidogenesis (Cain & Cidlowski, 2017). Significantly, zebrafish and humans' steroidogenic pathways are highly conserved (Dinarello et al., 2020).

Induction of GC secretion by circadian rhythm and stress is under the strict control of the hypothalamic-pituitary-adrenal/interrenal (HPA/HPI) axis **(Fig. 1.3)** (Alsop & Vijayan, 2008; Ulrich-Lai & Herman, 2009). Notably, the principal organs of the HPA axis are conserved in zebrafish and retain similar functions and structures except for adrenal glands, which are represented by two distinct tissues: the interrenal gland and chromaffin cells located in the head

kidney in fish. Interrenal tissue is homologous to the adrenal cortex in mammals (Alsop & Vijayan, 2008; Clark et al., 2011). Extrinsic or intrinsic stimuli such as physical and neurological stressors, circadian cues, and inflammatory cytokines activate the paraventricular nucleus of the hypothalamus to release corticotropin-releasing factor (CRF). This hormone acts on the anterior pituitary to initiate adrenocorticotropic hormone (ACTH) secretion into the blood vessels. The ACTH, in turn, stimulates GC secretion from the interrenal cells/adrenal gland. Finally, secreted GCs enter the circulation and spread throughout the body (Ulrich-Lai & Herman, 2009). This mechanism is regulated by the negative feedback of GCs acting on the pituitary and hypothalamus to block further release of ACTH and CRF, respectively **(Fig. 1.3).** This negative feedback loop is fundamental to terminate the stress response, thereby preventing the prolonged activity of GCs and maintaining homeostasis (Gjerstad et al., 2018).

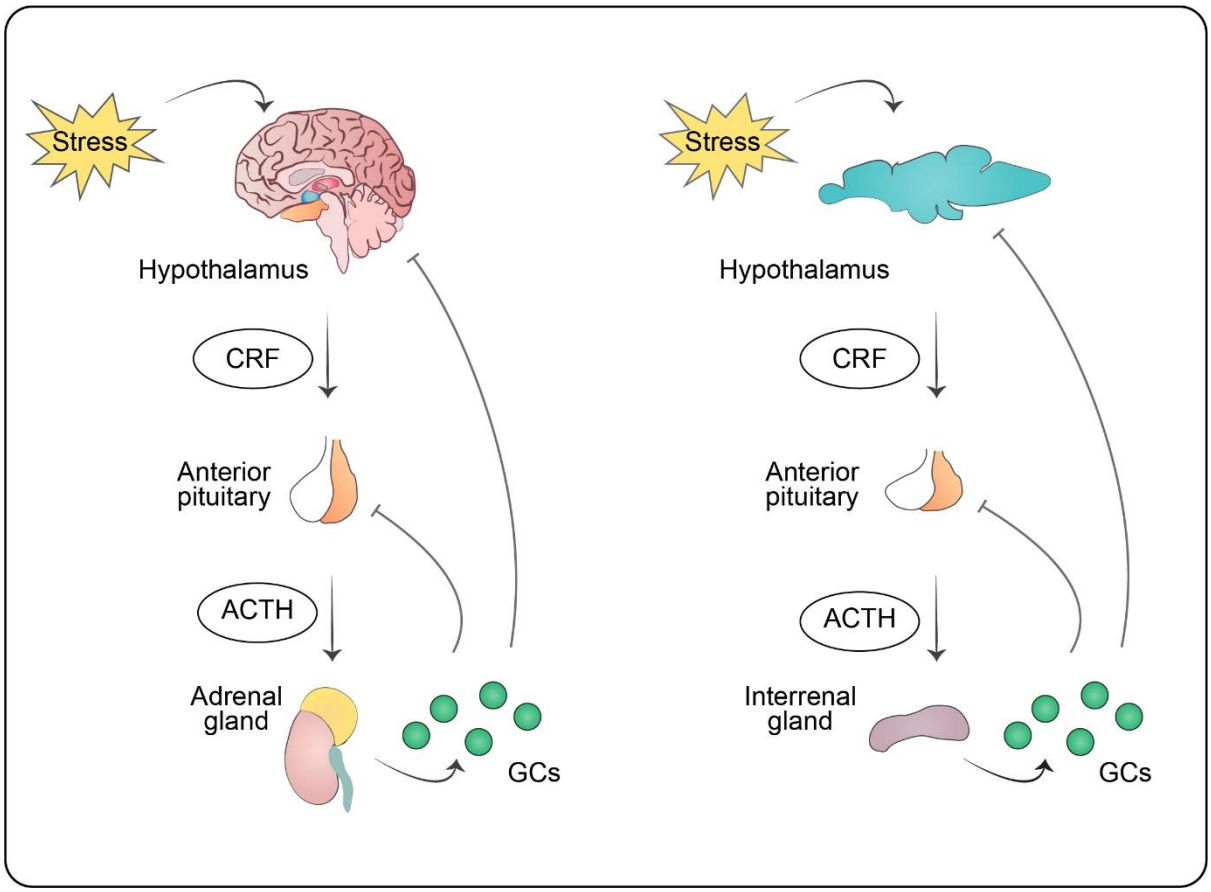

Figure 1.3. Activation of HPA/HPI axis upon stress. Intrinsic or extrinsic stressors activate the hypothalamus to release CRF, which in turn stimulates the anterior pituitary. Activated pituitary gland release ACTH into the vascular system. ACTH stimulates the secretion of GC from the adrenal gland

in mammals and the interrenal gland in zebrafish. GC regulates its own secretion by a negative feedback system acting on the anterior pituitary or hypothalamus to inhibit ACTH and CRF secretion, respectively. The scheme is adapted from (Collier et al., 2017). CRF: corticotropin-releasing factor, ACTH: adrenocorticotropic hormone, GCs: glucocorticoids.

Owing to their lipophilic nature, GCs can diffuse through the cell membrane and exert their function by binding primarily to the glucocorticoid receptor (GR). In some instances, mineralocorticoid receptor (MR), which are intracellular, ligand-depended transcription factors belonging to the nuclear receptor superfamily **(Fig. 1.4)**. While GR can exclusively bind to GCs, the MR have an affinity for both GCs and aldosterone (Timmermans et al., 2019). In the absence of its ligand, GR localizes to the cytoplasm in a multicomplex comprising of heat-shock proteins, immunophilins, and other chaperones. These chaperones play a critical role in the prevention of receptor degradation, receptor-ligand binding, and nuclear transportation of GR. Upon binding of GC, the GR complex undergoes conformational changes and translocates into the nucleus, where it activates or represses the target gene expression (Timmermans et al., 2019). The modes of GR-mediated gene regulations occur either directly by binding to DNA with specific binding motifs called glucocorticoid response elements (GREs), acting as transcription factors, or by altering the function of other transcription factors through physical protein-protein interactions. In addition to these genomic effects in the nucleus, activated GR has non-genomic functions in the cytoplasm and mitochondria (Cain & Cidlowski, 2017; Timmermans et al., 2019). GR can function as a monomer, dimer, and even tetramer depending on its subcellular localization, the presence or absence of ligand, or its DNA-binding status (Escoter-Torres et al., 2019). Acting on several cell types, endogenous GCs exert critical modulatory functions on the stress response, homeostasis, metabolism, development, and inflammation (Cain & Cidlowski, 2017).

Figure 1.4. Genomic effects of the GCs. Genomic actions of GCs mainly occur through GR-mediated transcription. GC binds to GR as part of a multicomplex in the cytoplasm. The ligand-bound GR undergoes conformational changes, dissociates from accessory proteins, and migrates from the cytosol to the nucleus to activate or suppress target gene transcription. In addition to GR, GC also binds with high affinity to MR. While GCs can only activate GR, MR can be activated both by GCs and its own ligands, such as aldosterone. hsp: heat shock protein, GR: glucocorticoid receptor, MR: mineralocorticoid receptor, GC: glucocorticoid.

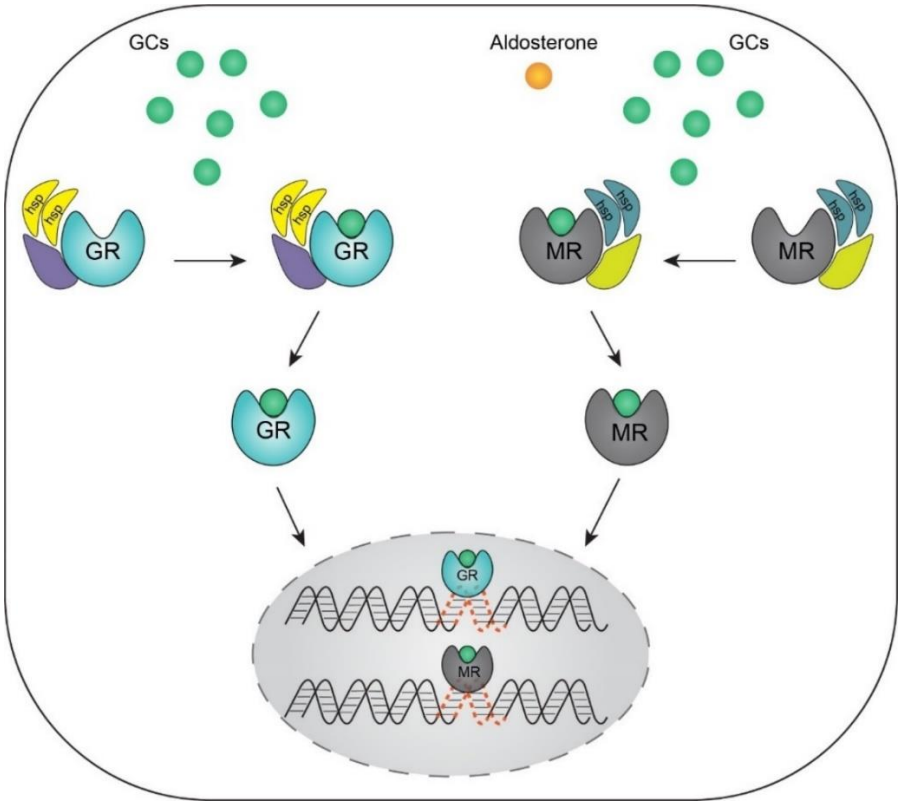

The human GR is encoded by the *NR3C1* gene comprising of nine exons located on chromosome 5 (Timmermans et al., 2019) and alternative splicing of exon 9 generates two isoforms: GRα and GRβ containing different C-terminal ends (Hollenberg et al., 1985; Oakleyt et al., 1999). GRα is the canonical receptor functioning in a ligand-dependent manner. On the other hand, the splice variant GRβ does not bind GCs but antagonizes the GRα transcriptional activity (Oakleyt et al., 1999; Timmermans et al., 2019). In addition to its dominant negative activity, genome-wide expression analyses showed the transcriptional regulation of several non-GRα genes by GRβ, indicating its intrinsic, GRα independent transcriptional activity (Kino et al., 2009; Lewis-Tuffin et al., 2007). Notably, the *NR3C1* gene encoding GRs in humans is strikingly similar to the zebrafish *nr3c1* gene in terms of structure, including the formation of splice variant Grβ isoform (Dinarello et al., 2020). Although a dominant negative effect of Grβ on Grα was reported *in vitro*, no such effect has been observed *in vivo*, indicating that zebrafish Grβ might not have a transcription regulatory role (Chatzopoulou et al., 2017).

GRs possess three main domains: an N terminal domain, a DNA-binding domain, and a C-terminal ligand-binding domain (Timmermans et al., 2019). GR interacts with co-regulators and the transcriptional machinery through the N terminal domain containing a major

transactivation domain called AF-1 (Nicolaides et al., 2010). The DNA-binding domain of GR has two zinc-finger motifs through which the GR binds to GRE. This domain is separated from the ligand binding domain by a hinge domain. Due to its flexible structure, this hinge region facilitates receptor dimerization, translocation to the nucleus, and interaction of GR dimers with GREs (Cain & Cidlowski, 2017). The ligand binding domain is responsible for the recognition and binding of its ligands. Moreover, this domain possesses a second transactivation domain named AF-2, which is critical for GR dimerization, translocation to the nucleus, and its interaction with co-activators/repressors (Nicolaides et al., 2010).

1.5.1 Mechanisms of GR-mediated transcriptional regulation

The ligand-bound GRs are able to activate or repress the expression of target genes transcriptionally. Previous studies proposed three basic mechanisms of GR-mediated transcriptional regulation in the nucleus (Oakley & Cidlowski, 2013). Classic transcriptional regulation by GR occurs through GR acting as a transcriptional factor and relies on direct contact of GR homodimers with GREs in the promoter region(s) of GC responsive genes **(Fig. 1.5)**. Binding of GR homodimers to GRE stimulates recruitment of co-regulators, including steroid receptor co-activators 1 (SRC1), GR-interacting protein 1 (GRIP1), and cAMP-responsive element-binding protein (CREB)-binding protein (CBP), thereby initiating the transcription (Cain & Cidlowski, 2017). By contrast, GR monomers can bind negative GREs (nGREs) and selectively recruit the co-repressors, including nuclear receptor co-repressor 1 and 2, hence resulting in suppression of the target gene transcription (Hudson et al., 2012).

The second mechanism of GR-mediated transcriptional regulation happens via tethering of ligand-bound GR to the chromatin through DNA-bound transcription factors, instead of GR binding to DNA itself (Oakley & Cidlowski, 2013) (**Fig. 1.5)**. GR-mediated immune suppression mainly occurs through protein-protein interactions between GR and other transcriptional factors; particularly, activator protein-1 (AP-1), the signal transducer and activator of transcriptions (STATs), nuclear factor-κB (NF-κB) which leads to repression of pro-inflammatory cytokine production (Cain & Cidlowski, 2017). On the other hand, several studies also revealed GR-mediated transcriptional induction of target genes via GR tethering (Ratman et al., 2013), indicating that both transactivation and transrepression are possible with this mechanism.

The third mode of GR-mediated transcriptional regulation occurs through the direct binding of GR to composite elements (**Fig. 1.5)**. These composite elements are DNA sequences encompassing both a GRE half-site and a response element for diverse transcription factors that 'partners' with GR in the modulation of transcription activity (Cain & Cidlowski, 2017). Notably, this mode of crosstalk, like others, can incite both induction and repression of transcription. For example, the Notch4 promoter composite element contains a GRE half-site and an AP-1 motif. In this motif, AP-1 and GR were shown to synergistically activate the Nothch4 transcription in endothelial cells (J. Wu & Bresnick, 2007). On the other hand, the composite mechanism of GR-depended repression was reported in GC negative feedback mechanism. Interaction of GR and AP-1 at adjacent elements within nGRE results in inhibition of hypothalamic CRH gene transcription. Furthermore, mutations disrupting either GR or AP-1 binding were associated with loss of GC-dependent repression (Malkoski & Dorin, 1999).

GRs are expressed in nearly all cells in the body, so it is not surprising that mice lacking GR die soon after birth due to multiorgan dysfunction (Cole et al., 1995). However, the function of GR is known to vary in a tissue-specific manner. Indeed, chromatin immunoprecipitation sequencing (ChIP-seq) analyses showed little overlap of GR binding sites in different cell types and tissues, suggesting that the landscape of chromatin accessibility probably dictates which GREs are accessible for GR binding. This varying accessibility of GREs leads to cell-type-specific transcriptional modulation mediated by GRs (John et al., 2011).

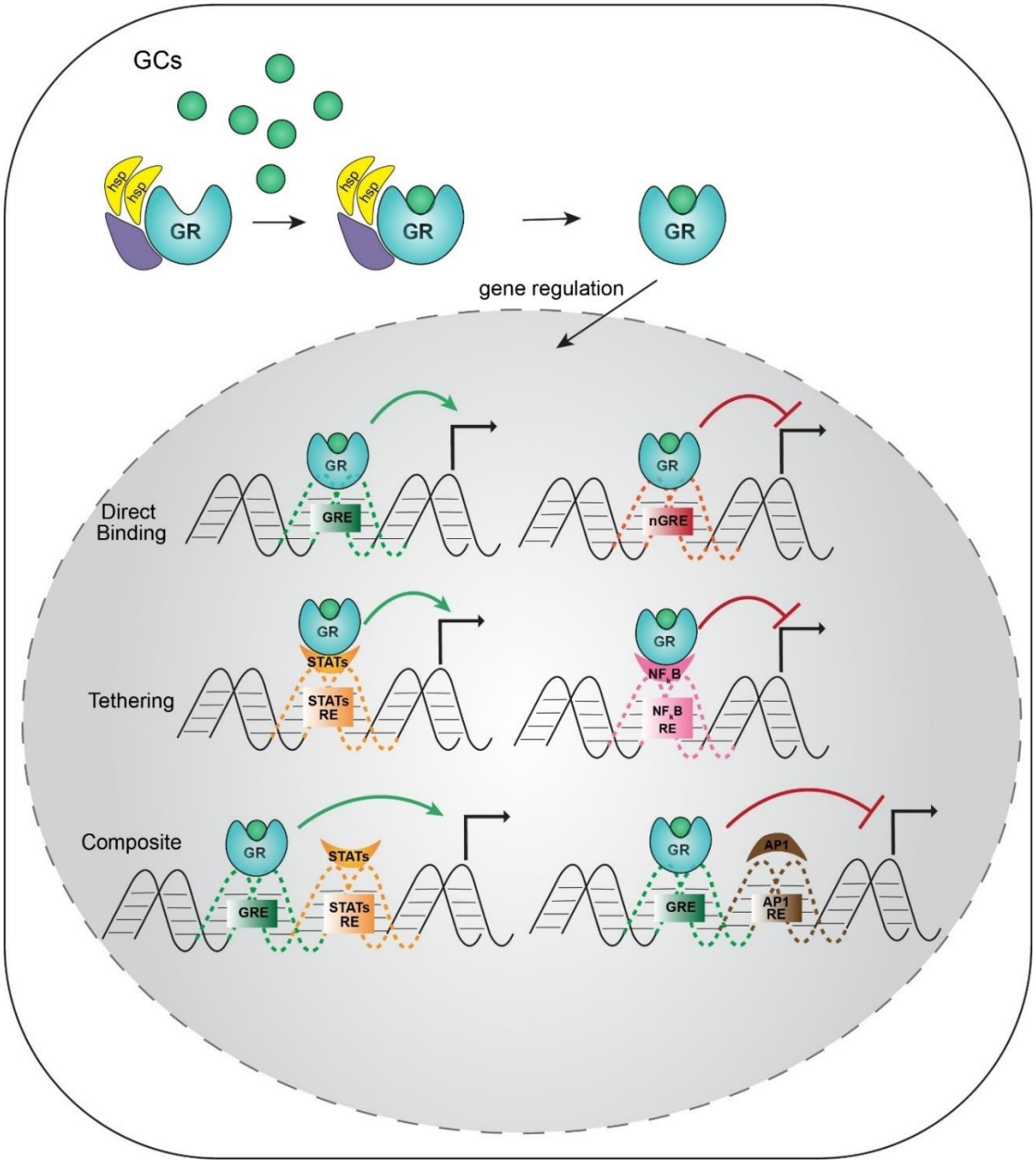

Figure 1.5. Mechanisms of GR mediated transcriptional regulation. GR regulates the target gene transcription by three different mechanisms; direct binding to GRE or nGRE sites, tethering in which GC-bound GR may physically interact with DNA-bound transcription factors, or composite binding in which GC-bound GR directly binds to DNA and physically interact with neighboring DNA-bound transcription factors. In all these modes of action, GR can both enhance and repress target gene transcription. hsp: heat shock protein, GR: glucocorticoid receptor, GCs: glucocorticoids, GRE: glucocorticoid response elements, nGRE: negative GRE, STAT: signal transducer and activator of transcriptions, RE: response element, NF-κB: nuclear factor-κB, AP-1: activator protein-1. Green lines indicate transcriptional activation, and red lines indicate transcriptional suppression. The scheme is adapted from (Dinarello et al., 2020).

1.5.2 Immunomodulation by GCs

GCs, acting through GR, impart pleiotropic effects on the immune system. Upon a prolonged or exaggerated inflammatory response, GRs fetter the inflammatory process, acting as a cellular rheostat to ensure that homeostasis is re-established. Accordingly, inflammation resolution occurs partly through GR-mediated transcriptional regulation (Busillo & Cidlowski, 2013; Cain & Cidlowski, 2017). For instance, GR represses the activity of the pro-inflammatory transcription factors AP-1 and NF-kB activation of which is facilitated by signaling cascades triggered by pro-inflammatory stimuli (Busillo & Cidlowski, 2013). Consequently, the expression of various pro-inflammatory cytokines, including IL4, IL1β, IFNγ, and TNF, are repressed (Cain & Cidlowski, 2017). Furthermore, GRs suppress the inflammatory profile by interfering with signal transduction in immune cells as well as inhibiting their maturation and function (Busillo & Cidlowski, 2013; Cain & Cidlowski, 2017). For instance, GRs blunt T cell activation directly by interfering with T cell receptor signaling and indirectly by regulating dendritic cell (DC) function, including antigen presentation, co-stimulation, and production of cytokines which are crucial for Th cell response. GC-induced apoptosis was reported in lymphocytes, DCs, and eosinophils (Cain & Cidlowski, 2017). While GCs are widely known for their immunosuppressive properties, GRs are also involved in the reinforcement of inflammation by enhancing the expression of the pro-inflammatory cytokines, including TNF, IL1, IL6, and IFNγ (Busillo & Cidlowski, 2013; Wiegers & Reul, 1998).

GR differentially modulates the activity of diverse STAT family proteins, which are transcription factors transferring signals from activated cytokine receptors to the nucleus. Earlier studies revealed the transcriptional synergy mediated by GR and some STATs at the target gene promoter. For instance, a molecular complex formed by GR and STAT5 through direct protein-protein interaction was shown to instigate synergistic activation of β-casein gene transcription *in vitro* (Stocklin et al., 1996). Furthermore, a recent genome-wide study revealed extensive genomic cooperation between GR and STAT3 at the regulatory domains. Langlais et al. performed ChIP-seq and expression profiling analyses, delineating that their co-recruitment to neighboring and composite binding sites, as well as STAT3 tethering to GR through protein-protein interaction, cause transcriptional synergism. Conversely, GR tethering to DNA-bound STAT3 represses the target gene transcription (Langlais et al., 2012).

Due to the immunosuppressive actions of GCs, they are widely used pharmacologically in the treatment of certain inflammatory and autoimmune diseases (Cain & Cidlowski, 2017). For example, corticosteroids, which locally suppress Th2 cell-mediated inflammation through inhibiting cytokine expression such as IL4, are the most effective and commonly used drugs for patients with asthma (Ogasawara et al., 2018; So et al., 2002; Umland et al., 1997). Despite to remarkable therapeutic potential of GCs, long-term GC treatment can lead to reduced sensitivity or resistance to GCs, triggering exaggerated inflammatory responses in some chronic diseases, including asthma, major depression, and cardiovascular conditions (Rodriguez et al., 2016). Besides, long-term treatment with pharmacological GCs was shown to result in several severe side effects, including disturbed wound healing and glucose metabolism, muscle and skin atrophy, and hypertension, etc. (Schäcke et al., 2002).

1.5.3 GCs in cardiac developments

GCs are indispensable for several biological activities, as explained above. Indeed, early postnatal death was reported in GR-deficient mice with several defects, including respiratory failure, impaired HPA axis, defective liver function, and enlarged adrenal glands (Cole et al., 1995). Although GCs are essential for the maturation of diverse tissues and organs during fetal development, rising evidence indicates that the level of GCs should be in balance for proper fetal growth. Stress conveyed through GCs can be transferred from the maternal to the fetal environment during pregnancy. Placenta critically regulates and limits those signals, forming a barrier with the help of 11β -hydroxysteroid dehydrogenase type 2, which converts cortisol to its inactive form called cortisone. Since this barrier is not complete, maternal GCs can cross the placenta and increase the GC levels in the fetus (Rafn Benediktsson et al., 1997). Excessive in-utero exposure to GCs during pregnancy due to high maternal and fetal concentrations was associated with fetal growth retardation in humans (Seckl & Holmes, 2007). Moreover, altered prenatal exposure to GCs was suggested as one of the critical factors underlying altered intrauterine and postnatal immunity and susceptibility to inflammation which leads to impaired fetal growth (Solano & Arck, 2020). Furthermore, supraphysiologic levels of GCs were also shown to be critical for zebrafish. Previous studies showed that zebrafish embryos injected with cortisol at the one-cell stage exhibited reduced cardiac performance, such as lowered

heart-beat and impaired cardiac development, as shown by pericardial edema and abnormal chamber formation (Nesan & Vijayan, 2012).

In addition to short-term consequences altering early development, exposure to excess GCs in utero is associated with fetal programming with subsequent effects on adult health with increased susceptibility to multiple disorders, including hypertension, hyperactivity of the HPA axis, and anxiety in adulthood (Seckl & Holmes, 2007). Higher blood pressure and lower birthweight, which are strongly associated with hypertension, were reported in the adult rats exposed to supraphysiologic levels of GCs in utero (R. Benediktsson et al., 1993). In addition, premature activation of the fetal HPA axis and subsequent activation of GR-mediated pathways due to maternal nutritional restriction was shown to elevate fetal GC levels and retard fetal growth, leading to long-term cardiometabolic consequences (Cottrell et al., 2012). Adult zebrafish with elevated GC action during embryogenesis exhibited enlarged heart with altered expression of maturation-related genes such as elevated levels of *vmyc* (homologs to mammalian B-MHC), suggesting cardiac hypertrophy (Wilson et al., 2015).

Various studies have been performed over the years to delineate the role the GR signaling in the heart, especially in cardiomyocytes. GR gain of function approaches using a transgenic mouse model overexpressing doxycycline-controlled GR in cardiomyocytes demonstrated aberrant heart rhythm (bradycardia) and cardiac conduction with atrioventricular block. Importantly, this conduction defect was reversed by the administration of doxycycline to shut off GR overexpression. Furthermore, *in vitro* studies using isolated cardiomyocytes from the same transgenic mice suggested cellular alterations underlying the phenotypes mentioned above. Isolated cardiomyocytes overexpressing human GR displayed ion channel remodeling and altered calcium homeostasis, which resulted in conduction defects (Sainte-Marie et al., 2007), indicating the cardiomyocyte-specific influence of GR.

In mammals, it was shown that GC levels dramatically increase in late gestation, in which most of the organs undergo maturational changes needed to survive extra-uterine life (Fowden et al., 1998). Furthermore, Rog-Zielinska et al. investigated the role of GR in late-gestation fetal heart maturation. Fetuses deficient in GR displayed reduced heart size, disorganized myofibrils, and cardiomyocyte alignment as well as impaired cardiac function in late gestation. To further evaluate whether these effects arise from the absence of GR within the heart and vasculature, they generated transgenic mice with conditional knockout of GR in cardiomyocytes and vascular smooth muscle cells. Similar to global GR deficient mice, fetal

hearts of conditional knockout of GR in muscle cells exhibited impaired heart maturation and function, suggesting cell-autonomous action of GR exerts in cardiomyocytes and vascular smooth muscle cell maturation (Eva A. Rog-Zielinska et al., 2013). Consistent with these results, smaller heart size and cardiac dysfunction were also noted in the zebrafish embryonic loss of function model, which was established by injection of Gr morpholino (Wilson et al., 2015). Thanks to the transient nature of morpholine knockdown, the majority of embryos could survive into adulthood, while Gr deficient fetuses die soon after birth. Hence, further observation of zebrafish Gr morphants revealed structural and functional abnormalities, including reduced heart size and underdeveloped trabeculae in adulthood (Wilson et al., 2015).

Furthermore, it was shown that mice deficient in GR, specifically in cardiomyocytes, die prematurely due to HF characterized by hypertrophy, left ventricle dilation, and systolic dysfunction. Dysregulated expression of several genes, which are known to be involved in the pathogenesis of cardiovascular disease, was also noted in these mice (Oakley et al., 2013). Recently, it was shown that these detrimental effects of GR deficiency were abolished in mice lacking both GR and MR in cardiomyocytes. These double knockout mice are protected from cardiac remodeling and dysfunction as well as early death observed in cardiomyocyte-specific GR knockout mice. By contrast, mice lacking only MR in cardiomyocytes exhibited proper heart morphology and functionality (Oakley et al., 2019). Emerging findings suggested that cardiomyocyte MR is dispensable for normal cardiac development and function, but under myocardial stress such as GR deficiency in cardiomyocytes or specific disease conditions, it becomes detrimental, contributing to the development and progression of cardiac diseases such as HF (Fraccarollo et al., 2011; Oakley et al., 2019).

1.6 The Immune System in Cardiac Homeostasis

It is becoming clear that the immune system not only defends against pathogens but also makes a critical contribution to normal cardiac development, function, and remodeling. Leukocytes, for example, play a life-long role in homeostasis and adaptation to disease conditions for various organs. Recently, elucidating the role of tissue-resident immune cells in homeostasis and pathological conditions has become a major research topic. In the heart, leukocyte infiltration occurs at gestation, and different types of these cells remain in the myocardium throughout adulthood (Swirski & Nahrendorf, 2018). Advanced lineage tracing

tools demonstrated that the heart contains heterogeneous macrophage populations with diverse origins and functions (Epelman et al., 2014). In addition to their canonical function as part of the immune system, recent studies showed that tissue-resident macrophages also play non-canonical roles in cardiac conduction and coronary development (Hulsmans et al., 2017; Leid et al., 2016).

To interact and communicate with other cells, immune cells release cytokines that are key mediators of immune response (J. M. Zhang & An, 2007). It is worth noting that elevated levels of several cytokines, including IL1β, IL17, TNFα, IL6, and IFNγ, were reported to participate in the development and progression of several cardiovascular diseases, highlighting the importance of immune system regulation to maintain cardiac homeostasis (Role of Cytokines and Inflammation in Heart Function during Health and Disease, 2018). On the other hand, the cardioprotective function of several cytokines was also noted in certain disease conditions. For instance, administration of IL10 was shown to suppress myocardial inflammation and mitigate pathological ventricular remodeling following myocardial infarction (Krishnamurthy et al., 2009). Although the traditional classification presents cytokines as pro- or anti-inflammatory owing to their immunomodulatory functions, emerging evidence extends our understanding of cytokine functions beyond being only inflammatory mediators to non-immune functions. Numerous cytokines are now known to elicit various pleiotropic effects depending on environmental conditions as well as tissue-specific milieu (Foti, 2017). IL13, for example, was reported to regulate glucose metabolism in the liver by acting directly on hepatocytes. In the heart, IL6 was implicated in cardiomyocyte metabolic homeostasis, and its deficiency was associated with cardiac lipotoxicity, thereby predisposing to cardiac dysfunction (Xu et al., 2018). Earlier *in vitro* studies showed that administration of IL11 resulted in resistance to cardiomyocyte death induced by oxidative stress, suggesting a possible cardioprotective function (R. Kimura et al., 2007). Furthermore, it was shown that IL4 exhibits critical functions in cardiac remodeling, fetal development, tissue regeneration, brain functions, and pathogenesis of cancer and fibrosis. (McCormick & Heller, 2015).

1.6.1 IL4 Signaling

IL4, a short four α-helix bundle glycoprotein, is one of the pleiotropic cytokines playing a crucial role in the modulation of immune responses (Wlodaver et al., 1992). It is mainly

produced by mast cells, basophils, Th2 cells, neutrophils, and eosinophils to orchestrate type 2 immunity which is known to be essential for the maintenance of homeostasis and regulation of tissue repair and fibrosis (Gieseck et al., 2017)

IL4 shows approximately 25% sequence homology with IL13 (Minty et al., 1993). Although they are structurally and functionally related cytokines and exert overlapping biological and immunoregulatory functions, they also play unique roles in various biological activities (A. E. Kelly-Welch et al., 2003; McCormick & Heller, 2015). Both *IL4* and *IL13* genes are encoded by adjacent genes located on chromosome 5 in humans. Due to the whole genome duplication event that occurred in teleost fish, zebrafish has two *il4/13* loci, namely *il4* and *il13*. While *il4* is located on chromosome 14, *il13* presents on chromosome 9 in zebrafish (Ohtani et al., 2008). Transcript and protein analysis showed zebrafish Il4 and Il13 share high homology with mammalian IL4 and IL13(Ohtani et al., 2008).

To exert its biological functions, IL4 signals via two types of heterodimeric receptors: type I and type II IL4R **(Fig. 1.6)**. Both IL4Rs comprise two transmembrane proteins. The type I receptor is composed of the IL4Ra chain (IL4Rα) and the common γ chain (γC). On the other hand, the type II receptor, also called IL13R, is composed of the IL4Rα chain and IL13Rα1 chain (IL13Ra1) (McCormick & Heller, 2015). IL4 possesses two binding epitopes. While one of the epitopes is for the high-affinity receptor chain IL4Rα, the other epitope is for the low-affinity IL13Rα1 and γc receptor chains (Mueller et al., 2002). In contrast to IL4, IL13 can only bind to type II IL4R complexes with high affinity but not type I complexes. In addition, IL13 can also bind to IL13Rα2 with higher affinity than IL13Rα1. However, IL13Rα2 was considered to function as a decoy receptor due to its short intracellular domain lacking signaling kinase part. Nevertheless, emerging evidence suggests that it plays a role in IL13 signaling (A. E. Kelly-Welch et al., 2003; McCormick & Heller, 2015).

Binding of IL4 to IL4Rα leads to dimerization with either γc or IL13Rα1, thus providing a new conformation of intracellular receptor domains to initiate of downstream phosphorylation cascade **(Fig. 1.6)**. The receptor dimerization activates Janus kinases (JAKs) associated with the cytoplasmic tail of the γc (JAK3), IL4Rα (JAK1), or IL13Rα1 (TYK2, JAK2) (Junttila, 2018). Activated Jaks, in turn, phosphorylates tyrosine residues in the cytoplasmic tail of IL4Rα , which serve as docking sites for downstream signaling molecules, including STATs and insulin receptor substrate family (IRS). While type I IL4R complex can

activate both STATs and IRS, type II IL4R can only phosphorylate STATs but is unable to activate IRS. Although IL4 signals preferentially through STAT6 and IRS-2 to induce downstream molecules, some cells can also engage STAT3 in response to IL4 stimulation (McCormick & Heller, 2015). Once the cytoplasmic tyrosine residues are phosphorylated, STATs are recruited to IL4Rα, where their tyrosine residues are phosphorylated. Then, phosphorylated STATs dimerize and translocate into the nucleus to bind to specific accessible DNA sequences within the promoter of target genes, regulating their transcription (A. Kelly-Welch et al., 2005).

Zebrafish genome analysis showed that the IL4R system is present in zebrafish (Wang & Secombes, 2015). Similar to mammals, zebrafish Il4rα comprises of an extracellular domain, a transmembrane domain, and a cytoplasmic domain. Furthermore, previous studies revealed that structural and functional features of the IL4Rα are also conserved in zebrafish (Zhu et al., 2012).

Figure 1.6. IL4 signaling pathways. IL4 can signal through two signaling complexes. Upon binding of IL4 to the IL4Rα chain, the IL4Rα dimerize with the common γC chain to form a type I receptor complex or IL13Rα1 chain to form a type II receptor complex. The dimerization of the type I receptor can activate JAKs and downstream STAT6 and IRS-2, while the type II complex can activate predominantly STAT6 but also STAT3 through the JAK family kinase TYK2. Phosphorylated STAT3/6 translocate to the nucleus to bind the promoter regions of IL4 responsive genes. IRS: insulin receptor substrate family, JAK: Janus kinases, STAT: signal transducer and activator of transcriptions, P: phosphorylated.

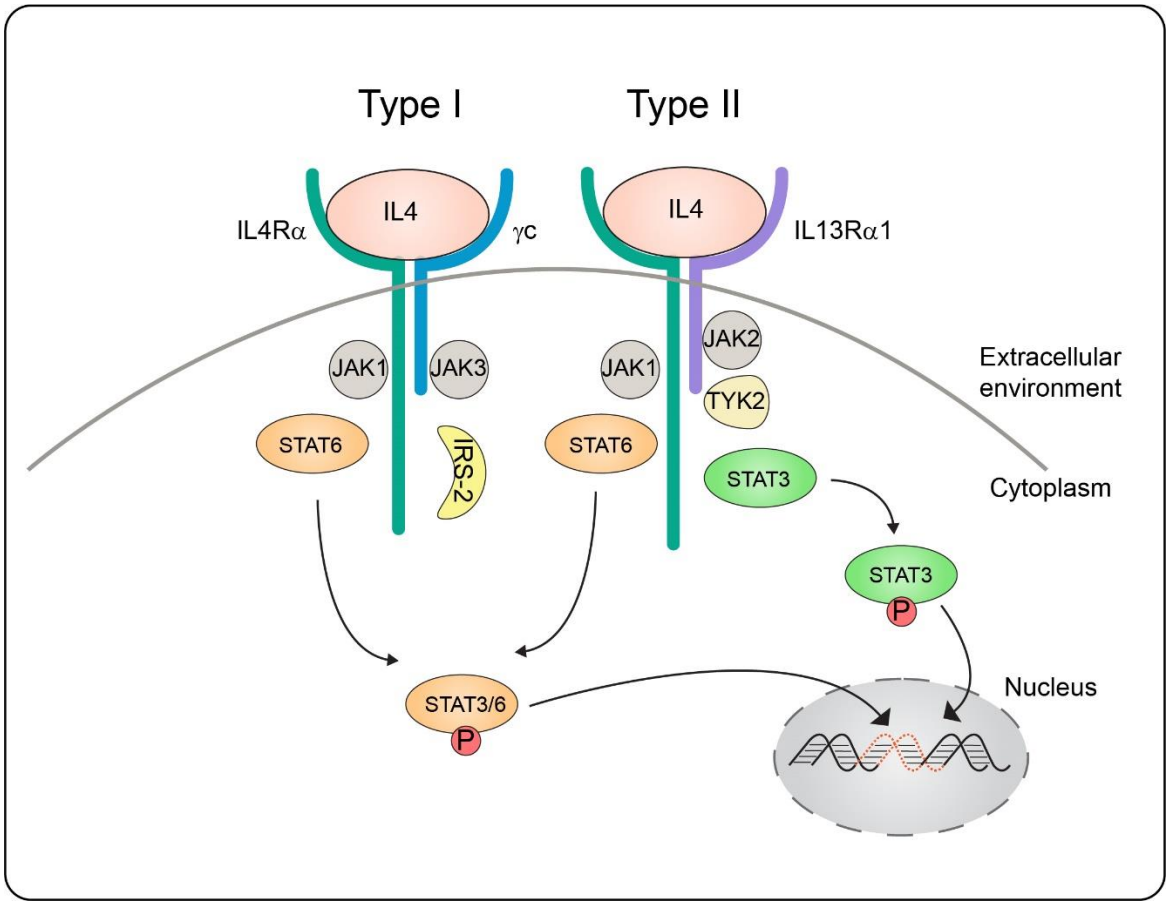

1.6.2 Biological Functions of IL4

IL4 has a pivotal role in type 2 mediated immune responses, acting as a critical player in a wide range of activities regulating inflammatory responses, thereby maintaining homeostasis. Some diverse IL4 responses are associated with allergic and fibrotic diseases (Gieseck et al., 2017). For instance, it promotes differentiation of naïve T cells to Th2 cells, B cell development and antibody production, immunoglobulin (Ig) class switching to IgE, proliferation and activation of mast cells, as well as expansion of basophils and eosinophils (Lloyd & Snelgrove, 2018). On the other hand, excessive activation of this response results in atopic reactions (Gieseck et al., 2017). In the presence of supraphysiological levels of IL4, the aforementioned immune activities mediated by IL4 contribute to the development of allergic inflammation (De Vries et al., 1999; Steinke & Borish, 2001). Besides, it was shown that IL4 induces mucin gene expression, hypersecretion of mucus, and eosinophilic inflammation in asthma (Gour & Wills-Karp, 2015). Hence, IL4 is one of the targeted cytokines for therapeutic interventions to temper

allergic diseases. For instance, GCs are used to inhibit excessive IL4 production and activity in the clinic (Ogasawara et al., 2018; So et al., 2002; Umland et al., 1997).

In addition to its pro-inflammatory functions in allergic disease, IL4 acts as an anti-inflammatory cytokine by inhibiting inflammatory cytokine production, including TNFα, IL6, IL1β, and other pro-inflammatory mediators (te Velde et al., 1990). Furthermore, IL4 stimulates the macrophage activation program toward the type 2 subset with wound healing phenotype known as alternatively activated macrophages **(Fig. 1.7)**. While classically activated macrophages (type 1 macrophages, M1) boost pro-inflammatory cytokines secretion, alternatively activated macrophages (type 2 macrophages, M2) oppose inflammation by secreting IL10 and transforming growth factor β (TGFβ) and promote tissue repair, extracellular matrix regulation, and wound healing (DM et al., 2008).

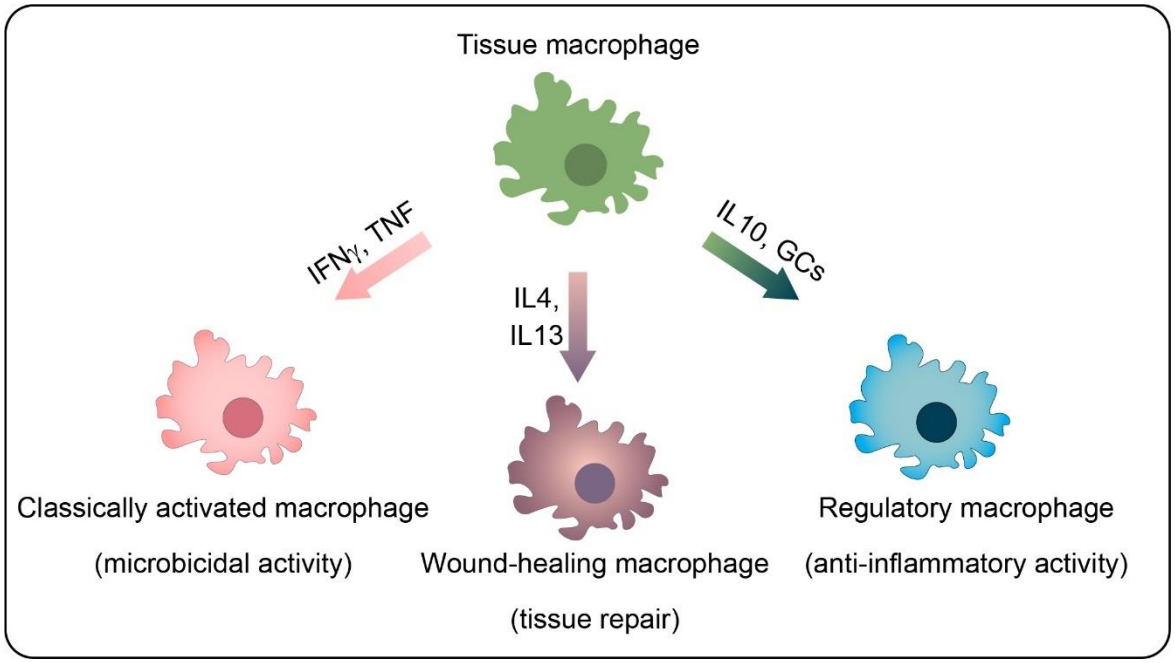

Figure 1.7. Polarization of macrophages in response to different environmental stimuli. In the presence of IFNγ and TNF, macrophages are classically polarized into pro-inflammatory phenotype (classically activated, M1) and involved in microbial activity. In contrast, wound healing macrophages (alternatively activated, M2) are induced by IL4 and contribute to tissue repair. Regulatory macrophages arise in response to different stimuli, including GCs and IL10, and suppress the immune response. IFNγ: interferon γ, TNF: tumor necrosis factor, IL: Interleukin, GCs: Glucocorticoids. The scheme is adapted from (DM et al., 2008)

In addition to its effects on immune cells, IL4 is also able to exert distinct functions by influencing other types of cells. Acting as a pro-fibrotic factor, for example, it induces proliferation and differentiation of fibroblasts into myofibroblasts, as well as promotes collagen production (Huang et al., 2015). Previous studies showed that IL4 is involved in the fibrotic remodeling of several organs, such as the heart during disease pathogenesis (Kanellakis et al., 2012; Roselló-Lletí et al., 2007). In addition to its effect on fibroblasts, IL4 secreted from myotubes was shown to signal myoblast recruitment and promote myoblast fusion with myotubes, suggesting a role for IL4 in regulating cell fusion during myogenesis (Horsley et al., 2003).

Among its multiple biological effects, IL4 is also involved in the modulation of neuroimmune function. A reduced level of IL4 was detected in the brain of a rat anxiety model (H. J. Lee et al., 2016) and the serum of a mouse depression model (Han et al., 2015). Accordingly, IL4 deficient mice exhibited anxiety-like behavior (Moon et al., 2015). Moreover, a similar inverse correlation of IL4 with anxiety was also reported in women in mid-pregnancy (Karlsson et al., 2017). A recent study showed an increased level of IL4 secretion in the brain of mice exposed to anxiolytic drugs, including imipramine and 3′-deoxyadenosine, which leads to reduced anxiety behaviors. Moreover, the anxiolytic action of these drugs was diminished upon inhibition of IL4 signaling, suggesting that the anxiolytic effect is mediated by IL4 (Gao et al., 2019). These findings show that IL4 plays a significant role in the pathophysiology of anxiety.

1.6.3 Opposite effects of IL4 in the heart

Although IL4 is known to be involved in various biological functions in diverse tissues and organs, its effect on the heart is still not fully uncovered yet. Particularly, the role of IL4 in cardiac development remains largely unknown to date. Most of the previous studies concentrated on the pro-fibrotic function of IL4 in the adult heart during cardiac fibrosis, which is a maladaptive cardiac remodeling and eventually leads to cardiac failure. Indeed, IL4 level was associated with cardiac fibrosis and left ventricular remodeling in patients with HF. Patients with hypertensive cardiomyopathy showed an even more significant correlation with IL4 levels (Roselló-Lletí et al., 2007). In murine models, it was demonstrated that cardiac mast cells orchestrate ventricular fibrosis through the secretion of cytokines in response to

hypertension. Increased level of IL4, for example, was reported in spontaneously hypertensive rats, and stabilization of mast cells in these animals was shown to neutralize myocardial IL4 levels and protect against cardiac fibrosis development (Levick et al., 2009). Kanellakis et al. confirmed the pro-fibrotic effect of IL4 in adult hearts and suggested a causal relationship between IL4 and cardiac fibrotic remodeling in hypertension using mice with aortic coarctation. Neutralization of IL4 was shown to mitigate left ventricular fibrosis in pressure-overloaded hearts (Kanellakis et al., 2012). Recently, this possible causal role of IL4 in cardiac fibrotic remodeling was further supported by using IL4 knockout mice, which exhibit blunted cardiac fibrosis. Accordingly, IL4 deficiency prevented the development of dilated cardiomyopathy in response to AngII-induced hypertension (Peng et al., 2015). In addition to cardiac fibrotic remodeling during disease pathogenesis, elevated levels of IL4 were also reported in aging mice during the development of age-associated interstitial cardiac fibrosis (Cieslik et al., 2011).

Despite the detrimental effect of IL4 when acting as a pro-fibrotic factor and contributing to cardiac remodeling in adult hearts, several studies proposed that IL4 can exert cardioprotective function under some conditions. Clinical studies indicated that increased levels of IL4 were associated with reduced risk for incidence of cardiovascular events (Engelbertsen et al., 2013). Lower levels of IL4, for example, were detected in patients with myocardial infarction who later developed left ventricular dysfunction (Szkodzinski et al., 2011). Furthermore, IL4 provides therapeutic benefits through the induction of macrophage polarization towards an anti-inflammatory phenotype in cardiac repair. Following the coronary artery ligation, which mimics the myocardial infarction, administration of IL4 was shown to induce the accumulation of M2-like macrophages in the infarct myocardium and augment cardiac repair and function in adult mice (Shintani et al., 2017).

Even though the evidence up to now suggests contradictory consequences for intricate interactions between IL4 and distinct cardiac resident cell types, depending on the underlying pathological circumstances, a common view seems to be a possible role for IL4 in the events that usually precede pathological cardiac remodeling.

1.7 Hypertension

Another major risk factor for extensive cardiovascular remodeling and HF is hypertension, defined as elevated blood pressure (González et al., 2018). Since initial adaptive remodeling induced by hypertension was reported to vary among patients and animal models, its cardioprotective role in reducing wall stress is still debated (Drazner, 2011). However, it is well-known that hypertension is a chronic condition in which persistent elevated cardiac demand and subsequent alterations lead to maladaptive remodeling and pathological responses inherent to HF (Drazner, 2011). For example, most patients with HF have a history of hypertension. In contrast, it was proposed that risks of developing HF later in life are reduced if hypertension is not present in middle age. (Messerli et al., 2017). In addition to HF, hypertension was reported to precede kidney failure, stroke, and cognitive impairment. Therefore, it is still the strongest risk factor for cardiovascular disease worldwide (Drazner, 2011).

This gateway position of hypertension makes it a critical target to prevent progression into HF. Nevertheless, despite the numerous therapeutic attempts to treat hypertension and/or counteract its progression, there is still no fully effective treatment to attenuate its cardiovascular comorbidities and subsequent end-organ damage (Ghatage et al., 2021). Indeed, a recent comprehensive analysis reported doubled number of hypertensive patients aged between 30-79 years in the last 10 years (Zhou et al., 2021).

The renin (REN) angiotensin system (RAS) is a well-known physiological system that regulates blood pressure by controlling sodium and water absorption. Dysregulated RAS plays a pivotal role in the pathogenesis and progression of hypertension (Te Riet et al., 2015a). Mechanistically, RAS is initiated by regulated secretion of renin from the juxtaglomerular apparatus cells of the kidney to circulation **(Fig. 1.8)**. Renin, in turn, cleaves angiotensinogen (AGT), which is a precursor protein produced in the liver to form angiotensin (Ang) I (Atlas, 2007). Notably, the circulating renin can act on AGT both systemically and locally in specific organs and tissues (Te Riet et al., 2015b). In the classic RAS pathway, angiotensinogen converting enzyme (ACE) mainly produced by vascular endothelial cells hydrolyses AngI to generate AngII, which can bind to AngII type 1 (AT1) and type 2 (AT2) receptors (Atlas, 2007). The binding of AngII to the AT1 receptor increases sodium-water retention, aldosterone and reactive oxygen species (ROS) production, blood pressure, and vasoconstriction. In

contrast, binding AngII to the AT2 receptor leads to vasodilation, counteracting the effect of the AT1 receptor (Paz Ocaranza et al., 2020). Hence, Ang II is widely accepted as the main modulator of the RAS. In addition to the ACE-AngII pathway, accumulating evidence pointed out other alternative pathways in which ACE2 can catalyze the cleavage of both Ang I and Ang II to Ang1-9 to Ang1-7, respectively. Importantly, Ang1-9 binding to Mas receptor and Ang1-7 binding to AT2 receptor result in vasodilation and reduced blood pressure, exerting anti-hypertensive effects. Therefore, this non-canonical RAS action was suggested as a cardioprotective pathway, counterbalancing the effect of AngII (Ghatage et al., 2021; Paz Ocaranza et al., 2020).

The action of AngII leading to pathophysiological events associated with cardiac damage is mainly mediated by the AT1 receptor (Paz Ocaranza et al., 2020). For instance, in addition to induction of blood pressure elevation, AngII acting through the AT1 receptor was shown to promote cardiac hypertrophy (Sadoshima & Izumo, 1993), fibrosis (Schieffer et al., 1994), and inflammation (G. Wolf et al., 2002), which are strongly associated with hypertension. Moreover, Kimura et al. showed that AngII-infused rats exhibit increased cardiac nicotinamide adenine dinucleotide phosphate (NADPH) oxidase activity, resulting in ROS-induced oxidative stress, which plays a critical role in the progression of cardiovascular disease and target organ damage (S. Kimura et al., 2005).

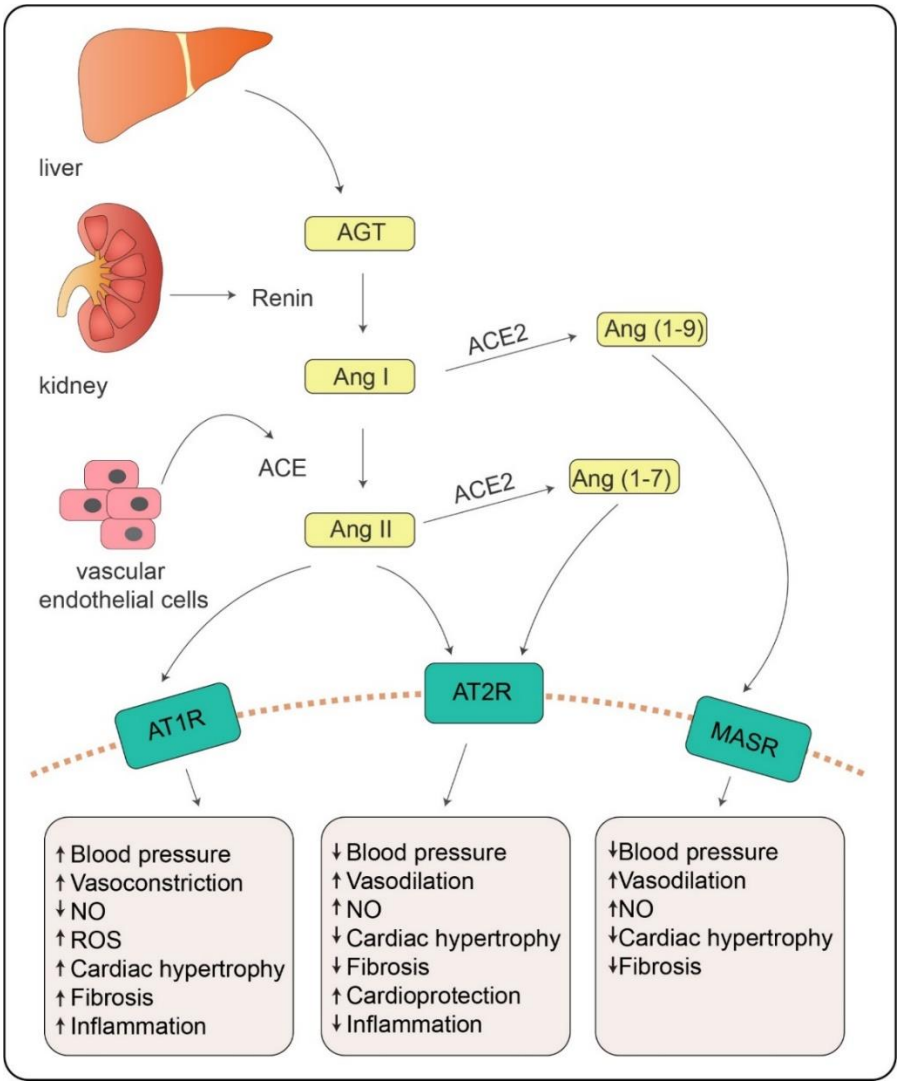

Figure 1.8. RAS. In the classical RAS pathway, renin secreted from the liver cleaves AngI from AGT, which is secreted from the liver. Vascular endothelial cells release ACE, which converts AngI to AngII, which in turn can bind to AT1R and AT2R. Activation of AT1R increases blood pressure, vasoconstriction, ROS, cardiac hypertrophy, fibrosis, and inflammation, whereas it reduces NO production. Signaling through the AT2R antagonizes the effects of AngII-AT1R. In the alternative pathways, Ang I and Ang II can be cleaved by ACE2 to produce Ang (1-9) to Ang (1-7), respectively. Both Ang (1-9) and (Ang1-7) exert cardioprotective and anti-hypertensive effects through binding to MASR and AT2R, respectively. AGT: Angiotensinogen, Ang: Angiotensin, AT1R: AngII type I receptor, AT2R: AngII type II receptor, ACE: angiotensinogen converting enzyme, NO: nitric oxide, ROS: reactive oxygen species.

1.7.1 Hypertensive cardiovascular remodeling

1.7.1.1 Cardiac remodeling in Hypertension

Cardiac remodeling, which frequently accompanies hypertension, occurs as an adaptive response to hemodynamic (i.e., increased wall stress) and nonhemodynamic factors (i.e., altered genotypes, vasculature, cytokines, etc.), which result in pressure or volume overload (Drazner, 2011). Hypertensive cardiac remodeling is the culmination of a complex chain of events, usually including cardiac hypertrophy, cardiomyocyte death, fibrosis, and inflammation (González et al., 2018). The primary response of cardiomyocytes to hypertensive stimuli is hypertrophic growth (Sugden & Clerk, 1998). It was suggested that the molecular alterations in cardiomyocytes during hypertrophic growth may prompt their death (Dickhout et al., 2011). Indeed, increased cardiomyocyte death was reported in hypertensive patients with HF (Ravassa et al., 2007).

Under pressure or volume overload, the heart develops concentric or eccentric hypertrophy, respectively, as a compensation mechanism **(Fig. 1.9).** High blood pressure results in elevated left ventricle wall stress, which is the tension in individual myocardial fibers. To normalize wall stress, the left ventricle increases wall thickness (with no reduction in chamber volume) and mass. This structural change is termed concentric hypertrophy. If the high blood pressure persists, hypertension progresses, and compensated hypertrophy transits into functional decompensation, leading to HFpEF. On the other hand, in the presence of volume overload, the heart develops eccentric hypertrophy, which is characterized by dilation of left ventricular chamber, ultimately leading to HFrEF (Messerli et al., 2017; Nadruz, 2015).

The classical view of hypertensive cardiac remodeling was proposed as concentric hypertrophy (Drazner, 2011). However, recent evidence showed that some patients with hypertension developed concentric hypertrophy while others exhibited eccentric hypertrophy (Cuspidi et al., 2012). Although the underlying reason for distinct cardiac remodeling patterns observed in hypertensive patients is still uncertain, it was proposed that different pathways might be involved in the progression of cardiac remodeling among patients due to the multifactorial nature of hypertension (Nadruz, 2015).

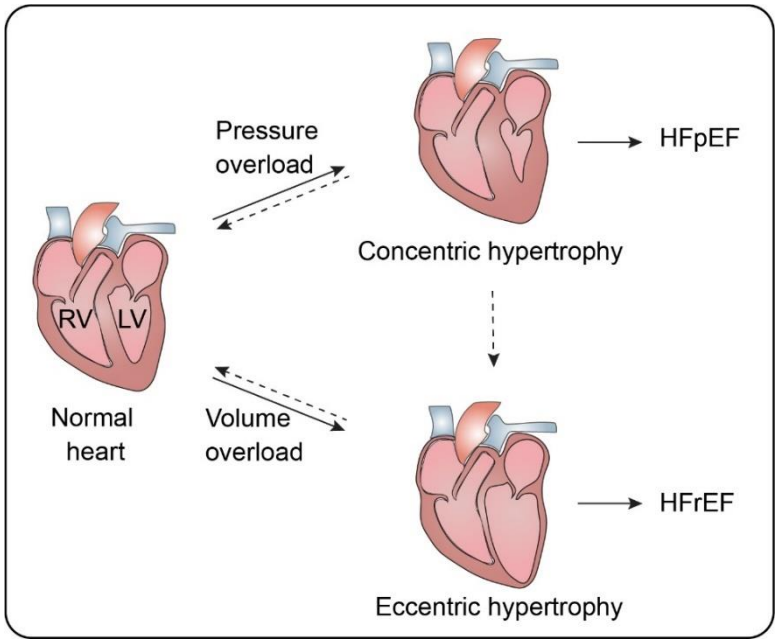

Figure 1.9. Progression from hypertension to HF. In response to various stimuli, left ventricle mass can increase from either wall thickening or chamber dilation. In the presence of pressure overload, the wall thickness of the left ventricle increases, resulting in concentric hypertrophy. Volume overload cause dilation in the left ventricular chamber, resulting in eccentric hypertrophy. Hypertensive stimuli can induce both eccentric and concentric hypertrophy. Patients with concentric hypertrophy can develop HFpEF, whereas patients with eccentric hypertrophy can develop HFrEF. RV: Right ventricle, LV: left ventricle. HFpEF: Heart failure with preserved ejection fraction, HFrEF: Heart failure with reduced ejection fraction.

1.7.1.2 Vascular remodeling in Hypertension

Under physiological conditions, vascular networks undergo structural alterations to establish functional and mature vasculature as well as to maintain blood flow homeostasis. This adaptive process involves cell growth, cell death, vessel pruning, and regression as well as ECM remodeling. It should be noted that vascular remodeling may involve all or some of these events depending on distinct physiological conditions and vascular beds (Korn & Augustin, 2015; Lyle & Taylor, 2019). In zebrafish, for instance, developmental vessel pruning and regression involving dynamic endothelial cell rearrangements were shown in the trunk and brain (Q. Chen et al., 2012; Franco et al., 2015; Lenard et al., 2015). In a pathological condition like hypertension, adaptive rearrangements lead to pathological vascular remodeling (Lyle & Taylor, 2019). Moreover, inflammation, apoptosis, endothelial dysfunction, and fibrosis are the other key events that were suggested to partake in these pathological vascular changes in hypertension (Rok Humar et al., 2005). However, the cause-and-effect relationship between the chain of events and hypertension is still debated.

1. INTRODUCTION

Vascular remodeling mostly emerges in hypertension and contributes to the progression of the disease. Particularly, microvascular regression, which is the loss of terminal arterioles and capillaries, was suggested to be one of the hallmarks of hypertension (R. Humar et al., 2009). For example, hypertensive rat models generated through surgical reduction of renal mass and exposure to the high-salt diet exhibited rapid microvascular rarefaction within a few days (Hansen-Smith et al., 1996). Furthermore, a reduction in the density of microvessels in several vascular beds, including skin, skeletal muscle, retina, and brain, was reported in hypertensive patients as well as animal models (Henrich et al., 1988; Serné et al., 2001; Sokolova et al., 1985; S. Wolf et al., 1994). Importantly, microcirculation is required for tissue perfusion enabling the exchange of nutrients and waste between blood and tissues to keep the tissues and organs healthy. Microvascular malformations leading to poor perfusion were proposed as a critical factor worsening the hypertension progression and contributing to target organ dysfunction (Levy et al., 2008). In microvessels, endothelial cell apoptosis, the process of programmed cell death, was suggested as the main mechanism of vascular remodeling under some conditions. Previous studies reported expanded endothelial cell apoptosis during microvascular rarefaction in hypertensive rat models (Kobayashi et al., 2005; Vega et al., 1999; Vogt et al., 2001).

The endothelial function has been viewed as a central factor in vascular remodeling. In physiological condition, endothelial cells secrete distinct vasodilation and vasoconstriction factors to maintain homeostasis. For instance, blood flow and shear stress promote nitric oxide (NO) production in endothelial cells as a vasodilation factor (Van Varik et al., 2012). NO affects contraction and relaxation of vascular smooth muscle cells, thereby regulating vessel tone and diameter. Hence, NO is an essential signaling molecule for endothelial health (Napoli & Ignarro, 2009). Previous studies showed that NO modulates vascular tone in developing zebrafish, as seen in humans (Pelster et al., 2005). Moreover, mice lacking endothelial NO synthase (eNOS) exhibited hypertensive characteristics with endothelial dysfunction (V. W. T. Liu & Huang, 2008). While physiological shear stress increases the abundance of eNOS (Napoli & Ignarro, 2009), in pathological conditions like hypertension, eNOS contributes to the elevated production of ROS, which inhibits NO activity (Higashi et al., 2012). Indeed, excessive ROS production was documented in hypertensive patients as well as animal models (Cai & Harrison, 2000; Dijkhorst-Oei et al., 1999). On top of that, it is known that high blood pressure causes augmented mechanical vascular wall stress. Taken together, growing evidence

indicates that altered blood flow, shear stress, and ROS imbalance promote endothelial dysfunction indicated by reduced NO bioavailability and increased oxidative stress, vasoconstriction, and pro-inflammatory factors in response to hypertension. (Higashi et al., 2012; Van Varik et al., 2012). However, it should be noted that since oxidative stress and inflammation can initiate and modulate each other, establishing causality between them remains challenging.

1.7.2 Dysregulated Immune Activity In Hypertension

The immune system is one of the pivotal mediators of hypertension pathogenesis and end-organ damage. Low-grade inflammation is involved in the initiation and maintenance of blood pressure elevation. It was postulated that a modest increase in blood pressure induced by hypertensive stimuli such as AngII may lead to tissue injury and oxidative damage, thereby inducing the production of danger-associated molecular patterns (DAMPs) and neo-antigens when the hypertensive stimuli persist over time. DAMPs and neoantigens, in turn, stimulate innate immune cells to secrete pro-inflammatory cytokines and to further activate adaptive immune cells. (Drummond et al., 2019; Harrison et al., 2010). It was proposed that activated immune cells infiltrate into different tissues, such as the kidney, heart, vessels, and brain, where they stimulate oxidative stress and chronic inflammation. In turn, oxidative stress and inflammatory response cause a further increase in blood pressure, subsequently leading to target organ remodeling, including fibrosis, vessel stiffening and regression, cardiac hypertrophy and dysfunction, and cognitive impairment (Harrison et al., 2010; Norlander et al., 2018). Also, elevated levels of inflammatory markers such as C-Reactive Protein, IL1β, IL17, TNFα, IL6 were detected in patients with hypertension (Bautista et al., 2005; De Ciuceis et al., 2017; Dörffel et al., 1999). Furthermore, the attenuated hypertensive response was documented in $IL17^{-/-}$ (Madhur et al., 2010), $TNF\alpha^{-/-}$ (Sriramula et al., 2008) or $IL6^{-/-}$ (D. L. Lee et al., 2006) mice in response to AngII infusion or $IFN\gamma^{-/-}$ mice (Garcia et al., 2012) in response to aldosterone infusion.

The role of lymphocyte infiltration in the pathogenesis of hypertension was shown by loss of function studies using *Rag1*$^{-/-}$ rodent models. Guzik et al. reported that vascular infiltration of T cells contributes to blood pressure elevation, vascular oxidative stress, and dysfunction in mice with AngII or DOCA-salt hypertension. Interestingly, Rag1 deficient mice

exhibited blunted hypertensive response induced with either Ang II infusion or DOCA-salt. Accordingly, they noted that AngII-mediated hypertensive response was recovered by the adoptive transfer of T cells but not B cells in *Rag1*$^{-/-}$ mice (Guzik et al., 2007). In consistent with these results, attenuated hypertensive responses were also observed in Rag1 mutant Dahl SS rats in response to salt-induced hypertension (Mattson et al., 2013). Likewise, another study also reported that severe combined immunodeficient (SCID) mice were protected from Ang II-induced hypertension (Crowley et al., 2010).

In addition to adaptive immune cells, several studies suggested that innate immune cells, particularly monocytes/macrophages, play significant roles in hypertension pathogenesis. Macrophages are known to be the most widely available and dispersed innate immune cells, proposed to be critical intermediaries in tissues and organs targeted in hypertension (Harwani, 2018). Indeed, previous studies showed that deficiency of these cells protects rodent models against experimental hypertension, highlighting their contribution to the pathogenesis of hypertension. For example, mice harboring a mutation in the gene encoding the macrophage colony-stimulating factor (m-CSF), leading to macrophage deficiency, showed mitigated hypertensive response, including attenuated blood pressure elevation, vascular remodeling, endothelial dysfunction, and vascular inflammation in hypertension induced by Ang II (De Ciuceis et al., 2005) and DOCA-salt (Ko et al., 2007). These findings were extended by another study using the Cre-Lox system to induce diphtheria toxin receptors in lysozyme M (LysM)$^{+}$ myelomonocytic cells in mice. Selective ablation of LysM^{+} cells by low dose diphtheria toxin prevented AngII-induced blood pressure rise and vascular dysfunction in mice. Notably, reconstituting these mice with monocytes restored hypertensive responses caused by Ang II (Wenzel et al., 2011). Furthermore, depletion of perivascular macrophages in the brain was shown to attenuate vascular oxidative stress and ameliorates cerebrovascular and cognitive dysfunction in a mouse model of hypertension (Faraco et al., 2016). Recently, it was reported that elevated IL10 production from macrophages in the heart results in cardiac fibrosis and diastolic dysfunction in a hypertensive mouse model (Hulsmans et al., 2018).

1.8 Zebrafish as a Model Organism For Cardiovascular Research

The zebrafish, *Danio rerio,* is a small freshwater fish belonging to the family of cyprinidae. In the 1980s, George Streisinger reported several characteristics of the zebrafish,

such as external fertilization, optical translucency during early development, small size in adulthood (3-5 cm), short generation time (2-3 months), and production of large clutches of embryos (200-300 eggs per week), which can facilitate large-scale forward genetic screens in a vertebrate model (Chakrabarti et al., 1983; Grunwald & Streisinger, 1992; Streisinger et al., 1981). Due to these characteristics, he proposed the usage of zebrafish as a laboratory model to study early development. It is advantageous that zebrafish exhibit very fast organogenesis. The fertilized egg reaches the embryonic stage where the heart tube starts to contract by 24 hpf. The embryo starts to hatch around 2 days post fertilization (dpf) and develops into larvae by 3 dpf. Within 3 dpf, zebrafish develop most of the primary organs, such as heart, liver, and nervous system (Poon & Brand, 2013). On top of this, the zebrafish genome is fully sequenced. Remarkably, approximately 70% of human genes have at least one orthologue in the zebrafish genome, and 82% of disease genes identified in humans are also present in the zebrafish genome (Howe et al., 2013).

External development of zebrafish embryos enables effortless visualization and manipulation during development. Furthermore, the optical translucency of zebrafish embryos offers the significant advantage of identifying cellular behaviors during the early stages of development in live animals. The ability to perform live imaging of the embryonic heart at the cellular level in physiological or pathological condition is crucial to gain better insights into the dynamic process and cellular interactions orchestrating cardiovascular development and remodeling. Furthermore, the external development of zebrafish streamlines chemical administration. Most small molecules can be diluted into fish water as they can directly diffuse into zebrafish. Alternatively, they can be injected into zebrafish at the desired developmental stage (Cassar et al., 2020; Kaufman et al., 2009). These advantages of zebrafish not only provide a robust and affordable test platform for therapeutic approaches but also facilitate the establishment of novel models for studying cardiovascular disease by simple manipulations. Several advantages of zebrafish, including external development, optical translucency, and genetic tractability, put zebrafish in a highly favorable position as a powerful model organism at the forefront of cardiovascular research.

1.9 Aim of the Thesis

Cardiovascular disease is still the leading cause of death, and there is an urgent need for novel and efficient therapeutic approaches. However, due to complex, multi-system events governing cardiovascular development and remodeling, underlying mechanism are still not fully elucidated. It is becoming clear that the immune system, including immune cells and molecules secreted from them, contributes to a wide range of physiological and pathological events in the heart. Particularly, cytokines serving as molecular messengers between cells not only play a significant role in the modulation of the immune response, but also participate in organ development and function. In line with this notion, the dysregulated immune system was proposed as one of the underlying mechanisms of cardiovascular remodeling. Furthermore, aberrant cytokine activity was implicated in various cardiovascular diseases. In a condition like stress and sodium retention, dysregulated immune response contributes to adverse cardiovascular remodeling, ultimately leading to HF. Even though a plethora of studies are trying to shed light on the mechanism behind pathological cardiac remodeling, it is still necessary to investigate and gain further insight into stress and hypertension pathogenesis to prevent the transition from adverse cardiovascular remodeling into HF. Therefore, the general aim of the study was to investigate cardiac remodeling and development to improve our comprehension of disease pathogenesis leading to potentially more effective treatment options. To achieve the main goal of the project, this dissertation is divided into two parts based on the specific aims presented below

Part-1: Early life stress experience predisposes the cardiovascular system to pathologic remodeling in adulthood. How stress increases susceptibility to cardiovascular diseases like HF remains to be elucidated. Apart from their well-characterized function in the orchestration of stress response, GCs are known to elicit pleiotropic function in the immune system and regulate the expression of various cytokines such as IL4 in certain cells under some conditions. On top of that, IL4 was shown to be inversely correlated with stress/anxiety disorders which prompts an intriguing hypothesis that IL4 might play a role in the stress response of the developing heart through its antagonistic effect on GR signaling. Previous studies implied IL4 as a pro-fibrotic factor, and its deficiency prevents pathologic cardiac remodeling in pressure-overloaded hearts. However, given the pleiotropic effect of IL4 on different cells, we still lack a complete understanding of its actions in non-immune organs. In particular, the role of IL4 in

the development and maintenance of cardiac tissue homeostasis, regardless of any stressors, is still elusive. In the first part, therefore, my objective was to

1. Investigate how stress experienced in early life influence cardiac development and what are the cellular and molecular mechanism underlying pathologic cardiac remodeling in response to stress.
2. Uncover the possible interaction between IL4 and stress signaling during cardiac development
3. Elucidate the role of IL4 signaling in the developing heart

In the first part, zebrafish and mouse models as well as cell culture models, were utilized to achieve the goals described above in order to identify a potential target in the stress regulatory pathway for therapeutic interventions in early life before the onset of cardiovascular disease.

Part-2: Cardiovascular remodeling is a complex process and involves a series of events that require crosstalk of various signaling pathways and interaction of different organs. Pathological cardiovascular remodeling is often implicated in hypertension, one of the strongest risk factors for HF. Despite decades of scrutiny, due to the complex nature of hypertension, along with its systemic detrimental effects, the precise mechanisms of the initiation and progression as well as its transition into cardiovascular disease remains to be illuminated. Aberrant immune cell activation and subsequent inflammation were proposed as critical factors governing cardiovascular structural and functional alterations in the pathogenesis of hypertension. However, the cause-and-effect relationship of inflammation with hypertension and its related comorbidities is still debated. Although several anti-inflammatory therapies have been launched to prevent the progression of hypertension and the development of HF, their efficacy is still questionable. In addition to immune-targeted therapeutic interventions, non-immune approaches such as RAS blockers have been used for a long time; however, over half of the patients do not respond to any of those therapies. Therefore, there is still an urgent need for novel therapeutic approaches for patients with hypertension. One of the major bottlenecks for this is the lack of a comprehensive hypertension model that can recapitulate key aspects of the disease process characterized in humans. In the second part of this dissertation, I aimed to establish a zebrafish model of ion imbalance as a hypertension model in order to

1. Reveal cellular processes underlying immune cell-driven end organ damage
2. Identify the molecular mediators of the cellular events
3. Examine the manipulation of the identified pathway(s) to prevent or reverse the progression of hypertension

2 Materials and Methods

2.1 Materials

2.1.1 Laboratory devices

	SUPPLIER	CAT NUMBER
Agarose Gel Chamber	Thermo Scientific	Owl Easycast B1
Bacteria Incubator	Infors HT	-
Cell Culture Incubator	Binder	CB210
Centrifuge	Eppendorf	5417R
Confocal Microscope LSM 800	Zeiss	LSM 800
Electrophoresis Power Supply	BioRad	PowerPac Basic
Fluorescence-Activated Cell Sorting (FACS)	BD Biosciences	Aria II
Fluorescent Microscope	Olympus	SZX16
Heating Block	Eppendorf	5382000015
High-Speed Camera	Ximea	MQ003-MG-CM
Incubator Zebrafish	Velp Scientifica	FOC215L
Incubator 37°C	LLG Labware	uni INCU 20
Magnetic Stirrer	VWR	VMS-C7
Magnetic Stir Bar	Carl Roth	X171.1
Microscale	Fisher Scientific	PAS214
Microinjector	World Precision Instr.	PV820
Microinjection Molds	MDC, self-made	-
Microwave	Exquisit	-
Mini Centrifuge	Santa Cruz	-
Mini Vortex	Carl Roth	HXH6.1
Nano Drop / Photometer	Eppendorf	D30
Needle Puller	Narishige	PC-100
Pipette 10, 100, 200, and 1000 µl	Eppendorf	Research Plus
Pipetboy	Integra	Acu 2
PCR Machine	Eppendorf	6337000019
Ph-Meter	Mettler-Toledo	Five Easy
Real-Time PCR Machine	Thermo Fisher	Step One Plus
Shaker (Rotator)	Stuart	SRT6
Stereomicroscope	Leica	S6
Thermo Block	Eppendorf	5382000015
Transmitted Light Microscope	Zeiss	Axiovert 40CFL

Uv Transilluminator	Alpha Imager HP	-
Vortex Device	Grant Bio	PV-1
Water Bath	GFL	11347017J
Weighing Balance	Kern	EW4200

2.1.2 Laboratory materials

	SUPPLIER	CAT NUMBER
Adhesive Film-25 covers	LIFE Technologies	4360954
Bacterial culture tubes	TPP	352059
Cell Strainer 40µm	Neolab	352340
Centrifuge tubes (15 and 50 ml)	TPP	91015, 91050
Flow cytometry tubes	Falcon	352058
Forceps	Dumont	-
Gauge needle	B.Braun	4657705
Glass Capillaries	Science Products	GB120F-8P
Microcentrifuge tubes (1.5 and 2 ml)	Sarstedt	72.706.400, 72.695.400
qPCR plates (Fast Optical 96-Well Reaction Plate)	Life Technologies	4346907
Pellet Pestle, 1.5 ml	Fisher Scientific	11872913
Petri dish (35, 60, and 100 mm)	Sarstedt	82.1135.500, 83.3901, 82.1473
Plastic pipette 3 mL	Pastette	LW4111
PCR tubes	Sarstedt	72.991.002
pellet pestle	Fisher Scientific	11872913
pellet pestle gun	Fisher Scientific	12-141-361
Pipette tips (10, 200, and 1000 µl)	Sarstedt	701130, 70.760.002, 70.1186
Serological pipette tips (10 and 25 ml)	Sarstedt	86.1254.001, 86.1685.001
Syringes	B.Braun	9161406V

2.1.3 Solutions and Buffers

30x Danieau's medium

Reagent	Final concentration	Amount
NaCl	1740 mM	101,7 g
KCl	21 mM	1,56 g
MgSO4	12 mM	2,96 g
Ca(NO3)2	18 mM	4,25 g
HEPES	150 mM	35,75 g
MilliQ H_2O		Add to 1 L
Total		1 L

1x PTU

Reagent	Final concentration	Amount
N-Phenylthiourea (PTU)	0.003%	30 mg
1x Danieau's medium	1x	Add to 1 L
Total		1 L

1:750 Ion-Poor Solution

Reagent	Final concentration	Amount
1x Danieau's medium	1:750	1333 µl
MilliQ H2O		Add to 1 L
Total		1 L

1:1500 Ion-Poor Solution

Reagent	Final concentration	Amount
1x Danieau's medium	1:1500	667 µl
MilliQ H2O		Add to 1 L
Total		1 L

1xPBS

Reagent	Final concentration	Amount
PBS	1x	5 tablets
MilliQ H2O		Add to 1 L
Total		1 L

1xPBST

Reagent	Final concentration	Amount
1xPBS	1x	Add to 500 mL
Triton X 100	0.3%	1.5 ml
Total		500 ml

4% PFA/PBT

Reagent	Final concentration	Amount
1xPBT	1x	30 ml
PFA 16%	4%	10 ml
Total		40 ml

10 % KOH

Reagent	Final concentration	Amount
KOH 10%	10 %	10g
MilliQ H_2O		Add to 100 ml
Total		100 ml

Bleaching solution

Reagent	Final concentration	Amount
H_2O_2 30%	3%	100 µl
KOH 10%	0.5%	50 µl
PBT	1x	850 µl
Total		1 ml

Tricaine

Reagent	Final concentration	Amount
Tricaine	4 mg/mL	2 g
1x Danieau’s medium	1x	Add to 500 ml
Total		500 mL

2 % agarose

Reagent	Final concentration	Amount
Agarose, NEEO	2%	2 g
MilliQ H_2O	1x	Add to 100 ml
Total		100 mL

Immunostaining blocking solution

Reagent	Final concentration	Amount
Goat serum	5%	500 µl
BSA	1%	0,1 g
DMSO	1%	100 µl
PBST	1%	Add to 10 ml
Total	1x	10 ml

Hybridization Buffer

Reagent	Final concentration	Amount
Formamide	50% formamide	25ml
20 X SSC	5X SSC	12,5 ml
Heparin 5 mg/ml	50µg/ml	0.5 ml
tRNA 50 mg/ml	500µg/ml	0.5 ml
Tween 20 (20%)	0.1 %	0.25 ml
Acide citrique 1M		0.46 ml
water		To 50 ml

2.1.4 Chemicals and Reagents

	SUPPLIER	CAT NUMBER
4-hydroxytamoxifen (4-OHT)	Sigma	H7904
Acetic Acid	Carl Roth	6755.1
Agarose, Low Melting Point	Sigma	A4018
Agarose NEEO Ultra Qualität	Carl Roth	2267.3
Anti-Digoxigenin- AP Fab fragments	Roche	11093274910
Ampicillin	Sigma	A9518
Bacterial LB Agar	Carl Roth	X969.2
Bacterial LB Medium	Carl Roth	964.2
Bovine Serum Albumin	Serva	11943.02
Calcium Nitrate ($Ca(NO_3)_2$)	Honeywell	C1396
Chloroform	Fisher Chemical	C/4960/15

Citric acid	Serva	38640
Dexamethasone	Sigma	D1756
Dexamethasone- Suitable for cell culture	Sigma	D4902
Dimethyl Sulfoxide (DMSO)	Th. Geyer	23419.3
Dream*Taq* DNA Polymerase	Life Technologies	K1082
DNaseI	Roche	10104159001
Dulbecco's Modified Eagle Medium, high glucose, GlutaMAX	GIBCO	31966021
Ethanol	Carl Roth	9065.2
5-Ethynyl-2′-deoxyuridine (EdU)	Santa Cruz	sc-284628
Fetal Bovine Serum	GIBCO	10270106
Fibronectin Bovine Protein, Plasma	Thermo Fisher	33010-018
Fluoromount Aqueous Mounting Medium	Sigma	F4680
Formaldehyde 16% (W/V)	VWR International	PIER28908
Formamide	Thermo Fisher	17899
Gel Red Nucleic Acid Stain	Linaris	41003
GeneRuler 1kb DNA Ladder	Thermo Fisher	SM0311
Glycogen	Serva,	23550
Goat serum	Sigma	G6767
HBSS	LIFE Technologies	14175095
Heparin	Sigma	H3393-100KU
Hydrochloric Acid (HCl)	Sigma	H1758
Hydrogen Peroxide (H2O2) 30%	ChemCruz	sc-203336A
HEPES	Carl Roth	9105.4
Isopropanol	Carl Roth	7343.2
Liberase TL Research Grade	Roche	5401020001
Loading Dye (Orange G)	Carl Roth	0318.2
Magnesium Sulfate (MgSO4)	ChemCruz	sc-211764
Master Mix Taq 2x	New England Biolabs	M0270
Methanol	Roth	4627.1
Mifepristone	Sigma	M8046
N-Phenylthiourea (PTU)	Sigma	P7629
Penicillin-Streptomycin (10.000 U/ml)	Thermo Fisher	15140122
Paraformaldehyde (PFA)	Sigma	P6148
Phenol/Chloroform/Isoamyl alcohol	Roth	A156.2
Phenol Red	Sigma	P0290
Phosphate-Buffered Saline (PBS)	Sigma	P4417
Phusion High-Fidelity DNA Polymerase	Life Technologies	F530L
Pluron F-68 polyol, 100 ml	MP Biomedicals	092750049
Potassium Chloride (KCl)	ChemCruz	sc-203207
Potassium Hydroxide (KOH)	Alfa Aesar	A16199

Pronase	Roche	11459643001
Proteinase K	Sigma	3115879001
Recombinant Murine IL4	PeproTech	214-14
Ribonucleic acid from torula yeast	Sigma	R6625
RNase H	Life Technologies	EN0201
SOC-Medium	New England Biolabs	B9020S
Sodium Acetate	Calbiochem	567418-500GM
Sodium Chloride (NaCl)	Serva	39781.02
SYBR Safe DNA Gel Staining Solution	Life Technologies	S33102
T4 Ligase	New England Biolabs	B0202S
O.C.T Compound	Sakura Tissue Tek	4583
Tricaine (3-amino benzoic acidethylester)	MDC Facility	-
Tris	Sigma	T1503
TRIzol	Life Technologies	15596026
Trypsin	GIBCO	15090046
Trypsin-EDTA	Sigma	T4049
Triton X 100	Carl Roth	3051.3
Trizma hydrochloride	Sigma	T2694
Tween 20	Santa Cruz	SC-29113
Water H2O RNase/DNase free	LIFE Technologies	R0581
Wheat Germ Agglutinin-Conjugated CF555	Biotium	29076-1

2.1.5 Critical Commercials/Kits

	SUPPLIER	CAT NUMBER
Cold Fusion Cloning Kit	System Biosciences	MC010A-1
Click-iT™ EdU imaging kit	Thermo Fisher	C10640
Click-iT TUNEL Alexa Fluor 647	Thermo Fisher	C10247
Cold Fusion Cloning Kit	System Biosciences	MC010A-1
Fast Red TR/Naphthol AS-MX	Sigma	F4648
Phusion High-Fidelity PCR Kit	Life Technologies	F553L
Luna Universal qPCR Master Mix	New England BioLabs	M3003
mMESSAGE mMACHINE	Life Technologies	AM1340
NucleoSpin Gel and PCR Clean-up	Macherey-Nagel	740609.250
NucleoSpin Plasmid kit	Macherey-Nagel	740588.250
SMART-Seq HT kit	TaKaRa	634455
SuperScript III First Strand Kit	Life Technologies	18080051

2.1.6 Antibodies

	SUPPLIER	CAT NUMBER
Monoclonal Mouse Anti-Human IL4	R&D systems	MAB204
Monoclonal Mouse 6X-HIS	Invitrogen	MA1-21315
Polyclonal Chick Anti-GFP	Thermo Fisher	A10262
Polyclonal Rabbit RFP	MBL	PM005
Monoclonal Mouse Anti-Proliferating Cell Nuclear Antigen (PCNA)	Dako	M0879
Monoclonal Mouse Anti Cardiac Troponin T2	Abcam	AB33589
Polyclonal Rabbit Anti-Ki-67 Antibody	Millipore	AB9260
Monoclonal Rat Anti-mCherry	Thermo Fisher	M11217
Monoclonal Mouse Anti-Interferon Gamma	Abcam	AB211784
Monoclonal Mouse anti-V5	ThermoFisher	R960-25
Alexa Fluor 488 Anti-chicken	Thermo Fisher	A10262
Alexa Fluor 647 Anti-mouse	Cell Signaling	4410S
Alexa Fluor 555 Anti-rabbit	Cell Signaling	4413
Alexa Fluor 488 Anti-rabbit	Cell Signaling	4412
Alexa Fluor 488 Anti-mouse	Cell Signaling	4408S
Alexa Fluor 555 Anti-rat	Cell Signaling	4417

2.1.7 RT-PCR Primers

	Forward primer	**Reverse primer**
agt	GGGCTCTGATGCCAGTTTTA	CGTCATCTCAAACACCACCTT
bcl2l1	GCAGATTGTGTTATGGGTATGAGC	GGTTGCAGGGGTAGTTCCTC
c-myc	GGCAGCGATTCAGAAGATGAAG	CCGTCTCGTGCCTTTTCTGT
cyclinD1	GCCAAACTGCCTATACATCAG	TGTCGGTGCTTTTCAGGTAC
gapdh	GTGGAGTCTACTGGTGTCTTC	GTGCAGGAGGCATTGCTTACA
ifng1	AAGATTCTCAGCTACATAATGCACACC	ATGCTCATCAGTAGATTCTGCTCAC
il1b	TGGACTTCGCAGCACAAAATG	CACTTCACGCTCTTGGATGA
il4	CTGTTGGTACTTACATTGGTCCCC	AGTGTCCTGTCTCATATATGTCAGGT
il4r	AGCAGCCAGCAGACTGAAAT	ATGGGATCGTCACAAAGTGCT

il6	ATGACGGCATTTGAAGGGGT	CGCGTTAGACATCTTTCCGTG
il10	TCACGTCATGAACGAGATCC	CCTCTTGCATTTCACCATATCC
il12	GAAACTCAACTGACCTCAACTG	CTTTATCTGGCTTGACAATGTCTC
il13ra1	GCATGTCAGAGCTTCCTCCG	AGACCTTGTTGGTGGCAACT
il13ra2	GAGCGATGGAGGAGTGTTCG	ATTGGTACAGGCGCACTTCA
ren	ATGCTTCTGGAAATGTCCGG	TGCCGGAAGAGCTGTGGCTT
socs1a	GCGCTCTGAGGAAACCTCTA	GAGACTCATCGGTCGTTTTAGT
stat3	GGACTTCCCGGACAGTGAG	ATCGCTTGTGTTGCCAGAG
tnfa	AAGGAGAGTTGCCTTTACCG	ATTGCCCTGGGTCTTATGG

2.1.8 Softwares

	ORIGIN	IDENTIFIER
Fiji/ImageJ	NIH	https://fiji.sc/
Imaris	Oxford Instruments	https://imaris.oxinst.com/
Prism	GraphPad Software	https://www.graphpad.com/scientific-software/prism/
FlowJo	BD (Becton, Disckinson & Company)	https://www.flowjo.com/solutions/flowjo
Matlab	The MathWorks	https://www.mathworks.com/products/ matlab.html
ZEN software	Zeiss	

2.2 Methods

2.2.1 Animal care and strains

Zebrafish maintenance

Zebrafish were maintained under standard conditions in accordance with institutional (Max Delbruck Center for Molecular Medicine), State (LAGeSo Berlin), and German ethical and animal welfare guidelines. Briefly, zebrafish embryos were collected and raised until 5 dpf in Danieau's solution in an incubator at 28,5 ºC. Afterward, the larvae were transferred to an aquarium tank system and raised until desired age with light-dark cycle of 14h light and 10h of dark. For live imaging experiments, 1-phenyl-2-thiourea (PTU) was added to Danieau's solution (0.003% (w/v)) starting from 1 dpf to block the skin pigmentation of embryos. If necessary, chorion was removed by adding 1 mg/ml of pronase to 1dpf embryos in the petri dish overnight, and then the solution of embryos was changed the next day. All zebrafish experiments were performed on larvae up to 7 dpf.

Transgenic lines used in this study are:

- Tg(myl7:MKATE-CAAX)^{sd11} (Lin et al., 2012),
- Tg(myl7:H2B-GFP)^{zf521} (Mickoleit et al., 2014),
- TgBAC(csf1ra:GAL4-VP16)^{i186} (Gray et al., 2011),
- Tg(UAS-E1B:NTR-mCherry)^{c264} (Davison et al., 2007),
- Tg(5xUAS:EGFP)^{zf82} (Asakawa et al., 2008),
- Tg(kdrl:Hsa.HRAS-mCherry)^{s896} (Chi et al., 2008),
- *Tg(myl7:GFP)^{f1}* (Geoffrey Burns et al., 2005),
- Tg(kdrl:EGFP)^{s843} (Beis et al., 2005),
- Tg(myl7:Cre-ERT2)^{pd12} (Kikuchi et al., 2010),
- Tg(myl7:GAL4)^{s740} (Sawamiphak et al., 2017),
- Tg(actb2:loxP-DsRed-loxP-dnstat3EGFP)^{s928} (Fang et al., 2013),
- Tg(fli:nls-mcherry)^{ubs10} (Heckel et al., 2015),
- Tg(wt1b:EGFP)^{li1} (Perner et al., 2007).

2.2.2 Microinjections in zebrafish embryos

2% agarose dissolved in Danieau's solution by heating in a microwave was used for the preparation of injection plates. Agarose solution was poured into a 10 cm Petri dish, and a special mold with lanes was placed on the agarose solution. After it solidified, the mold was removed. Then, the injection plates were kept at 4 ºC and warmed up at room temperature before injection.

For the setting of the mating up, the male and female zebrafish were placed in a special breeding tank with a transparent separator in the evening. The divider was removed in the next morning, and the eggs were collected from the bottom of the tanks within 20 minutes. Fine-tipped injection needles were prepared from glass capillaries using a needle puller. Next, the injection needle was loaded with an injection mix, and then the tip of the needle was broken using forceps. 1-2-cell stage eggs were aligned in the injection plate, and injection mix was injected into the cell. Injected embryos were kept in fresh Danieau's solution. Embryos were checked under a stereomicroscope in the evening, and unfertilized/dead embryos were removed.

2.2.3 Real-time PCR

Larval Heart dissection

5 dpf larvae expressing GFP under the control of cardiomyocyte-specific myosin light chain 7 (*myl7*) promoter were used to detect the hearts for dissection under the fluorescent microscope. Larvae were anesthetized with 0.016% tricaine, and then hearts were dissected under a fluorescent microscope using forceps in a petri dish. Dissected hearts were immediately transferred into a 1.5 ml tube containing cold PBS on ice. Every 20 min, PBS was removed from collected hearts, and then they were stored in TRIzol reagent at -80°C until usage.

RNA isolation

RNA was isolated from pooled whole zebrafish larvae (n=50) of desired developmental stages or isolated hearts (n=250-300) using TRIzol reagent. Briefly, pooled larvae or hearts

were homogenized with a pellet pestle until the tissue was disrupted. 0.2 volumes of chloroform were added to enable phase separation of RNA from DNA and protein. The upper aqueous phase containing RNA was transferred into a new tube, and 1 volume of isopropanol was added for the precipitation of RNA. After 2 times wash with 75% ethanol, the pellet containing RNA was resuspended in RNase-free water. To remove remaining genomic DNA, samples were treated with 1 unit of DNase I according to the manufacturer's instructions. Then, an equal volume of 1:1 phenol/chloroform was added, and samples were mixed by inverting the tubes. The upper aqueous phase containing RNA was transferred into a new tube, and RNA was precipitated by adding 0.1 volumes of 3M NaOAC and 2-3 volumes of absolute ice-cold ethanol. The pellet was washed twice with ice-cold %70 ethanol and resuspended in RNAse-free water.

cDNA Synthesis

cDNA was obtained using the SuperScript III First Strand Kit according to the manufacturer's instructions. 1-3 µg of RNA was reverse transcribed using oligo(dT), and samples were incubated for 50 min at 50 ºC followed by 5 min at 85 ºC. cDNA samples were stored at -20 ºC until usage.

Real-Time quantitative PCR (RT-qPCR)

All RT-qPCR analyses were performed in triplicates. Primers were designed to bind exon-exon junctions. RT-qPCR was performed using Luna Universal qPCR Master Mix according to the manufacturer's protocol and run on a StepOnePlus Real-Time PCR System. Primers used for qPCR are listed in section 2.1.7. *GapdH* or *actin* was used as endogenous control.

2.2.4 Generation of Transgenic Constructs

myl7:RFP

To generate the myl7:RFP, the *myl7* promoter and the *RFP* gene were amplified and inserted into the pTol2 vector using the Cold Fusion Cloning Kit (System Biosciences).

myl7:il4rΔC-RFP

To generate a zebrafish cDNA library, 5 dpf zebrafish larvae were anesthetized with Tricaine (0.168 mg/ml) and pooled together. Total RNA was isolated with TRIzol reagent, and 1-2 µg of RNA was reverse transcribed using the SuperScript III First Strand Kit as explained. *il4r* lacking the cytoplasmic domain (*il4rΔC*) was PCR amplified from the zebrafish cDNA library. pTol2 vector plasmid containing *myl7 and RFP* gene was digested with NheI and NcoI restriction enzymes, and *il4rΔC* gene was inserted into pTol2 plasmid using *NheI* and *NcoI* cloning sites. Primers used for the cloning were

NheI-kozak-il4r.F: GATTGCTAGCGCCGCCACCATGAAGTTCAATGTTTCGTTT and NcoI-il4rdeltaC.R: GACACCATGGCCAAAAAACAGATGAAGGTCAT.

myl7:mKATE-GR

To generate mKATE-GR, zebrafish GR (zGR) was amplified from the PCS2+zGRa plasmid (Schaaf et al., 2008). mKATE fragment was amplified from the pTol2-UAS-mKATE vector by PCR adding Gly-Gly-Gly-Gly-Ser (G4S) linker sequence to the C-terminus of the mKATE gene with the reverse primer. Then, mKATE-G4S and zGR were cloned into pTol2 vector plasmid using Cold Fusion Cloning Kit.

hsp70l:il4-6XHIS

il4 open reading frame was amplified from the zebrafish cDNA library, which was generated from 54 hpf zebrafish embryos. 6xHIS epitope sequence was added to the C-terminus of *il4* by PCR and then inserted downstream of *hsp70l* promoter in a vector containing a *cryaa:Cerulean* expression cassette and I–SceI recognition sites.

2.2.5 Generation of Transgenic Animals

To generate the *Tg(hsp70l:il4-6XHIS)*^{md74} line, the construct was injected into 1-2-cell stage embryo with I-SceI meganuclease for genomic insertion of the transgene. Injected embryos were sorted for Cerulean expression in the lens using fluorescent microscopy.

Positive embryos were raised to adulthood and then screened for founders. The offspring of identified founders were raised and expanded.

Zebrafish embryos at the 1-2-cell stage were injected either with *myl7:mKATE-GR*, *myl7:il4rΔC-RFP or myl7:RFP* construct. Injected embryos were sorted for mKATE/RFP expression in the heart using fluorescent microscopy and kept in fresh Danieau`s medium until 5 dpf. Live imaging of each positive fish was performed on day 3 and day 5.

2.2.6 Treatments

Stress

4 dpf zebrafish larvae were treated with vibrational stimulus by shaking for 16h with 1h shake at 300 rpm - 1h rest cycles. Control larvae were kept in similar conditions but without a vibration-based stressor. After 16h, larvae were fixed with 4% PFA for 2h at room temperature and kept in 100% methanol at -20 ºC for immunostaining.

Drug

Dexamethasone (dex) and mifepristone (mif) were reconstituted at 20 mg/ml in DMSO. Larvae were bathed with 100 μM dex or 10 μM mif in Danieau's medium, including 0.5% DMSO to increase permeabilization. Control larvae were kept in Danieau's medium with 0.5% DMSO. For morphological and functional analysis, larvae were treated from 2 dpf until 5 dpf. For qPCR analysis, 5 dpf larvae were treated for 2h. Following 2h treatment, whole larvae or hearts dissected from treated larvae were collected immediately and kept in TRIzol at -80 ºC until usage. To assess cardiomyocyte proliferation, 4 dpf larvae were treated for 16h followed by fixation with 4% PFA for 2h at room temperature and kept in 100% methanol at -20 ºC for immunostaining.

4-hydroxytamoxifen (4-OHT) was used to induce Cre-ERT2 expression. 4-OHT was reconstituted at 10mM in ethanol. 1 dpf embryos were bathed with 6 μM 4-OHT in Danieau's medium for 24h in the dark. Then, the drug was removed, and embryos were kept in fresh Danieau's solution until 4 dpf.

Heat-induction

To enable overexpression of *il4-6xHis* expression, embryos carrying *hsp70l:il4-6XHIS* transgene were exposed to 38 ºC in a preheated water bath for 1.5 h. After 1.5h treatment, they were transferred to a fish incubator and maintained in standard conditions. To assess morphological and functional analysis, larvae were heat-shocked daily, starting from 1 dpf until 5 dpf. For qPCR analysis, 5 dpf larvae were exposed to 38 ºC for 1.5 h, followed by 2h recovery. After 2h, hearts from the larvae anesthetized with tricaine were dissected. To assess cardiomyocyte proliferation, 4 dpf larvae were heat shocked for 16h and then fixed with 4% PFA for 2h at room temperature. After fixation, larvae were kept in 100% methanol at -20 ºC for immunostaining.

Ion-poor

Ion-poor solution was prepared by diluting Danieau's solution 750-fold or 1500-fold with deionized water. Eggs were collected and reared in fresh Danieau's solution until 2 dpf. Then, a clutch of embryos was divided into two groups, one of which was subjected to Danieau's solution diluted 750-fold with deionized water while the other group was exposed to standard Danieau's solution. 2 days after treatment, medium of larvae treated with ion-poor solution was changed with fresh Danieau's solution diluted 1500-fold with deionized water and solution of control larvae were replaced with fresh Danieau's solution. Fish were kept until desired age up to 7 dpf.

Neutralizing antibody

Neutralizing antibody for IL4 (IL4-nAB) was reconstituted at 0.5 mg/ml in PBS. 4 dpf zebrafish larvae were anesthetized with tricaine, and 2 nl (10 μg/ml) IL4-nAB was injected intrapericardially. Similarly, an equal amount of anti-6X-HIS antibody in PBS was injected intrapericardially as a control. Injected fish were kept in fresh Danieau's solution for 16h. The next day, larvae were fixed with 4% PFA for 2h at room temperature and kept in 100% methanol at -20 ºC for immunostaining

Anti-Ifnγ and anti-V5 antibodies (for control) were diluted to 150 μg/ml in deionized water. 2 nl of anti-Ifnγ antibody solution was injected into the pericardial sac of 3 dpf or 5 dpf

larvae which were anesthetized with tricaine. The solution of larvae was changed with fresh Danieau's solution or ion-poor solution after injection.

2.2.7 Cardiac Functional Analysis

5 dpf or 7 dpf larvae were embedded in 1% low-melting agarose. 6-10 seconds-long movies of the ventricle and a segment of the dorsal aorta were acquired at 300 frames per second using a transmitted light microscope equipped with a 40X objective and a high-speed camera. To calculate diastolic and systolic speed, ventricular areas at the end of the diastole ($area_{VD}$) and systole ($area_{VS}$) were calculated using Fiji. Changes in the ventricular area between diastole and systole over 4 cycles were calculated during diastole (time change from systole to diastole: $t_{Dcycle2}$-$t_{Scycle1}$) as diastolic speed ($speed_{VD}$) and during systole (time change from diastole to systole: $t_{Dcycle1}$-$t_{Scycle1}$) as systolic speed ($speed_{VS}$) following the equation below:

$$diastolic\ speed = \frac{|\mathrm{areaVDcycle2} - \mathrm{areaVScycle1}|}{\mathrm{tDcycle2} - \mathrm{tScycle1}}$$

$$systolic\ speed = \frac{|\mathrm{areaVScycle1} - \mathrm{areaVDcycle1}|}{\mathrm{tDcycle1} - \mathrm{tScycle1}}$$

The width and length of the ventricle at the end of diastole ($width_{VD}$ and $length_{VD}$) and systole ($width_{VS}$ and $length_{VS}$) were measured using Fiji. Diastolic ventricular volume ($volume_{VD}$) and systolic ventricular volume ($volume_{VS}$) were calculated as:

$$volume\ VD = \frac{\pi \times lengthVD \times width\ VD^2}{6}$$

$$volume\ VS = \frac{\pi \times lengthVS \times width\ VS^2}{6}$$

Then, EF and fractional shortening (FS) were calculated as:

$$EF = 100 \times \frac{(volumeVD - volumeVS)}{volume\ VD}$$

$$FS = 100 \times \frac{(widthVD - widthVS)}{width\ VD}$$

To calculate blood flow velocity, kymograms of blood cell movement in the dorsal aorta were created using the Velocity Measurement Tool in Fiji (http://dev.mri.cnrs.fr/projects/imagej-macros/wiki/Velocity_Measurement_Tool). Then, peak systolic (max) speed and end-diastolic (min) speed were analyzed from kymograms using a Matlab code (Chhatbar et al., 2013). Resistive index (RI) was calculated as:

$$RI = \frac{\max speed - \min speed}{\max speed}$$

2.2.8 Fluorescence- Activated Cell Sorting (FACS)

FACS was performed using *csf1ra:GAL4; UAS:NTR-mCherry* larvae. Whole larvae were dissociated in 0.26 unit/ml Liberase-TL in HBSS solution containing 1x Pluronic F-68 polyol and incubated on a thermomixer at 37ºC for 25-30 minutes at 750 rpm. Every 5 minutes, samples were mixed by pipetting and, at the last mixing, passed through a 20-gauge needle to enhance separation into single cells. Next, 1% BSA in HBSS solution was added to stop dissociation, and samples were centrifuged at 200g for 7 min at 4°C. The pellet was washed with and resuspended in sorting buffer (0.05% BSA in HBSS solution). The single cells were filtered through a 40 μm strainer and then sorted with a FACS Aria II machine. mCherry positive cells (macrophages) were sorted, collected in 250 μl TRIzol, frozen in liquid nitrogen, and then stored at -80°C.

2.2.9 RNA-Sequencing

Total RNA was extracted from FACS-sorted macrophages using TRIzol, as explained above. Samples were submitted to the Sequencing Facility (Genewitz), where the RNA was then processed for next-generation sequencing. Illumina-compatible sequencing libraries were prepared using the SMART-Seq HT kit following the manufacturer's protocol. After quality control of the libraries, they were sequenced by Illumina HiSeq (2x150 bp). Data output was approximately 350M reads per lane. Trimming for removal of adapter sequences was done by Trimmomatic v.0.36. GRCz11 zebrafish transcriptome from Ensembl was used as the reference genome for pseudo-mapping with Kallisto (v0.46.1), and also unique transcript counts were gathered in this step. Tximport (v1.22.0) was used to summarize the transcript level counts to gene counts. In this step, genes with over 10 counts were kept. The batch effect and other possible variations are accounted for using RUVseq v1.28.0 with k=3 setting. Differential expression analysis was done with DESeq2 (v1.34.0), comparing control and ion-poor treated groups. Log2 gold changes and p-values were acquired by the Wald test. Adjusted p-values lower than 0.05 and log2 fold change greater than 1 were set as a threshold to consider the genes as differentially expressed.

2.2.10 Zebrafish Immunofluorescent staining

Antibody Staining

Larvae were anesthetized with tricaine and fixed with 4% PFA + 0.3% triton at 4°C overnight or room temperature for 2h. After washing three times with PBS buffer containing 0.3% (V/V) Triton (PBST), larvae were permeabilized with a 1:20 dilution of Trypsin-EDTA in PBST for 40 min for 5 dpf fish and 45 min for 7 dpf on ice. For antigen retrieval, samples were incubated in 150 mM Tris-HCl (pH 9) at room temperature for 5 min followed by 15 min at 70°C. After blocking larvae with 5% goat serum, 1% BSA, 1% DMSO, and 0.3% Triton X-100 in PBS (blocking solution) for 1h at room temperature, samples were incubated in primary antibody for 3-4 days at 4°C on the rotator followed by three times washing with PBST. Next, secondary antibodies were added to the blocking solution for 2-3 days at 4°C on the rotator. After washing three times with PBST, larvae were mounted in

a fluoromount aqueous mounting medium and imaged with a Zeiss LSM880 NLO confocal microscopy system. Antibodies used in immunostaining are listed in section 2.1.6.

TUNEL staining

Cell death was detected by the TdT-mediated dUTP Nick-End Labeling (TUNEL) technique using a Click-iT TUNEL Alexa Fluor 647 kit according to the manufacturer's protocol. Briefly, fixed larvae were incubated in TdT reaction buffer (200ul for 6 larvae) at 37°C for 3 h. After washing, the solution was replaced with Click-iT reaction buffer (200ul for 6 larvae) and incubated at room temperature with protection from light for 1 h. Next, larvae were washed, and immunostaining was performed as described above. For positive control, larvae were treated with DNase I solution for 30 min at room temperature.

2.2.11 In-situ hybridization

Probes were generated by PCR amplification of a 54 hpf cDNA library. Primers used for probe generation were:

IL4.F: ATGAAGACCTGAAGATCTCAACATCTGGATACATC

IL4R.F: GTTTCGTTTGCGAATAGGGAAGCAG

T7IL4.R:TAATACGACTCACTATAGGGTTATGTCCTTTGAGCCGAG

T7IL4R.R: TAATACGACTCACTATAGGGGAGCAGTGGTGAAATGAACTG

ifng1.F: ATGATTGCGCAACACATGATGGGCT

T7ifng1.R: TAATACGACTCACTATAGGGACCTCTATTTAGACTTTTGC

ifngr1.F:GTTGGATACAAACTCTGTGGTAATAATAATGCGGATATTGATCTGTC

T7ifngr1.R: TAATACGACTCACTATAGGGGAAAGCTCATGTACGCCTCG

il4, il4r, ifng1, and *ifngr1* expressions were assessed by *in situ* hybridization. Larvae were anesthetized with tricaine and fixed with 4% PFA in PBS at 4°C overnight. Next, larvae were washed with PBS buffer containing 0.1% tween20 (PBT), dehydrated, and incubated in methanol at -20°C for at least 2h. After rehydration and washing with PBT, larvae were permeabilized with proteinase K (10μg/ml) for 30 min and then treated with 4% PFA in PBS

for 20 min to stop the proteinase K digestion. After washing 5 times with PBT, a hybridization mix was prepared, and larvae were incubated for 4-5h at 70 °C. Then the hybridization mix was replaced with 30-50 ng of antisense DIG-labeled RNA probe diluted in the hybridization mix, and larvae were kept at 70 °C overnight. After several washes, larvae were incubated for 5-6h under agitation in PBT containing 2mg/ml BSA and %2 goat serum, followed by incubation with anti-Digoxigenin-AP Fab fragments (1:5000-10000) overnight at 4°C. After washing several times with PBT and Trizma buffer, fish were incubated with Fast Red TR/Naphthol AS-MX dissolved in Trizma buffer and incubated overnight at 4°C.

2.2.12 Confocal microscopy

For morphological analysis of the larval heart, anesthetized larvae were mounted in 1% low-melting agarose in a petri dish filled with Danieau's buffer with tricaine and then imaged with a Zeiss LSM880 NLO confocal microscopy system using a 20X water immersion objective.

For time-lapse imaging, larvae were anesthetized and embedded in 1% low-melting agarose in a petri dish. Then, the dishes were filled with Danieau's buffer with tricaine. Confocal Z-stacks were acquired from the brain of 4 dpf larvae every 40 min for 16h with a Zeiss LSM880 NLO confocal microscopy system using a 20X water immersion objective.

2.2.13 Mouse maintenance

2.2.14 Mouse cardiomyocyte primary culture

Isolation of cardiomyocytes from neonatal mouse

P0 C57BL/6N mice pups were used for neonatal cardiomyocyte culture. First, pups were disinfected using 70% ethanol and anesthetized. Then, hearts were dissected and dissociated by repeated enzymatic digestion (0.08% trypsin in PBS and 50 µg/ml DNaseI). After dissociation, cells were cultivated in DMEM, high glucose, GlutaMAX supplement containing 10% fetal calf serum, and Penicillin-Streptomycin (10.000 U/ml) at 37°C in 95% air/5% CO_2. 100 µl of cell suspension containing $0.6x10^5$ to $3.1x10^5$ cells was plated on glass coverslips

(12 mm in diameter) pre-coated with 10 μg/ml bovine plasma fibronectin in 24 well-plate. After cells were attached to the coverslips, additional medium was added, and cells were incubated for 24h.

Treatment

Cardiomyocytes cultured on coverslip in 24 well-plate were treated with 100nM dex, 10 ng/ml recombinant murine IL4, dex (100 nM) plus recombinant IL4 (10ng/ml), or ethanol as vehicle control in serum-free medium for 24h. 2 μM EdU was added to each well for the last 12 h of treatment.

2.2.15 Mouse Immunocytochemistry

After treatment, cardiomyocytes were washed with PBS and fixed with 4% PFA in PBS. For permeabilization, cells were treated with Triton X-100 (0.1%) for 20 min, followed by incubation with blocking solution for 1h. After blocking, cells were incubated with primary antibodies (1:300 mouse cardiomyocyte marker Tnnt2) overnight at 4°C and then washed with PBS. Next, cells were incubated with secondary antibodies (1:1000 goat anti-mouse Alexa488). EdU staining was performed using the Click-iT™ EdU imaging kit according to the manufacturer's protocol. The cell nuclei were stained with DAPI (1 μg/ml). Then, coverslips were mounted and imaged with a Zeiss LSM880 confocal microscopy system.

2.2.16 Mouse Immunofluorescent staining

BALB/c-Il4ratm1Sz/J (Noben-Trauth et al. 1997) mice were purchased from the Jackson Laboratory. Mice were genotyped by PCR with three primers (Il4ra_wt: TGTGGGCTCAGAGTGACCAT; Il4ra_mut: CCAGACTGCCTTGGGAAAAG; Il4ra_common: CAGGGAACAGCCCAGAAAAG) which leads to amplification of 441 bp (wild type allele) and 247 bp (mutant allele) DNA fragments. P0 neonatal hearts were collected, rinsed with PBS, and incubated with 4% PFA overnight at 4°C, followed by washing with PBS.

Then, tissues were embedded in paraffin, and 7µm sections were subjected to immunofluorescent staining. First, sections were deparaffinized and rehydrated by immersing the slides through xylene, 100% ethanol, 95% ethanol, 70% ethanol, 50% ethanol, and deionized water step by step, incubating for 10 minutes in each solution. Then, antigen retrieval was performed with citrate buffer (10 mM citric acid, 0,05% Tween 20, pH 6) for 15 min in a microwave. Next, samples were blocked with a PBS solution supplemented with 3% BSA, 5% goat serum, and 0.3 % Tween 20 for 1h at room temperature. Then, primary antibodies (1:200 anti-Tnnt2 and 1:100 anti-Ki-67) were diluted in blocking solution and applied to the sections overnight at 4°C. After three times washing with PBS, secondary antibodies (1:500 anti-mouse Alexa647 and 1:500 anti-rabbit Alexa488) and 1:200 dilution of WGA in blocking solution were applied to the sections and incubated for 1h at room temperature, followed by three times washing with PBS. Finally, sections were mounted and imaged with Zeiss LSM880 NLO confocal microscopy.

2.2.17 Image Analysis

Mouse Heart immunofluorescence analyses

$Tnnt2^+$, $Ki67^+$, and WGA^+ positive cells were counted using ImageJ. Cardiomyocyte proliferation was determined by $Tnnt2^+/Ki67^+$ double-positive cells. 25000 square micron areas from each section were used for this quantification. To determine *in vitro* neonatal cardiomyocyte proliferation upon IL4 and/or dex treatment, cardiomyocytes showing EdU-labeled nuclei that were co-localized with H2B-GFP were counted using ImageJ.

Zebrafish heart analysis

All z-stack planes covering the whole cardiac ventricle or atrium of zebrafish larvae were used for analyses. To assess trabeculation, compact wall and trabecular cardiomyocytes were counted from confocal z-stacks at 10µm intervals, and 40µm of the ventricle for each heart was used for quantification. Membrane marker (mKATE-CAAX) and nuclear marker (H2B-GFP) were used to distinguish individual cardiomyocytes. Total cardiomyocyte numbers and endocardial cell numbers were counted using Imaris software. ImageJ was used to count epicardial cells and dead cells as well as to assess cardiomyocyte proliferation by counting

$PCNA^+$ and $H2B\text{-}GFP^+$ double-positive cells. The estimated volume of the ventricle was quantified using the Volumest plugin in ImageJ. Cardiomyocyte volume was quantified using the Segmentation Editor plugin ImageJ.

Vessel density

The vascular area in the brain was quantified using ImageJ. Brain vascular density was determined by normalizing the brain vascular area to the total area of brain parenchyma. Vascular volume in the trunk and brain was calculated using Imaris surface rendering.

2.2.18 Statistical analysis

Statistical analyses were carried out, and graphs were prepared by Graphpad Prism. For qRT-PCR data and changes in cardiomyocyte number between 3 dpf and 5 dpf, one-sample Student's t-tests were used to determine statistical significance. For statistical analysis of all other data, two-tailed Student's t-tests were used. Dixon's test was employed to detect outliers in all data sets. p values were corrected using the *Holm-Bonferroni* method in case of multiple comparisons. $p < 0.05$ was considered statistically significant. All data are presented as mean ± standard error of the mean.

3 Results

3.1 IL4 and GR antagonistic signaling in cardiomyocytes of developing heart during homeostasis and stress response

The first part of this chapter was already published in the article “Early-Life Stress Regulates Cardiac Development through an IL4-Glucocorticoid Signaling Balance” Cell Rep. 2020 Nov 17;33(7):108404 (https://doi.org/10.1016/j.celrep.2020.108404). All experiments and results were performed by Dilem Ceren Apaydin unless otherwise stated in the figure legends.

3.1.1 Activation of Gr signaling impairs cardiac development and ventricular function

To address how stress experienced during early life contributes to increased susceptibility to cardiovascular diseases during later life, I utilized zebrafish as a model organism. Due to the nature of the mammalian embryo, which grows inside the uterus, it is challenging to manipulate stress/GR signaling directly in the embryo during early development. To address this problem, I mimicked the late-gestational/early-postnatal developmental stages by exploiting zebrafish developmental stages pre-hatching (2 to 3 dpf) and early post-hatching periods (4 to 5 dpf). I treated 4 dpf larvae with vibrational stimulus causing water swirling and forced swimming to trigger brain-mediated stress response during zebrafish's early life **(Fig. 3.1a)**. This type of vibration-based stimulus as a stressor was previously reported to induce a brain-mediated stress response in zebrafish larvae (Castillo-Ramírez et al., 2019). To address the effect of stress on the developing heart, I assessed the cardiomyocyte proliferation in *Tg(myl7:H2B-GFP)*^{zf521} larvae, labeling cardiomyocyte nuclei by immunofluorescence staining of GFP and Proliferating Cell Nuclear Antigen (PCNA) which is a nuclear marker for cells in G1-S phase **(Fig. 3.1b)**. I found that larvae exposed to involuntary swimming show decreased cardiomyocyte proliferation compared to control siblings in the ventricle **(Fig. 3.1c)**. This data shows that brain-mediated stress induced by a physiological stressor mitigates the mitotic rate of cardiomyocytes during cardiac development in zebrafish.

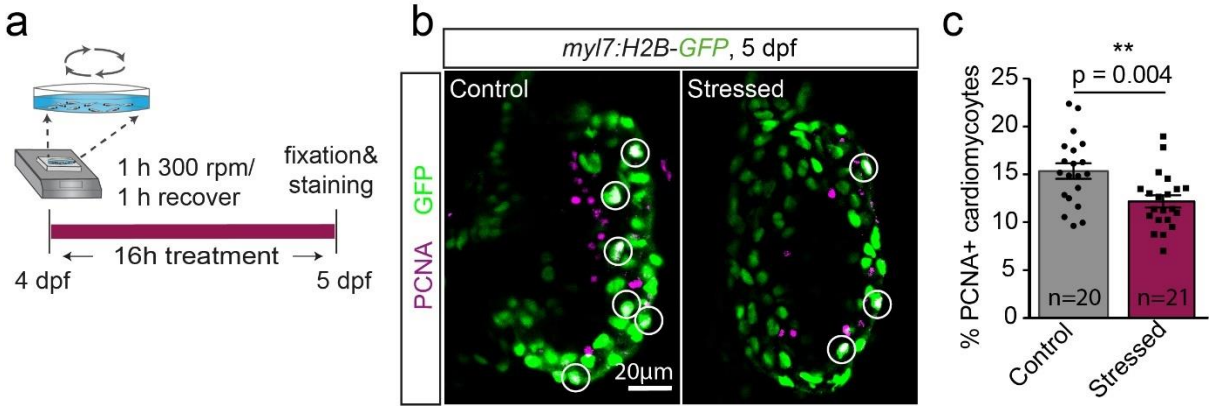

Figure 3.1. Zebrafish larvae exposed to vibrational stress exhibit impaired cardiomyocyte proliferation in the ventricle. a, Schematic illustration of the stress treatment for zebrafish larvae. 4 dpf larvae were exposed to forced swimming by shaking at 300 rpm for 1h followed by 1 h-long intervals without shaking over 16h or kept in similar conditions without shaking (control). b, Confocal projection of 5 dpf *Tg(myl7:H2B-GFP)*^{zf521} larval ventricle immunostained with antibodies against PCNA and GFP. Scale bar: 20 µm. c, Graph depicting the percentage of PCNA-positive (PCNA+) ventricular cardiomyocytes in 5 dpf *Tg(myl7:H2B-GFP)*^{zf521} larvae following vibrational stress. Data are presented as mean ± S.E.M. ** $p < 0.01$, t-test. n indicates the number of larvae used for experiments.

In response to stress, the HPI axis, homologous to the mammalian HPA axis, became activated to release GC, which is the primary stress hormone. GCs acting mainly through GR play crucial roles in several biological activities (Timmermans et al., 2019). To understand whether stress experienced in early life exerts its harmful effect on cardiac development acting through GR, I manipulated GR signaling by using a GR agonist dex in zebrafish larvae, starting from 2 dpf **(Fig. 3.2a)** to mimic mammalian late gestation developmental stage in which fetal GC levels rise (Andrés-Delgado & Mercader, 2016; Fowden et al., 1998). Following 3 days of 100uM dex treatment, I performed live imaging of 5 dpf *Tg(myl7:H2B-GFP)*^{zf521}*; Tg(myl7:mKate-CAAX* ^{sd11} larvae, in which cardiomyocyte nuclei and membrane fluorescently are labeled by H2B-GFP and mKATE-CAAX, respectively **(Fig. 3.2b)**. Thanks to the nuclear expression of GFP, I was able to quantify cardiomyocyte numbers using Imaris software and found that activation of Gr signaling causes a reduction of cardiomyocyte number in dex-treated larvae compared to control siblings **(Fig. 3.2c)**. Further morphological examination of the ventricle demonstrated increased ventricular volume in the presence of prolonged dex treatment **(Fig. 3.2d)**, indicating the development of ventricular hypertrophy.

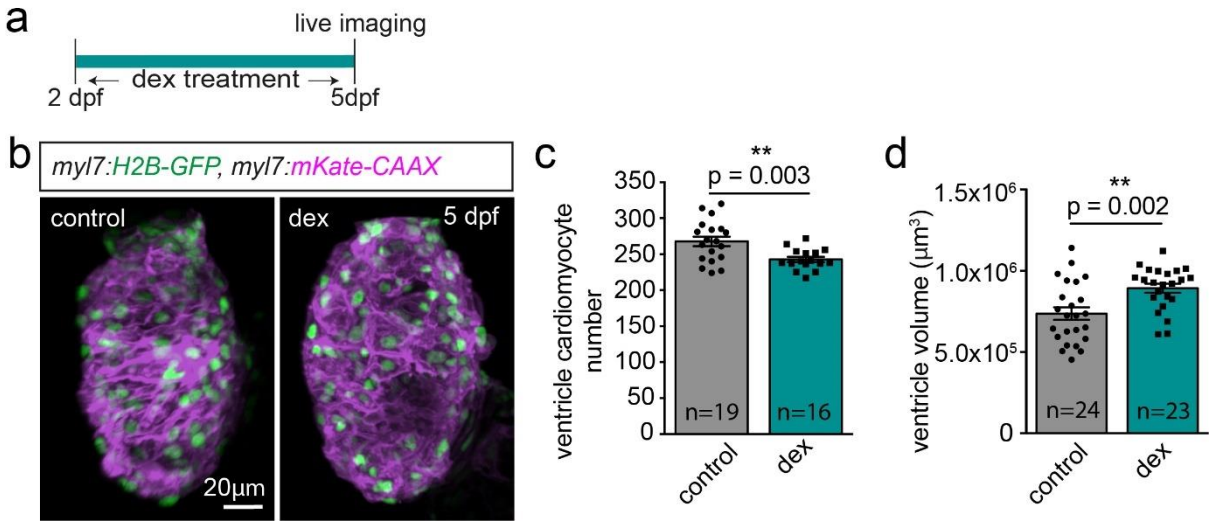

Figure 3.2. Dex-mediated Gr signaling activation leads to reduced ventricular cardiomyocyte number and increased ventricular size. a, Schematic representation of the dex treatment for zebrafish larvae. Larvae were treated with 100 µM dex or control medium from 2 dpf to 5 dpf. b, Confocal projection of 5 dpf *Tg(myl7:H2B-GFP)*^{zf521}*; Tg(myl7:mKate-CAAX* ^{sd11} larvae treated with either dex or control solution. Cardiomyocyte nuclei and membranes are labeled with H2B-GFP and mKate-CAAX, respectively. Scale bar: 20 µm c, Graph showing the average number of cardiomyocytes in the ventricle of 3-day dex-treated or control *Tg(myl7:H2B-GFP)*^{zf521}*; Tg(myl7:mKate-CAAX)*^{sd11} larvae. d, Graph depicting the quantification of average ventricle volume from 5 dpf *Tg(myl7:H2B-GFP)*^{zf521}*; Tg(myl7:mKate-CAAX)*^{sd11} larvae following dex or control treatment. Data are presented as mean ± S.E.M. ** $p < 0.01$, t-test. n indicates the number of larvae used for experiments. Ventricular volume quantification shown in d was performed by Cosco F.

To examine whether lower cardiomyocyte number upon activation of Gr signaling is a consequence of increased cardiomyocyte death, I assessed cardiomyocyte apoptosis in 5 dpf *Tg(myl7:H2B-GFP)*^{zf521} larvae by TUNEL assay coupled with GFP immunostaining 6h after dex or control treatment **(Fig. 3.3a)**. I detected negligible number of apoptotic cardiomyocytes in larvae treated with dex during development. This data indicates that cell death is not the reason for reduced cardiomyocyte number, suggesting that overactivation of Gr signaling might induce an anti-mitotic response as observed in larvae exposed to forced swimming. Furthermore, the data showing reduced cardiomyocyte numbers together with enlargement of the ventricular chamber upon dex treatment suggests that overactivation of Gr signaling might cause eccentric hypertrophy during heart development. In fact, cardiomyocytes often undergo

hypertrophic growth in response to increased demand during cardiac remodeling (Sugden & Clerk, 1998). To address this hypothesis, cardiomyocyte volume was quantified in 5 dpf *Tg(myl7:H2B-GFP)*^{zf521}*; Tg(myl7:mKate-CAAX)*^{sd11} larvae which were possible due to our ability to differentiate individual cardiomyocytes labeling their nuclei with H2B-GFP and membrane with mKATE-CAAX. Larvae exposed to 3-day dex treatment exhibited significantly increased cardiomyocyte size, highlighting hypertrophic cell growth **(Fig. 3.3b)**. These findings indicate that eccentric hypertrophy evidenced by enlarged ventricular volume, at least partially, results from cardiomyocyte hypertrophy upon overactivation of Gr signaling.

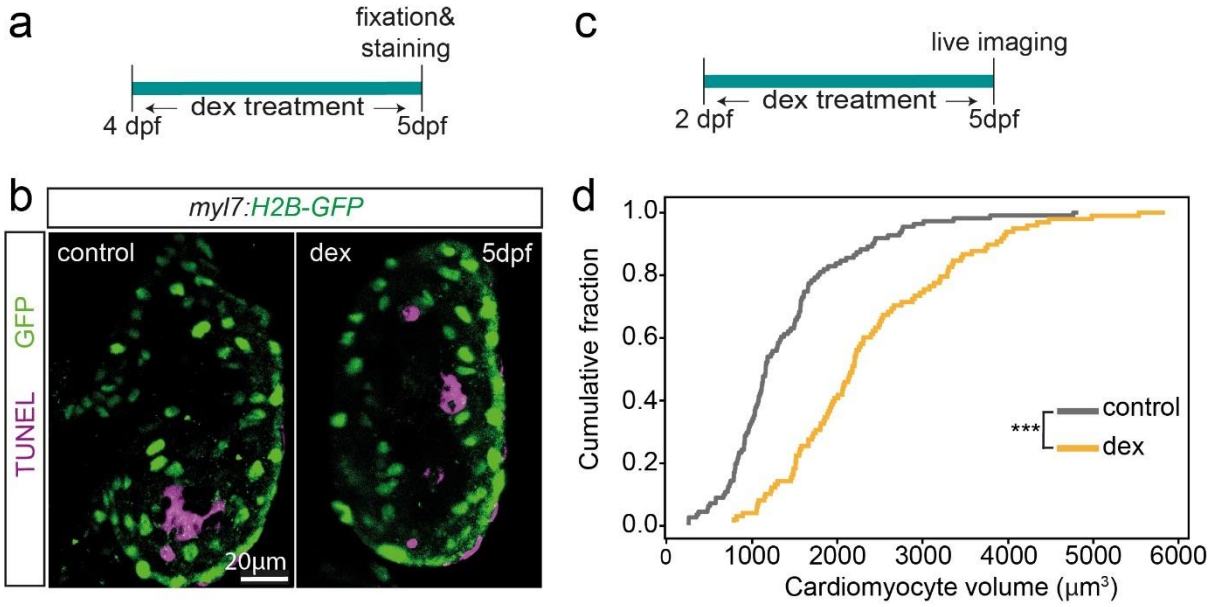

Figure 3.3. Activation of Gr signaling increases cardiomyocyte size but does not affect cardiomyocyte apoptosis. **a**, Schematic illustration of dex treatment used in zebrafish larvae for TUNEL assay. 5 dpf Larvae were treated with 100 µM dex or control medium for 6h. **b**, Confocal projections of 5 dpf *Tg(myl7:H2B-GFP)*^{zf521} larval heart exposed to either dex or control treatment, immunostained for GFP to label cardiomyocyte nuclei, and apoptosis was detected by TUNEL assay. Scale bar: 20 µm. **c**, Schematic representation of the dex treatment to assess cardiomyocyte size of zebrafish larvae. *Tg(myl7:H2B-GFP)*^{zf521}*; Tg(myl7:mKate-CAAX)*^{sd11} larvae were treated with 100 µM dex or control medium from 2 dpf to 5 dpf and live imaged. **d**, Graph showing the cumulative distribution of cardiomyocyte size in control and dex-treated larvae. *** $p < 0.001$, t-test. Cardiomyocyte sizes shown in d were quantified by Cosco F.

Another key morphogenetic process in the heart is the trabecular formation which requires crosstalk between the cardiac layers, cardiomyocyte delamination from the ventricular wall and expansion into the ventricular cavity, as well as cardiomyocyte proliferation. Cardiac

trabeculae are an essential muscular structure to increase surface area for nutrients and oxygen exchange and muscle mass for cardiac contractility. Therefore, I characterized the cardiac trabeculation to examine whether this critical developmental process is affected by the activation of Gr signaling. I performed live imaging of 5 dpf *Tg(myl7:H2B-GFP)* ^{zf521}*; Tg(myl7:mKate-CAAX)*^{sd11} larvae **(Fig. 3.4a,b)** and counted the number of both compact and trabecular cardiomyocytes. I found that larvae treated with dex for 3 days showed impaired trabeculation, as shown by reduced ratios of trabecular/compact wall cardiomyocytes **(Fig. 3.4c),** indicating another Gr-mediated morphological defect.

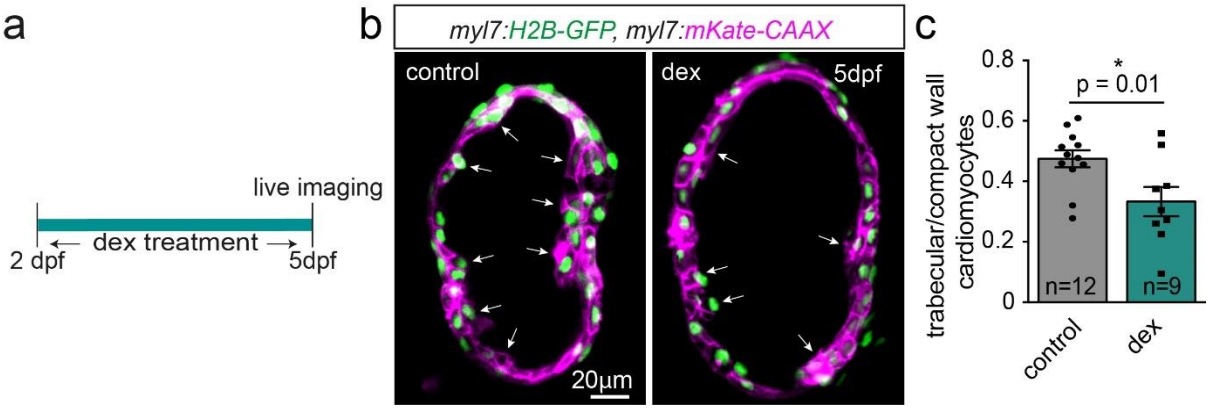

Figure 3.4. Activation of Gr signaling causes a severe defect in the trabecular formation of the developing heart. a, Schematic representation of the dex treatment for trabeculation assessment. Larvae were treated with 100 µM dex or control medium from 2 dpf to 5 dpf **b**, Confocal projections of 3-day dex treated or control *Tg(myl7:H2B-GFP)*^{zf521}*; Tg(myl7:mKate-CAAX)*^{sd11} larval ventricle. Cardiomyocyte nuclei and membranes are labeled with H2B-GFP and mKate-CAAX, respectively. White arrows indicate trabecular cardiomyocytes. Scale bar: 20 µm. **c**, Graph showing the ratio of trabecular/ compact wall cardiomyocyte numbers in dex treated and control larvae. Data are presented as mean ± S.E.M. * $p < 0.05$, t-test. n indicates the number of larvae used for experiments.

These findings suggest that adverse morphological alterations observed upon activation of Gr signaling might lead to functional impairments of the developing heart. The impaired trabecular formation, for example, was associated with cardiac dysfunction in cardiovascular diseases (M. Wu, 2018). Therefore, to elucidate this hypothesis, cardiac function was assessed by live imaging of the ventricle with a high-speed camera **(Fig. 3.5a)**. Diastolic and systolic speed were calculated as ventricular area change between diastole and systole by the time of one cycle. The striking reduction of diastolic and systolic speed, indicated by slower ventricular relaxation and contraction, was found in larvae treated with dex for 3 days compared to control

siblings **(Fig. 3.5b,c)**. In addition to diastolic and systolic speed, EF and FS, which are other critical systolic parameters associated with myocardial stiffening, were also calculated upon Gr activation. However, larvae exposed to 3-day dex treatment showed no alterations in EF and FS **(Fig. 3.5d)**.

Taken together, this data indicates that larvae exposed to Gr overactivation exhibit impaired cardiac function, possibly as a consequence of structural abnormalities, i.e., lower cardiomyocyte number, cardiac hypertrophy, and disrupted trabecular formation.

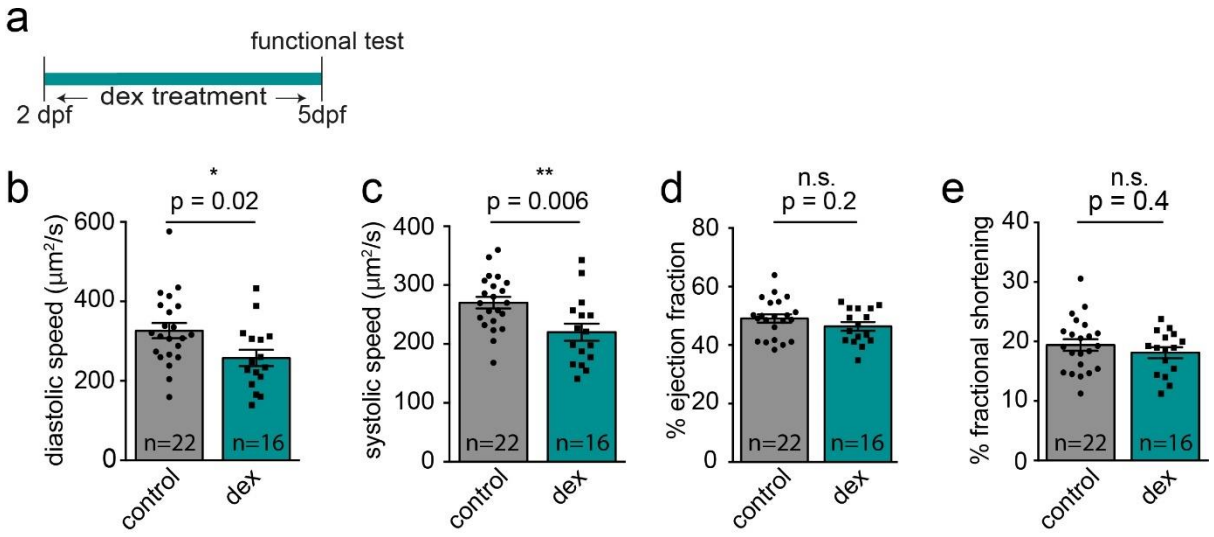

Figure 3.5. Zebrafish larvae exposed to dex treatment show reduced diastolic and systolic speeds but no change in EF and FS. a, Schematic representation of the dex treatment for cardiac function assessment. Larvae were treated with 100 µM dex or control medium from 2 dpf to 5 dpf. Parameters of cardiac function were assessed from 5 cycles for each fish. b-e, Graphs indicating diastolic speed (b), systolic speed (c), EF (d), FS (e). Data are presented as mean ± S.E.M. * $p < 0.05$, ** $p < 0.01$, n.s. not significant. t-test. n indicates the number of larvae used for experiments. Cardiac function was assessed by Cosco F.

3.1.2 Il4 stimulates cardiac development and enhances the ventricular function

In addition to stress response, GCs are involved in several other biological processes, one of which is immunomodulation. GCs attenuate the expression of numerous cytokines,

including IL1β, IL4, IL17, TNFα, IL6, and IFNγ, promoting the resolution of the inflammatory response (Cain & Cidlowski, 2017). On the other hand, prolonged exposure to stressors promotes inflammation which triggers pathological events in the heart (Effects of Stress on the Development and Progression of Cardiovascular Disease, 2018). In fact, disturbance of the immune system has been advocated as a contributing factor to cardiovascular diseases (Swirski & Nahrendorf, 2018). Given these previous findings, I reasoned that Gr-mediated abnormalities and/or dysregulation in the immune system during development might underlie the cardiac remodeling observed upon overactivation of Gr signaling in zebrafish larvae. The key factor in immune regulation is the cytokine network, which modulates the inflammatory response (Cain & Cidlowski, 2017). Therefore, I further aimed to explore the potential crosstalk between GR and cytokine signaling.

Apart from suppression of its expression by GCs, IL4 was inversely associated with stress/anxiety in humans as well as animal models, highlighting its potential for crosstalk with GR signaling (Han et al., 2015; Karlsson et al., 2017; H. J. Lee et al., 2016) To address this possibility further, the expression of Il4 and its receptor were examined in the developing zebrafish heart. *In situ* hybridization showed that *il4* mRNA was not detectable in the heart while its receptor, *il4r*, was expressed in cardiomyocytes of the developing zebrafish heart as early as 3 dpf **(Fig. 3.6a)**. On the other hand, *il4* expression was abundant in the thymus, a hematopoietic organ located close to the heart **(Fig. 3.6a)**. In addition to IL4, the levels of IFNγ signaling components, another signature cytokine, were examined as its level was also reported to be regulated by GR (Cain & Cidlowski, 2017). On the contrary, neither *Ifng1* nor its receptor was detectable in the developing heart **(Fig. 3.6b)**. These findings, together with previous reports, point out that IL4 is an appealing candidate for potential interaction with GR signaling during development.

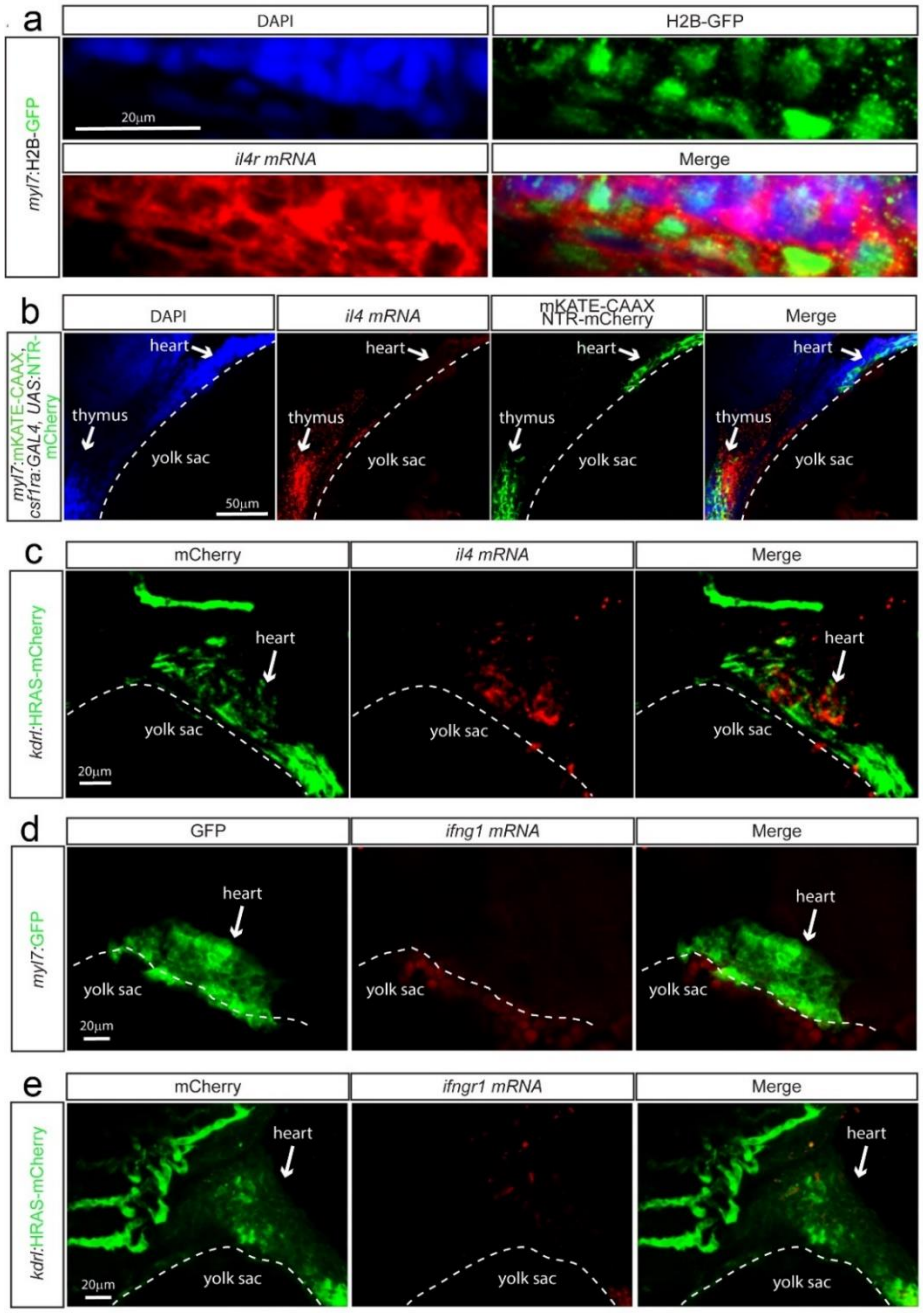

Figure 3.6. Cardiomyocytes of developing heart express *il4r*, but not *il4, ifng1, ifng1r*. a, *il4r* mRNA in situ hybridization on 3 dpf *Tg(myl7:H2B-GFP)*^{zf521} larvae. Cardiomyocyte nuclei are labeled with H2B-GFP. Scale bar: 20 μm. **b,** *il4* mRNA in situ hybridization on 3 dpf *Tg(myl7:mKate-CAAX)*^{sd11}*; Tg(csf1ra:Gal4)*^{i186}*; Tg(UAS:NTR-mCherry)*^{c26} larvae. Cardiomyocyte membranes were labeled with mKATE-CAAX, and myeloid cells were labeled with NTR-mCherry. Scale bar: 50 μm. **c,** *il4* mRNA in situ hybridization on *Tg(kdrl:HRAS-mCherry)*^{s896} larvae. Endocardial cells were labeled with HRAS-mCherry. Scale bar: 20 μm. **d,** *ifng1* mRNA in situ hybridization on 3 dpf *Tg(myl7:H2B-GFP)*^{zf521} larvae. Scale bar: 20 μm**. e,** *ifng1r* mRNA in situ hybridization on *Tg(kdrl:HRAS-mCherry)*^{s896} larvae. Scale bar: 20 μm. This data was generated by Sawamiphak S.

IL4, one of the pleiotropic cytokines, is known to be involved in the modulation of type 2 immune response along with several other biological activities. However, the developmental role of IL4 in the heart remains largely unknown. As its receptor is expressed in the developing myocardium, I reasoned that it might be involved in myocardial growth. To reveal the possible role of Il4 signaling in the developing zebrafish heart, I first characterized the effect of Il4 signaling manipulation on the morphology of the larval heart. **(Fig. 3.7a)** For this purpose, a transgenic line *Tg(hsp70:il4-6xHIS)*^{md74} allowing heat-inducible Il4 expression *(il4-6xHIS)* under the heat shock protein (*hsp70*) promoter was generated **(Fig. 3.7b)**. Following daily heat-induction of *il4-6xHIS* overexpression 4 consecutive days between 1-5 dpf, I performed live imaging of 5 dpf *Tg(hsp70:il4-6xHIS)*^{md74}, *Tg(myl7:H2B-GFP)*^{zf521}, *Tg(myl7:mKate-CAAX)*^{sd11} **(Fig. 3.7c)**. Characterization of ventricular morphology revealed that *il4-6xHIS* overexpression leads to increased ventricular volume **(Fig. 3.**7e), suggesting a hypertrophic growth of the ventricle, similar to findings obtained from larvae exposed to Gr overactivation**.** Interestingly, I noted a higher number of cardiomyocytes in larvae overexpressing *il4-6xHIS* compared to control siblings **(Fig. 3.7d),** indicating overgrowth of larval hearts in response to Il4 induction during development.

Not only trabecular deficiency but also excessive trabeculation were associated with cardiac defects as it is required for proper formation and function of the ventricular walls (M. Wu, 2018). Therefore, I reasoned that a high number of ventricular cardiomyocytes caused by Il4 induction might result in abnormal number of ventricular trabeculae, leading to hypertrabeculation. To address this hypothesis, I counted cardiomyocytes in the compact and trabecular layer of 5 dpf larvae exposed to daily *il4-6xHIS* heat-induction over 4 days. Unlike overactivation of Gr, I observed no alteration of trabecular layer formation as evidenced by similar ratios of trabecular/compact wall cardiomyocytes upon Il4 induction **(Fig. 3.7f, g),** indicating that newly formed cardiomyocytes are not populated specifically in compact layer or trabeculae. Instead, they seem to normally incorporate into the ventricular wall, leading to grossly normal myocardium during cardiac development.

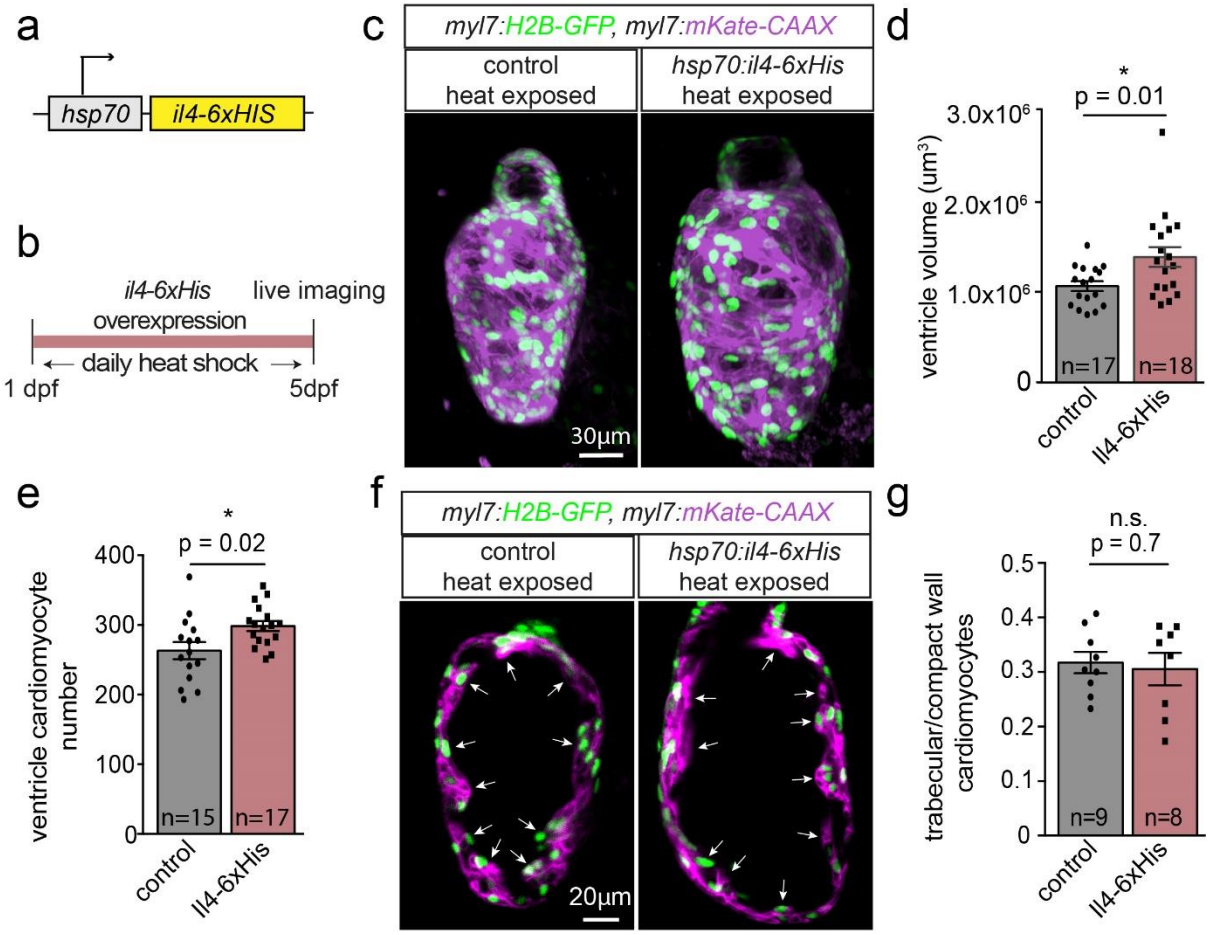

Figure 3.7. Heat-induced Il4 elevation leads to increased ventricular cardiomyocyte number and ventricle size without any trabeculae defect. a, Scheme of *hsp70:il4-6xHIS* transgene. b, Schematic illustration of daily Il4 induction. Larvae were exposed to daily heat shock at 38 ºC for 1.5h, starting from 1 dpf until 5 dpf. c, Confocal projection of 5 dpf *Tg(myl7:H2B-GFP)*^{zf521}, *Tg(myl7:mKate-CAAX)*^{sd11} control and *Tg(myl7:H2B-GFP)*^{zf521,} *Tg(myl7:mKate-CAAX)*^{sd11} *Tg(hsp70:il4-6xHIS)*^{md74} *il4-6xHIS* overexpressing larval ventricle. Scale bar: 30 µm. d-e, Graphs showing average number of ventricular cardiomyocyte (d) and ventricular volume (e) of control and *il4-6xHIS* overexpressing larvae. f, Confocal projection of 5 dpf control and *il4-6xHis* overexpressing *Tg(myl7:H2B-GFP)*^{zf521}; *Tg(myl7:mKate-CAAX)*^{sd11} ventricle. g, Graph depicting ratio of trabecular/compact wall cardiomyocyte numbers in 5 dpf larvae exposed to daily heat shock. Data are presented as mean ± S.E.M. * $p < 0.05$, t-test. n.s. not significant. n indicates the number of larvae used for experiments. Ventricular volume shown in d was quantified by Cosco F.

As cardiomyocytes are the muscle mass that provides the contractile force of the heart, supplemental cardiomyocytes upon *il4-6xHIS* overexpression might affect cardiac contractility. To test this hypothesis, cardiac function was assessed in 5 dpf larvae following

daily heat shock over 4 days **(Fig. 3.8a)**. Enhanced ventricular relaxation and contraction abilities evidenced by increased diastolic and systolic speed were observed upon *il4-6xHIS* overexpression compared to control siblings **(Fig. 3.8b,c)**. However, larvae exposed to Il4 induction exhibited no change in EF and FS **(Fig. 3.8d,e)**. These results, together with morphological characterizations, suggest that overgrowth of the heart through additional muscle mass might cause enhanced cardiac contractility upon Il4 induction without leading to any adverse structural and functional alterations.

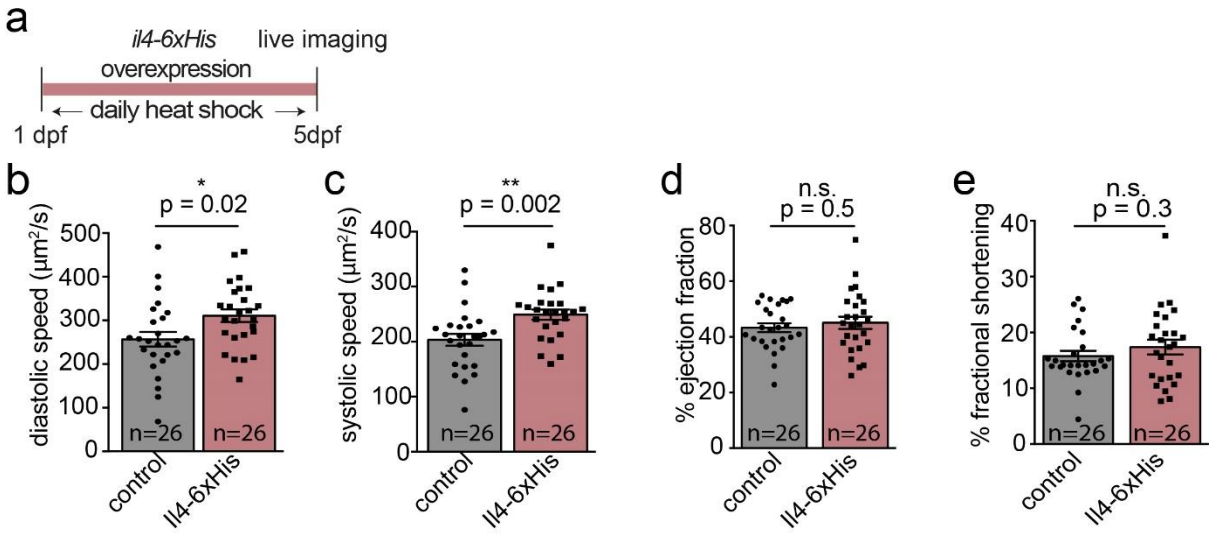

Figure 3.8. Il4 induction enhances the diastolic and systolic speeds of the developing heart. **a**, Schematic illustration of Il4 induction used for functional test. Larvae were exposed to heat shock daily at 38 ^{o}C for 1.5h from 1 dpf to 5 dpf. **b-e**, Bar graphs showing the average of diastolic speed **(b),** systolic speed **(c)**, EF **(d)**, FS **(e)** in 5 dpf *il4-6xHis*-overexpressing and control larvae. Data are presented as mean ± S.E.M. * $p < 0.05$, ** $p < 0.01$, n.s. not significant. t-test. n indicates the number of larvae used for experiments. Cardiac function was assessed by Cosco F.

Utilizing the gain-of-function tools, I showed improved myocardial growth in zebrafish larvae. The data showing a higher number of cardiomyocytes observed upon *il4-6xHIS* overexpression suggests a regulatory role for Il4 in cardiomyocytes' mitotic rate. To further investigate whether Il4 is required for the development of the heart, a loss-of-function approach was utilized by injection of Il4 neutralizing antibody (Il4-nAB), which was previously reported to efficiently inhibit Il4 signaling in zebrafish (Bhattarai et al., 2016). 16h after pericardial injection of Il4-nAB, I assessed the cardiomyocyte mitotic rate of 5 dpf *Tg(myl7:H2B-GFP)^{zf521}*

larvae by immunostaining for PCNA and GFP **(Fig. 3.9a)**. Interestingly, I found that larvae with Il4 deficiency exhibit decreased cardiomyocyte proliferation compared to control siblings, which were injected with an antibody against 6-histidine epitope as control **(Fig. 3.9b, c)**. Taken together, this data suggests that Il4 is required for cardiomyocyte mitotic activity in developing hearts, highlighting its pro-mitotic potential.

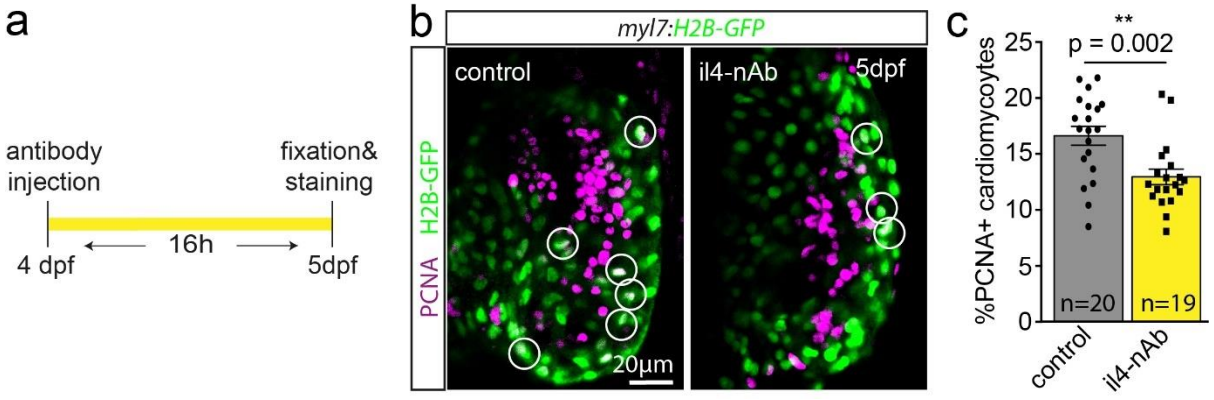

Figure 3.9. The deficiency of Il4 signaling is sufficient to inhibit cardiomyocyte proliferation in the developing heart. **a**, Schematic representation of antibody injection. 4 dpf *Tg(myl7:H2B-GFP)*^{zf521} larvae were injected with antibodies either against Il4 (Il4-nAB) or 6x-histidine repetitive sequence as control and fixed at 16h post-injection. **b,** Confocal projections of 5 dpf *Tg(myl7:H2B-GFP)*^{zf521} larvae injected with either Il4-nAB or control antibody. Scale bar: 20 µm. **c,** Graph showing average percentage of PCNA-positive (PCNA+) cardiomyocytes in the ventricle of 5 dpf larvae injected with either Il4-nAB or control antibody. Data are presented as mean ± S.E.M. ** $p < 0.01$, t-test. n indicates the number of larvae used for experiments. Antibody injection into pericardium was performed by Sawamiphak S.

3.1.3 Gr-Il4 interaction regulates cardiomyocyte proliferation in the atrium and the ventricle during development

Morphological characterization of larval hearts upon overactivation of either Gr or Il4 signaling pathways revealed opposite effects on cardiac development. I observed that stress/Gr signaling activation reduces cardiomyocyte number and proliferation. On the other hand, induction of Il4 increases cardiomyocyte number, as well as its inhibition attenuates cardiomyocyte proliferation. These opposite effects of Gr and Il4, together with previously

reported results showing regulation of IL4 activity by stress/GR signaling (Cain & Cidlowski, 2017; Han et al., 2015; Karlsson et al., 2017; H. J. Lee et al., 2016), highlights potential crosstalk between them during heart growth. These interesting outcomes prompt me to examine further whether they exert their developmental effects on the heart through modulating cardiomyocyte proliferation and whether their possible interaction takes place in the regulation of this process. For this purpose, I employed a combinatorial treatment to manipulate both pathways by exposing larvae to either dex, *il4-6xHIS* overexpression, dex together with *il4-6xHIS* overexpression, or control **(Fig. 3.10.a)**. 6h after treatment, I assessed the mitotic rate of cardiomyocytes by immunostaining for PCNA and GFP in 5 dpf *Tg(myl7:H2B-GFP)*^{zf521} and *Tg(myl7:H2B-GFP)*^{zf521}*; Tg(hsp70:il4-6xHIS)*^{md74} larvae. Consistent with the stress-mediated reduction in cardiomyocyte proliferation, in the presence of dex, larvae showed drastically lower proliferative rates in ventricular cardiomyocytes compared to control siblings (**Fig. 3.10b, c)**. On the other hand, larvae overexpressing *il4-6xHIS* exhibited a higher mitotic rate compared to control siblings (**Fig. 3.10b, c)**. Intriguingly, I found that this positive effect of Il4 on cardiomyocyte proliferation is mitigated when Gr signaling is also activated by dex treatment (**Fig. 3.10b, c).** Taken together, these results indicate that while GCs promote anti-mitotic response, Il4 acts as a pro-mitotic factor in cardiomyocytes during development.

Apart from the role of GCs in pathological settings, GCs exert a wide range of physiological effects which are essential for the proper development and maintenance of homeostasis (Cain & Cidlowski, 2017). In the heart, it was reported that GCs are required for cardiomyocyte maturation (Eva A. Rog-Zielinska et al., 2013; Wilson et al., 2015). After I revealed the action of stress/GCs as a cardiomyocyte mitotic brake in chronic condition, I aimed to investigate further whether Gr signaling is involved in any other developmental cardiac events apart from the adaptation of the heart in response to stress during myocardial growth. To examine the effect of Gr on the heart in normal physiology, I utilized a Gr antagonist, mif, to inhibit Gr signaling. Following 6h mif treatment, I assessed the cardiomyocyte proliferation by immunostaining for PCNA and GFP in 5 dpf *Tg(myl7:H2B-GFP)*^{zf521} larvae (**Fig. 3.10a, b).** Surprisingly, I found that decreased systemic Gr signaling leads to increased cardiomyocyte proliferation compared to control siblings (**Fig. 3.10c)**, indicating a hyperproliferative cardiomyocyte response of the developing heart to Gr deficiency.

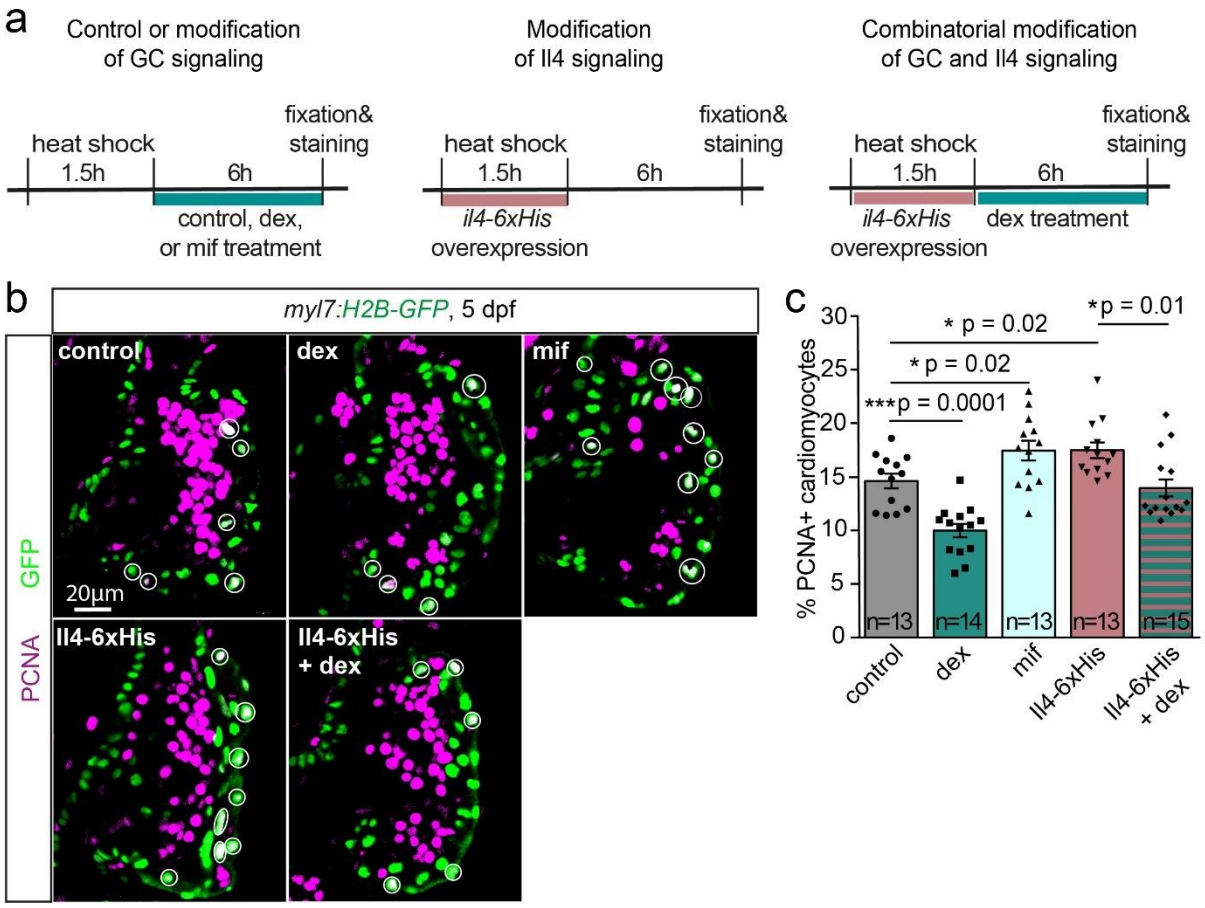

Figure 3.10. Gr and Il4 interactions regulate cardiomyocyte mitotic response in the developing heart. a, Schematic illustration of Gr agonist and antagonist treatment as well as heat-induced *il4-6xHis* expression. 5 dpf *Tg(hsp70:il4-6xHIS)*^{md74}*; Tg(myl7:H2B-GFP)*^{zf521} and *Tg(myl7:H2B-GFP)*^{zf521} larvae were heat shocked for 1.5h followed by control, dex or mif treatment for 6h. **b**, Confocal projections of 5 dpf ventricle of *Tg(hsp70:il4-6xHIS)*^{md74}, *Tg(myl7:H2B-GFP)*^{zf521}, and *Tg(myl7:H2B-GFP)*^{zf521} larvae immunostained with PCNA and GFP following the treatment. Scale bar: 20 µm. **c**, Graph showing the average percentage of PCNA-positive (PCNA+) cardiomyocytes in the ventricle. Data are presented as mean ± S.E.M * $p < 0.05$, ** $p < 0.01$ ***, $p < 0.001$, n.s. not significant. t-test. n indicates the number of larvae used for experiments.

To examine whether these regulatory effects of Gr and Il4 as well as their interaction observed in the ventricle, also exist in the atrium of the developing heart, I performed immunostaining for PCNA and GFP using 5 dpf *Tg(myl7:H2B-GFP)*^{zf521} and *Tg(hsp70:il4-6xHIS)*^{md74}, *Tg(myl7:H2B-GFP)*^{zf521} larvae which were exposed to the same kind of combinatorial treatment (**Fig. 3.11a, b).** Similar to the phenotype observed in the ventricle (**Fig. 3.10c)**, the pro-mitotic effect of Il4, anti-mitotic effect of Gr, and neutralization of these effects

in the presence of both Gr and Il4 activation were also confirmed in atrium cardiomyocytes (**Fig. 3.11c)**, highlighting that regulatory function of Il4-Gr interaction in cardiomyocyte mitotic activity is not restricted to the ventricle.

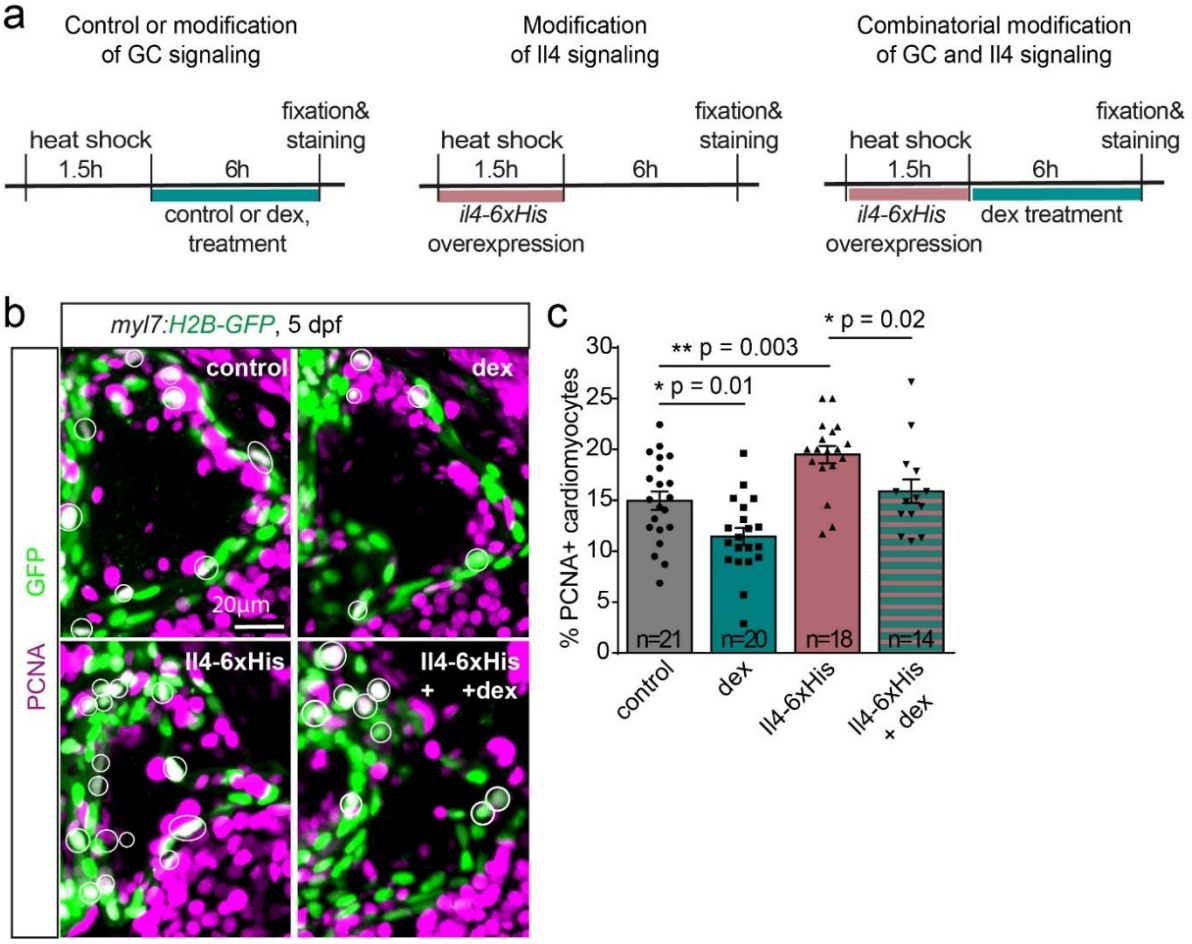

Figure 3.11. Regulation of cardiomyocyte proliferation by Gr and Il4 interactions is persisted in the atrium of the developing zebrafish heart. **a**, Schematic illustration of dex treatment and Il4 induction. 5 dpf *Tg(hsp70:il4-6xHIS)*^{md74}*; Tg(myl7:H2B-GFP)*^{zf521} and *Tg(myl7:H2B-GFP)*^{zf521} larvae were heat shocked for 1.5h followed by control or dex for 6h. **b,** Confocal projection of 5 dpf atrium of *Tg(hsp70:il4-6xHIS)*^{md74}, *Tg(myl7:H2B-GFP)*^{zf521,} and *Tg(myl7:H2B-GFP)*^{zf521} larvae PCNA and GFP immunostained after the treatment. Scale bar: 20 µm. **c**, Graph demonstrating the average percentage of PCNA-positive (PCNA+) cardiomyocytes in the atrium. Data are presented as mean ± S.E.M * $p < 0.05$, ** $p < 0.01$, n.s. not significant. t-test. n indicates the number of larvae used for experiments. Atrial cardiomyocyte proliferation shown in c was quantified by Sawamiphak S.

3.1.4 Gr signaling does not act upstream of Il4 signaling

To gain better insights into the antagonistic interaction between Gr and Il4 signaling during cardiac development, I first examined whether Gr transcriptionally regulates Il4 signaling components, acting upstream of Il4 signaling as observed in some physiological (Cain & Cidlowski, 2017) or pathological (Ogasawara et al., 2018; So et al., 2002; Umland et al., 1997) settings. I assessed *il4r, il13ra1, and il13a2* mRNA expression in the heart and *il4* mRNA expression in the whole body upon 2h dex treatment by qPCR (**Fig. 3.12)**. I found that neither expression of those cytokines nor their receptors were changed following dex treatment (**Fig. 3.12)**. This data shows that the opposite effect of Gr and Il4 in the heart is not mediated by transcriptional regulation of Il4 signaling by Gr signaling.

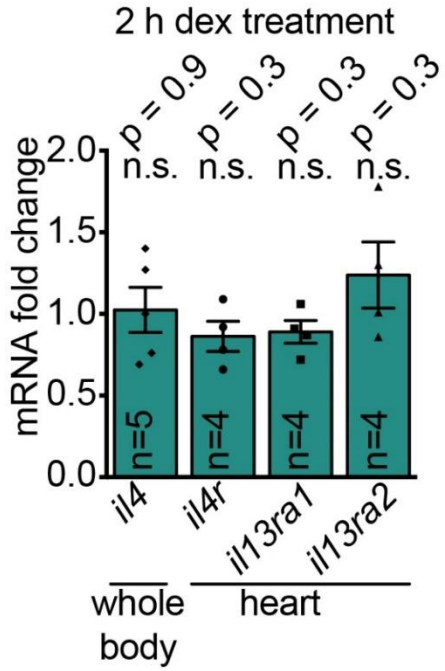

Figure 3.12. Expressions of *il4, il4r, il13ra1, and il13ra2* are not regulated by Gr signaling in the developing zebrafish heart. Graph showing the average mRNA fold change of *il4r, il13ra1, and il13ra2* in the heart and *il4* in the whole body in response to 2h dex treatment. Data are presented as mean ± S.E.M, n.s. not significant. t-test. n indicates biological replicas.

3.1.5 Stat3 is a critical mediator balancing the proliferation of cardiomyocytes

Activation of IL4 signaling starts with the binding of IL4 to IL4R, which induces phosphorylation of predominantly STAT6, but also STAT3, which in turn goes to the nucleus to regulate the target gene expression (McCormick & Heller, 2015). Similarly, GR acting as a transcription factor is involved in the transcriptional regulation of several target genes.

Interestingly, GR interactions with STAT3 and STAT6 in some cells were previously reported (Biola et al., 2000; Langlais et al., 2012). To better understand how Gr and Il4 function antagonistically to one another to balance cardiomyocyte proliferation, I first assessed the alteration of proliferation-related Stat6 target genes, *bcl2l1* and *socs1,* in the heart by qPCR upon overactivation of Il4 and Gr signaling (**Fig. 3.13a)**. I found upregulation of *bcl2l1* and *socs1* 2h after *il4-6xHIS* overexpression; however, I did not detect any change in their expression levels 2h after dex treatment (**Fig. 3.13b)**. Next, I examined the expression of Stat3 target genes, *c-myc, cyclinD1,* and *gata3,* which are involved in cell proliferation. Consistent with earlier findings of inverse effects of Gr and Il4 signaling on cardiomyocyte proliferation (**Fig. 3.10)**, I noted upregulation of *c-myc, cyclinD1,* and *gata3* upon *il4-6xHIS* overexpression in the heart while these pro-mitotic genes were downregulated upon dex dependent Gr activation (**Fig. 3.13c)**, suggesting that Stat3 might play a central role in the crosstalk of Gr and Il4 in the developing heart. To examine whether Gr-mediated transcriptional suppression of Stat3 underlies Il4-Gr crosstalk, I assessed *stat3* mRNA in the heart and whole body of 5 dpf larvae exposed to 2h dex treatment. No alteration of *stat3* expression was observed upon dex-mediated Gr activation (**Fig. 3.13c)**, indicating that deregulation of proliferation-related Stat3 target gene expression is not a consequence of an altered level of *stat3* but rather altered Stat3 activity.

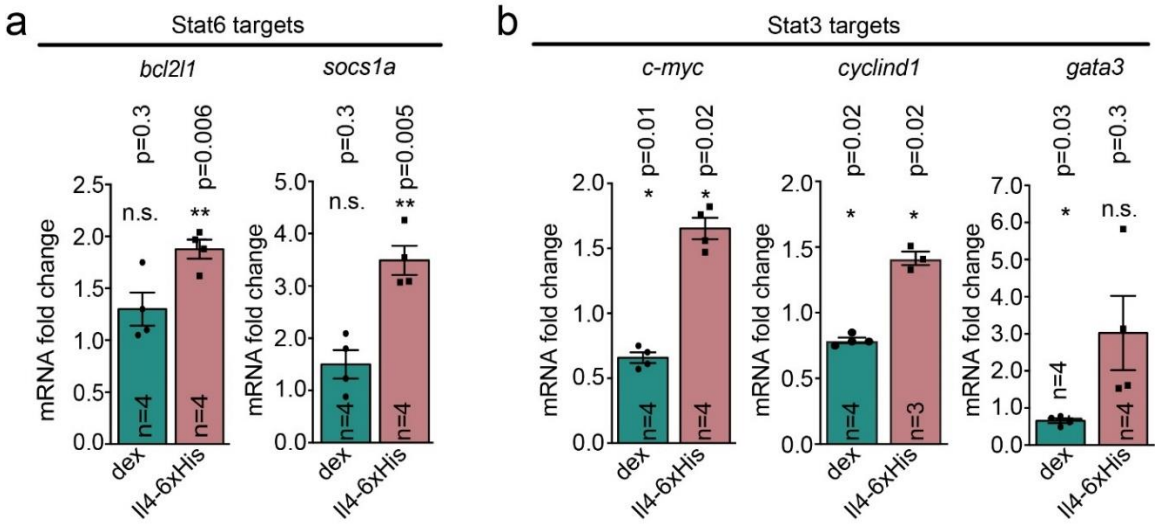

Figure 3.13. Stat3 mediates the proliferation regulatory effects of Il4 and Gr in the larval heart. **a-b**, Graph showing the average mRNA fold change of stat6 downstream genes*; bcl2l1, socs1a* **(a)**, and Stat3 downstream genes; *c-myc, cyclinD1,* and *gata3* **(b)** in the heart of wild-type larvae treated with dex or *Tg(hsp70:il4-6xHIS)*^{md74} larvae overexpressing *il4-6xHis.* Data

are presented as mean ± S.E.M, * $p < 0.05$, ** $p < 0.01$, n.s. not significant. t-test. n indicates biological replicas.

To further confirm the direct effect of Stat3 mediated by Gr and Il4 on cardiomyocyte proliferation, I took advantage of the Cre/Lox system for cardiomyocyte-specific expression of the dominant negative form of Stat3 (DNStat3) in zebrafish larvae. The DNStat3 was previously constructed by a tyrosine-to-phenylalanine mutation in the activation loop preventing tyrosine phosphorylation and shown to inhibit endogenous Stat3 signaling in zebrafish (Conway, 2006). Embryos were exposed to 4-OHT from 1 to 2 dpf to induce DNStat3 specifically in cardiomyocytes, and 5 dpf larvae were treated with either Il4 induction or mif (**Fig. 3.14a,d)**. Proliferating cardiomyocytes in developing hearts were labeled with PCNA and GFP by immunostaining (**Fig. 3.14b, e)**. Interestingly, the expression of DNStat3 in cardiomyocytes impaired cardiomyocyte proliferation and neutralized the mitogenic effect of Il4 induction (**Fig. 3.14b, c)**. Similarly, the positive mitotic effect of mif-mediated Gr inhibition on cardiomyocytes was mitigated in the presence of DNStat3 expression in cardiomyocytes (**Fig. 3.14e, f)**. In consistent with qPCR data, these findings show that Stat3 is a critical regulator of mitotic activity in cardiomyocytes.

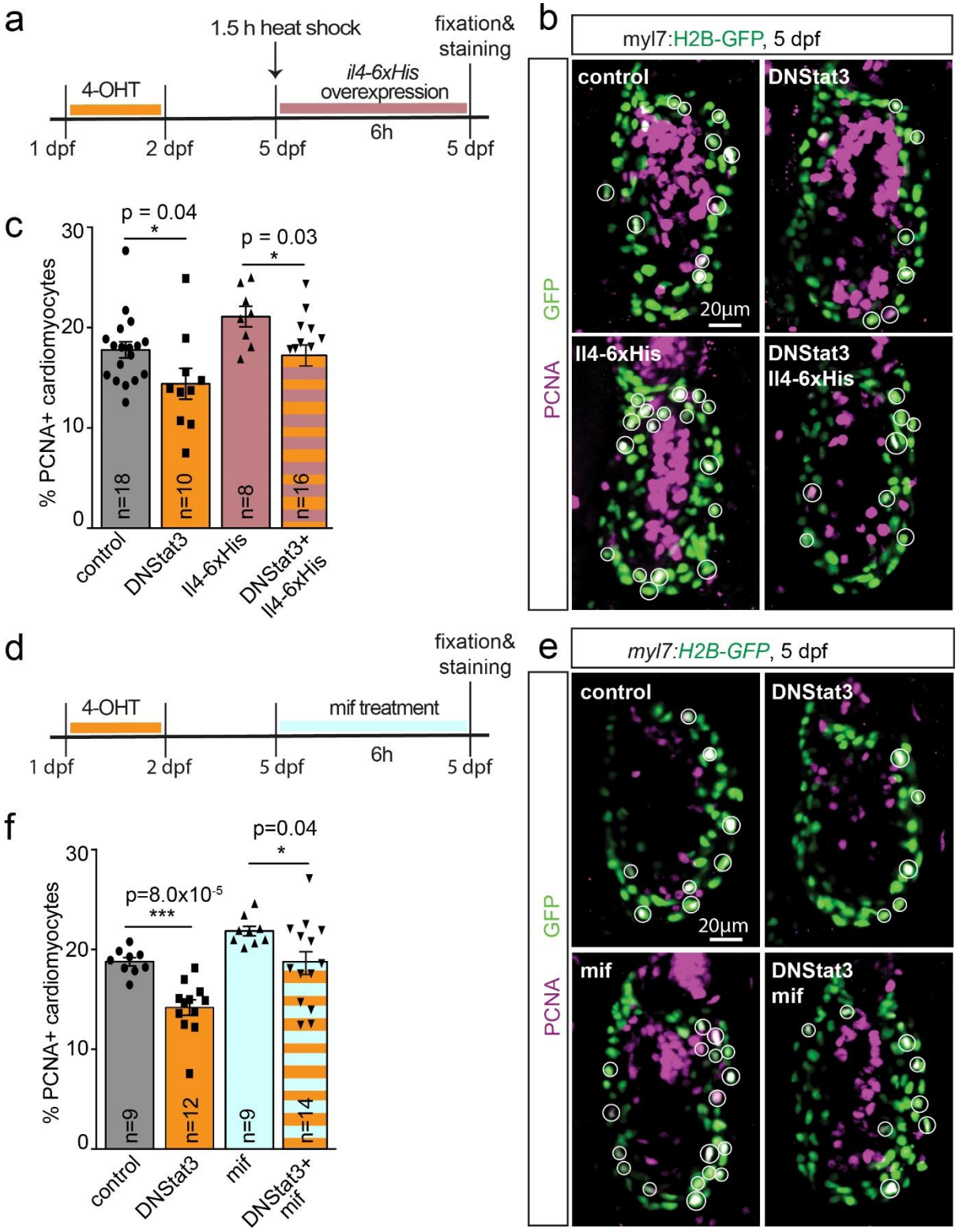

Figure 3.14. Gr-Il4 crosstalk through Stat3 is required to modulate cardiomyocyte proliferation in the developing heart. a, Schematic representation of *il4-6xHis* overexpression treatment performed in b,c. 1 dpf *Tg(hsp70:il4-6xHIS)*^{md74}; *Tg(myl7:H2B-GFP)*^{zf521}; *Tg(myl7:Cre-ERT2)*^{pd12};

Tg(actb2:loxP-DsRed-loxP-dnstat3 EGFP)^{s928} and *Tg(myl7:H2B-GFP)*^{zf521}*; Tg(myl7:Cre-ERT2)*^{pd12}*; Tg(actb2:loxP-DsRed-loxP-dnstat3 EGFP)*^{s928} larvae were treated with 6uM 4-OHT for 24h to express *Cre-ERT2* specifically in cardiomyocytes. 5 dpf larvae were exposed to heat shock at 38 ºC for 1.5h, followed by 6h incubation. **b,** Confocal projections of 5 dpf PCNA and GFP immunostained control, *DNstat3* overexpressing, *il4-6xHis* overexpressing, and *DNstat3 and il4-6xHis* overexpressing larval ventricles. Scale bar: 20 µm. **c,** Graph showing the average percentage of PCNA-positive (PCNA+) cardiomyocytes in the ventricle of control and DNStat3-expressing hearts with and without *il4-6xHis* overexpression. **d,** Schematic representation of mif treatment performed in e,f. *Tg(myl7:H2B-GFP)*^{zf521} *; Tg(myl7:Cre-ERT2)*^{pd12}*; Tg(actb2:loxP-DsRed-loxP-dnstat3 EGFP)*^{s928} larvae were treated with 6uM 4-OHT at 1 dpf for 24h. 2 dpf larvae were treated with 10uM mif until 5 dpf. **e,** Confocal projections of 5 dpf PCNA and GFP immunostained control, *DNstat3* overexpressing, mif treated, and *DNstat3* overexpressing and mif treated larvae. **f**, Graph depicting the average percentage of PCNA-positive (PCNA+) cardiomyocytes upon mif treatment in the ventricle of control and DNStat3-expressing hearts with mif or control treatment. Scale bar: 20 µm. Data are presented as mean ± S.E.M * $p < 0.05$, ***, $p < 0.001$, n.s. not significant. t-test. n indicates the number of larvae used for experiments. The data was generated by Sawamiphak S.

3.1.6 Cell-Autonomous signaling of GC and Il4 regulates the proliferation of cardiomyocytes through modulation of Stat3 activity

GCs are known to be involved in the regulation of growth hormone secretion. Accordingly, the pathological level of GCs was shown to inhibit growth (Mazziotti & Giustina, 2013). The impaired cardiac growth upon dex-mediated Gr activation observed in zebrafish larvae might be a consequence of systemic complications caused by excessive Gr activation. However, the attenuated proliferative rate in the presence of DNStat3 expression, specifically in cardiomyocytes, indicates that Gr and Il4 play a significant role in cardiomyocyte proliferation and affect cardiac development by a cell-autonomous signaling mechanism. To investigate whether cell-autonomous action of Gr and Il4 control mitotic rate, I generated constructs to allow me to activate Gr signaling and inhibit Il4 signaling, specifically in cardiomyocytes using the *myl7* promoter.

First, I generated a plasmid expressing zebrafish *gr* followed by a flexible polypeptide linker and *mKATE* inserted downstream of the *myl7* promoter *(myl7: mKATE-GR)* (**Fig. 3.15a).** To assess the effect of cardiomyocyte-specific Gr overexpression on mitotic activity, I injected

mKATE-GR construct into 1-2 cell stage *Tg(myl7:H2B-GFP)^{zf521}* embryos and performed PCNA immunostaining (**Fig. 3.15b)**. Thanks to the mosaic expression of mKATE-GR, I could assess the proliferative rate of both mKate-GR^{+} and mKate-GR^{-} cardiomyocytes in the same hearts. I noted severely reduced mitotic rates of mKATE-GR^{+} cardiomyocytes compared to mKATE-GR^{-} cardiomyocytes in 5 dpf hearts, providing further support for the anti-mitotic effect of Gr on cardiomyocytes (**Fig. 3.15c)**. Notably, this evidence also reflects that stress-mediated GC rise blocks the cell cycle reentry in a cell in a cell-autonomous way rather than through growth hormone secretion.

Next, I utilized a cell type specific loss of function approach to interfere with endogenous Il4r, specifically in cardiomyocytes. For this purpose, I generated a construct harboring a truncated form of *Il4r* fused to *RFP* and placed downstream of the *myl7* promoter *(myl7:Il4rΔC-RFP)* (**Fig. 3.15a).** Notably, the truncated Il4r lacks the cytoplasmic domain, including Stat docking sites required for downstream transcriptional activity, acting as a dominant negative receptor. Previous *in vitro* studies reported the competitive potential of the truncated IL4R with endogenous IL4 signaling, resulting in suppressed endogenous machinery (Gandhi et al., 2014). I injected Il4rΔC-RFP construct into 1-2 cell stage *Tg(myl7:H2B-GFP)^{zf521}* embryos and assessed the cell proliferation at 5 dpf by PCNA immunostaining (**Fig. 3.15b)**. In consistent with the impairment in cell proliferation seen in larvae injected with (Il4nAB) antibody, I found that a barely detectable level of Il4rΔC-RFP^{+} cardiomyocytes entered the cell cycle in 5 dpf hearts, providing further support for the requirement of Il4 signaling specifically in cardiomyocytes for proliferation in the developing heart (**Fig. 3.15d)**.

Being expressed at very high levels via the myl7 promoter might cause some side effects on cell survival, thereby causing the reduction of cell numbers independently of mitotic control. To test this hypothesis, I assessed the mitotic rate of cardiomyocytes in larvae with the mosaic expression of only the fluorescent cassettes under the control of the *myl7* promoter *(myl7:RFP)* (**Fig. 3.15a).** There was no significant change in percentages of PCNA+ cardiomyocytes between the RFP+ and RFP- populations in the same heart, indicating that RFP expression alone does not alter mitotic rate (**Fig. 3.15b, e).** Comparable levels of the proliferative cardiomyocytes in RFP+ and RFP- populations suggest that mitotic defects observed in mKATE-GR and Il4rΔC-RFP injected hearts are not a consequence of overexpression of the constructs.

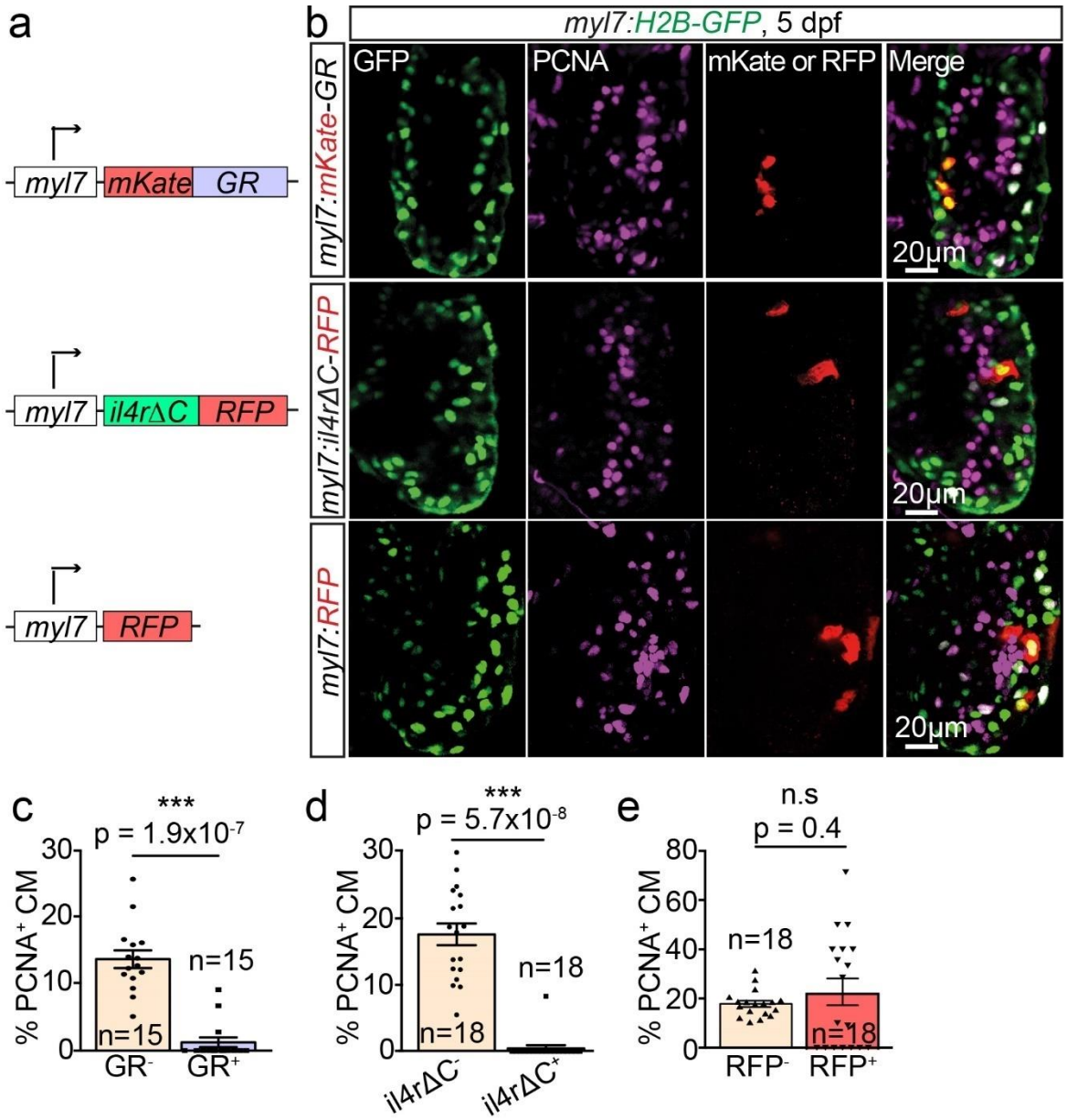

Figure 3.15. Gr and Il4 function as proliferation regulators during cardiac development in a cardiomyocyte-specific manner. a, Schematic representation of transgenic constructs. **b**, Confocal projections of 5 dpf larvae injected with either *myl7:mKate-GR*, *myl7:Il4rΔC-RFP*, or *myl7:RFP* plasmids at the 1-2 cell stage. **c-e**, Graphs demonstrating the average percentage of PCNA-positive (PCNA+) cardiomyocytes containing either mKATE-GR **(c)**, Il4rΔC-RFP **(d)**, or RFP **(e)** in the ventricle of 5 dpf larvae. Scale bar: 20 μm. Data are presented as mean ± S.E.M. * $p < 0.05$, *** $p < 0.001$, n.s. not significant. t-test. n indicates the number of larvae used for experiments.

The cells expressing either *myl7:mKate-GR* or *myl7:Il4rΔC-RFP* constructs might be sick and dying over time, which might be the reason for largely absent proliferative cardiomyocytes in the 5 dpf larval heart. To test this hypothesis, I assessed the cell death by

TUNEL staining and found no increased cell death in larvae injected with either *myl7:mKate-GR*, *myl7:Il4rΔC-RFP*, or *myl7:RFP* plasmids (**Fig. 3.16a)**. Concurrently, live imaging of larvae injected with either *myl7:mKate-GR* or *myl7:Il4rΔC-RFP* showed no change in cell numbers expressing Gr or Il4rΔC in the same larvae at 3 and 5 dpf (**Fig. 3.16b)**. Notably, as expected in normal development, the number of cardiomyocytes expressing only RFP significantly increased in myl7:RFP injected larvae during this developmental stage.

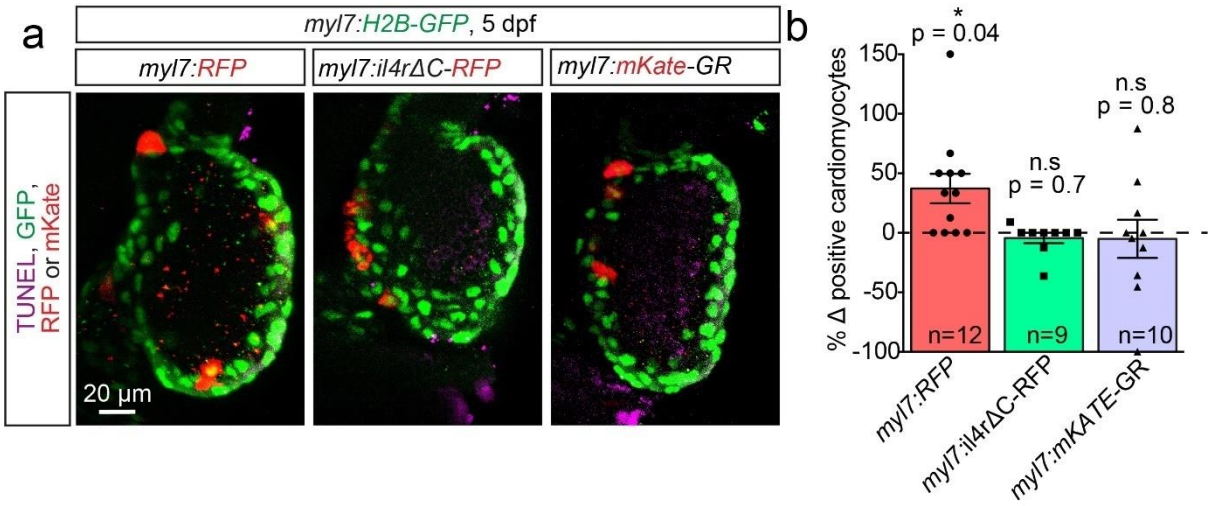

Figure 3.16. Cardiomyocyte-specific overexpression of Gr and dominant negative form of Il4r do not induce cardiomyocyte apoptosis. a, Confocal projections of TUNEL stained larvae injected with either *myl7:mKate-GR*, *myl7:Il4rΔC-RFP*, or *myl7:RFP* plasmids at the 1-2 cell stage. b, Graphs showing the average change of cardiomyocyte numbers in the ventricle between 3 dpf and 5 dpf. Scale bar: 20 µm. Data are presented as mean ± S.E.M. * $p < 0.05$, n.s. not significant, t-test. n indicates the number of larvae used for experiments. Live imaging was performed by Corradi L.

3.1.7 Activation of Gr and Il4 signaling do not alter endocardial and epicardial development

The heart wall is a highly organized tissue consisting of endocardium, myocardium, and epicardium layers. Not only cardiomyocytes but also endothelial and epicardial cells as well as intercellular communications between them play crucial roles in normal cardiac development and function (Bornhorst & Abdelilah-Seyfried, 2021; Kikuchi, Gupta, et al., 2011; Kikuchi, Holdway, et al., 2011; Quijada et al., 2020). I further aimed to address whether the regulatory effect of Gr and Il4 on cardiac development is limited to cardiomyocytes or also influences the

development of other cardiac cells, which might subsequently contribute to structural and functional alterations in the heart. To test this hypothesis, I characterized the morphologies of endocardium and epicardium in response to the manipulation of Il4 and Gr signaling. Interestingly, live imaging of *Tg(fli:nls-mcherry)*^{ubs10}and *Tg(wt1b:EGFP)*^{li1} larvae in which endothelial cells nuclei were labeled with mCherry and epicardial cells were labeled with EGFP, showed no aberrant morphological alterations upon activation of Gr signaling by 3-day dex treatment compared to control siblings (**Fig. 3.17a-c)**. Although dex-treated larvae showed a slight decrease in endothelial cell numbers observed in the ventricle, it was not statistically significant (**Fig. 3.17d)**. In addition, I found epicardial cell numbers were comparable in control and dex-treated larvae (**Fig. 3.17e).**

Similarly, following daily heat-induced Il4 elevation, 5 dpf *Tg(fli:nls-mcherry)*^{ubs10} *Tg(hsp70:il4-6xHIS)*^{md74} and *Tg(wt1b:EGFP)*^{li1} *Tg(hsp70:il4-6xHIS)*^{md74} larvae showed that formations of endocardium and epicardium were not altered in developing heart as evidenced by no overt alterations in morphology (**Fig. 3.17f, g)** and cell number (**Fig. 3.17h, i)**. Taken together, the data showing myocardium restricted effect of Gr and Il4 signaling suggests that Gr and Il4 modulate cardiac development through regulation of cardiomyocyte proliferation.

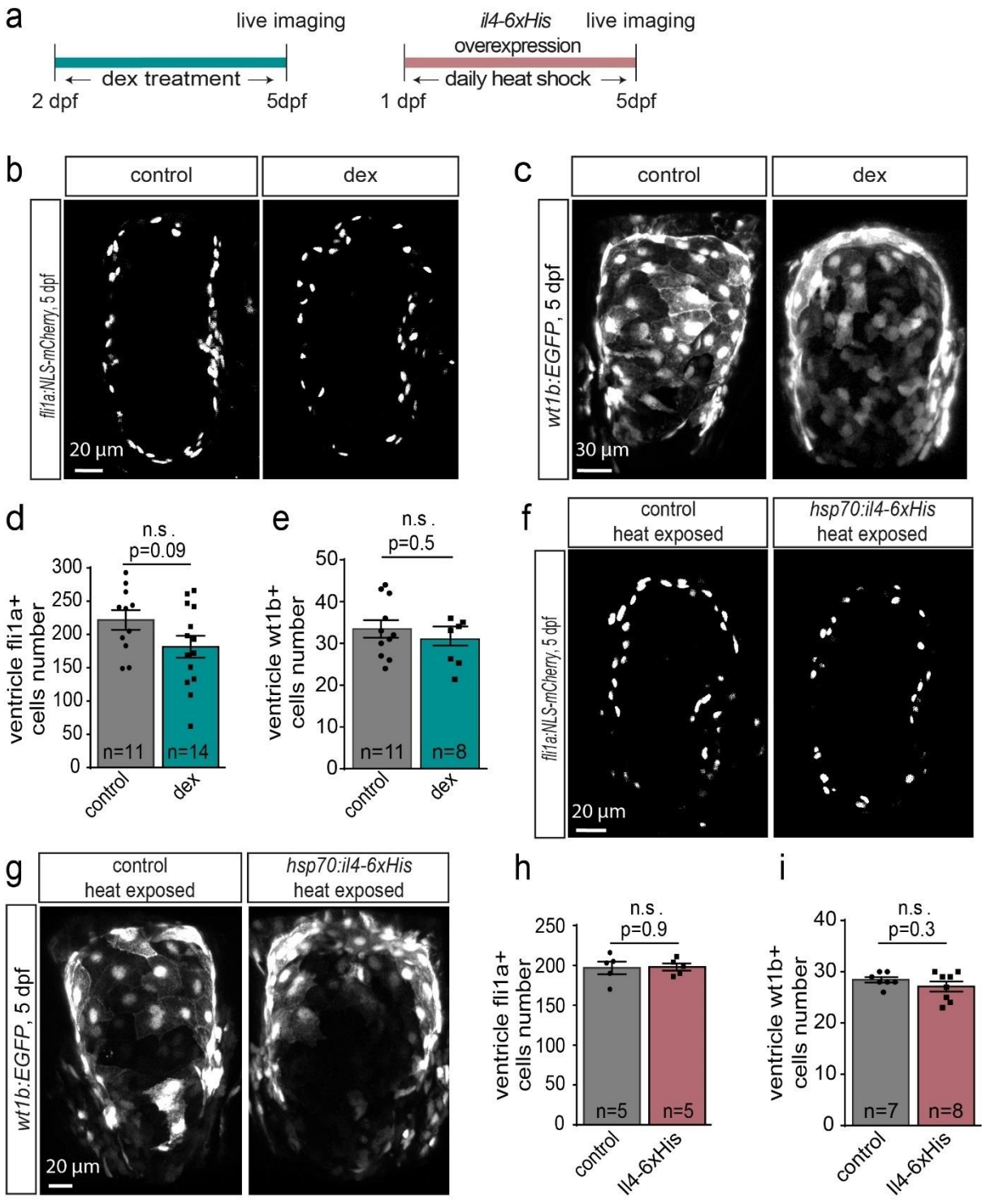

Figure 3.17. Endocardial and epicardial cell numbers are not affected in the presence of Gr and Il4 overactivation. a, Schematic representation of dex treatment and Il4 induction. **b-c,** Confocal projections of dex treated or control 5 dpf *Tg(fli:nls-mcherry)*^{ubs10} ventricle **(b)**, and *Tg(wt1b:EGFP)*^{li1} **(c)** ventricle. Endothelial cell nuclei are labeled with NLS-mCherry. Scale bar: 20 µm. Epicardial cells are labeled with EGFP. Scale bar: 30 µm. **d**, Graph depicting the average numbers of endothelial cells

(fli1a+) in the ventricle of 3-day dex treated or control siblings. **e**, Graph showing the average number of epicardial cells (wt1b+) in the ventricle upon 3-day dex treatment or control. **f**, Confocal projections of 5 dpf *Tg(fli:nls-mcherry)*^{ubs10} larval heart following daily heat-induction for *il4-6xHIS* overexpression. Scale bar: 20 µm. **g**, Confocal projections of 5 dpf *Tg(wt1b:EGFP)*^{li1} larval heart exposed to daily Il4 induction. Scale bar: 20 µm **h**, Graph indicating fli1a+ endothelial cell numbers in the ventricle of *Tg(fli:nls-mcherry)*^{ubs10} larvae upon daily *il4-6xHIS* overexpression. **i**, Graph depicting the average number of wt1b+ epicardial cells in the 5 dpf larvae overexpressing *il4-6xHIS* or control. Data are presented as mean ± S.E.M, n.s. not significant. t-test. n indicates the number of larvae used for experiments. Confocal images were taken by Corradi L.

3.1.8 IL4Rα is indispensable for cardiomyocyte proliferation in neonatal mouse heart

Up to now, in this study, I revealed a previously unknown role of Il4 signaling in heart development. Next, I aimed to reveal whether this pro-mitotic effect is evolutionarily conserved in a higher organism. To test this hypothesis, IL4R-α null mice, which were previously reported to lack the IL4 functional activity (Noben-Trauth et al., 1997), were utilized. Immunostaining was performed using proliferation marker Ki67, labeling cells during G1-M phases as well as the cardiomyocyte marker Troponin T2 (Tnnt2) in sections of P0 hearts (**Fig. 3.18a).** Ki67+ and Tnnt2+ cells were counted to assess cardiomyocyte proliferation in the neonatal heart. *Il4ra*$^{-/-}$ mice exhibited lower percentages of cardiomyocyte entering the cell cycle compared to control *Il4ra*$^{+/+}$ hearts, and to a lesser extent in *Il4ra*$^{+/-}$ hearts, indicating that IL4 signaling is required for cardiomyocyte proliferation also in the developing mouse heart (**Fig. 3.18b)**. Taken together, this data confirms the mitogenic effect of IL4 during cardiac development also in mammals.

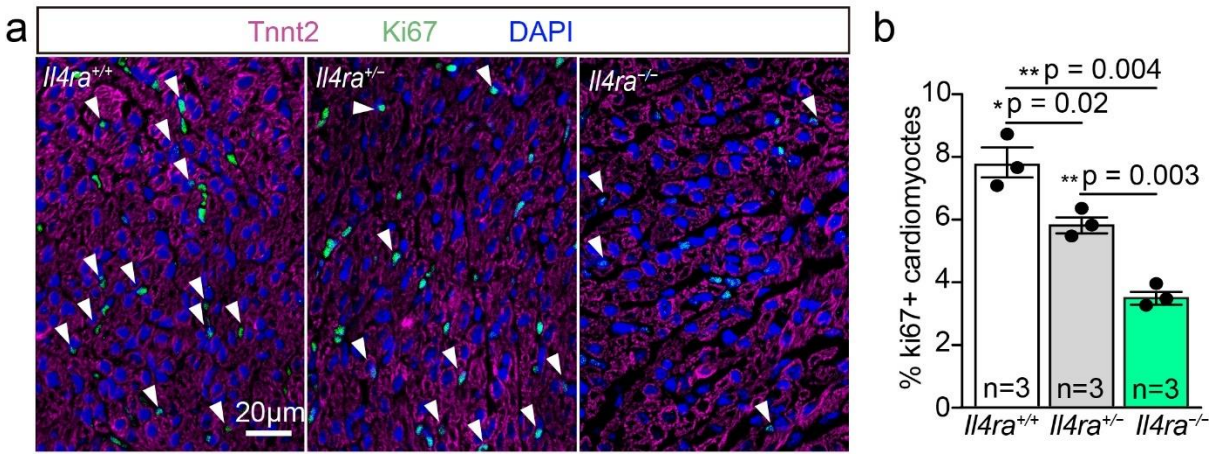

Figure 3.18. IL4Rα loss of function decreases the mitotic rate of cardiomyocytes in neonatal mice. **a**, Confocal projections of P0 heart sections from *Il4ra*$^{+/+}$, *Il4ra*$^{+/-}$, and *Il4ra*$^{-/-}$ mice. Cardiomyocytes and proliferative cells were stained with Tnnt2 and Ki67, respectively. Cell nuclei were marked with DAPI. White arrows indicate proliferative cardiomyocytes (Tnnt2+Ki67+). Scale bar: 20 µm. **b**, Graph showing the average percentage of Ki67+Tnnt2+ cardiomyocytes in P0 *Il4ra*$^{+/+}$, *Il4ra*$^{+/-}$ and *Il4ra*$^{-/-}$ mice. Data are presented as mean ± S.E.M. * $p < 0.05$, ** $p < 0.01$, n.s. not significant, t-test. n indicates the number of mice used for experiments. The data was generated by Morocho-Jaramillo PA.

3.1.9 GR and IL4 signaling regulates the proliferation of mouse cardiomyocytes

The evolutionary conserved pro-mitotic role of IL4 prompted me to investigate further its possible interaction with GR signaling in the developing mouse. For this purpose, I treated cardiomyocytes, which were isolated from P0 neonatal mice and cultured for 2 days, with either dex, recombinant IL4, dex plus recombinant IL4, or a control solution for 24h. Following thymidine analog 5-Ethynyl-2´-deoxyuridine (EdU) incorporation for 12h, immunocytochemistry was performed to assess cardiomyocyte proliferation (**Fig. 3.19a,b)**. In consistent with *in vivo* data obtained from zebrafish larval heart, dex treatment drastically lowered the mitotic activity in cardiomyocytes compared to control (**Fig. 3.19c)**. On the contrary, activation of IL4 signaling significantly increased the cardiomyocyte proliferation rate, similar to my results obtained from the zebrafish heart upon *il4-6xHIS* overexpression (**Fig. 3.19c)**. Importantly, in agreement with the modulatory effect of GR and IL4 crosstalk on cardiomyocyte proliferation noted in zebrafish larvae, mouse cardiomyocytes isolated from developing heart showed an attenuated pro-mitotic effect of IL4 upon dex-mediated GR

activation (**Fig. 3.19c)**. Taken together, these results further support that activation of GR signaling acts as a cardiomyocyte mitotic brake whereas IL4 acts as a mitogenic factor in the developing heart as well as strongly suggest that the antagonistic effect of GC and IL4 on mitotic activity is also conserved in different vertebrates.

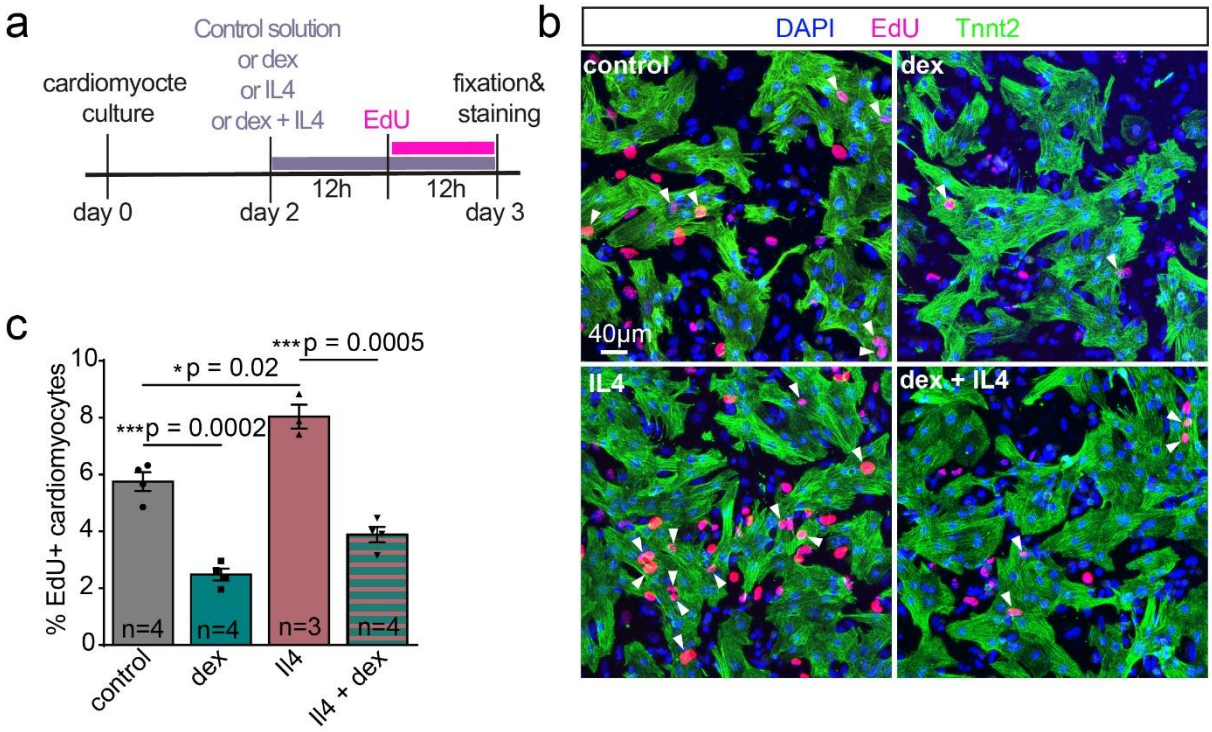

Figure 3.19. Regulation of cardiomyocyte proliferation by GR-IL4 crosstalk is conserved in neonatal mice. a, Representative scheme of control, dex, rIL4, and EdU treatment. **b**, Confocal projections of cultured neonatal mouse cardiomyocytes treated with either control, dex, rIL4, or dex+rIL4 solution. Scale bar: 40 µm. Cardiomyocytes were immunostained with Tnnt2. Proliferating cells were stained with EdU. DAPI was used to label cell nuclei. **c**, Graphs indicating the average percentage of EdU+ cardiomyocytes following the treatment. Data are presented as mean ± S.E.M. * $p < 0.05$, *** $p < 0.000$, t-test. n indicates the number of biological replicates. Isolation of cardiomyocytes from neonatal mice and immunocytochemistry were performed by Rathjen FG. Cardiomyocyte proliferation shown in c was quantified by Sawamiphak S.

3.2 Ifnγ-driven cerebrovascular remodeling in a zebrafish hypertension model

The second part of this chapter will be included in the article "Interferon-γ drives macrophage reprogramming, cerebrovascular remodelling, and cognitive dysfunction in a zebrafish and a mouse model of ion imbalance and pressure overload" Cardiovasc Res. 2023 May 22;119(5):1234-1249 (https://doi.org/10.1093/cvr/cvac188). All experiments and results in this part were performed by Dilem Ceren Apaydin unless otherwise stated in the figure legends.

3.2.1 Establishment of a 5-day ion poor treatment

Underlying mechanisms of hypertension onset and its transition to a more complicated disease state such as HF, are needed to develop effective targeted therapies (Lerman et al., 2019). To gain better insights into cellular and molecular mechanisms governing the incipience of hypertension and associated comorbidities, I established an ion imbalance zebrafish model requiring simple and short manipulation compared to other hypertensive animal models. An ion-poor treatment approach was previously reported to sufficiently promote RAS-dependent Na+ uptake (Kumai et al., 2014). Modifying this previous approach, I reared embryos in standard Danieau's solution until 2 dpf. After that, I divided a clutch of embryos into 2 groups. The experimental group was subjected to gradual reduction of ion concentrations, 750-fold dilution for 2 days, and then 1500-fold dilution until desired age up to 7 dpf, while control embryos were always kept in Danieau's solution (**Fig. 3.20)**.

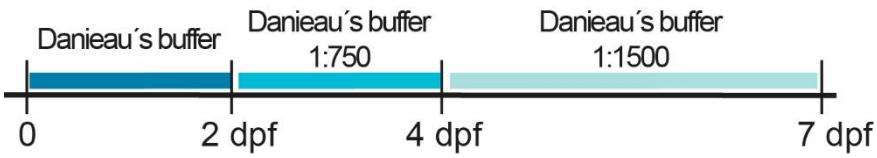

Figure 3.20. Schematic representation of ion-poor treatment. Embryos were reared in Danieau's solution until 2 dpf and then exposed to 750-fold diluted Danieau's solution until 4 dpf, followed by exposure to 1500-fold dilution until desired age up to 7 dpf. Control embryos were kept in Danieau's solution.

3.2.2 Elevated angiotensin and renin expression in response to 5-day ion-poor treatment

Increased blood pressure is a major hallmark of hypertension. RAS is one of the key regulators of blood pressure and water-electrolyte balance. Dysregulated RAS contributes to blood pressure elevation, leading to the development of hypertension (Te Riet et al., 2015a). To address whether the ion imbalance zebrafish model recapitulates excessive RAS activation, I assessed the temporal change of *ang* and *ren* expression by qRT-PCR following 1-3 day ion-poor treatment (**Fig. 3.21)**. I observed a slightly elevated *agt* level, but not *ren*, in the first day of ion-poor treatment (**Fig. 3.21)**. The increase of *agt* mRNA level became significant in response to 2-day ion poor treatment while *ren* remained unchanged. Following 3-day treatment, I detected significantly upregulated *ren* expression and even more increased *agt* expression (**Fig. 3.21)**. Collectively, I showed that ion-poor treatment leads to the gradual activation of RAS mirroring key phenotypes of human HFpEF.

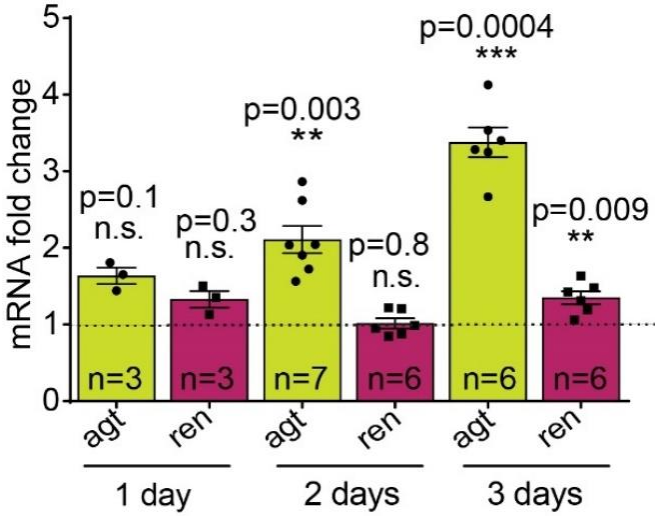

Figure 3.21. The hypertensive zebrafish model exhibits a gradual increase in *agt* expression. Graph showing the average mRNA fold change of *agt* and *ren* in the whole body upon ion-poor treatment. Data are presented as mean ± S.E.M, ** p < 0.01, *** p < 0.001 n.s. not significant. t-test. n indicates biological replicas.

3.2.3 Arterial hypertension in response to 5-day ion-poor treatment

To further characterize the ion imbalance zebrafish model to see whether it can recapitulate the systemic and cardiovascular features of hypertension, I first assessed the blood flow velocity in the dorsal aorta of control or ion-poor treated larvae. It was shown that patients with hypertension exhibit decreased blood flow velocity measured in different vascular beds (A et al., 2003; S et al., 1994; SY et al., 2019; Tsubata et al., 2019). Interestingly, I detected

reduced end-diastolic (**Fig. 3.22a, b)** and peak systolic velocity (**Fig. 3.22a, c)**. Resistive index is a measurement defined from both peak systolic and end-diastolic velocities in vessels, and increased resistive index, which is positively correlated with vascular stiffening, was reported in hypertensive patients (Okura et al., 2004; Viazzi et al., 2014). I calculated resistive index with the formula previously used: (peak systolic velocity - end-diastolic velocity)/ peak systolic velocity (Viazzi et al., 2014) and found that larvae exposed to ion-poor treatment showed higher arterial resistive index compared to control siblings (**Fig. 3.22d)**. Taken together, I showed that 5-day ion poor treatment is sufficient to induce arterial hypertension in zebrafish larvae, recapitulating another key characteristic of human hypertension.

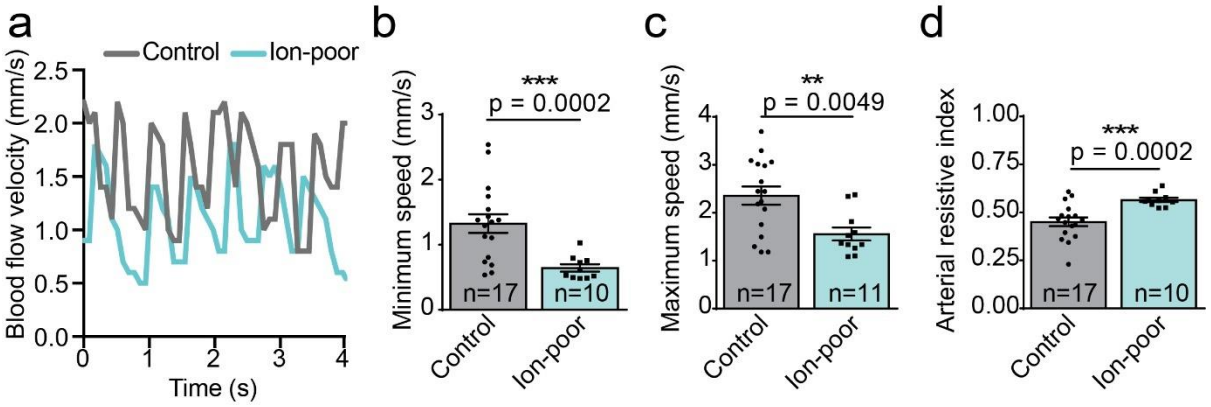

Figure 3.22. 5-day ion poor treatment leads to arterial hypertension in zebrafish larvae. **a**, Line graph showing representative blood flow velocities of control and ion-poor treated larvae. **b-d**, graphs depicting minimum speed (end-diastolic velocity) **(b)**, maximum speed (peak systolic velocity) **(c)**, and arterial resistive index **(d)** in control and ion-poor treated larvae. Data are presented as mean ± S.E.M. ** $p < 0.01$, *** $p < 0.001$, t-test. n indicates the number of larvae used for experiments.

3.2.4 Diastolic dysfunction in the zebrafish model of ion imbalance

Cardiac dysfunction was widely implicated in hypertensive heart disease. Particularly, diastolic dysfunction indicating impaired myocardium relaxation and filling, is a critical sign for transition to HFpEF (Drazner, 2011). To address whether the zebrafish model of ion imbalance phenotypes the functional alterations in the heart detected in patients with HFpEF, ventricles of zebrafish larvae exposed to 5-days treatment either with ion-poor or control solution were imaged by a high-speed camera. Diastolic function was assessed by calculating

diastolic speed based on ventricular movement during relaxation. I found that ion-poor treatment reduces diastolic speed, reflecting impaired ventricular relaxation ability (**Fig. 3.23a).** Although I noticed a subtle decrease in systolic speed calculated based on ventricular movement during contraction, it was not significantly different between ion-poor and control treated larvae (**Fig. 3.23b).** Further functional characterizations revealed that neither EF (**Fig. 3.23c)** nor FS (**Fig. 3.23d)** was altered upon ion-poor treatment. Taken together, these results show that larvae exposed to 5-day ion-poor treatment show diastolic dysfunction but preserved systolic functions, resembling HFpEF characteristics in humans.

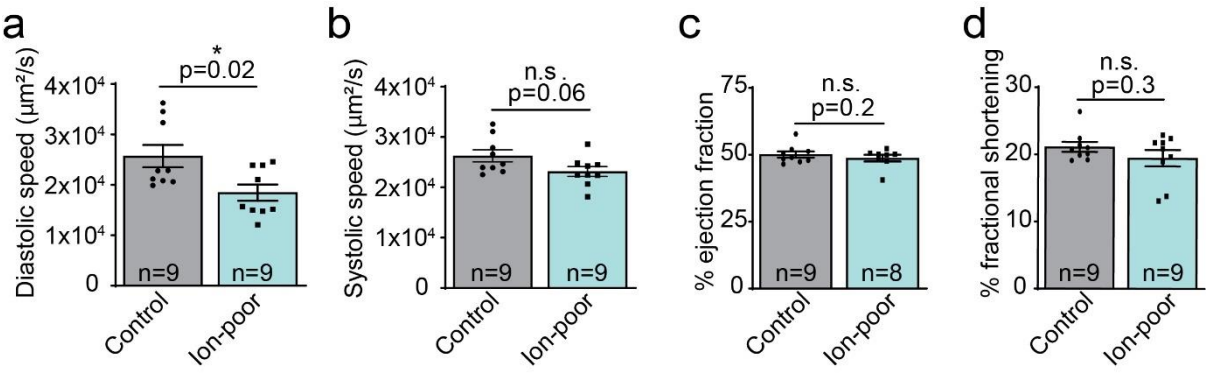

Figure 3.23. Diastolic, but not systolic, function is impaired in the hypertensive zebrafish model. Graphs presenting average diastolic speed calculated from ventricular movement during relaxation **(a)**, systolic speed calculated based on ventricular movement during contraction **(b)**, EF **(c)**, and FS **(d)** in 7 dpf larvae upon control or ion poor treatment. Data are presented as mean ± S.E.M. * $p < 0.05$, n.s. not significant, t-test. n indicates the number of larvae used for experiments.

3.2.5 Hypertrophic remodeling of heart in the zebrafish model of ion imbalance

As functional abnormalities are common consequences of adverse structural remodeling in the heart, I reasoned that hypertensive cardiac remodeling might underlie the impaired mechanical relaxation in ion-poor induced hypertensive zebrafish. Ventricular hypertrophy is the most common morphological abnormality reported in cardiac response to hypertension. To compensate for sustained pressure overload induced by hypertensive stimuli, cardiomyocytes are known to undergo hypertrophic transformation, which can ultimately progress to maladaptive failure (Rossi & Carillo, 1991; Schiattarella & Hill, 2015). To address whether 5-

day ion-poor treatment leads to pathological adaptation of cardiomyocyte populations in hypertension response, I performed live imaging of *Tg(myl7:H2B-GFP)*^{zf521}*; Tg(myl7:mKate-CAAX)*^{sd11} larvae treated with either ion-poor or control solution (**Fig. 3.24a)**. Following 5-day ion-poor treatment, larvae showed enlarged cardiomyocyte volume in the compact layer of the ventricle compared to control siblings (**Fig. 3.24b)**, indicating hypertrophic cardiomyocyte growth.

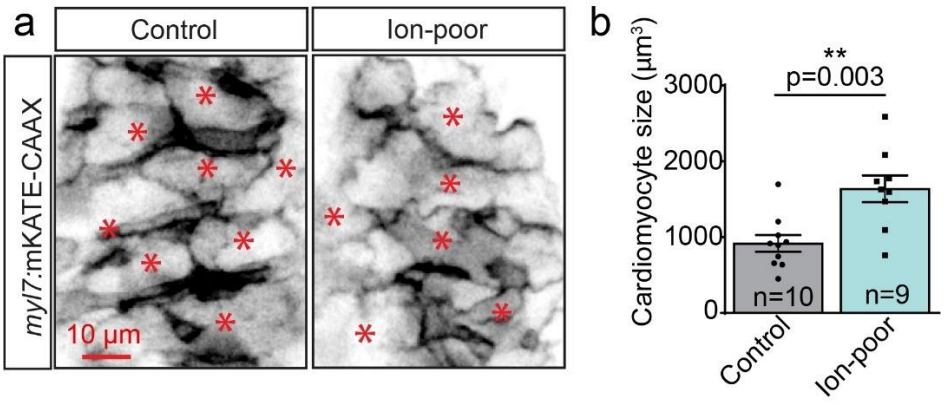

Figure 3.24. 5-day ion poor treatment leads to cardiomyocyte hypotrophy in zebrafish larvae. **a,** Confocal projection displaying ventricle of 7 dpf *Tg(myl7:mKate-CAAX)*^{sd11} larvae exposed to 5-day ion poor treatment or control solution. Cardiomyocyte membranes are labeled with mKate-CAAX. **b**, Graph showing the average cardiomyocyte size in the compact layer of the ventricle upon 5-day ion poor treatment or control solution. Scale bar: 10 µm. Data are presented as mean ± S.E.M. ** $p < 0.01$, t-test. n indicates the number of larvae used for experiments. Quantification of cardiomyocyte size was performed by Sawamiphak S.

Cardiomyocyte loss due to cell death was associated with the duration and severity of hypertension (Ravassa et al., 2007). To further investigate how zebrafish heart responds to ion-poor hypertensive stimuli, I examined *Tg(myl7:H2B-GFP)*^{zf521}*; Tg(myl7:mKate-CAAX)*^{sd11} larvae following 5-day ion-poor treatment (**Fig. 3.25a, c)**. Interestingly, cardiomyocyte numbers were comparable in control and ion-poor treated larvae (**Fig. 3.25b)**. In addition, ion-poor treated larvae exhibited unaltered ventricular volume (**Fig. 3.25d).** These data, together with cardiomyocyte hypertrophy, imply the development of concentric hypertrophy in response to ion-poor hypertensive stimuli.

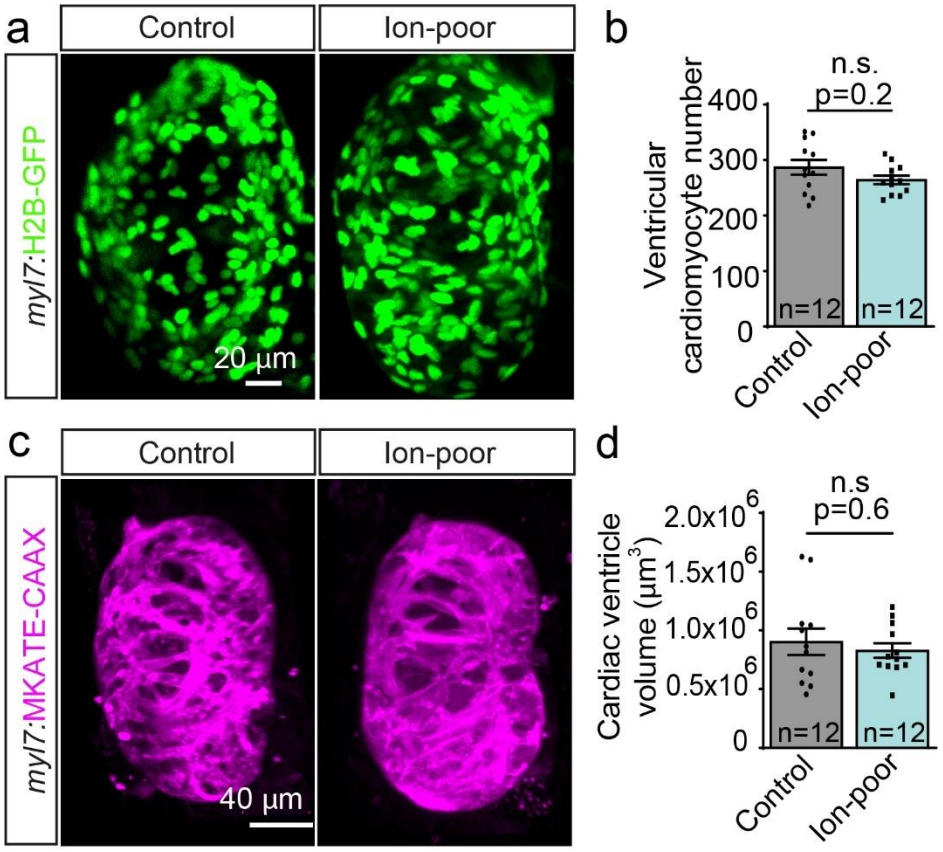

Figure 3.25. Hypertensive ion poor treatment does not affect ventricular cardiomyocyte number and ventricle size. **a**, Confocal images of 7 dpf control or ion poor treated *Tg(myl7:H2B-GFP)*^{zf521} larval hearts. Cardiomyocyte nuclei are labeled with H2B-GFP. Scale bar: 20 µm. **b**, Graph depicting the average cardiomyocyte number in the ventricle upon 5-day ion poor treatment or control solution. **c,** Confocal images of 7 dpf *Tg(myl7:mKate-CAAX)*^{sd11} larval treated with control or ion-poor treatment. Cardiomyocyte membranes are labeled with mKate-CAAX. Scale bar: 40 µm. **d**, Graph showing the average ventricle volume in zebrafish larvae following 5-day control or ion-poor treatment. Data are presented as mean ± S.E.M., n.s. not significant, t-test. n indicates the number of larvae used for experiments. Quantification of ventricular volume shown in d was done by Cosco F.

3.2.6 Vascular regression and increased cell death in hypertensive brain

The vascular structure is one of the target organs affected by hypertension, and vessels commonly undergo remodeling in response to hypertensive stimuli. Regression of the vessels in different vascular beds was reported in hypertensive patients as well as hypertensive animal models (François Feihl et al., 2006). To examine vascular structures in response to ion-poor hypertensive stimuli, trunk and brain of 5 dpf *kdrl:HRAS-mCherry* transgenic larvae labeling

endothelial cells with HRAS-mCherry were imaged following 3-day treatment (**Fig. 3.26a, c**). Interestingly, larvae exposed to ion-poor treatment for 3 days displayed no abnormal vasculature morphology in the trunk containing the balanced network of major artery and vein (**Fig. 3.26a**). To assess vessel regression, vascular density was calculated as a percentage of total tissue volume. While it was not altered in the trunk (**Fig. 3.26b**), reduction of vessel density was observed in the brain (**Fig. 3.26d**), indicating cerebrovascular regression.

Apoptosis of endothelial cells was suggested as a primary mechanism of hypertensive vascular regression (Ravassa et al., 2007). To reveal mechanisms of cerebrovascular regression in response to ion-poor mediated hypertensive stimuli, apoptosis of endothelial cells was assessed by terminal deoxynucleotidyl transferase dUTP nick end labeling (TUNEL) assay (**Fig. 3.26c**). Intriguingly, there was no significantly increased endothelial cell death in the brain vasculature of larvae exposed to ion-poor treatment (**Fig. 3.26e**). In contrast, increased parenchymal cell death in the brain after 3-day ion-poor treatment was observed (**Fig. 3.26f**). Concurrently, reduced brain volume was detected following 5-day ion-poor treatment (**Fig. 3.26g**). This data indicates that another mechanism, rather than endothelial cell apoptosis, might drive cerebrovascular regression in hypertension response.

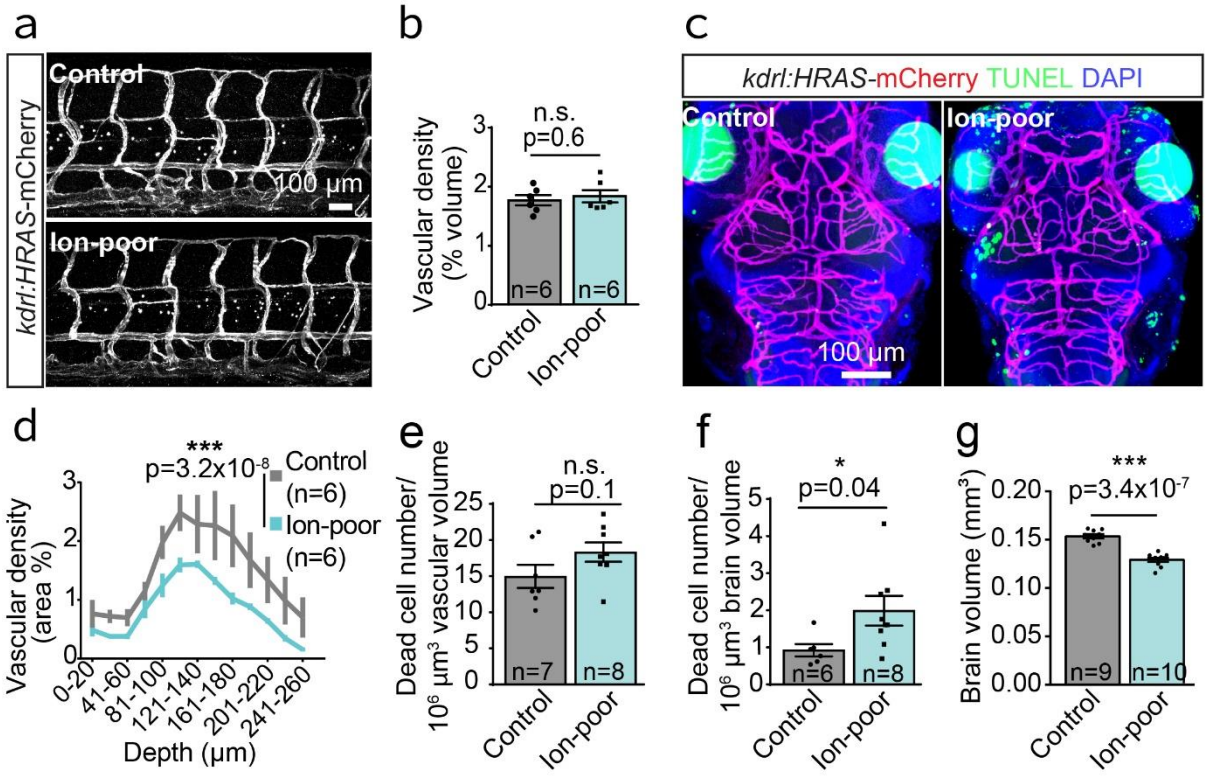

Figure 3.26. Hypertensive stimuli induce cerebrovascular regression and non-endothelial cell death in the zebrafish brain. **a,** Confocal projection of trunk in 5 dpf *Tg(kdrl:Hsa.HRAS-mCherry)*^{s896} larvae exposed to 3-day ion poor treatment or control solution. Endothelial cells were labeled with HRAS-mCherry. **b,** Graph displaying vascular density in the trunk of 3-day ion poor treated or control siblings. **c,** Confocal projection of 5 dpf *Tg(kdrl:Hsa.HRAS-mCherry)*^{s896} brain of 3-day ion poor treated or control siblings. Death cells were labeled with TUNEL, and cell nuclei were labeled with DAPI. **d,** Graph showing cerebrovascular density throughout the brain parenchyma in 5 dpf larvae treated with ion poor or control solution for 3 days. **e-f,** Graphs depicting TUNEL+ dead cell number in the cerebral vessels **(e)** and brain parenchyma **(f)** in ion-poor treated and control siblings. **g,** Graph displaying the average brain volume of 7 dpf larvae treated with control or ion-poor solution for 5 days. Scale bar: 100 µm. Data are presented as mean ± S.E.M., * $p < 0.05$, *** $p < 0.001$ n.s. not significant, t-test. n indicates the number of larvae used for experiments. The data was generated by Seth B and Sawamiphak S.

3.2.7 Macrophage-endothelial cell interaction and endothelial cell retraction mediate cerebrovascular regression

Independent of apoptosis, pruning and trimming of vascular beds, including endothelial cell retraction, migration, and redeployment in the remaining vasculature, occur during developmental vascular remodeling (Franco et al., 2015; Korn & Augustin, 2015; Lenard et al., 2015). However, it is unknown whether these dynamic endothelial cell rearrangements are involved in hypertensive cerebrovascular remodeling. Furthermore, monocytes/macrophages, which are key mediators of inflammation, were reported to play a critical role in vascular remodeling induced by hypertension (De Ciuceis et al., 2005; Javeshghani et al., 2013; Leibovitz et al., 2009; Wenzel et al., 2011). To assess these cellular processes as well as possible alteration of macrophage behaviors in ion-poor induced hypertensive brain vasculature, time-lapse imaging of *Tg(kdrl:Hsa.HRAS-mCherry)*^{s896}*; TgBAC(csf1ra:GAL4-VP16)*^{i186}*; UAS:EGFP* transgenic larvae labeling endothelial cells with mCherry and monocytes/macrophages with EGFP, was performed. Similar vessel regression process observed in the vascular remodeling of developing vessels in which endothelial cells retracted from the same vascular segment and migrated away was noticed in larvae exposed to 2-day ion-poor treatment, whereas this process was detected scarcely in control siblings (**Fig. 3.2a).** Interestingly, monocyte/macrophage interactions with endothelial cells in hypertensive brains

were noted. Surprisingly, these macrophage-endothelial cell contacts were detected preceding vessel regression in the brain (**Fig. 3.27),** suggesting a role for this contact in the vessel regression process.

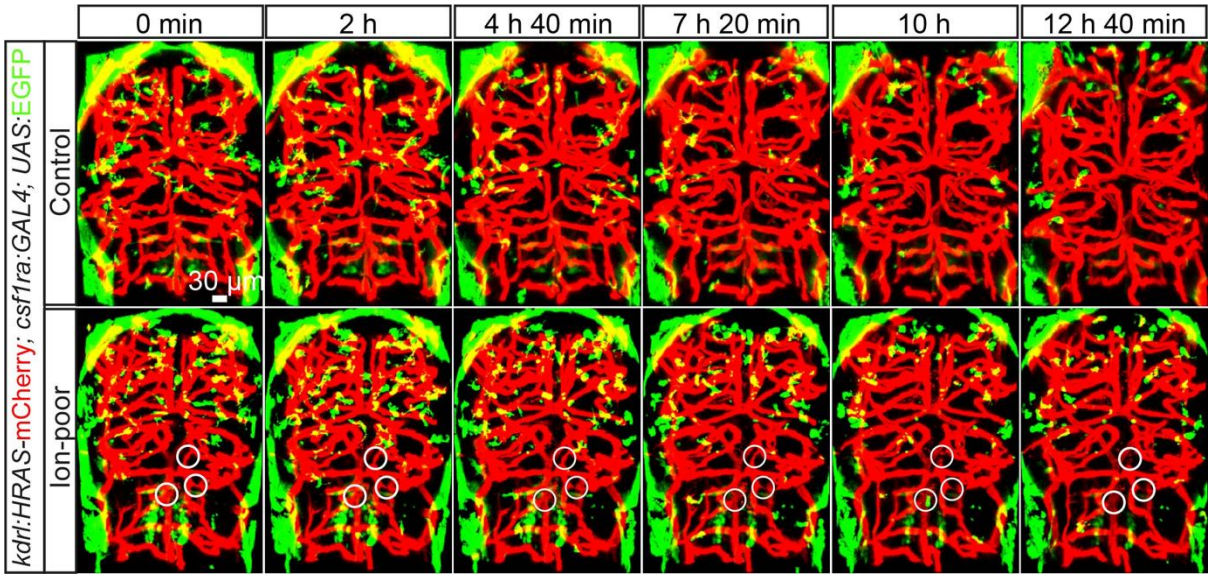

Figure 3.27. Cerebrovascular regression occurs through endothelial cell retraction and migration in the hypertensive zebrafish brain. Time-lapse imaging of 4 dpf *Tg(kdrl:Hsa.HRAS-mCherry)*^{s896}, *TgBAC(csf1ra:GAL4-VP16)*^{i186}, *Tg(UAS:EGFP)* larvae at 2 days of ion poor treatment and control siblings. Endothelial cells were labeled with HRAS-mCherry, and macrophage/microglia were labeled with EGFP. White circles indicate endothelial retraction events. Representative images were selected frames obtained from the movie. Scale bar: 30 µm. The data was generated by Seth B and Apaydin O.

3.2.8 Induction of Systemic Inflammation in the ion-poor-induced hypertensive response

Several pro-inflammatory cytokines, including IL1β, IL17, TNFα, and IL6, shape and exaggerate hypertensive response through mechanisms that remain to be determined (Bautista et al., 2005; De Ciuceis et al., 2017; Dörffel et al., 1999). To investigate the dynamics of the relationship between the progression of hypertension and the elevation of pro-inflammatory cytokines, I assessed the expression level of several cytokines, which are associated with hypertension, at different time points by qPCR. Expression levels of *ifng, il1b, il6, il12, tnfa,* and *il10* were unaffected in the presence of 1-day ion-poor treatment (**Fig.3.28a)**. However, 2

days of treatment led to a slight upregulation (approximately 1.5 folds) of the pro-inflammatory cytokine *ifng* and *il1b*, although it was not statistically meaningful (**Fig.3.28b)**. Importantly, larvae exposed to prolonged ion-poor treatment until 3 days exhibited significant elevation of *ifng* (over 2-fold) and *il1b* (over 8-fold) mRNA levels (**Fig.3.28c)**, suggesting induction of systemic inflammation in response to ion-poor mediated hypertensive stimuli.

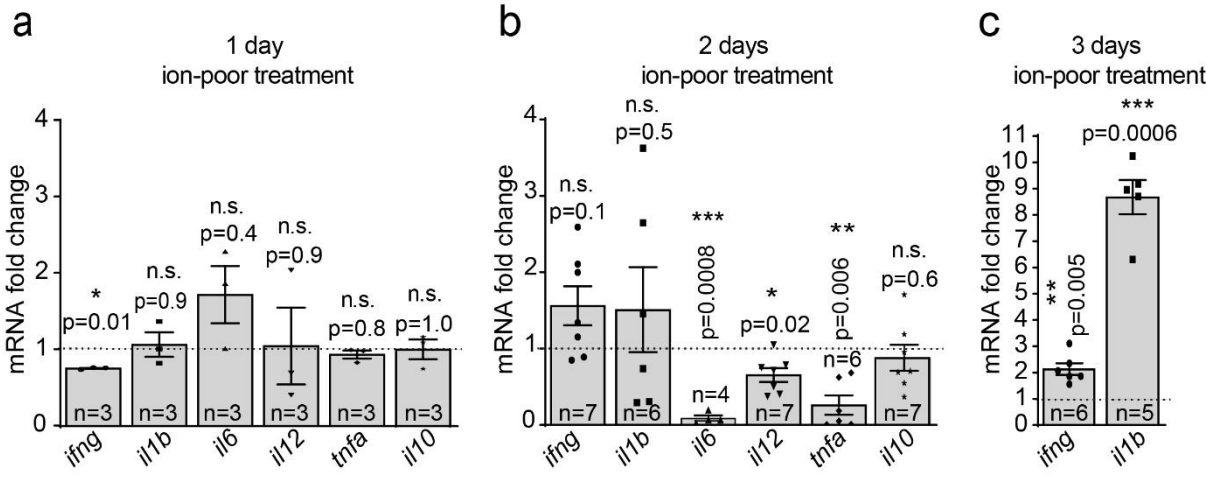

Figure 3.28. Hypertensive ion-poor treatment induces progressive elevation of systemic inflammation characterized by *ifng* and *il1b* upregulation. Graphs depicting mRNA fold change of the cytokines detected by qRT-PCR at 1 day (a), 2 days (b), and 3 days (c) of ion-poor treatment. Data are presented as mean ± S.E.M, * $p < 0.01$, ** $p < 0.01$, *** $p < 0.001$ n.s. not significant. t-test. n indicates biological replicas.

3.2.9 Downregulation of homeostasis and neuroprotection-related genes in macrophages in response to hypertensive stimuli

IFNγ is known to be involved in macrophage polarization towards the inflammatory phenotype. Subsequently, these classically activated macrophages further promote inflammation by secreting pro-inflammatory cytokines such as IL1β (DM et al., 2008; Pelegrin & Surprenant, 2009). My findings, together with previous reports, suggest an intriguing hypothesis that elevation of *ifng* might be the signature event affecting macrophage function and promoting their contact with brain vessels, ultimately leading to regression. To this end, a better understanding of the role of macrophages in hypertension-driven vascular remodeling is required. To gain further insight into downstream signaling, Ifnγ loss of function approach was

employed to test change in the transcriptional profile of control or hypertensive monocytes/macrophages. 3 dpf *TgBAC(csf1ra:GAL4-VP16)^{i186}; Tg(UAS-E1B:NTR-mCherry)^{c264}* larvae, which were exposed to 1day ion-poor or control treatment (prior to induction of systemic inflammation and cerebrovascular regression), were intrapericardially injected with either anti-Ifnγ antibody to mitigate Ifnγr1 signaling or V5 antibody as a control (**Fig.3.29a)**. After 3-day of treatment, control and hypertensive monocytes/macrophages were sorted by FACS (**Fig.3.29b)** and analyzed RNA-seq (**Fig.3.29c-e)**.

Interestingly, differential expression analysis pointed out dampened innate immune and tissue homeostatic function of macrophages in hypertensive response (**Fig.3.29c,d)**. Particularly, the expression of disintegrin and metalloproteinase domain 10b (*ada10b*), histidine ammonia-lyase (*hal*), and lysine demethylase 5A (*kdm5a*), which are critical genes related to anti-inflammatory response and resolution of inflammation, were downregulated in ion-poor treated macrophages. Moreover, complement factor H related 5 (*cfhl5*) and bactericidal and innate immune effector peptides NK-lysin (*nkl.3 and nkl.4*), which are involved in complement system regulation, were also suppressed in hypertensive macrophages (**Fig.3.29c, d)**. Importantly, ion-poor mediated hypertensive stimuli blunted the neuro and vascular protective factors including *bmp5*, nucleobindin 2a (*nucb2a*), and plexin D1 (*plxnd1*) (**Fig.3.29c,d)**. Notably, blocking Ifnγ signaling with anti-Ifnγ antibody injection rescued the expression of these critical genes (**Fig.3.29c,e)**.

Figure 3.29. Ifnγ signaling drives alteration of macrophage phenotype in response to hypertensive stimuli. a, Control and ion-poor treated 5 dpf *TgBAC(csf1ra:GAL4-VP16)^{i186}; Tg(UAS-E1B:NTR-mCherry)^{c264}* larvae, which were subjected to either anti-V5 or anti-Ifnγ injection at 3 dpf, were utilized to isolate macrophages by FACS for RNA-seq. **b,** Heatmap illustrating the genes differentially expressed in control injected with anti-V5 and hypertensive macrophages injected with either anti-V5 or Ifnγ (adjusted p-value < 0.05). **c-d,** Volcano plots depicting upregulated (red) and downregulated (blue) genes in ion-poor treated macrophages compared to control macrophages (c) as well as ion-poor+anti-Ifnγ compared to ion-poor treated macrophages (d). Grey dots depict the genes at similar levels between groups. RNA-seq was performed by utilizing 3 biological replicates per each group. Antibody injection and FACS were performed by Apaydin O. Sample preparation was performed by Seth B. RNA-seq analysis was done by Goldaper IK.

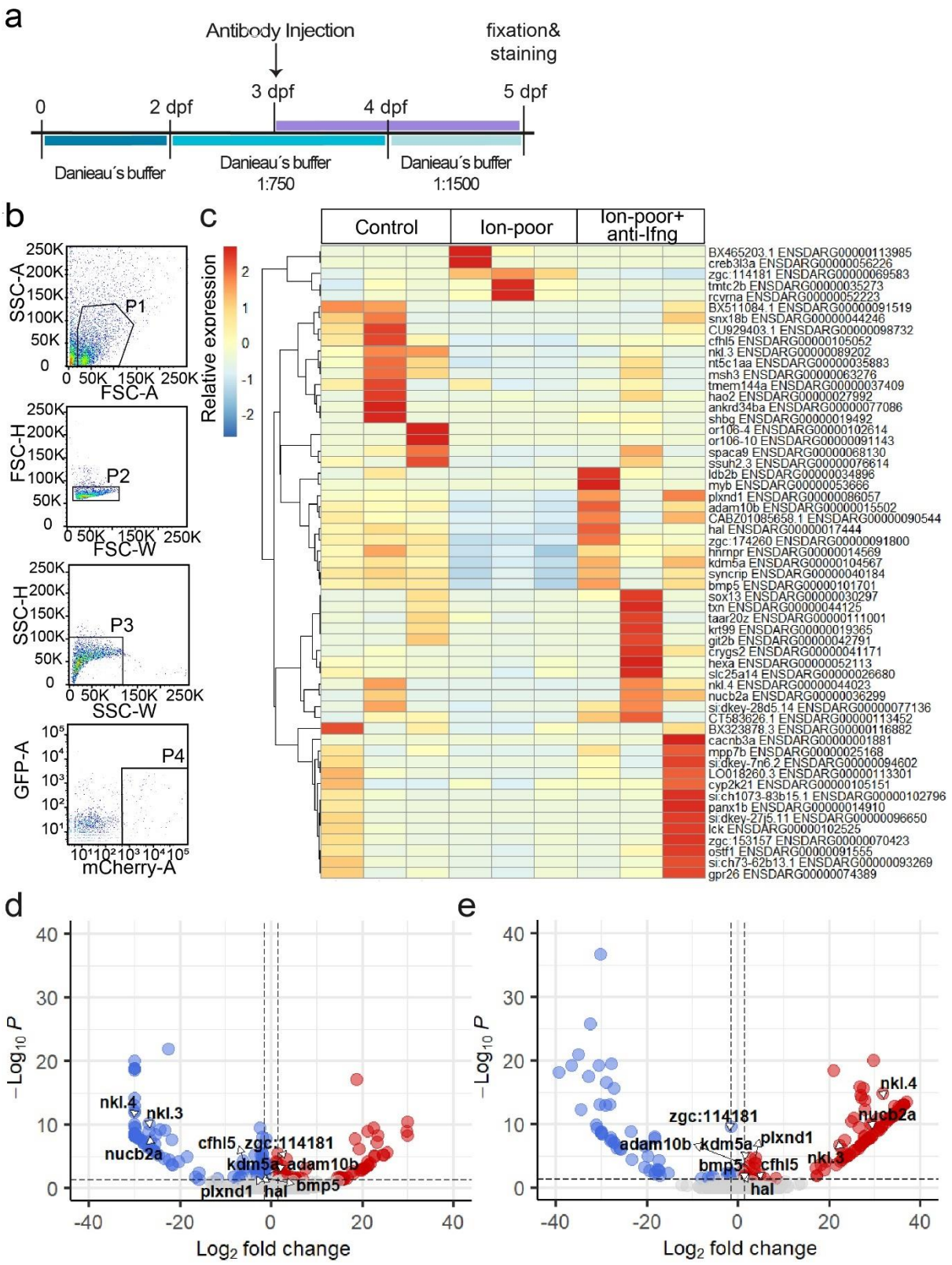
a
Antibody Injection
fixation&
staining
0
2 dpf
3 dpf
4 dpf
5 dpf
Danieau´s buffer
Danieau´s buffer
1:750
Danieau´s buffer
1:1500
b
SSC-A
FSC-A
P1
FSC-H
FSC-W
P2
SSC-H
SSC-W
P3
GFP-A
mCherry-A
P4
c
Control
Ion-poor
Ion-poor+
anti-Ifng
Relative expression
BX465203.1 ENSDARG00000113985
creb3l3a ENSDARG00000056226
zgc:114181 ENSDARG00000069583
tmtc2b ENSDARG00000035273
rcvrna ENSDARG00000052223
BX511084.1 ENSDARG00000091519
snx18b ENSDARG00000044246
CU929403.1 ENSDARG00000098732
cfhl5 ENSDARG00000105052
nkl.3 ENSDARG00000089202
nt5c1aa ENSDARG00000035883
msh3 ENSDARG00000063276
tmem144a ENSDARG00000037409
hao2 ENSDARG00000027992
ankrd34ba ENSDARG00000077086
shbg ENSDARG00000019492
or106-4 ENSDARG00000102614
or106-10 ENSDARG00000091143
spaca9 ENSDARG00000068130
ssuh2.3 ENSDARG00000076614
ldb2b ENSDARG00000034896
myb ENSDARG00000053666
plxnd1 ENSDARG00000086057
adam10b ENSDARG00000015502
CABZ01085658.1 ENSDARG00000090544
hal ENSDARG00000017444
zgc:174260 ENSDARG00000091800
hnrnpr ENSDARG00000014569
kdm5a ENSDARG00000104567
syncrip ENSDARG00000040184
bmp5 ENSDARG00000101701
sox13 ENSDARG00000030297
txn ENSDARG00000044125
taar20z ENSDARG00000111001
krt99 ENSDARG00000019365
git2b ENSDARG00000042791
crygs2 ENSDARG00000041171
hexa ENSDARG00000052113
slc25a14 ENSDARG00000026680
nkl.4 ENSDARG00000044023
nucb2a ENSDARG00000036299
si:dkey-28d5.14 ENSDARG00000077136
CT583626.1 ENSDARG00000113452
BX323878.3 ENSDARG00000116882
cacnb3a ENSDARG00000001881
mpp7b ENSDARG00000025168
si:dkey-7n6.2 ENSDARG00000094602
LO018260.3 ENSDARG00000113301
cyp2k21 ENSDARG00000105151
si:ch1073-83b15.1 ENSDARG00000102796
panx1b ENSDARG00000014910
si:dkey-27j5.11 ENSDARG00000096650
lck ENSDARG00000102525
zgc:153157 ENSDARG00000070423
ostf1 ENSDARG00000091555
si:ch73-62b13.1 ENSDARG00000093269
gpr26 ENSDARG00000074389
d
−Log10 P
Log2 fold change
nkl.4
nkl.3
nucb2a
cfhl5
zgc:114181
kdm5a
adam10b
bmp5
plxnd1
hal
e
−Log10 P
Log2 fold change
zgc:114181
adam10b
kdm5a
plxnd1
bmp5
cfhl5
nkl.3
hal
nkl.4
nucb2a

3.2.10 Anti-Ifnγ treatment mitigates hypertensive cerebrovascular regression

Transcriptome analysis showing altered macrophage phenotype in hypertensive response and its prevention by anti-Ifnγ treatment suggest a pivotal role for Ifnγ signaling in the progression of hypertension. Specifically, the rescued genes involved in vasculo/neuro protective function of hypertensive macrophages upon anti-Ifnγ treatment indicates that Ifnγ signaling might drive the rarefaction in brain vasculature caused by ion-poor mediated hypertensive stimuli. To further address this hypothesis, cerebrovascular regression was assessed in 5-day ion-poor or control treated *Tg(kdrl:Hsa.HRAS-mCherry)*^{s896} larvae subjected to either anti-V5 or anti- Ifnγ injection at 3-days of treatment, a stage where cerebrovascular regression was notable (**Fig.3.30a,b)**. Consisted with vascular regression as observed in 3-day ion poor treated larval brain, 5-day treatment resulted in decreased vascular density in the brain of *Tg(kdrl:Hsa.HRAS-mCherry)*^{s896} larvae (**Fig.3.30b,c)**. Interestingly, blockage of Ifnγ signaling restored this hypertensive cerebrovascular regression (**Fig.3.30b, c)**. These data indicate that rarefaction detected in the brain vasculature in response to hypertensive stimuli is, at least partially, mediated by Ifnγ signaling, highlighting a causal role of Ifnγ in hypertensive cerebrovascular remodeling.

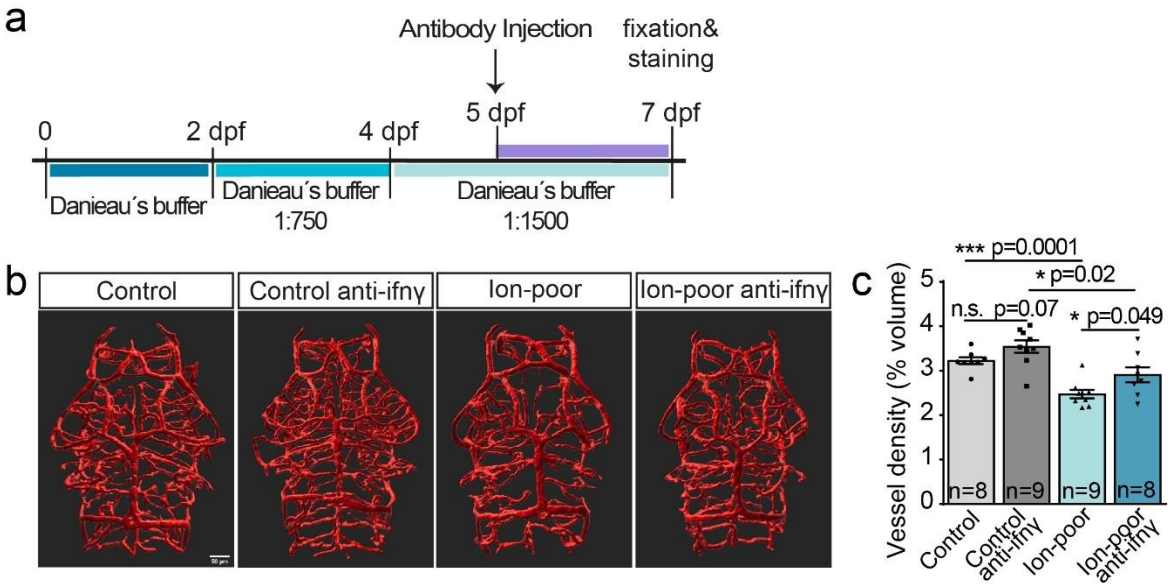

Figure 3.30. Ifnγ inhibition partly rescues cerebrovascular regression in hypertensive zebrafish. **a,** Schematic representation of antibody injection and ion-poor treatment. Anti-V5 or anti-Ifnγ antibodies were injected into the pericardial sac at 3 days of ion-poor treatment, and cerebral vasculature was examined at 5-days of ion-poor treatment. **b,** Confocal projection of 7 dpf control or ion poor treated *Tg(kdrl:Hsa.HRAS-mCherry)*^{s896} larvae injected with either anti-V5 (as control) or anti-Ifnγ. **c**, Graph showing the average vascular density in the brain of anti-V5-injected, anti-Ifnγ injected, ion-poor-treated anti-V5 injected, and ion-poor-treated anti-Ifnγ injected larvae. Data are presented as mean ± S.E.M., * $p < 0.05$, *** $p < 0.001$, n.s. not significant, t-test. n indicates the number of larvae used for experiments. Antibody injection was performed by Apaydin O. The data was generated by Seth B and Sawamiphak S.

3.2.11 Anti-Ifnγ treatment attenuates ion-poor-mediated arterial hypertension but not diastolic dysfunction

To further test the therapeutic potential of anti-Ifnγ treatment in other cardiovascular comorbidities caused by ion-poor mediated hypertensive stimuli and characterize potential causal interaction between them, I examined arterial hypertension and diastolic function following 5-day ion-poor treatment and 2-day anti-Ifnγ treatment (**Fig.3.31a)**. I noted that impairment of arterial flow velocity in both systole and diastole upon ion-poor treatment was attenuated in larvae subjected to anti-Ifnγ treatment (**Fig.3.31b-d)**. On the contrary, administration of the anti-Ifnγ antibody did not rescue the ion-poor induced diastolic dysfunction (**Fig.3.31e)**, suggesting that diastolic dysfunction might not be mediated by Ifnγ signaling in ion-poor mediated hypertensive response.

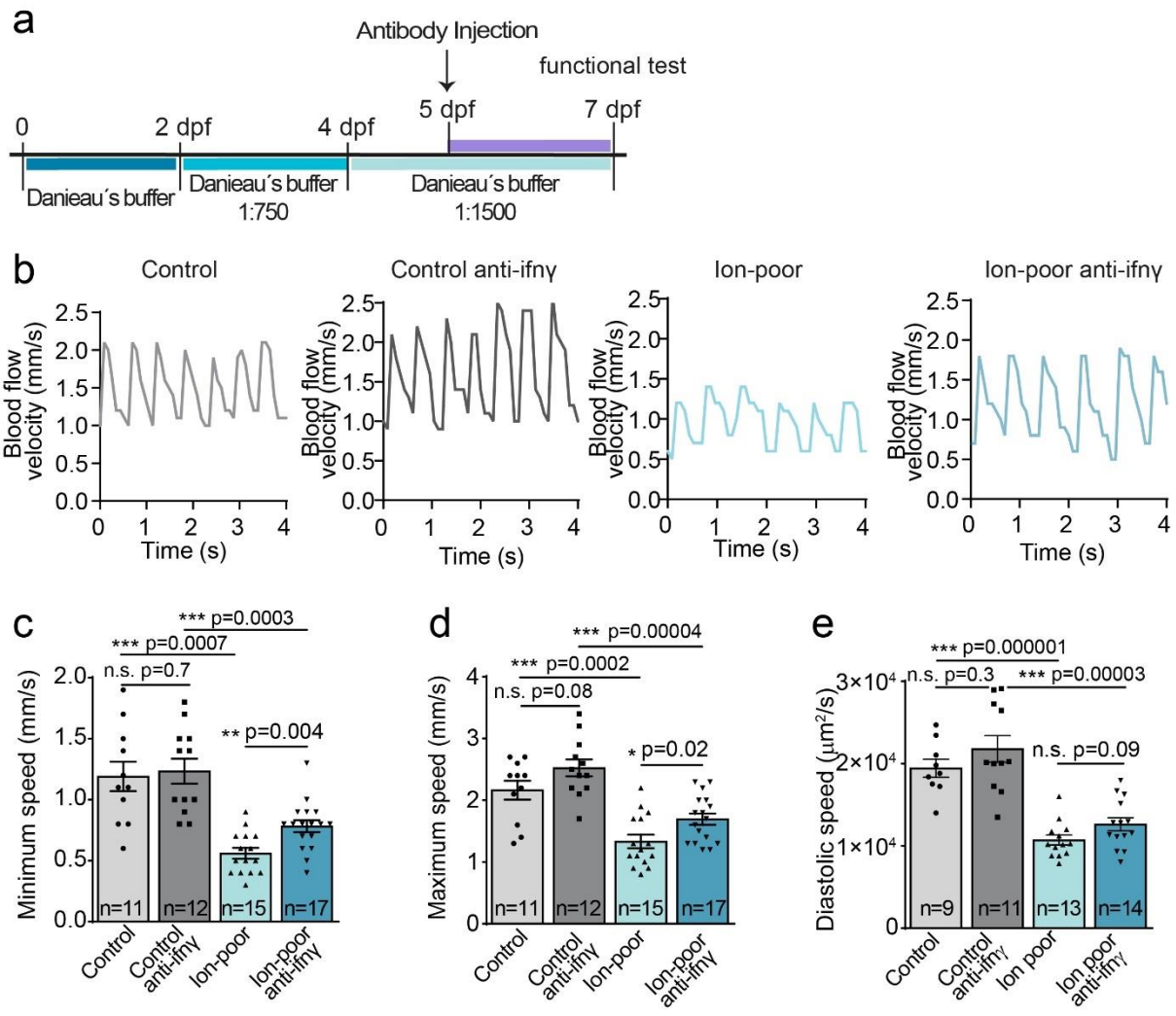

Figure 3.31. Ifnγ inhibition restores reduced blood flow but not diastolic dysfunction in hypertensive zebrafish. a, Schematic representation of antibody injection and ion-poor treatment. Anti-V5 (control) or anti-Ifnγ antibodies were injected into the pericardial sac at 5 dpf. The cardiac functional assay was performed at 7 dpf. **b,** Line graph showing representative blood flow velocities of anti-V5-injected, anti-Ifnγ injected, ion-poor-treated anti-V5 injected, and ion-poor-treated anti-Ifnγ injected larvae. **c-e**, Graphs displaying the average minimum speed (end-diastolic velocity) (c), maximum speed (peak systolic velocity) (d), and ventricular diastolic speed (e) in control or ion poor treated larvae injected with either anti-V5 or anti-Ifnγ. Data are presented as mean ± S.E.M. * $p < 0.05$, ** $p < 0.01$, *** $p < 0.001$, t-test. n indicates the number of larvae used for experiments.

4 Discussion

Cardiovascular disease is the leading cause of death globally. A growing number of studies suggested that adversities experienced in early life can severely increase the risk of ischemic heart disease, coronary heart disease, and myocardial infarction, which are the most frequent causes of HF in late adulthood (Dong et al., 2004; Lawson et al., 2020; Murphy et al., 2017; Su et al., 2015). Therefore, it is necessary to gain better mechanistic insights into developmental perturbations caused by early life exposure to stress and their transition to adverse programming of cardiovascular events.

Considering the complexity and intricacy of cardiac development with multiple systems involved, it is not unexpected that diverse systems and their crosstalk would also be involved in the pathogenesis of the cardiovascular disease, not just in cardiac homeostasis. Due to the immune system's remarkable nature, immune cells and their mediators, cytokines, modulate numerous biological activities acting locally or systemically. Particularly, cytokines are critical messengers assisting communication between different cells that can be nearby or distant. It is becoming evident that cytokine signaling as well as occasional cross-talking with other pathways, take part in the maintenance of proper cardiac development and function alongside the pathological adversities associated with cardiovascular disease. It is well-known that the dysregulated immune system and inflammation contribute to cardiovascular remodeling and its progression into HF. Hypertension is a major risk factor for HF, and aberrant immune activity is primarily implicated in the transition of hypertension to severe disease conditions. On the other hand, the causative role of cytokines leading to inflammation in hypertension-related comorbidities remains to be elucidated. Therefore, during my doctoral studies, utilizing mostly zebrafish but also mouse and in vitro models, I investigated different cytokine signaling pathways to advance our understanding of inter-organ crosstalk during cardiac development and remodeling, which in turn could allow targeting of identified cytokine pathways for novel intervention strategies to prevent or rescue pathological remodeling.

In the first part of the discussion section, I will discuss the antagonistic interaction between Gr and Il4 as a critical modulator of myocardial growth. Then I will follow the discussion with how Gr overactivation due to the stress experienced in early life affects cardiac development to ultimately result in adverse cardiac remodeling. In the second part, I will

discuss the role of Ifnγ signaling in pathological cardiovascular remodeling focusing on hypertension as a model while establishing the ion imbalance zebrafish model to achieve it.

4.1 Il4 and GC antagonistic signaling in cardiomyocytes of developing heart during homeostasis and stress response

4.1.1 Cardiac developmental program influenced by early life stress

GCs are known to be required for fetal growth, tissue development, and maturation (Cole et al., 1995). In the heart, for example, GR signaling activated by GCs was reported to induce structural and functional maturation of zebrafish and mouse myocardium (Eva A. Rog-Zielinska et al., 2013; Wilson et al., 2015). Moreover, mice deficient in cardiomyocyte GR exhibited aberrant gene expression associated with cardiovascular disease and died prematurely from HF (Oakley et al., 2013). On the other hand, fetal exposure to excess endogenous and exogenous GCs or maternal stress was shown to retard intrauterine growth. It was proposed that these unfavorable intrauterine environments culminate in early life programming with adverse consequences on cardiovascular and metabolic systems as well as mental health conditions in adulthood (Seckl & Holmes, 2007). Accordingly, growing evidence also points out a positive correlation between early life stress and HF. Owing to the pleiotropic effect of GCs, previous studies indicated that dysregulated GR signaling induced by pre/post-natal adversities might lead to inflammation, suggesting an underlying mechanism of cardiovascular diseases with potential inflammatory origin (Danese et al., 2007; Hostinar et al., 2015; Solano & Arck, 2020). However, the precise mechanism where stress responses in early life result in adverse cardiovascular outcomes with increased susceptibility to cardiovascular disease, particularly HF, in later life is still not defined.

Since mammalian model organisms develop in utero, exposure to stress during cardiac morphogenesis is hindered. Therefore, it is challenging to provide an animal model to investigate the developmental origin of cardiovascular disease caused by stress. Previous findings resulted exclusively from pharmacological approaches or genetic modifications in GR for manipulation of stress response mechanisms. However, maternal delivery of exogenous GC used in most frequently in earlier studies leaves an important question that whether the developmental effects observed in these studies are stress responses. Although GC is often

considered a “stress hormone” mediating physiological response to stress, they are also known to be involved in numerous other biological processes independent of the stress response. Furthermore, molecules other than GC can trigger the stress response as well (MacDougall-Shackleton et al., 2019). To elucidate this enigma, I utilized the advantages of the zebrafish model, which develop externally, allowing us easy application of physical challenges as well as pharmacological and genetic manipulations to modulate Gr signaling. I performed the experiments using zebrafish larvae at pre-hatching (2-3 dpf) and early post-hatching (4-5 dpf) developmental stages, similar to late-gestational/early-postnatal developmental periods of mammalian hearts. Thus, I was able to assess the impact of brain-mediated stress on cardiac morphogenesis using a zebrafish model.

An early life stress model was previously established in zebrafish. Castillo-Ramírez et al. utilized water vortex flow to create a forceful swimming pattern leading to reconfiguration of the HPA axis function and GC response in zebrafish larvae (Castillo-Ramírez et al., 2019). Modifying this method, I generated water currents to challenge larvae with involuntary swimming during early development to assess its effect on the heart. This work presents the first evidence that brain-processed stress experienced in early life impairs cardiac developmental programs through suppressing cardiomyocyte proliferation in the ventricle. The data presented here showed enlarged size in cardiomyocytes as seen in rat cardiomyocytes (Ren et al., 2012) as well as increased ventricular volume upon GR activation, suggesting eccentric ventricular hypertrophy. Importantly, a trend of eccentric ventricular hypertrophy was detected in ventricles with fewer cardiomyocytes (Tracy, 2013), consistent with the data presented here. Under certain conditions such as increased cardiac workload, the heart is known to undergo structural and functional alterations to compensate for the current demand (Gjesdal et al., 2011). This hypertrophic remodeling, on the other hand, is known to be a strong predictor of adverse cardiovascular events and precedes HF (Gjesdal et al., 2011; Kuroda et al., 2015; Velagaleti et al., 2014). This report suggests that activation of Gr signaling leads to eccentric hypertrophy during development which might increase the prevalence of unfavorable cardiovascular outcomes in later life.

Trabeculation is a critical morphogenetic process required for normal cardiac development and function (M. Wu, 2018). During trabeculation, cardiomyocytes are known to be highly proliferative, and impaired cardiomyocyte proliferation leads to a cardiac trabecular defect during cardiac development (J. Liu et al., 2010). The premature trabecular layer

observed in the developing zebrafish heart might be due to an anti-mitotic response in cardiomyocytes induced by Gr activation. It was also reported that impairment in cardiac trabeculation ultimately results in HF (J. Liu et al., 2010; M. Wu, 2018). The data obtained from the cardiac functional analysis showed dex-induced cardiac dysfunction characterized by decreased ability of ventricular relaxation and contraction in zebrafish larvae. Surprisingly, other systolic parameters, i.e., EF and FS, were unaltered in dex-treated larvae. These findings indicate that 3-day GR activation during myocardial growth does not affect myocardial stiffness, suggesting the development of adaptive remodeling in the heart. Growing evidence suggests increased myocardial stiffness as a transitional state from compensated hypertrophy to decompensated HF in patients (Hieda et al., 2020; Makarenko et al., 2004). Hence, the importance of exposure time to excessive GCs cannot be ruled out, and it will be essential to investigate further the effect of prolonged exposure to GCs on systolic parameters in later developmental stages.

Although stress/GR signaling in pathological settings was linked to cardiovascular disease, the physiological role of GR signaling in the heart is not well-known. Earlier studies only showed its contribution to cardiomyocyte maturation during myocardial growth (E A Rog-Zielinska et al., 2015; Eva A. Rog-Zielinska et al., 2013; Wilson et al., 2015). Surprisingly, the data presented in this study shows that mif-mediated Gr inhibition causes hyperproliferation of cardiomyocytes in zebrafish larvae, indicating that a certain amount of Gr signaling is essential to prevent hyperplastic growth of myocardium. Previous studies showed that mice lacking GR signaling, specifically in cardiomyocytes, exhibit increased heart weight and left ventricular mass without fibrosis and hypertrophic response (Oakley et al., 2013). These findings would also suggest possible hyperplastic growth of the heart, which may, in turn, lead to structural and functional abnormalities culminating in cardiovascular disease. Indeed, cardiomyocyte-specific GR knockout mice were reported to die prematurely from spontaneous cardiovascular disease (Oakley et al., 2013). Thus, these results presented in this dissertation widen the functional role of GR beyond the adaptive response to stress by implicating it as a possible regulator of between proliferation and maturation of cardiomyocytes in the developing heart. However, these results still require further investigations to understand the physiological role of GR in the developing heart and possibly preserving resilience against heart disease in adulthood.

4.1.2 Stat3 signaling as a potential target for early life interventions

Since persisting abnormalities induced by early life stress initiate complex and variable downstream cardiac outcomes leading to cardiovascular disease, it was suggested that therapeutic approaches targeting these initial cardiac events might be more effective than targeting the downstream cardiovascular events in the later stages of disease (Suglia et al., 2018). Accordingly, a better mechanistic understanding of early life stress-mediated cardiovascular programming is needed to provide a target for early intervention.

GCs exert immunomodulatory functions by inhibiting the expression of various cytokines, including IL4, IL6, IL17, and IFNγ (Cain & Cidlowski, 2017). Cytokines are widely appreciated mediators of intercellular communication among cells and are thought to be involved in the coordination of several physiological and pathological functions (J. M. Zhang & An, 2007). In fact, the dysregulated immune system was proposed as a causal mechanism of pathological remodeling and subsequent cardiovascular disease (Swirski & Nahrendorf, 2018). To further investigate whether this is the mechanism how stress/Gr signaling imposes perturbations on the heart leading to early cardiac programming, I focused on the identification of potential cytokine signaling interfering with Gr signaling in the developing heart.

In search of various cytokines which might crosstalk with Gr signaling, Il4 became the leading potential candidate. *in situ* data presented here revealed that while *il4r* was expressed in cardiomyocytes of developing heart, expressions of *ifngr1* and its ligand were not detected in the developing heart. Additionally, earlier studies suggested that IL4 level might be regulated by stress/GR signaling under certain pathological conditions (Gemou-Engesaeth et al., 2002; So et al., 2002; Umland et al., 1997). In addition to GCs, stress-mediated regulation of IL4 level was implicated in rat anxiety models where their brains exhibited decreased level of IL4 (H. J. Lee et al., 2016). Similarly, previous studies also proposed an inverse correlation of IL4 with anxiety and depression. For instance, increased depression symptoms in pregnant women were associated with Th1/Th2 imbalance, evidenced by elevated IFNγ/IL4 ratio (Karlsson et al., 2017). Therefore, it is logical to consider that there might be an interaction between these two signaling pathways. Here, I showed that the anti-mitotic effect of stress/Gr is restored by induction of Il4, highlighting crosstalk between them to balance cardiomyocyte proliferation in the developing heart. Notably, my data obtained from neonatal mice cardiomyocyte culture

reveals that IL4 and GC antagonistic signaling in cardiomyocytes is also evolutionarily conserved among the different vertebrates.

Although GR signaling was previously shown to regulate the level of IL4 in some cells under certain conditions, qPCR results presented here indicate that the Il4 signaling components, including *il4* and *il4r* were not transcriptionally controlled by Gr signaling. Instead, this work shows evidence of a novel Gr-Il4 crosstalk mechanism in the cardiomyocytes acting through atypical signaling transducer Stat3 during development. DNSTAT3 was shown to inhibit STAT3 signaling by competing with endogenous STAT3 for receptor interactions (Conway, 2006). The data showing neutralized mitotic activity in zebrafish cardiomyocytes expressing DNStat3 in the presence of mif-mediated Gr inhibition as well as excessive Il4, provides further proof that the antagonistic interaction between Gr and Il4 signaling as proliferation regulators through modulation of Stat3 activity to balance cardiomyocyte mitosis not only upon exposure to stress, but also during physiological cardiac development. These findings indicate that STAT3 signaling might be a critical stress control pathway, highlighting its potential for future therapeutic interventions.

Emerging evidence point out the beneficial effects of STAT3 on the heart. Previous studies proposed an enhanced regenerative capacity with cell cycle reentry through STAT3 in cardiomyocytes in mice (Miyawaki et al., 2017) and zebrafish (Fang et al., 2013) after myocardial damage, highlighting a potential cardioprotective function of STAT3. However, its role in cardiomyocyte mitotic response was proposed to be limited to the regeneration process as cardiomyocytes expressing DNStat3 exhibited no reduced mitotic activity in the young adult zebrafish (Fang et al., 2013). By contrast, here, I showed that Stat3 signaling is indispensable for cardiomyocyte mitosis in zebrafish heart, at least during early development. In fact, the mitotic activity of cardiomyocytes is known to be limited in late development in the absence of any injury. Only %5 cardiomyocytes, for instance, were shown to be proliferative in juvenile fish (Bertozzi et al., 2021). Furthermore, it was demonstrated that the downregulation of STAT3 predisposes HF. For example, mice lacking STAT3 expression in cardiomyocytes exhibited enhanced cardiac fibrosis, impaired cardiac function, and developed HF (Hilfiker-Kleiner et al., 2004; Jacoby et al., 2003). On the other hand, excessive activation of STAT3 is known to induce cardiomyocyte hypertrophy and inflammation (Haghikia et al., 2014), indicating that balanced STAT3 activity in cardiomyocytes is required for cardiac

homeostasis. Notably, this work shows the effect of Stat3 on myocardial growth is regulated by the antagonistic interaction of Gr and Il4 during physiological development.

Most of the cytokines act through the JAK/STAT intracellular signaling cascade leading to the phosphorylation of STATs which translocate to the nucleus and regulate the transcription of the target genes by working in coordination with other molecules. GR was shown to interfere with the STAT signaling, resulting in opposite outcomes (Cain & Cidlowski, 2017). The findings presented in this work reveal that Gr interferes with Il4-activated Stat3 signaling, leading to suppression of Stat3-targeted pro-mitotic gene expression in cardiomyocytes. My data showing no change in the level of *stat3* upon Gr activation indicates that Gr-mediated transcriptional repression of Stat3 itself could not underlie Il4-Gr crosstalk. A previous comprehensive study revealed dual activities of GR-STAT3 crosstalk, depending on tethering between GR and STAT3. In this study, Langlais et al. proposed that GR tethering to DNA-bound STAT3 represses the transcriptional activity while STAT3 tethering to GR leads to transcriptional synergism (Langlais et al., 2012). Therefore, it is possible that binding Gr to DNA-bound Stat3 through direct protein-protein interaction in cardiomyocytes might result in suppression of Stat3 targeted gene expression involved in cell division. Alternatively, Gr might also influence the phosphorylation of Stat3, thereby competing with Il4r. However, the scope of this study did not cover the mechanistic interaction between Gr and Il4-activated Stat3. Further work will be required to pinpoint the mode of GR-mediated STAT3 targeted gene regulation in the cardiomyocytes during development.

4.1.3 A non-immune signaling function of Il4 in the regulation of cardiac growth

Emerging evidence uncovered that cytokines, at least some of them, are critical for the homeostatic control of distinct tissues (Foti, 2017; Swirski & Nahrendorf, 2018). Although the non-immune function of cytokines is beginning to draw more attention, the developmental roles of most of the cytokines remain unknown. IL4 is a pleiotropic cytokine coordinating several biological processes. It was shown that IL4 secreted from a subset of skeletal muscle cells during development acts as a recruitment factor mediating myoblast fusion with myotubes which is indispensable for skeletal myogenesis (Horsley et al., 2003). However, previous studies reported contradictory findings about the effect of IL4 on the heart. Several studies

indicated it as a pro-fibrotic factor in the adult heart under pathological conditions (Kanellakis et al., 2012; Levick et al., 2009; Peng et al., 2015; Roselló-Lletí et al., 2007). On the other hand, some studies demonstrated the beneficial effects of IL4 acting as a cardioprotective agent (Engelbertsen et al., 2013; Shintani et al., 2017). Despite varying reports on the effect of IL4 on the adult heart, the role of IL4 during myocardial development remains largely unknown.

This study reports for the first time that IL4 acts as a pro-mitotic factor for cardiomyocytes during myocardial growth. Notably, the findings obtained from *Il4ra*$^{-/-}$ mutant mice indicated that IL4 signaling is indispensable for cardiomyocyte mitotic activity in the developing heart, revealing that this developmental role of IL4 is evolutionary conserved in vertebrates. Furthermore, I showed that *il4-6xHIS* overexpression causes increased cardiomyocyte number and enlarged ventricle but normal development of endocardium and epicardium, indicating that the pro-mitotic effect of Il4 signaling might be cardiomyocyte-specific in the developing heart. It is known that the proliferation rate of cardiomyocytes is a critical factor for cardiac trabeculae formation during development (J. Liu et al., 2010; Samsa et al., 2013). For instance, endocardial-specific Notch1 intracellular domain inhibitor Fkbp1a deficiency, which causes activation of Notch1 signaling, was shown to induce cardiomyocyte proliferation and hypertrabeculation (H. Chen et al., 2013). However, the results presented here showed that enhanced cardiomyocyte mitotic rate due to over-activation of Il4 signaling did not alter the cardiomyocyte abundance in the compact and trabecular layers. Besides, functional characterization of larvae upon Il4 induction revealed improved cardiac diastolic and systolic function but no alterations in other systolic parameters. These findings, in agreement with evidence showing normal trabecular development, suggest newly formed cardiomyocytes incorporated into the myocardium without leading to aberrant cardiac development. Accordingly, overgrowth of the myocardium might be the reason for enhanced cardiac function observed upon IL4 induction.

4.1.4 Cell-Autonomous Signaling by the Gr and Il4r in cardiomyocytes

GCs are known to be involved in the regulation of growth hormone production, resulting in competing effects on the hypothalamus and pituitary gland (Mazziotti & Giustina, 2013). Earlier studies showed that growth hormone enhances heart development and function through induction of cell cycle re-entry and hypertrophy in cardiomyocytes (Brüel et al., 2007).

Furthermore, it was suggested that growth hormone deficiency caused by excessive exposure to exogenous or endogenous GCs might be an important contributor to adverse cardiovascular outcomes (Mazziotti & Giustina, 2013). Therefore, it is worth to investigate further whether the perturbation effect of GR activation is a secondary effect of growth hormone or specific to cardiomyocytes. The results obtained from cardiomyocyte-specific overexpression of Gr show that anti-mitotic response induced by Gr signaling occurs, at least partially, directly through activation of Gr expressed on cardiomyocytes instead of indirectly through regulation of growth hormone secretion. Additionally, I introduced interference to endogenous Il4 signaling using the expression of a truncated version of Il4r in cardiomyocytes. Subsequently, I observed that Il4 exerts pro-mitotic effect through induction of Il4 signaling specifically in cardiomyocytes, thus further proving that Il4 signaling is required for cardiomyocyte proliferation during cardiac development. In sum, these findings together with the results obtained from the cardiomyocyte specific DNStat3 expression show that the antagonistic interaction between Gr and Il4 occurs by competing for modulation of Stat3 activation in cardiomyocytes autonomously.

It is known that cytokines exert their functions by acting on the same cells secreted through autocrine action, on nearby cells through paracrine action, or on distant cells through endocrine action (J. M. Zhang & An, 2007). The *in situ* data showing the expression of *il4* in the thymus of developing zebrafish but not in cardiomyocytes suggests a possible involvement of the immune system in the orchestration of cardiac development. However, the scope of this dissertation could not address the direct contribution of immune cell-derived Il4 to the regulation of cardiomyocyte mitotic rate. Further studies using immune cell-specific Il4 knockout lines will be needed to reveal whether Il4 secreted from these cells govern myocardial growth.

In conclusion, a novel inter-organ crosstalk between the brain, heart, and possibly immune system is demonstrated to modulate cardiomyocyte proliferation, thereby maintaining the physiological growth of the heart by the results discussed in this section **(Fig. 4.1)**. The mentioned crosstalk is implicated via the regulation of GCs through HPI axis, regulation of Gr and Il4 signaling on cardiomyocytes, and regulation of Il4 production in the thymus. In line with previous studies, my results demonstrate that activation of Gr signaling and exposure to early life stress disrupts cardiac development. Besides, this work provides further insights into its mechanism. I showed that stress-mediated GR activation acts as a mitotic brake through

regulation of Stat3 activity, thereby leading to morphological and functional abnormalities. On the other hand, Il4 signaling might play a significant role in counteracting the anti-mitotic response of stress-mediated GR activation by exerting a pro-mitotic function acting through Stat3 in cardiomyocytes. All in all, these findings show that STAT3 might be targeted to rescue stress-mediated cardiac programming and inhibit its progression into cardiac failure.

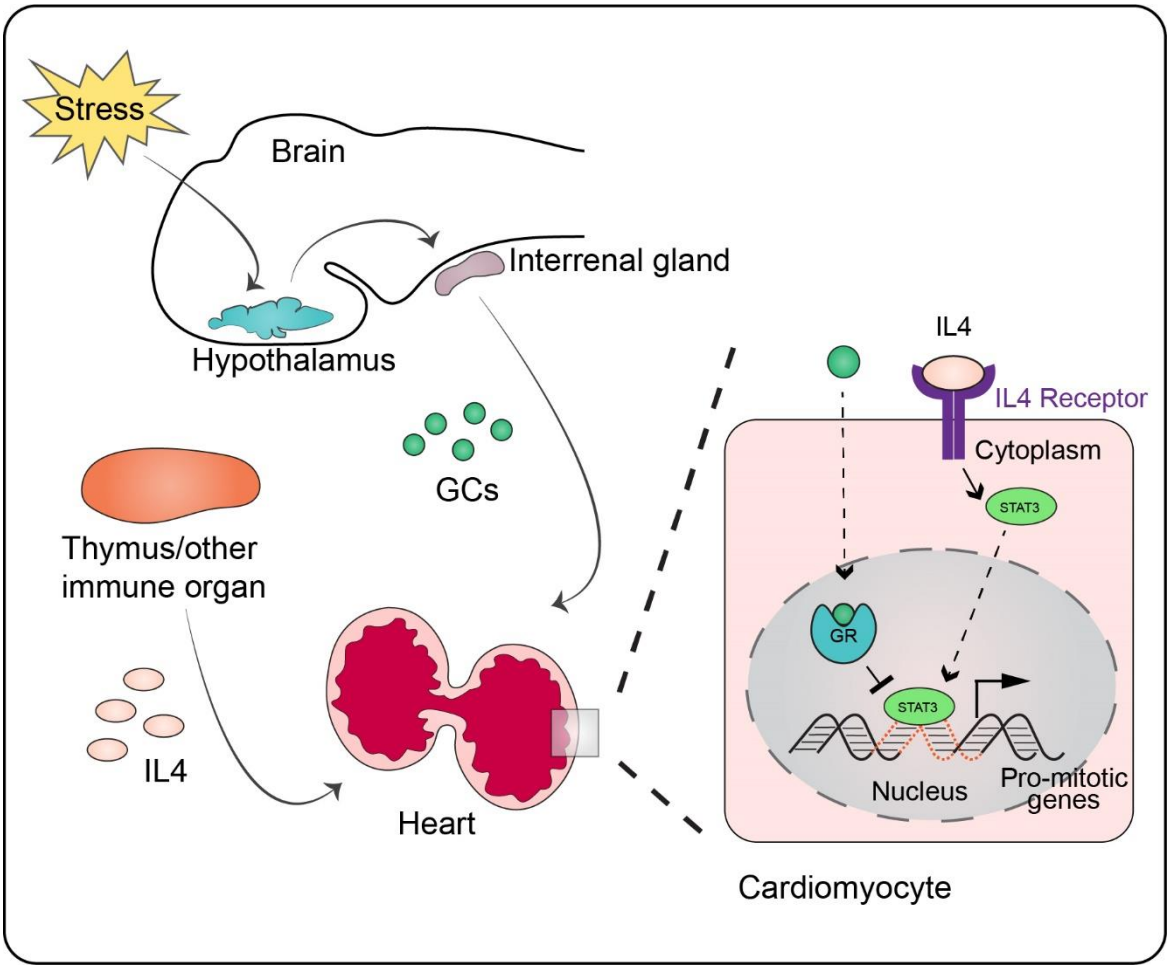

4.2 Ifng-driven cerebrovascular remodeling and arterial hypertension in a zebrafish model of hypertension

4.2.1 Zebrafish model of ion imbalance

Hypertension was proposed as the most predominant risk factor for cardiovascular diseases (Drazner, 2011). Although the precise mechanism governing the progression of hypertension is not determined yet, adverse cardiovascular remodeling, including a series of events such as dysregulated RAS, hypertrophy, vascular alterations, and inflammation, was proposed as an important determinant for the transition from hypertension to HF (Drazner, 2011; Kuroda et al., 2015; Lyle & Taylor, 2019). As dysregulated RAS system is a critical predictor of hypertension, most of the current treatment strategies target RAS to achieve healthy blood pressure. For example, RAS blockers which are ACE inhibitors, Ang receptor blockers, or renin inhibitors, have been used to treat high blood pressure. These anti-hypertensive drugs help to lower blood pressure in patients with essential hypertension (Drummond et al., 2019; Oparil & Schmieder, 2015). However, reaching physiological blood pressure in patients with resistant hypertension is difficult. Although these patients take a combination of antihypertensive drugs to balance blood pressure, they remain at high risk for target organ damage (Carey et al., 2018). Growing evidence highlights that hypertensive patients with normalized blood pressure after treatment still carry increased residual risk of cardiovascular events (Blacher et al., 2010; Struthers, 2013). Therefore, better mechanistic insights into the pathogenesis of hypertension are crucial to identify novel targets for future interventions.

Several animal models were established to study the pathogenesis of hypertension as well as to evaluate therapeutic strategies. Rodent models of hypertension were generated mainly by genetic manipulations (Lerman et al., 2019). The most common genetic strains used in hypertension research are spontaneously hypertensive rats (Okamoto & Aoki, 1963) and DahI salt-sensitive rats (Dahl et al., 1962). In addition to genetic modifications, pharmacological treatments such as Ang II, aldosterone, deoxycorticosterone acetate (DOCA)-salt, and vasodilation inhibitors such as N-nitro-L- arginine methyl ester were utilized to generate experimental models of hypertension (Lerman et al., 2019). However, hypertension is a complex disease damaging multiple organs, and there are several hypertension-related

comorbidities. On top of that, due to its multifactorial nature, the etiology of hypertension remains poorly understood. Hence, experimental models of hypertension often fail to recapitulate all the systemic and cardiovascular features of hypertension observed in humans.

This work provides means to study cellular and molecular mechanisms underlying the onset of hypertension and associated end-organ damage by establishing a zebrafish hypertension model which requires minimal manipulation in a short time, unlike its mammalian counterparts. To establish a zebrafish model of ion imbalance, I modified a previously established ion-poor treatment which was shown to induce rapid RAS activation and Na(+) uptake in zebrafish larvae (Kumai et al., 2014) and characterized this novel model whether it can capture the key aspects of human hypertension. I showed that exposure to ion-poor stimuli is sufficient to drive hypertension-associated morphological and functional adversities, including not only early RAS elevation but also arterial hypertension. Notably, the data showing ion-poor hypertensive stimuli induced cardiac remodeling characterized by concentric hypertrophy and diastolic dysfunction without any overt systolic dysfunction is similar to incipient HFpEF phenotypes (Drazner, 2011), indicating progression of hypertension upon prolonged ion-poor treatment.

Recently, an increased level of circulating AGT was associated with left ventricular diastolic dysfunction in humans (Millen et al., 2018). Considering hypertension, diastolic dysfunction, and HFpEF as a part of a continuous disease spectrum, they suggested circulating AGT concentration as a marker for the severity of the disease. The data presented here is consistent with patient results, providing further support for the potential of AGT as an early marker for the diagnosis of HFpEF. Furthermore, the level of renin was shown to be inconsistent among the patients with essential hypertension. While some hypertensive patients have mild to moderate elevation in plasma level activity of renin, others have normal or suppressed level of renin. In fact, it has been debated that preservation of normal renin levels may partake in blood pressure increase in hypertension (Atlas, 2007). Similarly, I did not observe any increase in ren mRNA in the early treatment period. Its expression became significantly increased, although it was around only 1.3-fold increase after 3-day of ion-poor treatment.

4.2.2 Cerebrovascular regression in hypertensive zebrafish brain

Hypertension is often presented with maladaptive vascular remodeling, which plays a significant role in subtle damage to organs, including the heart, kidney, and brain (François Feihl et al., 2008; R. Humar et al., 2009). It was previously shown that hypertension causes structural and functional alterations in cerebral vessels, which are strongly associated with cognitive dysfunction and blood-brain barrier impairment (Paiardi et al., 2009; Pires et al., 2013). In line with these previous findings, the work presented here demonstrates ion-poor hypertensive stimuli mediated cerebrovascular regression in zebrafish larvae.

To date, the precise mechanisms of hypertensive vascular remodeling, specifically in cerebral vessels, are not fully elucidated. It is interesting to explore further the morphological rearrangements and cellular processes driving hypertension-induced cerebrovascular remodeling utilizing the robustness of the zebrafish model. Evidence presented here indicates that apoptosis of endothelial cells might not be the primary mechanism underlying the cerebrovascular regression as hypertensive zebrafish brain exhibited no induction of cell death in the cerebral vessels. Instead, the data obtained from live imaging of the larval brain demonstrated a dynamic process of endothelial cells which includes retraction from vessels and migration away, resulting in regression of vessels without the contribution of endothelial cell death. Although these dynamic endothelial cell rearrangements were reported in the developmental vascular remodeling (Q. Chen et al., 2012; Franco et al., 2015; Korn & Augustin, 2015), this study shows for the first time their involvement in hypertension-driven vascular regression. Moreover, ion-poor hypertensive stimulus resulted in reduction of brain volume compared to control siblings, possibly due to increased cell death observed in brain parenchyma. Also, insufficient oxygen supply to the brain due to cerebrovascular regression might contribute to brain volume reduction in response to a hypertensive stimulus. Similarly, previous studies also noted smaller brain volume associated with increased risk of cognitive decline and dementia in hypertensive patients (Beauchet et al., 2013; Celle et al., 2012; Shang et al., 2021).

4.2.3 Altered tissue homeostatic and neuroprotective function of hypertensive macrophages

Macrophages are known to play pivotal roles in angiogenesis and vascular remodeling during development, wound healing, and disease. However, the angiogenic potential of macrophages has been debated due to conflicting results showing that they are involved in both angiogenesis and regression (Jetten et al., 2014; Willenborg et al., 2012; Zajac et al., 2013). Macrophages are a highly heterogeneous cell population and exert diverse functions by changing their phenotype in response to different environmental stimuli (DM et al., 2008). Gurevich et al. showed that ablation of macrophages at various stages of wound healing after injury results in impaired vessel regression and sprouting, proposing that temporal phenotypical switch of macrophages and their subsequent inflammatory state are critical determinants of vascular fate (Gurevich et al., 2018). Recently, Graney et al. showed that not only the phenotype of macrophages is important, but also their time spent in the microenvironment and the condition of the environment are critical issues. This study using a 3D tissue-engineered human blood vessel network reported that proinflammatory macrophages (M1) promote vascularization in the short term (1 day after seeding) while they lead to vessel regression in the long term (3 days after seeding) (Graney et al., 2020). In fact, vessel regression is a natural process occurring not only during vessel maturation but also during vascular remodeling to maintain homeostasis of vascular structure (Korn & Augustin, 2015). Therefore, diverse macrophage subtypes possibly behave differently over time by changing their behavior, favoring either angiogenesis or regression.

Due to their characteristics mentioned above, macrophages have the potential to be involved in hypertensive vascular remodeling, thereby contributing to end-organ damage (Kossmann et al., 2014; Moore et al., 2015). However, their mechanism of action in different vascular beds under diverse situations remains unknown. Mechanistically, earlier studies proposed that macrophages mediate vascular regression through phagocytosis of apoptotic endothelial cells and inducing endothelial cell death, as reported in retinal development (Lang & Bishop, 1993; Lobov et al., 2005; Rao et al., 2007). Similar macrophage-driven vessel regression through resembling mechanism, but depending on macrophage phenotype, was also shown in zebrafish and mouse wound angiogenesis (Gurevich et al., 2018). In contrast to previous studies proposing the macrophage-induced apoptosis of endothelial cells as a

mechanism of vessel regression, the data presented in this dissertation shows that cerebrovascular regression in hypertensive zebrafish is independent of endothelial cell death. Thus, it is intriguing to consider that there might be other mechanisms of macrophage-orchestrated vessel regression, at least in the cerebral vessels in response to ion-poor hypertensive stimuli. Interestingly, a direct physical interaction between macrophages and endothelial cells in unstable vessels were noted during vessel development and repair in zebrafish (Gerri et al., 2017). Therefore, it is worth to further explore dynamic macrophage behavior in the hypertensive cerebrovascular regression. Thanks to the optical translucency of zebrafish larva, this study demonstrated that macrophages were coupled to cerebral vessel regression process, interacting with vessels prior to regression, providing new mechanistic insights into cellular interactions during cerebrovascular remodeling in response to hypertension.

Furthermore, the macrophage-specific transcriptome profiling presented here identifies potential candidate molecules for therapeutic approaches. Interestingly, while some genes involved in homeostasis and neuroprotection were downregulated, genes related to neurodegenerative disease were upregulated in hypertensive macrophages. For example, Carnosine dipeptidase 1 (cndp1), one of the genes found upregulated in hypertensive macrophages, was previously associated with dementia (Heywood et al., 2015). On the other hand, BMPs, downregulated in hypertensive macrophages, are known to be critically important for brain development, neurogenesis, and neural plasticity (Jensen et al., 2021). Particularly, BMP5/7 was reported to modulate the development of noradrenergic locus (Tilleman et al., 2010) and midbrain dopaminergic neurons (Jovanovic et al., 2018), which are related to cognitive and memory functions (Nobili et al., 2017; Poe et al., 2020). Recently, it was proposed that BMP5/7 exerts neuroprotection in a mouse model of Parkinson's disease (Vitic et al., 2021). Besides its function in the brain, BMPs are also known to play essential roles in vascular development, homeostasis, and remodeling in response to shear and oxidative stress. BMP signaling was also proposed as an important modulator of cerebrovascular angiogenesis and the functional blood-brain barrier (Araya et al., 2008), and impaired BMP signaling was implicated in neurovascular disorders (Cunha et al., 2017; García de Vinuesa et al., 2016; Goumans et al., 2018)

Another gene downregulated in hypertensive macrophages by transcriptomic profiling, Neucleobindin-2 (NUCB2), is a precursor protein physiologically cleaved into three peptide

fragments, including nesfatin-1 (H. Shimizu et al., 2009). Like BMP5/7, Nesfatin-1 was proposed to protect dopaminergic neurons against neurodegeneration in the mouse model of Parkinson's disease (Shen et al., 2017). Recently, decreased blood level of nesfatin-1 was noted in patients with Parkinson's disease (Emir et al., 2019). Furthermore, other studies provided evidence indicating that Nesfatin-1 has neuroprotective effects through modulating pro-apoptotic and pro-inflammatory responses in brain injury models (Özsavcí et al., 2011; Tang et al., 2012).

Another important candidate determined here in this work is PlxnD1 which is a cell surface receptor**.** PlxnD1 was proposed to play a vital role in cardiac morphogenesis, as seen in mice deficient in PlxnD1 exhibited cardiac and vascular defects (Gitler et al., 2004). In zebrafish, PlxnD1 morphants demonstrated abnormalities in the patterning of the developing vascular networks (Torres-Vázquez et al., 2004). Notably, under different disease conditions, both beneficial and detrimental effects of PlxnD1 on vascular remodeling were reported by several studies. PlxnD1 in endothelial cells was shown to activate an anti-angiogenic downstream cascade, leading to dysregulation of angiogenesis in ischemic retinopathy (Fukushima et al., 2011; Yang et al., 2015). On the other hand, brain endothelial-specific *Plxnd1* knockout mice exhibited blood-brain barrier disruption and severe brain damage as well as delayed recovery due to insufficient and aberrant vasculature after ischemic stroke (Yu et al., 2022), suggesting that PlxnD1 signaling may exert different functions depending on the tissue and pathological conditions. Intriguingly, PlxnD1 signaling in macrophages was reported to elevate the pro-angiogenic activity of macrophages as characterized by macrophage-mediated endothelial cell activation through VEGFR2 (Meda et al., 2012), indicating a possible role for it in macrophage-endothelial cell communication.

Surprisingly, transcriptional profiling in macrophages also revealed blunted expression of several key regulators of innate immunity, inflammatory resolution, and anti-inflammatory response in macrophages upon ion-poor hypertensive stimuli. Innate immune function related genes such as complement factor H related 5 (*cfhl5*) and NK-lysin 3 and 4 (*nkl.3 and nkl.4*) were suppressed in hypertensive macrophages. The complement system, one of the critical effector mechanisms of innate immunity, is strictly regulated to protect the host tissue from damage and disease. Factor H related proteins are known to be essential regulators of the complement system (Skerka et al., 2013). Moreover, NK-lysin is an antimicrobial peptide that is also one of the crucial effector components of the innate immune system (J. Chen et al.,

2015). Importantly, up-regulation of *nkl.4* was reported in zebrafish against viral infection, implying its involvement also in zebrafish innate immune response (Pereiro et al., 2015).

Taken together, the transcriptional state of hypertensive macrophages determined in this study for the first time associates these differentially expressed critical factors involved in vasculo/neuro protection, homeostasis, and neurodegenerative diseases, with innate immune cell function and brain remodeling in hypertension. Due to the induction of low-grade inflammation in hypertension, the involvement of proinflammatory macrophages in hypertension pathogenesis has been highlighted mostly through their inflammatory response (Harwani, 2018). Notably, this report revealing transcriptional changes related to the innate immune function of macrophages indicates that the involvement of macrophages in hypertension pathogenesis may not be through canonical pro-inflammatory response but rather related to alterations of macrophage homeostatic and neuro/vasculo protective function. In conclusion, this work would help guide future therapeutic strategies for hypertension, highlighting the importance of derangements in macrophage functions in response to hypertension.

4.2.4 Ifnγ signaling as a potential target for hypertension-associated comorbidities

The onset and progress of hypertension mostly vary in patients and animal models due to its multifactorial characteristic (Drazner, 2011; Lerman et al., 2019). Certainly, this is one of the reasons for the not fully revealed mechanism of pathogenesis as well as ineffective therapeutic interventions. Previous studies showed the involvement of inflammation in experimental models and patients with hypertension (Caillon et al., 2019; Drummond et al., 2019). For instance, elevated levels of IL1β, IL17, IFNγ, TNFα, and IL6 were reported in hypertensive patients (Bautista et al., 2005; De Ciuceis et al., 2017; Dörffel et al., 1999). Importantly, those cytokines were also associated with renal and vascular dysfunction, resulting in elevated sodium reabsorption (McMaster et al., 2015). Therefore, inflammation might play a key role in the progression of hypertension into more severe cardiovascular diseases. Several pro-inflammatory cytokines were implicated in the pathogenesis of HF. Indeed, the inflammatory cascade initiated by these cytokines was suggested as a causative role in several cardiovascular diseases (Mehra et al., 2005).

It was proposed that hypertensive stimuli such as AngII induce the accumulation of immune cells in the tissues such as the kidney and perivascular region of arteries and arterioles. These infiltrated cells release pro-inflammatory cytokines and promote oxidative stress, which affects vascular homeostasis (De Ciuceis et al., 2005; Kossmann et al., 2014; Liao et al., 2008). Accordingly, systemic inflammation was suggested as an underlying mechanism of structural and functional remodeling of microvessels, which subsequently triggers maladaptive cardiac remodeling and impaired cardiac function (Paulus & Tschöpe, 2013). Additionally, it was suggested that low-grade inflammation stimulates endothelial activation and oxidative stress, which leads to reduction in the bioavailability of nitrogen oxide and consequently contributes to cardiomyocyte stiffness, ventricular dysfunction, and HF (Franssen et al., 2016; Zanoli et al., 2020). Taken together, these findings implicate that dysregulated immune cell activation and subsequent inflammation are the key players in hypertension pathogenesis and end-organ damage.

It is worth mentioning that hypertension pathogenesis involves a harmony of distinct events. Although the contribution of the immune system to various pathological events during hypertension is well-accepted, the cause-and-effect relationships of inflammation with hypertension and hypertension-related comorbidities such as vascular regression remain unclear. Therefore, I aimed to delineate the temporal relationship between inflammation and the development of hypertension. I detected unsignificant upregulation of proinflammatory cytokines *ifng* and *il1b* after only 2-day of ion-poor treatment in which angiotensinogen upregulation was already detected. Interestingly, their increases became significant on the third day of treatment, in which cerebral vessel regression became detectable, suggesting a causative role of inflammation in cerebrovascular remodeling. Although with these data, I cannot reveal the direct effect of RAS dysregulation on induction of inflammatory cascade, these findings propose that elevation of angiotensinogen in response to ion-poor treatment may promote systemic inflammation marked by *ifng* and drastic *il1b* upregulation, ultimately resulting in vascular remodeling in the brain. Further investigation will be needed to determine whether the levels of these pro-inflammatory cytokines are directly induced by elevated RAS activity.

Earlier studies reported elevated levels of IL1β secretion from peripheral blood monocytes of hypertensive patients after *ex vivo* stimulation with AngII (Dörffel et al., 1999). Moreover, it was suggested that IL1R deficiency protects the mice from AngII-induced blood pressure elevation (J. Zhang et al., 2016). IL1β was shown to promote the secretion of other

pro-hypertensive cytokines, such as IL6 (Rothman et al., 2020), highlighting its potential for inflammation-targeted therapy for hypertension. In recent years, a human monoclonal antibody neutralizing the IL1β (canakinumab) was proposed as an anti-inflammatory therapy for cardiovascular disease in which inflammation plays a critical pathophysiological role. Anti-inflammatory Thrombosis Outcome Study (CANTOS) reported that anti-IL1β targeted antibody therapy reduces inflammation and cardiovascular events in patients with prior myocardial infarction (Ridker et al., 2017). Given the pivotal role of inflammation in the development and progression of hypertension, it is tempting to test the beneficial potential of canakinumab to prevent the onset of hypertension. Indeed, a recent study confirmed the reduced risk of cardiovascular events in patients with previous myocardial infarction; however, this study reported no alteration in blood pressure or the development of incident hypertension in patients with the inhibition of IL1β (Rothman et al., 2020), highlighting that there might me additional drivers involved in hypertension pathogenesis.

The partial success of the IL1β-targeted antibody urged me to address the therapeutic potential of other candidate molecules. Early upregulation of Ifnγ in hypertensive response where other cytokines remained unchanged makes Ifnγ signaling a prominent candidate for therapeutic interventions targeting hypertensive cardiovascular remodeling. Furthermore, IFNγ, which is a prototypical inflammatory cytokine produced by mostly T cells, is a well-known stimulus for classical macrophage activation, which leads to macrophage release of pro-inflammatory cytokines such as IL1β (DM et al., 2008; Pelegrin & Surprenant, 2009), suggesting that IFNγ signaling might be upstream of IL1 signaling, further highlighting its potential. The data presented here shows for the first time that Ifnγ signaling underlies, at least partially, hypertensive cerebrovascular remodeling. Furthermore, the findings demonstrated that inhibition of Ifnγ signaling with an anti-Ifnγ antibody restored not only cerebral vessels from regression but also mitigated arterial hypertension, reinforcing the therapeutic potential of anti-Ifnγ treatment.

On the other hand, with the administration of anti-Ifnγ, I could not recover the diastolic dysfunction caused by ion-poor hypertensive stimuli. Given that it was antibody-based manipulation of target signaling, it is possible that either concentration of antibody or the treatment time was not sufficient to rescue the phenotype. Alternatively, functional remodeling of the cardiac ventricle in hypertension response might be driven by Ifnγ-independent

mechanisms. In fact, previous studies support this observation where IFNγ-deficiency attenuated hypertensive response evidenced by blunted blood pressure elevation in response to AngII infusion (Kamat et al., 2015; Saleh et al., 2015) or combinatorial chronic aldosterone infusion, uninephrectomy and salt feeding condition (Garcia et al., 2012) but exaggerated left ventricular hypertrophy and worsened diastolic dysfunction. Furthermore, IFNGR deficiency was shown to ameliorate cardiac damage by reducing cardiac hypertrophy, infiltration of immune cells, and accumulation of cardiac fibronectin and collagen without altering blood pressure elevation caused by AngII infusion in mice (Markó et al., 2012). Altogether, in line with previous findings, the data presented here imply the role of other mechanisms driving cardiac remodeling in response to different hypertensive stimuli.

Finally, a comprehensive analysis of molecular mechanisms underlying macrophage-mediated alteration of the cerebrovascular system uncovered that inhibition of Ifnγ signaling protects macrophages from activation of the hypertension-driven transcriptional program. Importantly, the transcriptome profiling in macrophages suggests that blunted macrophage paracrine signaling through Ifnγ may alter cerebrovascular remodeling during hypertension, providing further insight into the mechanisms behind their actions.

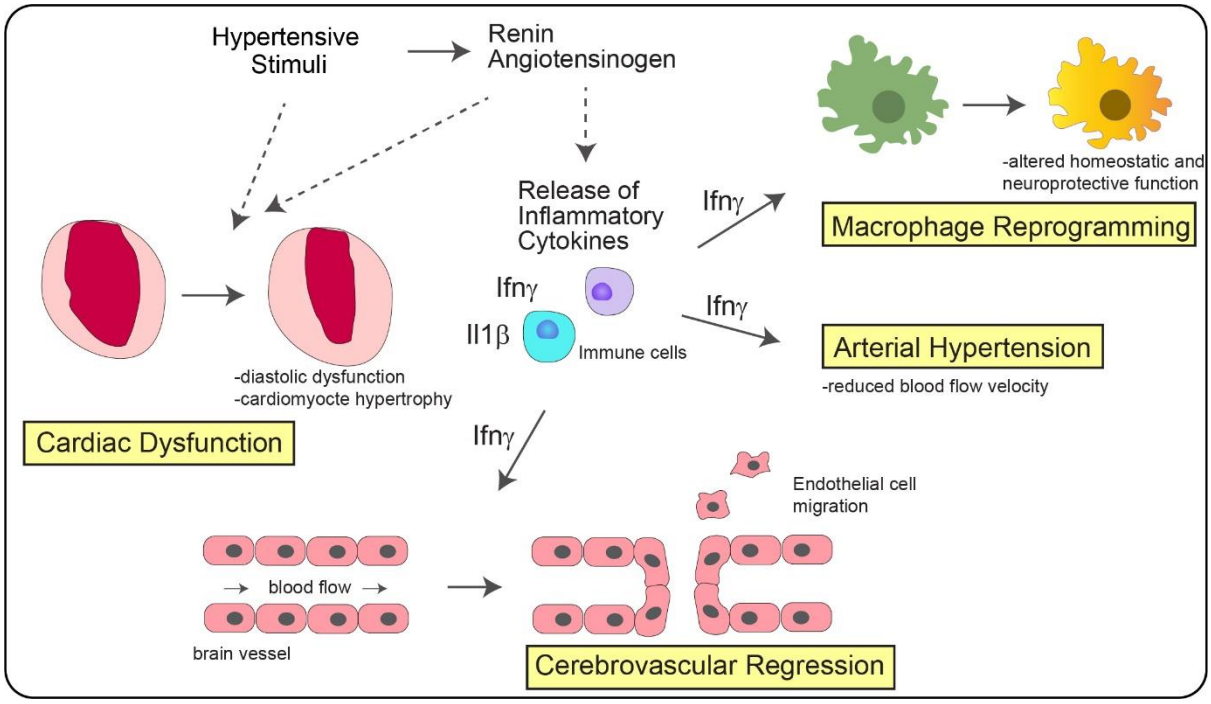

5 Bibliography

Alastalo, H., Räikkönen, K., Pesonen, A. K., Osmond, C., Barker, D. J. P., Heinonen, K., Kajantie, E., & Eriksson, J. G. (2013). Early life stress and blood pressure levels in late adulthood. *Journal of Human Hypertension*, *27*(2), 90–94. https://doi.org/10.1038/jhh.2012.6

Alsop, D., & Vijayan, M. M. (2008). Development of the corticosteroid stress axis and receptor expression in zebrafish. *American Journal of Physiology - Regulatory Integrative and Comparative Physiology*, *294*(3), 711–719. https://doi.org/10.1152/AJPREGU.00671.2007/SUPPL_FILE/SUPPLEMENTAL_MATERIAL.PDF

Andrés-Delgado, L., & Mercader, N. (2016). Interplay between cardiac function and heart development. *Biochimica et Biophysica Acta*, *1863*(7Part B), 1707. https://doi.org/10.1016/J.BBAMCR.2016.03.004

Arackal, A., & Alsayouri, K. (2020). Histology, Heart. *StatPearls*. http://www.ncbi.nlm.nih.gov/pubmed/31424727

Araya, R., Kudo, M., Kawano, M., Ishii, K., Hashikawa, T., Iwasato, T., Itohara, S., Terasaki, T., Oohira, A., Mishina, Y., & Yamada, M. (2008). BMP signaling through BMPRIA in astrocytes is essential for proper cerebral angiogenesis and formation of the blood-brain-barrier. *Molecular and Cellular Neuroscience*, *38*(3), 417–430. https://doi.org/10.1016/j.mcn.2008.04.003

Asakawa, K., Suster, M. L., Mizusawa, K., Nagayoshi, S., Kotani, T., Urasaki, A., Kishimoto, Y., Hibi, M., & Kawakami, K. (2008). Genetic dissection of neural circuits by Tol2 transposon-mediated Gal4 gene and enhancer trapping in zebrafish. *Proceedings of the National Academy of Sciences of the United States of America*, *105*(4), 1255–1260. https://doi.org/10.1073/pnas.0704963105

Atlas, S. A. (2007). The renin-angiotensin aldosterone system: Pathophysiological role and pharmacologic inhibition. *Journal of Managed Care Pharmacy*, *13*(8 SUPPL. B). https://doi.org/10.18553/jmcp.2007.13.s8-b.9

Role of cytokines and inflammation in heart function during health and disease, 23 Heart Failure Reviews 733 (2018). https://doi.org/10.1007/s10741-018-9716-x

Bautista, L. E., Vera, L. M., Arenas, I. A., & Gamarra, G. (2005). Independent association between inflammatory markers (C-reactive protein, interleukin-6, and TNF-α) and essential hypertension. *Journal of Human Hypertension*, *19*(2), 149–154. https://doi.org/10.1038/sj.jhh.1001785

Beauchet, O., Celle, S., Roche, F., Bartha, R., Montero-Odasso, M., Allali, G., & Annweiler, C. (2013). Blood pressure levels and brain volume reduction: A systematic review and meta-analysis. *Journal of Hypertension*, *31*(8), 1502–1516. https://doi.org/10.1097/HJH.0b013e32836184b5

Beis, D., Bartman, T., Jin, S.-W., Scott, I. C., D'Amico, L. A., Ober, E. A., Verkade, H., Frantsve, J., Field, H. A., Wehman, A., Baier, H., Tallafuss, A., Bally-Cuif, L., Chen, J.-N., Stainier, D. Y. R., & Jungblut, B. (2005). Genetic and cellular analyses of zebrafish atrioventricular cushion and valve development. *Development*, *132*(18), 4193–4204.

https://doi.org/10.1242/dev.01970

Benediktsson, R., Lindsay, R. S., Noble, J., Seckl, J. R., & Edwards, C. R. W. (1993). Glucocorticoid exposure in utero: new model for adult hypertension. *The Lancet*, *341*(8841), 339–341. https://doi.org/10.1016/0140-6736(93)90138-7

Benediktsson, Rafn, Calder, A. A., Edwards, C. R. W., & Seckl, J. R. (1997). Placental 11β-hydroxysteroid dehydrogenase: A key regulator of fetal glucocorticoid exposure. *Clinical Endocrinology*, *46*(2), 161–166. https://doi.org/10.1046/j.1365-2265.1997.1230939.x

Bertozzi, A., Wu, C. C., Nguyen, P. D., Vasudevarao, M. D., Mulaw, M. A., Koopman, C. D., de Boer, T. P., Bakkers, J., & Weidinger, G. (2021). Is zebrafish heart regeneration "complete"? Lineage-restricted cardiomyocytes proliferate to pre-injury numbers but some fail to differentiate in fibrotic hearts. *Developmental Biology*, *471*, 106–118. https://doi.org/10.1016/J.YDBIO.2020.12.004

Bhattarai, P., Thomas, A. K., Cosacak, M. I., Papadimitriou, C., Mashkaryan, V., Froc, C., Reinhardt, S., Kurth, T., Dahl, A., Zhang, Y., & Kizil, C. (2016). IL4/STAT6 Signaling Activates Neural Stem Cell Proliferation and Neurogenesis upon Amyloid-β42 Aggregation in Adult Zebrafish Brain. *Cell Reports*, *17*(4), 941–948. https://doi.org/10.1016/j.celrep.2016.09.075

Biola, A., Andréau, K., David, M., Sturm, M., Haake, M., Bertoglio, J., & Pallardy, M. (2000). The glucocorticoid receptor and STAT6 physically and functionally interact in T-lymphocytes. *FEBS Letters*, *487*(2), 229–233. https://doi.org/10.1016/S0014-5793(00)02297-3

Blacher, J., Evans, A., Arveiler, D., Amouyel, P., Ferrières, J., Bingham, A., Yarnell, J., Haas, B., Montaye, M., Ruidavets, J.-B. B., Ducimetière, P., & Group, on behalf of the P. S. (2010). Residual cardiovascular risk in treated hypertension and hyperlipidaemia: the PRIME Study. *Journal of Human Hypertension*, *24*(1), 19–26. https://doi.org/10.1038/jhh.2009.34

Bornhorst, D., & Abdelilah-Seyfried, S. (2021). Strong as a Hippo's Heart: Biomechanical Hippo Signaling During Zebrafish Cardiac Development. *Frontiers in Cell and Developmental Biology*, *9*, 2192. https://doi.org/10.3389/FCELL.2021.731101/BIBTEX

Brown, D., Samsa, L., Qian, L., & Liu, J. (2016). Advances in the Study of Heart Development and Disease Using Zebrafish. *Journal of Cardiovascular Development and Disease*, *3*(2), 13. https://doi.org/10.3390/jcdd3020013

Brüel, A., Christoffersen, T. E. H., & Nyengaard, J. R. (2007). Growth hormone increases the proliferation of existing cardiac myocytes and the total number of cardiac myocytes in the rat heart. *Cardiovascular Research*, *76*(3), 400–408. https://doi.org/10.1016/J.CARDIORES.2007.06.026

Busillo, J. M., & Cidlowski, J. A. (2013). The five Rs of glucocorticoid action during inflammation: ready, reinforce, repress, resolve, and restore. *Trends in Endocrinology and Metabolism: TEM*, *24*(3), 109. https://doi.org/10.1016/J.TEM.2012.11.005

Cai, H., & Harrison, D. G. (2000). Endothelial dysfunction in cardiovascular diseases: The role of oxidant stress. *Circulation Research*, *87*(10), 840–844. https://doi.org/10.1161/01.RES.87.10.840

Caillon, A., Paradis, P., & Schiffrin, E. L. (2019). Role of immune cells in hypertension. *British Journal of Pharmacology*, *176*(12), 1818–1828. https://doi.org/10.1111/bph.14427

Cain, D. W., & Cidlowski, J. A. (2017). Immune regulation by glucocorticoids. *Nature Reviews Immunology*, *17*(4), 233–247. https://doi.org/10.1038/nri.2017.1

Carey, R. M., Calhoun, D. A., Bakris, G. L., Brook, R. D., Daugherty, S. L., Dennison-Himmelfarb, C. R., Egan, B. M., Flack, J. M., Gidding, S. S., Judd, E., Lackland, D. T., Laffer, C. L., Newton-Cheh, C., Smith, S. M., Taler, S. J., Textor, S. C., Turan, T. N., & White, W. B. (2018). Resistant hypertension: Detection, evaluation, and management a scientific statement from the American Heart Association. *Hypertension*, *72*(5), E53–E90. https://doi.org/10.1161/HYP.0000000000000084

Cassar, S., Adatto, I., Freeman, J. L., Gamse, J. T., Iturria, I., Lawrence, C., Muriana, A., Peterson, R. T., Van Cruchten, S., & Zon, L. I. (2020). Use of Zebrafish in Drug Discovery Toxicology. *Chemical Research in Toxicology*, *33*(1), 95–118. https://doi.org/10.1021/acs.chemrestox.9b00335

Cassidy-Bushrow, A. E., Peters, R. M., Johnson, D. A., & Templin, T. N. (2012). Association of depressive symptoms with inflammatory biomarkers among pregnant African-American women. *Journal of Reproductive Immunology*, *94*(2), 202–209. https://doi.org/10.1016/j.jri.2012.01.007

Castillo-Ramírez, L. A., Ryu, S., & De Marco, R. J. (2019). Active behaviour during early development shapes glucocorticoid reactivity. *Scientific Reports*, *9*(1), 1–9. https://doi.org/10.1038/s41598-019-49388-3

Celle, S., Annweiler, C., Pichot, V., Bartha, R., Barthélémy, J. C., Roche, F., & Beauchet, O. (2012). Association between ambulatory 24-hour blood pressure levels and brain volume reduction: A cross-sectional elderly population-based study. *Hypertension*, *60*(5), 1324–1331. https://doi.org/10.1161/HYPERTENSIONAHA.112.193409

Chakrabarti, S., Streisinger, G., Singer, F., & Walker, C. (1983). Frequency of γ-ray induced specific locus and recessive lethal mutations in mature germ cells of the zebrafish, brachydanio rerio. *Genetics*, *103*(1), 109–123. https://doi.org/10.1093/genetics/103.1.109

Chatzopoulou, A., Schoonheim, P. J., Torraca, V., Meijer, A. H., Spaink, H. P., & Schaaf, M. J. M. (2017). Functional analysis reveals no transcriptional role for the glucocorticoid receptor β-isoform in zebrafish. *Molecular and Cellular Endocrinology*, *447*, 61–70. https://doi.org/10.1016/j.mce.2017.02.036

Chen, H., Zhang, W., Sun, X., Yoshimoto, M., Chen, Z., Zhu, W., Liu, J., Shen, Y., Yong, W., Li, D., Zhang, J., Lin, Y., Li, B., VanDusen, N. J., Snider, P., Schwartz, R. J., Conway, S. J., Field, L. J., Yoder, M. C., … Shou, W. (2013). Fkbp1a controls ventricular myocardium trabeculation and compaction by regulating endocardial Notch1 activity. *Development*, *140*(9), 1946–1957. https://doi.org/10.1242/DEV.089920

Chen, J., Huddleston, J., Buckley, R. M., Malig, M., Lawhon, S. D., Skow, L. C., Lee, M. O., Eichler, E. E., Andersson, L., & Womack, J. E. (2015). Bovine NK-lysin: Copy number variation and functional diversification. *Proceedings of the National Academy of Sciences of the United States of America*, *112*(52). https://doi.org/10.1073/pnas.1519374113

Chen, Q., Jiang, L., Li, C., Hu, D., Bu, J., Cai, D., & Du, J. (2012). Haemodynamics-Driven Developmental Pruning of Brain Vasculature in Zebrafish. *PLOS Biology*, *10*(8), e1001374. https://doi.org/10.1371/journal.pbio.1001374

Chhatbar, P. Y., Kara, P., PY, C., P, K., Chhatbar, P. Y., & Kara, P. (2013). Improved blood velocity measurements with a hybrid image filtering and iterative Radon transform

algorithm. *Frontiers in Neuroscience*, *7*(7 JUN), 106. https://doi.org/10.3389/fnins.2013.00106

Chi, N. C., Shaw, R. M., De Val, S., Kang, G., Jan, L. Y., Black, B. L., & Stainier, D. Y. R. (2008). Foxn4 directly regulates tbx2b expression and atrioventricular canal formation. *Genes and Development*, *22*(6), 734–739. https://doi.org/10.1101/gad.1629408

Christian, L. M., Franco, A., Glaser, R., & Iams, J. D. (2009). Depressive symptoms are associated with elevated serum proinflammatory cytokines among pregnant women. *Brain, Behavior, and Immunity*, *23*(6), 750–754. https://doi.org/10.1016/j.bbi.2009.02.012

Chrousos, G. P. (2009). Stress and disorders of the stress system. *Nature Reviews Endocrinology 2009 5:7*, *5*(7), 374–381. https://doi.org/10.1038/nrendo.2009.106

Chrousos, G. P., & Gold, P. W. (1992). The Concepts of Stress and Stress System Disorders: Overview of Physical and Behavioral Homeostasis. *JAMA: The Journal of the American Medical Association*, *267*(9), 1244–1252. https://doi.org/10.1001/jama.1992.03480090092034

Cieslik, K. A., Taffet, G. E., Carlson, S., Hermosillo, J., Trial, J. A., & Entman, M. L. (2011). Immune-inflammatory dysregulation modulates the incidence of progressive fibrosis and diastolic stiffness in the aging heart. *Journal of Molecular and Cellular Cardiology*, *50*(1), 248–256. https://doi.org/10.1016/j.yjmcc.2010.10.019

Clark, K. J., Boczek, N. J., & Ekker, S. C. (2011). Stressing zebrafish for behavioral genetics. *Reviews in the Neurosciences*, *22*(1), 49–62. https://doi.org/10.1515/RNS.2011.007

Cole, T. J., Blendy, J. A., Monaghan, A. P., Krieglstein, K., Schmid, W., Aguzzi, A., Fantuzzi, G., Hummler, E., Unsicker, K., & Schütz, G. (1995). Targeted disruption of the glucocorticoid receptor gene blocks adrenergic chromaffin cell development and severely retards lung maturation. *Genes and Development*, *9*(13), 1608–1621. https://doi.org/10.1101/gad.9.13.1608

Collier, A. D., Kalueff, A. V., & Echevarria, D. J. (2017). Zebrafish models of anxiety-like behaviors. *The Rights and Wrongs of Zebrafish: Behavioral Phenotyping of Zebrafish*, 45–72. https://doi.org/10.1007/978-3-319-33774-6_3/COVER/

Conway, G. (2006). STAT3-dependent pathfinding and control of axonal branching and target selection. *Developmental Biology*, *296*(1), 119–136. https://doi.org/10.1016/j.ydbio.2006.04.444

Cottrell, E. C., Holmes, M. C., Livingstone, D. E., Kenyon, C. J., & Seckl, J. R. (2012). Reconciling the nutritional and glucocorticoid hypotheses of fetal programming. *The FASEB Journal*, *26*(5), 1866–1874. https://doi.org/10.1096/fj.12-203489

Crowley, S. D., Song, Y. S., Lin, E. E., Griffiths, R., Kim, H. S., & Ruiz, P. (2010). Lymphocyte responses exacerbate angiotensin II-dependent hypertension. *American Journal of Physiology - Regulatory Integrative and Comparative Physiology*, *298*(4). https://doi.org/10.1152/ajpregu.00373.2009

Cunha, S. I., Magnusson, P. U., Dejana, E., & Lampugnani, M. G. (2017). Deregulated TGF-β/BMP signaling in vascular malformations. *Circulation Research*, *121*(8), 981–999. https://doi.org/10.1161/CIRCRESAHA.117.309930

Cuspidi, C., Sala, C., Negri, F., Mancia, G., & Morganti, A. (2012). Prevalence of left-

ventricular hypertrophy in hypertension: an updated review of echocardiographic studies. *Journal of Human Hypertension*, *26*(6), 343–349. https://doi.org/10.1038/JHH.2011.104

Dahl, L. K., Heine, M., & Tassinari, L. (1962). Role of genetic factors in susceptibility to experimental hypertension due to chronic excess salt ingestion. *Nature*, *194*(4827), 480–482. https://doi.org/10.1038/194480b0

Danese, A., Pariante, C. M., Caspi, A., Taylor, A., & Poulton, R. (2007). Childhood maltreatment predicts adult inflammation in a life-course study. *Proceedings of the National Academy of Sciences of the United States of America*, *104*(4), 1319–1324. https://doi.org/10.1073/pnas.0610362104

Davison, J. M., Akitake, C. M., Goll, M. G., Rhee, J. M., Gosse, N., Baier, H., Halpern, M. E., Leach, S. D., & Parsons, M. J. (2007). Transactivation from Gal4-VP16 transgenic insertions for tissue-specific cell labeling and ablation in zebrafish. *Developmental Biology*, *304*(2), 811–824. https://doi.org/10.1016/j.ydbio.2007.01.033

De Ciuceis, C., Agabiti-Rosei, C., Rossini, C., Airò, P., Scarsi, M., Tincani, A., Tiberio, G. A. M., Piantoni, S., Porteri, E., Solaini, L., Duse, S., Semeraro, F., Petroboni, B., Mori, L., Castellano, M., Gavazzi, A., Agabiti-Rosei, E., & Rizzoni, D. (2017). Relationship between different subpopulations of circulating CD4+ T lymphocytes and microvascular or systemic oxidative stress in humans. *Blood Pressure*, *26*(4), 237–245. https://doi.org/10.1080/08037051.2017.1292395

De Ciuceis, C., Amiri, F., Brassard, P., Endemann, D. H., Touyz, R. M., & Schiffrin, E. L. (2005). Reduced vascular remodeling, endothelial dysfunction, and oxidative stress in resistance arteries of angiotensin II-infused macrophage colony-stimulating factor-deficient mice: evidence for a role in inflammation in angiotensin-induced vascular injury. *Arteriosclerosis, Thrombosis, and Vascular Biology*, *25*(10), 2106–2113. https://doi.org/10.1161/01.ATV.0000181743.28028.57

De Vries, J. E., Carballido, J. M., & Aversa, G. (1999). Receptors and cytokines involved in allergic TH2 cell responses. *Journal of Allergy and Clinical Immunology*, *103*(5 SUPPL.), S492–S496. https://doi.org/10.1016/S0091-6749(99)70166-1

Dickhout, J. G., Carlisle, R. E., & Austin, R. C. (2011). Interrelationship between cardiac hypertrophy, heart failure, and chronic kidney disease: Endoplasmic reticulum stress as a mediator of pathogenesis. *Circulation Research*, *108*(5), 629–642. https://doi.org/10.1161/CIRCRESAHA.110.226803

Dijkhorst-Oei, L. T., Stroes, E. S. G., Koomans, H. A., & Rabelink, T. J. (1999). Acute simultaneous stimulation of nitric oxide and oxygen radicals by angiotensin II in humans in vivo. *Journal of Cardiovascular Pharmacology*, *33*(3), 420–424. https://doi.org/10.1097/00005344-199903000-00012

Dinarello, A., Licciardello, G., Fontana, C. M., Tiso, N., Argenton, F., & Valle, L. D. (2020). Glucocorticoid receptor activities in the zebrafish model: a review. *Journal of Endocrinology*, *247*(3), R63–R82. https://doi.org/10.1530/JOE-20-0173

DM, M., JP, E., Mosser, D. M., Edwards, J. P., DM, M., & JP, E. (2008). Exploring the full spectrum of macrophage activation. *Nature Reviews Immunology*, *8*(12), 958–969. https://doi.org/10.1038/nri2448

Dong, M., Giles, W. H., Felitti, V. J., Dube, S. R., Williams, J. E., Chapman, D. P., & Anda, R. F. (2004). Insights into causal pathways for ischemic heart disease: Adverse childhood

experiences study. *Circulation*, *110*(13), 1761–1766. https://doi.org/10.1161/01.CIR.0000143074.54995.7F

Dörffel, Y., Lätsch, C., Stuhlmüller, B., Schreiber, S., Scholze, S., Burmester, G. R., & Scholze, J. (1999). Preactivated peripheral blood monocytes in patients with essential hypertension. *Hypertension*, *34*(1), 113–117. https://doi.org/10.1161/01.HYP.34.1.113

Drazner, M. H. (2011). The progression of hypertensive heart disease. *Circulation*, *123*(3), 327–334. https://doi.org/10.1161/CIRCULATIONAHA.108.845792

Drummond, G. R., Vinh, A., Guzik, T. J., & Sobey, C. G. (2019). Immune mechanisms of hypertension. *Nature Reviews Immunology*, *19*(8), 517–532. https://doi.org/10.1038/s41577-019-0160-5

Emir, G. K., Ünal, Y., Yılmaz, N., Tosun, K., & Kutlu, G. (2019). The association of low levels of nesfatin-1 and glucagon-like peptide-1 with oxidative stress in Parkinson's disease. *Neurological Sciences*, *40*(12), 2529–2535. https://doi.org/10.1007/s10072-019-03975-4

Engelbertsen, D., Andersson, L., Ljungcrantz, I., Wigren, M., Hedblad, B., Nilsson, J., & Björkbacka, H. (2013). T-helper 2 immunity is associated with reduced risk of myocardial infarction and stroke. *Arteriosclerosis, Thrombosis, and Vascular Biology*, *33*(3), 637–644. https://doi.org/10.1161/ATVBAHA.112.300871

Epelman, S., Lavine, K. J., Beaudin, A. E., Sojka, D. K., Carrero, J. A., Calderon, B., Brija, T., Gautier, E. L., Ivanov, S., Satpathy, A. T., Schilling, J. D., Schwendener, R., Sergin, I., Razani, B., Forsberg, E. C., Yokoyama, W. M., Unanue, E. R., Colonna, M., Randolph, G. J., & Mann, D. L. (2014). Embryonic and adult-derived resident cardiac macrophages are maintained through distinct mechanisms at steady state and during inflammation. *Immunity*, *40*(1), 91–104. https://doi.org/10.1016/j.immuni.2013.11.019

Escoter-Torres, L., Caratti, G., Mechtidou, A., Tuckermann, J., Uhlenhaut, N. H., & Vettorazzi, S. (2019). Fighting the fire: Mechanisms of inflammatory gene regulation by the glucocorticoid receptor. *Frontiers in Immunology*, *10*(AUG), 1859. https://doi.org/10.3389/fimmu.2019.01859

Fang, Y., Gupta, V., Karra, R., Holdway, J. E., Kikuchi, K., & Poss, K. D. (2013). Translational profiling of cardiomyocytes identifies an early Jak1/Stat3 injury response required for zebrafish heart regeneration. *Proceedings of the National Academy of Sciences of the United States of America*, *110*(33), 13416–13421. https://doi.org/10.1073/pnas.1309810110

Faraco, G., Sugiyama, Y., Lane, D., Garcia-Bonilla, L., Chang, H., Santisteban, M. M., Racchumi, G., Murphy, M., Van Rooijen, N., Anrather, J., & Iadecola, C. (2016). Perivascular macrophages mediate the neurovascular and cognitive dysfunction associated with hypertension. *Journal of Clinical Investigation*, *126*(12), 4674–4689. https://doi.org/10.1172/JCI86950

Feihl, François, Liaudet, L., Levy, B. I., & Waeber, B. (2008). Hypertension and microvascular remodelling. *Cardiovascular Research*, *78*(2), 274–285. https://doi.org/10.1093/cvr/cvn022

Feihl, François, Liaudet, L., Waeber, B., & Levy, B. I. (2006). Hypertension. *Hypertension*, *48*(6), 1012–1017. https://doi.org/10.1161/01.HYP.0000249510.20326.72

Felitti, V. J., Anda, R. F., Nordenberg, D., Williamson, D. F., Spitz, A. M., Edwards, V., Koss, M. P., & Marks, J. S. (1998). Relationship of childhood abuse and household dysfunction

to many of the leading causes of death in adults: The adverse childhood experiences (ACE) study. *American Journal of Preventive Medicine*, *14*(4), 245–258. https://doi.org/10.1016/S0749-3797(98)00017-8

Foti, M. (2017). Introduction to Cytokines as Tissue Regulators in Health and Disease. *Cytokine Effector Functions in Tissues*, 3–30. https://doi.org/10.1016/B978-0-12-804214-4.00019-1

Fowden, A. L., Li, J., & Forhead, A. J. (1998). Glucocorticoids and the preparation for life after birth: are there long-term consequences of the life insurance? *Proceedings of the Nutrition Society*, *57*(1), 113–122. https://doi.org/10.1079/PNS19980017

Fraccarollo, D., Berger, S., Galuppo, P., Kneitz, S., Hein, L., Schütz, G., Frantz, S., Ertl, G., & Bauersachs, J. (2011). Deletion of cardiomyocyte mineralocorticoid receptor ameliorates adverse remodeling after myocardial infarction. *Circulation*, *123*(4), 400–408. https://doi.org/10.1161/CIRCULATIONAHA.110.983023

Franco, C. A., Jones, M. L., Bernabeu, M. O., Geudens, I., Mathivet, T., Rosa, A., Lopes, F. M., Lima, A. P., Ragab, A., Collins, R. T., Phng, L.-K. K., Coveney, P. V., & Gerhardt, H. (2015). Correction: Dynamic Endothelial Cell Rearrangements Drive Developmental Vessel Regression (PLoS Biol, 2015). *PLoS Biology*, *13*(4), e1002125. https://doi.org/10.1371/journal.pbio.1002163

Franssen, C., Chen, S., Unger, A., Korkmaz, H. I., De Keulenaer, G. W., Tschöpe, C., Leite-Moreira, A. F., Musters, R., Niessen, H. W. M., Linke, W. A., Paulus, W. J., & Hamdani, N. (2016). Myocardial Microvascular Inflammatory Endothelial Activation in Heart Failure With Preserved Ejection Fraction. *JACC: Heart Failure*, *4*(4), 312–324. https://doi.org/10.1016/j.jchf.2015.10.007

Fukushima, Y., Okada, M., Kataoka, H., Hirashima, M., Yoshida, Y., Mann, F., Gomi, F., Nishida, K., Nishikawa, S. I., & Uemura, A. (2011). Sema3E-PlexinD1 signaling selectively suppresses disoriented angiogenesis in ischemic retinopathy in mice. *Journal of Clinical Investigation*, *121*(5), 1974–1985. https://doi.org/10.1172/JCI44900

Gandhi, H., Worch, R., Kurgonaite, K., Hintersteiner, M., Schwille, P., Bökel, C., & Weidemann, T. (2014). Dynamics and interaction of Interleukin-4 receptor subunits in living cells. *Biophysical Journal*, *107*(11), 2515–2527. https://doi.org/10.1016/j.bpj.2014.07.077

Gao, T., Li, B., Hou, Y., Luo, S., Feng, L., Nie, J., Ma, Y., Xiao, L., Chen, X., Bao, H., Lu, X., Huang, F., Wang, G., Xiao, C., & Du, J. (2019). Interleukin-4 signalling pathway underlies the anxiolytic effect induced by 3-deoxyadenosine. *Psychopharmacology*, *236*(10), 2959–2973. https://doi.org/10.1007/s00213-019-5186-7

Garcia, A. G., Wilson, R. M., Heo, J., Murthy, N. R., Baid, S., Ouchi, N., & Sam, F. (2012). Interferon-γ ablation exacerbates myocardial hypertrophy in diastolic heart failure. *American Journal of Physiology - Heart and Circulatory Physiology*, *303*(5), H587–H596. https://doi.org/10.1152/ajpheart.00298.2012

García de Vinuesa, A., Abdelilah-Seyfried, S., Knaus, P., Zwijsen, A., & Bailly, S. (2016). BMP signaling in vascular biology and dysfunction. *Cytokine and Growth Factor Reviews*, *27*, 65–79. https://doi.org/10.1016/j.cytogfr.2015.12.005

Gemou-Engesaeth, V., Fagerhol, M. K., Toda, M., Hamid, Q., Halvorsen, S., Groegaard, J. B., & Corrigan, C. J. (2002). Expression of activation markers and cytokine mRNA by

peripheral blood CD4 and CD8 T cells in atopic and nonatopic childhood asthma: effect of inhaled glucocorticoid therapy. *Pediatrics*, *109*(2). https://doi.org/10.1542/PEDS.109.2.E24

Geoffrey Burns, C., Milan, D. J., Grande, E. J., Rottbauer, W., Macrae, C. A., & Fishman, M. C. (2005). High-throughput assay for small molecules that modulate zebrafish embryonic heart rate. *Nature Chemical Biology*, *1*(5), 263–264. https://doi.org/10.1038/NCHEMBIO732

Gerri, C., Marín-Juez, R., Marass, M., Marks, A., Maischein, H. M., & Stainier, D. Y. R. (2017). Hif-1α regulates macrophage-endothelial interactions during blood vessel development in zebrafish. *Nature Communications*, *8*. https://doi.org/10.1038/ncomms15492

Ghatage, T., Goyal, S. G., Dhar, A., & Bhat, A. (2021). Novel therapeutics for the treatment of hypertension and its associated complications: peptide- and nonpeptide-based strategies. *Hypertension Research 2021 44:7*, *44*(7), 740–755. https://doi.org/10.1038/s41440-021-00643-z

Gieseck, R. L., Wilson, M. S., & Wynn, T. A. (2017). Type 2 immunity in tissue repair and fibrosis. *Nature Reviews Immunology 2017 18:1*, *18*(1), 62–76. https://doi.org/10.1038/nri.2017.90

Gitler, A. D., Lu, M. M., & Epstein, J. A. (2004). PlexinD1 and semaphorin signaling are required in endothelial cells for cardiovascular development. *Developmental Cell*, *7*(1), 107–116. https://doi.org/10.1016/j.devcel.2004.06.002

Gjerstad, J. K., Lightman, S. L., & Spiga, F. (2018). Role of glucocorticoid negative feedback in the regulation of HPA axis pulsatility. *Stress*, *21*(5), 403–416. https://doi.org/10.1080/10253890.2018.1470238

Gjesdal, O., Bluemke, D. A., & Lima, J. A. (2011). Cardiac remodeling at the population level—risk factors, screening, and outcomes. *Nature Reviews Cardiology 2011 8:12*, *8*(12), 673–685. https://doi.org/10.1038/nrcardio.2011.154

Glover, V. (2015). Prenatal stress and its effects on the fetus and the child: Possible Underlying biological mechanisms. *Advances in Neurobiology*, *10*, 269–283. https://doi.org/10.1007/978-1-4939-1372-5_13

Godoy, L. D., Rossignoli, M. T., Delfino-Pereira, P., Garcia-Cairasco, N., & Umeoka, E. H. de L. (2018). A comprehensive overview on stress neurobiology: Basic concepts and clinical implications. *Frontiers in Behavioral Neuroscience*, *12*, 127. https://doi.org/10.3389/FNBEH.2018.00127/BIBTEX

González, A., Ravassa, S., López, B., Moreno, M. U., Beaumont, J., San José, G., Querejeta, R., Bayés-Genís, A., & Díez, J. (2018). Myocardial remodeling in hypertension toward a new view of hypertensive heart disease. *Hypertension*, *72*(3), 549–558. https://doi.org/10.1161/HYPERTENSIONAHA.118.11125

Goumans, M. J., Zwijsen, A., ten Dijke, P., & Bailly, S. (2018). Bone morphogenetic proteins in vascular homeostasis and disease. *Cold Spring Harbor Perspectives in Biology*, *10*(2), a031989. https://doi.org/10.1101/cshperspect.a031989

Gour, N., & Wills-Karp, M. (2015). IL-4 and IL-13 signaling in allergic airway disease. *Cytokine*, *75*(1), 68–78. https://doi.org/10.1016/j.cyto.2015.05.014

Graney, P. L., Ben-Shaul, S., Landau, S., Bajpai, A., Singh, B., Eager, J., Cohen, A., Levenberg, S., & Spiller, K. L. (2020). Macrophages of diverse phenotypes drive vascularization of engineered tissues. *Science Advances*, *6*(18). https://doi.org/10.1126/sciadv.aay6391

Gray, C., Loynes, C. A., Whyte, M. K. B., Crossman, D. C., Renshaw, S. A., & Chico, T. J. A. (2011). Simultaneous intravital imaging of macrophage and neutrophil behaviour during inflammation using a novel transgenic zebrafish. *Thrombosis and Haemostasis*, *105*(5), 811–819. https://doi.org/10.1160/TH10-08-0525

Grunwald, D. J., & Streisinger, G. (1992). Induction of recessive lethal and specific locus mutations in the zebrafish with ethyl nitrosourea. *Genetical Research*, *59*(2), 103–116. https://doi.org/10.1017/S0016672300030317

Gurevich, D. B., Severn, C. E., Twomey, C., Greenhough, A., Cash, J., Toye, A. M., Mellor, H., & Martin, P. (2018). Live imaging of wound angiogenesis reveals macrophage orchestrated vessel sprouting and regression. *The EMBO Journal*, *37*(13). https://doi.org/10.15252/embj.201797786

Guzik, T. J., Hoch, N. E., Brown, K. A., McCann, L. A., Rahman, A., Dikalov, S., Goronzy, J., Weyand, C., & Harrison, D. G. (2007). Role of the T cell in the genesis of angiotensin II induced hypertension and vascular dysfunction. *The Journal of Experimental Medicine*, *204*(10), 2449–2460. https://doi.org/10.1084/jem.20070657

Haghikia, A., Ricke-Hoch, M., Stapel, B., Gorst, I., & Hilfiker-Kleiner, D. (2014). STAT3, a key regulator of cell-to-cell communication in the heart. *Cardiovascular Research*, *102*(2), 281–289. https://doi.org/10.1093/CVR/CVU034

Han, A., Yeo, H., Park, M. J., Kim, S. H., Choi, H. J., Hong, C. W., & Kwon, M. S. (2015). IL-4/10 prevents stress vulnerability following imipramine discontinuation. *Journal of Neuroinflammation*, *12*(1), 1–16. https://doi.org/10.1186/s12974-015-0416-3

Hansen-Smith, F. M., Morris, L. W., Greene, A. S., & Lombard, J. H. (1996). Rapid microvessel rarefaction with elevated salt intake and reduced renal mass hypertension in rats. *Circulation Research*, *79*(2), 324–330. https://doi.org/10.1161/01.RES.79.2.324

Harrison, D. G., Vinh, A., Lob, H., & Madhur, M. S. (2010). Role of the adaptive immune system in hypertension. *Current Opinion in Pharmacology*, *10*(2), 203–207. https://doi.org/10.1016/j.coph.2010.01.006

Harwani, S. C. (2018). Macrophages Under Pressure: The Role of Macrophage Polarization in Hypertension. *Translational Research : The Journal of Laboratory and Clinical Medicine*, *191*, 45. https://doi.org/10.1016/J.TRSL.2017.10.011

Heckel, E., Boselli, F., Roth, S., Krudewig, A., Belting, H. G., Charvin, G., & Vermot, J. (2015). Oscillatory flow modulates mechanosensitive klf2a expression through trpv4 and trpp2 during heart valve development. *Current Biology*, *25*(10), 1354–1361. https://doi.org/10.1016/j.cub.2015.03.038

Henrich, H. A., Romen, W., Heimgärtner, W., Hartung, E., & Bäumer, F. (1988). Capillary rarefaction characteristic of the skeletal muscle of hypertensive patients. *Klinische Wochenschrift 1988 66:2*, *66*(2), 54–60. https://doi.org/10.1007/BF01713011

Heywood, W. E., Galimberti, D., Bliss, E., Sirka, E., Paterson, R. W., Magdalinou, N. K., Carecchio, M., Reid, E., Heslegrave, A., Fenoglio, C., Scarpini, E., Schott, J. M., Fox, N. C., Hardy, J., Bahtia, K., Heales, S., Sebire, N. J., Zetterburg, H., & Mills, K. (2015).

Identification of novel CSF biomarkers for neurodegeneration and their validation by a high-throughput multiplexed targeted proteomic assay. *Molecular Neurodegeneration*, *10*(1), 64. https://doi.org/10.1186/s13024-015-0059-y

Hieda, M., Sarma, S., Hearon, C. M., Dias, K. A., Martinez, J., Samels, M., Everding, B., Palmer, D., Livingston, S., Morris, M., Howden, E., & Levine, B. D. (2020). Increased Myocardial Stiffness in Patients with High-Risk Left Ventricular Hypertrophy: The Hallmark of Stage-B Heart Failure with Preserved Ejection Fraction. *Circulation*, 115–123. https://doi.org/10.1161/CIRCULATIONAHA.119.040332

Higashi, Y., Kihara, Y., & Noma, K. (2012). Endothelial dysfunction and hypertension in aging. *Hypertension Research*, *35*(11), 1039–1047. https://doi.org/10.1038/hr.2012.138

Hilfiker-Kleiner, D., Hilfiker, A., Fuchs, M., Kaminski, K., Schaefer, A., Schieffer, B., Hillmer, A., Schmiedl, A., Ding, Z., Podewski, E., Podewski, E., Poli, V., Schneider, M. D., Schulz, R., Park, J. K., Wollert, K. C., & Drexler, H. (2004). Signal Transducer and Activator of Transcription 3 Is Required for Myocardial Capillary Growth, Control of Interstitial Matrix Deposition, and Heart Protection From Ischemic Injury. *Circulation Research*, *95*(2), 187–195. https://doi.org/10.1161/01.RES.0000134921.50377.61

Hollenberg, S. M., Weinberger, C., Ong, E. S., Cerelli, G., Oro, A., Lebo, R., Brad Thompson, E., Rosenfeld, M. G., & Evans, R. M. (1985). Primary structure and expression of a functional human glucocorticoid receptor cDNA. *Nature*, *318*(6047), 635–641. https://doi.org/10.1038/318635a0

Horsley, V., Jansen, K. M., Mills, S. T., & Pavlath, G. K. (2003). IL-4 acts as a myoblast recruitment factor during mammalian muscle growth. *Cell*, *113*(4), 483–494. https://doi.org/10.1016/S0092-8674(03)00319-2

Hostinar, C. E., Lachman, M. E., Mroczek, D. K., Seeman, T. E., & Miller, G. E. (2015). Additive contributions of childhood adversity and recent stressors to inflammation at midlife: Findings from the MIDUS study. *Developmental Psychology*, *51*(11), 1630–1644. https://doi.org/10.1037/dev0000049

Howe, K., Clark, M. D., Torroja, C. F., Torrance, J., Berthelot, C., Muffato, M., Collins, J. E., Humphray, S., McLaren, K., Matthews, L., McLaren, S., Sealy, I., Caccamo, M., Churcher, C., Scott, C., Barrett, J. C., Koch, R., Rauch, G. J., White, S., … Stemple, D. L. (2013). The zebrafish reference genome sequence and its relationship to the human genome. *Nature*, *496*(7446), 498–503. https://doi.org/10.1038/nature12111

Huang, X. L., Wang, Y. J., Yan, J. W., Wan, Y. N., Chen, B., Li, B. Z., Yang, G. J., & Wang, J. (2015). Role of anti-inflammatory cytokines IL-4 and IL-13 in systemic sclerosis. *Inflammation Research*, *64*(3–4), 151–159. https://doi.org/10.1007/s00011-015-0806-0

Hudson, W. H., Youn, C., & Ortlund, E. A. (2012). The structural basis of direct glucocorticoid-mediated transrepression. *Nature Structural & Molecular Biology 2012 20:1*, *20*(1), 53–58. https://doi.org/10.1038/nsmb.2456

Hulsmans, M., Clauss, S., Xiao, L., Aguirre, A. D., King, K. R., Hanley, A., Hucker, W. J., Wülfers, E. M., Seemann, G., Courties, G., Iwamoto, Y., Sun, Y., Savol, A. J., Sager, H. B., Lavine, K. J., Fishbein, G. A., Capen, D. E., Da Silva, N., Miquerol, L., … Nahrendorf, M. (2017). Macrophages Facilitate Electrical Conduction in the Heart. *Cell*, *169*(3), 510-522.e20. https://doi.org/10.1016/J.CELL.2017.03.050

Hulsmans, M., Sager, H. B., Roh, J. D., Valero-Muñoz, M., Houstis, N. E., Iwamoto, Y., Sun,

Y., Wilson, R. M., Wojtkiewicz, G., Tricot, B., Osborne, M. T., Hung, J., Vinegoni, C., Naxerova, K., Sosnovik, D. E., Zile, M. R., Bradshaw, A. D., Liao, R., Tawakol, A., … Nahrendorf, M. (2018). Cardiac macrophages promote diastolic dysfunction. *Journal of Experimental Medicine*, *215*(2), 423–440. https://doi.org/10.1084/jem.20171274

Humar, Rok, Resink, T., & Battegay, E. J. (2005). Vascular remodeling in hypertension. *Hypertension: Principles and Practice*, 85–98. https://doi.org/10.1161/hy09t1.096249

Humar, R., Zimmerli, L., & Battegay, E. (2009). Angiogenesis and hypertension: An update. *Journal of Human Hypertension*, *23*(12), 773–782. https://doi.org/10.1038/jhh.2009.63

Jacoby, J. J., Kalinowski, A., Liu, M. G., Zhang, S. S. M., Gao, Q., Chai, G. X., Ji, L., Iwamoto, Y., Li, E., Schneider, M., Russell, K. S., & Fu, X. Y. (2003). Cardiomyocyte-restricted knockout of STAT3 results in higher sensitivity to inflammation, cardiac fibrosis, and heart failure with advanced age. *Proceedings of the National Academy of Sciences of the United States of America*, *100*(22), 12929–12934. https://doi.org/10.1073/PNAS.2134694100/ASSET/63AAF1E8-0AB5-4756-8BF2-30D91A6FF5C4/ASSETS/GRAPHIC/PQ2134694005.JPEG

Javeshghani, D., Barhoumi, T., Idris-Khodja, N., Paradis, P., & Schiffrin, E. L. (2013). Reduced Macrophage-Dependent Inflammation Improves Endothelin-1–Induced Vascular Injury. *Hypertension*, *62*(1), 112–117. https://doi.org/10.1161/HYPERTENSIONAHA.113.01298

Jensen, G. S., Leon-Palmer, N. E., & Townsend, K. L. (2021). Bone morphogenetic proteins (BMPs) in the central regulation of energy balance and adult neural plasticity. *Metabolism: Clinical and Experimental*, *123*, 154837. https://doi.org/10.1016/j.metabol.2021.154837

Jetten, N., Verbruggen, S., Gijbels, M. J., Post, M. J., De Winther, M. P. J., & Donners, M. M. P. C. (2014). Anti-inflammatory M2, but not pro-inflammatory M1 macrophages promote angiogenesis in vivo. *Angiogenesis*, *17*(1), 109–118. https://doi.org/10.1007/s10456-013-9381-6

John, S., Sabo, P. J., Thurman, R. E., Sung, M. H., Biddie, S. C., Johnson, T. A., Hager, G. L., & Stamatoyannopoulos, J. A. (2011). Chromatin accessibility pre-determines glucocorticoid receptor binding patterns. *Nature Genetics*, *43*(3), 264–268. https://doi.org/10.1038/ng.759

Jovanovic, V. M., Salti, A., Tilleman, H., Zega, K., Jukic, M. M., Zou, H., Friedel, R. H., Prakash, N., Blaess, S., Edenhofer, F., & Brodski, C. (2018). BMP/SMAD pathway promotes neurogenesis of midbrain dopaminergic neurons in vivo and in human induced pluripotent and neural stem cells. *Journal of Neuroscience*, *38*(7), 1662–1676. https://doi.org/10.1523/JNEUROSCI.1540-17.2018

Junttila, I. S. (2018). Tuning the Cytokine Responses: An Update on Interleukin (IL)-4 and IL-13 Receptor Complexes. *Frontiers in Immunology*, *9*(JUN), 888. https://doi.org/10.3389/FIMMU.2018.00888

Kamat, N. V., Thabet, S. R., Xiao, L., Saleh, M. A., Kirabo, A., Madhur, M. S., Delpire, E., Harrison, D. G., & Mcdonough, A. A. (2015). RENAL TRANSPORTER ACTIVATION DURING ANGIOTENSIN II HYPERTENSION IS BLUNTED IN IFN-γ−/− AND IL-17A −/− MICE. *Hypertension*, *65*(3), 569. https://doi.org/10.1161/HYPERTENSIONAHA.114.04975

Kanellakis, P., Ditiatkovski, M., Kostolias, G., & Bobik, A. (2012). A pro-fibrotic role for interleukin-4 in cardiac pressure overload. *Cardiovascular Research*, *95*(1), 77–85. https://doi.org/10.1093/cvr/cvs142

Karlsson, L., Nousiainen, N., Scheinin, N. M., Maksimow, M., Salmi, M., Lehto, S. M., Tolvanen, M., Lukkarinen, H., & Karlsson, H. (2017). Cytokine profile and maternal depression and anxiety symptoms in mid-pregnancy—the FinnBrain Birth Cohort Study. *Archives of Women's Mental Health*, *20*(1), 39–48. https://doi.org/10.1007/s00737-016-0672-y

Kaufman, C. K., White, R. M., & Zon, L. (2009). Chemical genetic screening in the zebrafish embryo. *Nature Protocols*, *4*(10), 1422–1432. https://doi.org/10.1038/nprot.2009.144

Kelly-Welch, A. E., Hanson, E. M., Boothby, M. R., & Keegan, A. D. (2003). Interleukin-4 and interleukin-13 signaling connections maps. *Science*, *300*(5625), 1527–1528. https://doi.org/10.1126/science.1085458

Kelly-Welch, A., Hanson, E. M., & Keegan, A. D. (2005). Interleukin-4 (IL-4) pathway. *Science's STKE : Signal Transduction Knowledge Environment*, *2005*(293). https://doi.org/10.1126/stke.2932005cm9

Kikuchi, K., Gupta, V., Wang, J., Holdway, J. E., Wills, A. A., Fang, Y., & Poss, K. D. (2011). Tcf21+ epicardial cells adopt non-myocardial fates during zebrafish heart development and regeneration. *Development*, *138*(14), 2895–2902. https://doi.org/10.1242/dev.067041

Kikuchi, K., Holdway, J. E., Major, R. J., Blum, N., Dahn, R. D., Begemann, G., & Poss, K. D. (2011). Retinoic Acid Production by Endocardium and Epicardium Is an Injury Response Essential for Zebrafish Heart Regeneration. *Developmental Cell*, *20*(3), 397–404. https://doi.org/10.1016/j.devcel.2011.01.010

Kikuchi, K., Holdway, J. E., Werdich, A. A., Anderson, R. M., Fang, Y., Egnaczyk, G. F., Evans, T., MacRae, C. A., Stainier, D. Y. R., & Poss, K. D. (2010). Primary contribution to zebrafish heart regeneration by gata4(+) cardiomyocytes. *Nature*, *464*(7288), 601–605. https://doi.org/10.1038/NATURE08804

Kimura, R., Maeda, M., Arita, A., Oshima, Y., Obana, M., Ito, T., Yamamoto, Y., Mohri, T., Kishimoto, T., Kawase, I., Fujio, Y., & Azuma, J. (2007). Identification of cardiac myocytes as the target of interleukin 11, a cardioprotective cytokine. *Cytokine*, *38*(2), 107–115. https://doi.org/10.1016/J.CYTO.2007.05.011

Kimura, S., Zhang, G. X., Nishiyama, A., Shokoji, T., Yao, L., Fan, Y. Y., Rahman, M., Suzuki, T., Maeta, H., & Abe, Y. (2005). Role of NAD(P)H oxidase- and mitochondria-derived reactive oxygen species in cardioprotection of ischemic reperfusion injury by angiotensin II. *Hypertension*, *45*(5), 860–866. https://doi.org/10.1161/01.HYP.0000163462.98381.7f

Kino, T., Manoli, I., Kelkar, S., Wang, Y., Su, Y. A., & Chrousos, G. P. (2009). Glucocorticoid receptor (GR) β has intrinsic, GRα-independent transcriptional activity. *Biochemical and Biophysical Research Communications*, *381*(4), 671–675. https://doi.org/10.1016/j.bbrc.2009.02.110

Effects of stress on the development and progression of cardiovascular disease, 15 Nature Reviews Cardiology 215 (2018). https://doi.org/10.1038/nrcardio.2017.189

Ko, E. A., Amiri, F., Pandey, N. R., Javeshghani, D., Leibovitz, E., Touyz, R. M., & Schiffrin, E. L. (2007). Resistance artery remodeling in deoxycorticosterone acetate-salt hypertension is dependent on vascular inflammation: Evidence from m-CSF-deficient

mice. *American Journal of Physiology - Heart and Circulatory Physiology*, *292*(4), 1789–1795. https://doi.org/10.1152/ajpheart.01118.2006

Kobayashi, N., DeLano, F. A., & Schmid-Schönbein, G. W. (2005). Oxidative stress promotes endothelial cell apoptosis and loss of microvessels in the spontaneously hypertensive rats. *Arteriosclerosis, Thrombosis, and Vascular Biology*, *25*(10), 2114–2121. https://doi.org/10.1161/01.ATV.0000178993.13222.f2

Korn, C., & Augustin, H. G. (2015). Mechanisms of Vessel Pruning and Regression. *Developmental Cell*, *34*(1), 5–17. https://doi.org/10.1016/j.devcel.2015.06.004

Kossmann, S., Hu, H., Steven, S., Schönfelder, T., Fraccarollo, D., Mikhed, Y., Brähler, M., Knorr, M., Brandt, M., Karbach, S. H., Becker, C., Oelze, M., Bauersachs, J., Widder, J., Münzel, T., Daiber, A., & Wenzel, P. (2014). Inflammatory monocytes determine endothelial nitric-oxide synthase uncoupling and nitro-oxidative stress induced by Angiotensin II. *Journal of Biological Chemistry*, *289*(40), 27540–27550. https://doi.org/10.1074/jbc.M114.604231

Krishnamurthy, P., Rajasingh, J., Lambers, E., Qin, G., Losordo, D. W., & Kishore, R. (2009). IL-10 inhibits inflammation and attenuates left ventricular remodeling after myocardial infarction via activation of STAT-3 and suppression of HuR. *Circulation Research*, *104*(2), e9. https://doi.org/10.1161/CIRCRESAHA.108.188243

Kumai, Y., Bernier, N. J., Perry, S. F., Y, K., NJ, B., SF, P., Kumai, Y., Bernier, N. J., Perry, S. F., Y, K., NJ, B., SF, P., Kumai, Y., Bernier, N. J., & Perry, S. F. (2014). Angiotensin-II promotes Na+ uptake in larval zebrafish, Danio rerio, in acidic and ion-poor water. *Journal of Endocrinology*, *220*(3), 195–205. https://doi.org/10.1530/JOE-13-0374

Kuroda, K., Kato, T. S., & Amano, A. (2015). Hypertensive cardiomyopathy: A clinical approach and literature review. *World Journal of Hypertension*, *5*(2), 41. https://doi.org/10.5494/wjh.v5.i2.41

Lang, R. A., & Bishop, J. M. (1993). Macrophages are required for cell death and tissue remodeling in the developing mouse eye. *Cell*, *74*(3), 453–462. https://doi.org/10.1016/0092-8674(93)80047-I

Langlais, D., Couture, C., Balsalobre, A., & Drouin, J. (2012). The Stat3/GR Interaction Code: Predictive Value of Direct/Indirect DNA Recruitment for Transcription Outcome. *Molecular Cell*, *47*(1), 38–49. https://doi.org/10.1016/j.molcel.2012.04.021

Lawson, C. A., Zaccardi, F., Squire, I., Okhai, H., Davies, M., Huang, W., Mamas, M., Lam, C. S. P., Khunti, K., & Kadam, U. T. (2020). Risk factors for heart failure: 20-year population-based trends by sex, socioeconomic status, and ethnicity. *Circulation: Heart Failure*. https://doi.org/10.1161/CIRCHEARTFAILURE.119.006472

Lee, D. L., Sturgis, L. C., Labazi, H., Osborne, J. B., Fleming, C., Pollock, J. S., Manhiani, M., Imig, J. D., & Brands, M. W. (2006). Angiotensin II hypertension is attenuated in interleukin-6 knockout mice. *American Journal of Physiology - Heart and Circulatory Physiology*, *290*(3). https://doi.org/10.1152/ajpheart.00708.2005

Lee, H. J., Park, H. J., Starkweather, A., An, K., & Shim, I. (2016). Decreased Interleukin-4 Release from the Neurons of the Locus Coeruleus in Response to Immobilization Stress. *Mediators of Inflammation*, *2016*. https://doi.org/10.1155/2016/3501905

Leibovitz, E., Ebrahimian, T., Paradis, P., & Schiffrin, E. L. (2009). Aldosterone induces arterial stiffness in absence of oxidative stress and endothelial dysfunction. *Journal of*

Hypertension, *27*(11), 2192–2200. https://doi.org/10.1097/HJH.0b013e328330a963

Leid, J., Carrelha, J., Boukarabila, H., Epelman, S., Jacobsen, S. E. W., & Lavine, K. J. (2016). Primitive Embryonic Macrophages are Required for Coronary Development and Maturation. *Circulation Research*, *118*(10), 1498–1511. https://doi.org/10.1161/CIRCRESAHA.115.308270

Lenard, A., Daetwyler, S., Betz, C., Ellertsdottir, E., Belting, H.-G. G., Huisken, J., & Affolter, M. (2015). Endothelial Cell Self-fusion during Vascular Pruning. *PLoS Biology*, *13*(4), e1002126. https://doi.org/10.1371/journal.pbio.1002126

Lerman, L. O., Kurtz, T. W., Touyz, R. M., Ellison, D. H., Chade, A. R., Crowley, S. D., Mattson, D. L., Mullins, J. J., Osborn, J., Eirin, A., Reckelhoff, J. F., Iadecola, C., & Coffman, T. M. (2019). Animal Models of Hypertension: A Scientific Statement From the American Heart Association. *Hypertension (Dallas, Tex. : 1979)*, *73*(6), e87–e120. https://doi.org/10.1161/HYP.0000000000000090

Levick, S. P., McLarty, J. L., Murray, D. B., Freeman, R. M., Carver, W. E., & Brower, G. L. (2009). Cardiac mast cells mediate left ventricular fibrosis in the hypertensive rat heart. *Hypertension*, *53*(6), 1041–1047. https://doi.org/10.1161/HYPERTENSIONAHA.108.123158

Levy, B. I., Schiffrin, E. L., Mourad, J. J., Agostini, D., Vicaut, E., Safar, M. E., & Struijker-Boudier, H. A. J. (2008). Impaired tissue perfusion a pathology common to hypertension, obesity, and diabetes mellitus. *Circulation*, *118*(9), 968–976. https://doi.org/10.1161/CIRCULATIONAHA.107.763730

Lewis-Tuffin, L. J., Jewell, C. M., Bienstock, R. J., Collins, J. B., & Cidlowski, J. A. (2007). Human Glucocorticoid Receptor β Binds RU-486 and Is TranscriptionallyActive. *Molecular and Cellular Biology*, *27*(6), 2266–2282. https://doi.org/10.1128/mcb.01439-06

Liao, T. D., Yang, X. P., Liu, Y. H., Shesely, E. G., Cavasin, M. A., Kuziel, W. A., Pagano, P. J., & Carretero, O. A. (2008). Role of inflammation in the development of renal damage and dysfunction in angiotensin II-induced hypertension. *Hypertension*, *52*(2), 256–263. https://doi.org/10.1161/HYPERTENSIONAHA.108.112706

Lin, Y. F., Swinburne, I., & Yelon, D. (2012). Multiple influences of blood flow on cardiomyocyte hypertrophy in the embryonic zebrafish heart. *Developmental Biology*, *362*(2), 242–253. https://doi.org/10.1016/j.ydbio.2011.12.005

Liu, J., Bressan, M., Hassel, D., Huisken, J., Staudt, D., Kikuchi, K., Poss, K. D., Mikawa, T., & Stainier, D. Y. R. (2010). A dual role for ErbB2 signaling in cardiac trabeculation. *Development*, *137*(22), 3867–3875. https://doi.org/10.1242/dev.053736

Liu, V. W. T., & Huang, P. L. (2008). Cardiovascular roles of nitric oxide: A review of insights from nitric oxide synthase gene disrupted mice. *Cardiovascular Research*, *77*(1), 19–29. https://doi.org/10.1016/j.cardiores.2007.06.024

Lloyd, C. M., & Snelgrove, R. J. (2018). Type 2 immunity: Expanding our view. *Science Immunology*, *3*(25). https://doi.org/10.1126/sciimmunol.aat1604

Lobov, I. B., Rao, S., Carroll, T. J., Vallance, J. E., Ito, M., Ondr, J. K., Kurup, S., Glass, D. A., Patel, M. S., Shu, W., Morrisey, E. E., McMahon, A. P., Karsenty, G., & Lang, R. A. (2005). WNT7b mediates macrophage-induced programmed cell death in patterning of the vasculature. *Nature*, *437*(7057), 417–421. https://doi.org/10.1038/nature03928

Lyle, A. N., & Taylor, W. R. (2019). The pathophysiological basis of vascular disease. *Laboratory Investigation*, *99*(3), 284–289. https://doi.org/10.1038/s41374-019-0192-2

MacDougall-Shackleton, S. A., Bonier, F., Romero, L. M., & Moore, I. T. (2019). Glucocorticoids and "Stress" Are Not Synonymous. *Integrative Organismal Biology*, *1*(1). https://doi.org/10.1093/iob/obz017

MacGrogan, D., Münch, J., & de la Pompa, J. L. (2018). Notch and interacting signalling pathways in cardiac development, disease, and regeneration. *Nature Reviews Cardiology 2018 15:11*, *15*(11), 685–704. https://doi.org/10.1038/s41569-018-0100-2

Madhur, M. S., Lob, H. E., McCann, L. A., Iwakura, Y., Blinder, Y., Guzik, T. J., & Harrison, D. G. (2010). Interleukin 17 promotes angiotensin II-induced hypertension and vascular dysfunction. *Hypertension*, *55*(2), 500–507. https://doi.org/10.1161/HYPERTENSIONAHA.109.145094

Maillet, M., Van Berlo, J. H., & Molkentin, J. D. (2013). Molecular basis of physiological heart growth: Fundamental concepts and new players. *Nature Reviews Molecular Cell Biology*, *14*(1), 38–48. https://doi.org/10.1038/nrm3495

Makarenko, I., Opitz, C. A., Leake, M. C., Neagoe, C., Kulke, M., Gwathmey, J. K., Del Monte, F., Hajjar, R. J., & Linke, W. A. (2004). Passive stiffness changes caused by upregulation of compliant titin isoforms in human dilated cardiomyopathy hearts. *Circulation Research*, *95*(7), 708–716. https://doi.org/10.1161/01.RES.0000143901.37063.2f

Malkoski, S. P., & Dorin, R. I. (1999). Composite glucocorticoid regulation at a functionally defined negative glucocorticoid response element of the human corticotropin-releasing hormone gene. *Molecular Endocrinology*, *13*(10), 1629–1644. https://doi.org/10.1210/mend.13.10.0351

Markó, L., Kvakan, H., Park, J.-K. K., Qadri, F., Spallek, B., Binger, K. J., Bowman, E. P., Kleinewietfeld, M., Fokuhl, V., Dechend, R., & Müller, D. N. (2012). Interferon-γ signaling inhibition ameliorates angiotensin ii-induced cardiac damage. *Hypertension*, *60*(6), 1430–1436. https://doi.org/10.1161/HYPERTENSIONAHA.112.199265

Martinez, C. A., Marteinsdottir, I., Josefsson, A., Sydsjö, G., Theodorsson, E., & Rodriguez-Martinez, H. (2022). Prenatal stress, anxiety and depression alter transcripts, proteins and pathways associated with immune responses at the maternal-fetal interface. *Biology of Reproduction*, *106*(3), 449–462. https://doi.org/10.1093/BIOLRE/IOAB232

Mattson, D. L., Lund, H., Guo, C., Rudemiller, N., Geurts, A. M., & Jacob, H. (2013). Genetic mutation of recombination activating gene 1 in Dahl salt-sensitive rats attenuates hypertension and renal damage. *American Journal of Physiology - Regulatory Integrative and Comparative Physiology*, *304*(6). https://doi.org/10.1152/ajpregu.00304.2012

Mazziotti, G., & Giustina, A. (2013). Glucocorticoids and the regulation of growth hormone secretion. *Nature Reviews. Endocrinology*, *9*(5), 265–276. https://doi.org/10.1038/NRENDO.2013.5

McCormick, S. M., & Heller, N. M. (2015). Commentary: IL-4 and IL-13 receptors and signaling. *Cytokine*, *75*(1), 38–50. https://doi.org/10.1016/j.cyto.2015.05.023

McMaster, W. G., Kirabo, A., Madhur, M. S., & Harrison, D. G. (2015). Inflammation, Immunity, and Hypertensive End-Organ Damage. *Circulation Research*, *116*(6), 1022–1033. https://doi.org/10.1161/CIRCRESAHA.116.303697

Meda, C., Molla, F., De Pizzol, M., Regano, D., Maione, F., Capano, S., Locati, M., Mantovani, A., Latini, R., Bussolino, F., & Giraudo, E. (2012). Semaphorin 4A Exerts a Proangiogenic Effect by Enhancing Vascular Endothelial Growth Factor-A Expression in Macrophages. *The Journal of Immunology*, *188*(8), 4081–4092. https://doi.org/10.4049/jimmunol.1101435

Mehra, V. C., Ramgolam, V. S., & Bender, J. R. (2005). Cytokines and cardiovascular disease. *Journal of Leukocyte Biology*, *78*(4), 805–818. https://doi.org/10.1189/JLB.0405182

Messerli, F. H., Rimoldi, S. F., & Bangalore, S. (2017). The Transition From Hypertension to Heart Failure: Contemporary Update. *JACC: Heart Failure*, *5*(8), 543–551. https://doi.org/10.1016/j.jchf.2017.04.012

Mickoleit, M., Schmid, B., Weber, M., Fahrbach, F. O., Hombach, S., Reischauer, S., & Huisken, J. (2014). High-resolution reconstruction of the beating zebrafish heart. *Nature Methods*, *11*(9), 919–922. https://doi.org/10.1038/nmeth.3037

Millen, A. M. E., Woodiwiss, A. J., Gomes, M., Michel, F., & Norton, G. R. (2018). Systemic Angiotensinogen Concentrations Are Independently Associated with Left Ventricular Diastolic Function in a Community Sample. *American Journal of Hypertension*, *31*(2), 212–219. https://doi.org/10.1093/ajh/hpx156

Minty, A., Chalon, P., Derocq, J. M., Dumont, X., Guillemot, J. C., Kaghad, M., Labit, C., Leplatois, P., Liauzun, P., Miloux, B., Minty, C., Casellas, P., Loison, G., Lupker, J., Shire, D., Ferrara, P., & Caput, D. (1993). Interleukin-13 is a new human lymphokine regulating inflammatory and immune responses. *Nature*, *362*(6417), 248–250. https://doi.org/10.1038/362248a0

Miyawaki, A., Obana, M., Mitsuhara, Y., Orimoto, A., Nakayasu, Y., Yamashita, T., Fukada, S. I., Maeda, M., Nakayama, H., & Fujio, Y. (2017). Adult murine cardiomyocytes exhibit regenerative activity with cell cycle reentry through STAT3 in the healing process of myocarditis. *Scientific Reports 2017 7:1*, *7*(1), 1–15. https://doi.org/10.1038/s41598-017-01426-8

Moon, M. L., Joesting, J. J., Blevins, N. A., Lawson, M. A., Gainey, S. J., Towers, A. E., McNeil, L. K., & Freund, G. G. (2015). IL-4 Knock Out Mice Display Anxiety-Like Behavior. *Behavior Genetics*, *45*(4), 451–460. https://doi.org/10.1007/s10519-015-9714-x

Moore, J. P., Vinh, A., Tuck, K. L., Sakkal, S., Krishnan, S. M., Chan, C. T., Lieu, M., Samuel, C. S., Diep, H., Kemp-Harper, B. K., Tare, M., Ricardo, S. D., Guzik, T. J., Sobey, C. G., & Drummond, G. R. (2015). M2 macrophage accumulation in the aortic wall during angiotensin ii infusion in mice is associated with fibrosis, elastin loss, and elevated blood pressure. *American Journal of Physiology - Heart and Circulatory Physiology*, *309*(5), H906–H917. https://doi.org/10.1152/ajpheart.00821.2014

Mueller, T. D., Zhang, J. L., Sebald, W., & Duschl, A. (2002). Structure, binding, and antagonists in the IL-4/IL-13 receptor system. *Biochimica et Biophysica Acta - Molecular Cell Research*, *1592*(3), 237–250. https://doi.org/10.1016/S0167-4889(02)00318-X

Murphy, M. O., Cohn, D. M., & Loria, A. S. (2017). Developmental origins of cardiovascular disease: Impact of early life stress in humans and rodents. *Neuroscience and Biobehavioral Reviews*, *74*, 453–465. https://doi.org/10.1016/j.neubiorev.2016.07.018

Nadruz, W. (2015). Myocardial remodeling in hypertension. *Journal of Human Hypertension*,

29(1), 1–6. https://doi.org/10.1038/jhh.2014.36

Napoli, C., & Ignarro, L. J. (2009). Nitric oxide and pathogenic mechanisms involved in the development of vascular diseases. *Archives of Pharmacal Research*, *32*(8), 1103–1108. https://doi.org/10.1007/s12272-009-1801-1

Nesan, D., & Vijayan, M. M. (2012). Embryo exposure to elevated cortisol level leads to cardiac performance dysfunction in zebrafish. *Molecular and Cellular Endocrinology*, *363*(1–2), 85–91. https://doi.org/10.1016/j.mce.2012.07.010

Nicolaides, N. C., Galata, Z., Kino, T., Chrousos, G. P., & Charmandari, E. (2010). The human glucocorticoid receptor: Molecular basis of biologic function. *Steroids*, *75*(1), 1–12. https://doi.org/10.1016/j.steroids.2009.09.002

Noben-Trauth, N., Shultz, L. D., Brombacher, F., Urban, J. F., Gu, H., & Paul, W. E. (1997). An interleukin 4 (IL-4)-independent pathway for CD4+ T cell IL-4 production is revealed in IL-4 receptor-deficient mice. *Proceedings of the National Academy of Sciences of the United States of America*, *94*(20), 10838. https://doi.org/10.1073/PNAS.94.20.10838

Nobili, A., Latagliata, E. C., Viscomi, M. T., Cavallucci, V., Cutuli, D., Giacovazzo, G., Krashia, P., Rizzo, F. R., Marino, R., Federici, M., De Bartolo, P., Aversa, D., Dell'Acqua, M. C., Cordella, A., Sancandi, M., Keller, F., Petrosini, L., Puglisi-Allegra, S., Mercuri, N. B., … D'Amelio, M. (2017). Dopamine neuronal loss contributes to memory and reward dysfunction in a model of Alzheimer's disease. *Nature Communications*, *8*(1), 1–14. https://doi.org/10.1038/ncomms14727

Norlander, A. E., Madhur, M. S., & Harrison, D. G. (2018). The immunology of hypertension. *The Journal of Experimental Medicine*, *215*(1), 21–33. https://doi.org/10.1084/jem.20171773

O'Connor, T. G., Winter, M. A., Hunn, J., Carnahan, J., Pressman, E. K., Glover, V., Robertson-Blackmore, E., Moynihan, J. A., Eun-Hyung Lee, F., & Caserta, M. T. (2013). Prenatal maternal anxiety predicts reduced adaptive immunity in infants. *Brain, Behavior, and Immunity*, *32*, 21–28. https://doi.org/10.1016/j.bbi.2013.02.002

Oakley, R. H., & Cidlowski, J. A. (2013). The Biology of the Glucocorticoid Receptor: New Signaling Mechanisms in Health and Disease. *The Journal of Allergy and Clinical Immunology*, *132*(5), 1033. https://doi.org/10.1016/J.JACI.2013.09.007

Oakley, R. H., Cruz-Topete, D., He, B., Foley, J. F., Myers, P. H., Xu, X., Gomez-Sanchez, C. E., Chambon, P., Willis, M. S., & Cidlowski, J. A. (2019). Cardiomyocyte glucocorticoid and mineralocorticoid receptors directly and antagonistically regulate heart disease in mice. *Science Signaling*, *12*(577). https://doi.org/10.1126/scisignal.aau9685

Oakley, R. H., Ren, R., Cruz-Topete, D., Bird, G. S., Myers, P. H., Boyle, M. C., Schneider, M. D., Willis, M. S., & Cidlowski, J. A. (2013). Essential role of stress hormone signaling in cardiomyocytes for the prevention of heart disease. *Proceedings of the National Academy of Sciences of the United States of America*, *110*(42), 17035–17040. https://doi.org/10.1073/pnas.1302546110

Oakleyt, R. H., Jewell, C. M., Yudt, M. R., Bofetiado, D. M., & Cidlowski, J. A. (1999). The dominant negative activity of the human glucocorticoid receptor β isoform. Specificity and mechanisms of action. *Journal of Biological Chemistry*, *274*(39), 27857–27866. https://doi.org/10.1074/jbc.274.39.27857

Ogasawara, N., Poposki, J. A., Klingler, A. I., Tan, B. K., Weibman, A. R., Hulse, K. E.,

Stevens, W. W., Peters, A. T., Grammer, L. C., Schleimer, R. P., Welch, K. C., Smith, S. S., Conley, D. B., Raviv, J. R., Soroosh, P., Akbari, O., Himi, T., Kern, R. C., & Kato, A. (2018). IL-10, TGF-β and glucocorticoid prevent the production of type 2 cytokines in human group 2 innate lymphoid cells. *The Journal of Allergy and Clinical Immunology*, *141*(3), 1147. https://doi.org/10.1016/J.JACI.2017.09.025

Ohtani, M., Hayashi, N., Hashimoto, K., Nakanishi, T., & Dijkstra, J. M. (2008). Comprehensive clarification of two paralogous interleukin 4/13 loci in teleost fish. *Immunogenetics*, *60*(7), 383–397. https://doi.org/10.1007/s00251-008-0299-x

Okamoto, K., & Aoki, K. (1963). Development of a strain of spontaneously hypertensive rats. *Japanese Circulation Journal*, *27*(3), 282–293. https://doi.org/10.1253/jcj.27.282

Okura, T., Watanabe, S., Miyoshi, K. I., Fukuoka, T., Higaki, J., T, O., S, W., K, M., T, F., J, H., Okura, T., Watanabe, S., Miyoshi, K. I., Fukuoka, T., & Higaki, J. (2004). Intrarenal and carotid hemodynamics in patients with essential hypertension. *American Journal of Hypertension*, *17*(3), 240–244. https://doi.org/10.1016/j.amjhyper.2003.10.005

Oparil, S., & Schmieder, R. E. (2015). New Approaches in the Treatment of Hypertension. *Circulation Research*, *116*(6), 1074–1095. https://doi.org/10.1161/CIRCRESAHA.116.303603

Özsavcí, D., Erşahin, M., Şener, A., Özakpinar, Ö. B., Toklu, H. Z., Akakín, D., Şener, G., & Yeğen, B. Ç. (2011). The novel function of nesfatin-1 as an anti-inflammatory and antiapoptotic peptide in subarachnoid hemorrhage-induced oxidative brain damage in rats. *Neurosurgery*, *68*(6), 1699–1708. https://doi.org/10.1227/NEU.0b013e318210f258

Paiardi, S., Rodella, L. F., De Ciuceis, C., Porteri, E., Boari, G. E. M., Rezzani, R., Rizzardi, N., Platto, C., Tiberio, G. A. M., Giulini, S. M., Rizzoni, D., & Agabiti-Rosei, E. (2009). Immunohistochemical evaluation of microvascular rarefaction in hypertensive humans and in spontaneously hypertensive rats. *Clinical Hemorheology and Microcirculation*, *42*(4), 259–268. https://doi.org/10.3233/CH-2009-1195

Paulus, W. J., & Tschöpe, C. (2013). A novel paradigm for heart failure with preserved ejection fraction: Comorbidities drive myocardial dysfunction and remodeling through coronary microvascular endothelial inflammation. *Journal of the American College of Cardiology*, *62*(4), 263–271. https://doi.org/10.1016/j.jacc.2013.02.092

Paz Ocaranza, M., Riquelme, J. A., García, L., Jalil, J. E., Chiong, M., Santos, R. A. S., & Lavandero, S. (2020). Counter-regulatory renin–angiotensin system in cardiovascular disease. *Nature Reviews Cardiology*, *17*(2), 116–129. https://doi.org/10.1038/s41569-019-0244-8

Pelegrin, P., & Surprenant, A. (2009). Dynamics of macrophage polarization reveal new mechanism to inhibit IL-1β release through pyrophosphates. *The EMBO Journal*, *28*(14), 2114–2127. https://doi.org/https://doi.org/10.1038/emboj.2009.163

Pelster, B., Grillitsch, S., & Schwerte, T. (2005). NO as a mediator during the early development of the cardiovascular system in the zebrafish. *Comparative Biochemistry and Physiology - A Molecular and Integrative Physiology*, *142*(2), 215–220. https://doi.org/10.1016/j.cbpb.2005.05.036

Peng, H., Sarwar, Z., Yang, X. P., Peterson, E. L., Xu, J., Janic, B., Rhaleb, N., Carretero, O. A., & Rhaleb, N. E. (2015). Profibrotic Role for Interleukin-4 in Cardiac Remodeling and Dysfunction. *Hypertension*, *66*(3), 582–589.

https://doi.org/10.1161/HYPERTENSIONAHA.115.05627

Pereiro, P., Varela, M., Diaz-Rosales, P., Romero, A., Dios, S., Figueras, A., & Novoa, B. (2015). Zebrafish Nk-lysins: First insights about their cellular and functional diversification. *Developmental and Comparative Immunology*, *51*(1), 148–159. https://doi.org/10.1016/j.dci.2015.03.009

Perner, B., Englert, C., & Bollig, F. (2007). The Wilms tumor genes wt1a and wt1b control different steps during formation of the zebrafish pronephros. *Developmental Biology*, *309*(1), 87–96. https://doi.org/10.1016/J.YDBIO.2007.06.022

Pfeffer, M. A., Shah, A. M., & Borlaug, B. A. (2019). Heart Failure With Preserved Ejection Fraction In Perspective. *Circulation Research*, *124*(11), 1598–1617. https://doi.org/10.1161/CIRCRESAHA.119.313572

Pires, P. W., Ramos, C. M. D., Matin, N., & Dorrance, A. M. (2013). The effects of hypertension on the cerebral circulation. *Https://Doi.Org/10.1152/Ajpheart.00490.2012*, *304*(12), 1598–1614. https://doi.org/10.1152/AJPHEART.00490.2012

Poe, G. R., Foote, S., Eschenko, O., Johansen, J. P., Bouret, S., Aston-Jones, G., Harley, C. W., Manahan-Vaughan, D., Weinshenker, D., Valentino, R., Berridge, C., Chandler, D. J., Waterhouse, B., & Sara, S. J. (2020). Locus coeruleus: a new look at the blue spot. *Nature Reviews Neuroscience*, *21*(11), 644–659. https://doi.org/10.1038/s41583-020-0360-9

Poon, K. L., & Brand, T. (2013). The zebrafish model system in cardiovascular research: A tiny fish with mighty prospects. *Global Cardiology Science and Practice*, *2013*(1), 4. https://doi.org/10.5339/gcsp.2013.4

Quijada, P., Trembley, M. A., & Small, E. M. (2020). The Role of the Epicardium during Heart Development and Repair. In *Circulation Research* (pp. 377–394). Lippincott Williams and Wilkins. https://doi.org/10.1161/CIRCRESAHA.119.315857

Rao, S., Lobov, I. B., Vallance, J. E., Tsujikawa, K., Shiojima, I., Akunuru, S., Walsh, K., Benjamin, L. E., & Lang, R. A. (2007). Obligatory participation of macrophages in an angiopoietin 2-mediated cell death switch. *Development*, *134*(24), 4449–4458. https://doi.org/10.1242/dev.012187

Ratman, D., Vanden Berghe, W., Dejager, L., Libert, C., Tavernier, J., Beck, I. M., & De Bosscher, K. (2013). How glucocorticoid receptors modulate the activity of other transcription factors: A scope beyond tethering. *Molecular and Cellular Endocrinology*, *380*(1–2), 41–54. https://doi.org/10.1016/j.mce.2012.12.014

Ravassa, S., González, A., López, B., Beaumont, J., Querejeta, R., Larman, M., & Díez, J. (2007). Upregulation of myocardial Annexin A5 in hypertensive heart disease: Association with systolic dysfunction. *European Heart Journal*, *28*(22), 2785–2791. https://doi.org/10.1093/eurheartj/ehm370

Ren, R., Oakley, R. H., Cruz-Topete, D., & Cidlowski, J. A. (2012). Dual role for glucocorticoids in cardiomyocyte hypertrophy and apoptosis. *Endocrinology*, *153*(11), 5346–5360. https://doi.org/10.1210/en.2012-1563

Rich-Edwards, J. W., Mason, S., Rexrode, K., Spiegelman, D., Hibert, E., Kawachi, I., Jun, H. J., & Wright, R. J. (2012). Physical and sexual abuse in childhood as predictors of early-onset cardiovascular events in women. *Circulation*, *126*(8), 920–927. https://doi.org/10.1161/CIRCULATIONAHA.111.076877

Ridker, P. M., Everett, B. M., Thuren, T., MacFadyen, J. G., Chang, W. H., Ballantyne, C., Fonseca, F., Nicolau, J., Koenig, W., Anker, S. D., Kastelein, J. J. P., Cornel, J. H., Pais, P., Pella, D., Genest, J., Cifkova, R., Lorenzatti, A., Forster, T., Kobalava, Z., … Glynn, R. J. (2017). Antiinflammatory Therapy with Canakinumab for Atherosclerotic Disease. *New England Journal of Medicine*, *377*(12), 1119–1131. https://doi.org/10.1056/nejmoa1707914

Rodriguez, J. M., Monsalves-Alvarez, M., Henriquez, S., Llanos, M. N., & Troncoso, R. (2016). Glucocorticoid resistance in chronic diseases. *Steroids*, *115*, 182–192. https://doi.org/10.1016/j.steroids.2016.09.010

Rog-Zielinska, E A, Craig, M.-A., Manning, J. R., Richardson, R. V, Gowans, G. J., Dunbar, D. R., Gharbi, K., Kenyon, C. J., Holmes, M. C., Hardie, D. G., Smith, G. L., & Chapman, K. E. (2015). Glucocorticoids promote structural and functional maturation of foetal cardiomyocytes: a role for PGC-1α. *Cell Death and Differentiation*, *22*(7), 1106. https://doi.org/10.1038/CDD.2014.181

Rog-Zielinska, Eva A., Thomson, A., Kenyon, C. J., Brownstein, D. G., Moran, C. M., Szumska, D., Michailidou, Z., Richardson, J., Owen, E., Watt, A., Morrison, H., Forrester, L. M., Bhattacharya, S., Holmes, M. C., & Chapman, K. E. (2013). Glucocorticoid receptor is required for foetal heart maturation. *Human Molecular Genetics*, *22*(16), 3269–3282. https://doi.org/10.1093/hmg/ddt182

Roger, V. L. (2013). Epidemiology of heart failure. *Circulation Research*, *113*(6), 646–659. https://doi.org/10.1161/CIRCRESAHA.113.300268

Roselló-Lletí, E., Rivera, M., Bertomeu, V., Cortés, R., Jordán, A., & González-Molina, A. (2007). Interleukin-4 and Cardiac Fibrosis in Patients With Heart Failure. *Revista Española de Cardiología (English Edition)*, *60*(7), 777–780. https://doi.org/10.1016/s1885-5857(08)60014-6

Rossi, M. A., & Carillo, S. V. (1991). Cardiac hypertrophy due to pressure and volume overload: distinctly different biological phenomena? *International Journal of Cardiology*, *31*(2), 133–141. https://doi.org/10.1016/0167-5273(91)90207-6

Rossignol, P., Hernandez, A. F., Solomon, S. D., & Zannad, F. (2019). Heart failure drug treatment. *The Lancet*, *393*(10175), 1034–1044. https://doi.org/10.1016/S0140-6736(18)31808-7

Rothman, A. M. K., MacFadyen, J., Thuren, T., Webb, A., Harrison, D. G., Guzik, T. J., Libby, P., Glynn, R. J., & Ridker, P. M. (2020). Effects of Interleukin-1β Inhibition on Blood Pressure, Incident Hypertension, and Residual Inflammatory Risk: A Secondary Analysis of CANTOS. *Hypertension*, 477–482. https://doi.org/10.1161/HYPERTENSIONAHA.119.13642

Sadoshima, J. I., & Izumo, S. (1993). Molecular characterization of angiotensin II-induced hypertrophy of cardiac myocytes and hyperplasia of cardiac fibroblasts critical role of the AT1 receptor subtype. *Circulation Research*, *73*(3), 413–423. https://doi.org/10.1161/01.RES.73.3.413

Sainte-Marie, Y., Cat, A. N. D., Perrier, R., Mangin, L., Soukaseum, C., Peuchmaur, M., Tronche, F., Farman, N., Escoubet, B., Benitah, J., & Jaisser, F. (2007). Conditional glucocorticoid receptor expression in the heart induces atrio-ventricular block. *The FASEB Journal*, *21*(12), 3133–3141. https://doi.org/10.1096/fj.07-8357com

Saleh, M. A., McMaster, W. G., Wu, J., Norlander, A. E., Funt, S. A., Thabet, S. R., Kirabo, A., Xiao, L., Chen, W., Itani, H. A., Michell, D., Huan, T., Zhang, Y., Takaki, S., Titze, J., Levy, D., Harrison, D. G., & Madhur, M. S. (2015). Lymphocyte adaptor protein LNK deficiency exacerbates hypertension and end-organ inflammation. *Journal of Clinical Investigation*, *125*(3), 1189–1202. https://doi.org/10.1172/JCI76327

Samsa, L. A., Yang, B., & Liu, J. (2013). Embryonic cardiac chamber maturation: Trabeculation, conduction, and cardiomyocyte proliferation. *American Journal of Medical Genetics, Part C: Seminars in Medical Genetics*, *163*(3), 157–168. https://doi.org/10.1002/ajmg.c.31366

Sawamiphak, S., Kontarakis, Z., Filosa, A., Reischauer, S., & Stainier, D. Y. R. (2017). Transient cardiomyocyte fusion regulates cardiac development in zebrafish. *Nature Communications*, *8*(1), 1–15. https://doi.org/10.1038/s41467-017-01555-8

Schaaf, M. J. M., Champagne, D., Van Laanen, I. H. C., Van Wijk, D. C. W. A., Meijer, A. H., Meijer, O. C., Spaink, H. P., & Richardson, M. K. (2008). Discovery of a functional glucocorticoid receptor β-isoform in zebrafish. *Endocrinology*, *149*(4), 1591–1598. https://doi.org/10.1210/en.2007-1364

Schäcke, H., Döcke, W. D., & Asadullah, K. (2002). Mechanisms involved in the side effects of glucocorticoids. *Pharmacology and Therapeutics*, *96*(1), 23–43. https://doi.org/10.1016/S0163-7258(02)00297-8

Schiattarella, G. G., & Hill, J. A. (2015). Is inhibition of hypertrophy a good therapeutic strategy in ventricular pressure overload? *Circulation*, *131*(16), 1435–1447. https://doi.org/10.1161/CIRCULATIONAHA.115.013894

Schieffer, B., Wirger, A., Meybrunn, M., Seitz, S., Holtz, J., Riede, U. N., & Drexler, H. (1994). Comparative effects of chronic angiotensin-converting enzyme inhibition and angiotensin II type 1 receptor blockade on cardiac remodeling after myocardial infarction in the rat. *Circulation*, *89*(5), 2273–2282. https://doi.org/10.1161/01.CIR.89.5.2273

Seckl, J. R., & Holmes, M. C. (2007). Mechanisms of disease: Glucocorticoids, their placental metabolism and fetal "programming" of adult pathophysiology. *Nature Clinical Practice Endocrinology and Metabolism*, *3*(6), 479–488. https://doi.org/10.1038/ncpendmet0515

Serné, E. H., Gans, R. O. B., Ter Maaten, J. C., Tangelder, G. J., Donker, A. J. M., & Stehouwer, C. D. A. (2001). Impaired skin capillary recruitment in essential hypertension is caused by both functional and structural capillary rarefaction. *Hypertension*, *38*(2), 238–242. https://doi.org/10.1161/01.HYP.38.2.238

Shang, X., Hill, E., Zhu, Z., Liu, J., Ge, B. Z., Wang, W., & He, M. (2021). The Association of Age at Diagnosis of Hypertension with Brain Structure and Incident Dementia in the UK Biobank. *Hypertension*, *78*, 1463–1474. https://doi.org/10.1161/HYPERTENSIONAHA.121.17608

Shen, X. L., Song, N., Du, X. X., Li, Y., Xie, J. X., & Jiang, H. (2017). Nesfatin-1 protects dopaminergic neurons against MPP + /MPTP-induced neurotoxicity through the C-Raf-ERK1/2-dependent anti-Apoptotic pathway. *Scientific Reports*, *7*(1), 40961. https://doi.org/10.1038/srep40961

Shimizu, H., Ohsaki, A., Oh-I, S., Okada, S., & Mori, M. (2009). A new anorexigenic protein, nesfatin-1. *Peptides*, *30*(5), 995–998. https://doi.org/10.1016/j.peptides.2009.01.002

Shimizu, I., & Minamino, T. (2016). Physiological and pathological cardiac hypertrophy.

Journal of Molecular and Cellular Cardiology, *97*, 245–262. https://doi.org/10.1016/j.yjmcc.2016.06.001

Shintani, Y., Ito, T., Fields, L., Shiraishi, M., Ichihara, Y., Sato, N., Podaru, M., Kainuma, S., Tanaka, H., & Suzuki, K. (2017). IL-4 as a Repurposed Biological Drug for Myocardial Infarction through Augmentation of Reparative Cardiac Macrophages: Proof-of-Concept Data in Mice. *Scientific Reports*, *7*(1), 1–14. https://doi.org/10.1038/s41598-017-07328-z

Skerka, C., Chen, Q., Fremeaux-Bacchi, V., & Roumenina, L. T. (2013). Complement factor H related proteins (CFHRs). *Molecular Immunology*, *56*(3), 170–180. https://doi.org/10.1016/j.molimm.2013.06.001

So, E. Y., Kim, S. H., Cho, B. S., Park, H. H., & Lee, C. E. (2002). Corticosteroid inhibits IL-4 signaling through down-regulation of IL-4 receptor and STAT6 activity. *FEBS Letters*, *518*(1–3), 53–59. https://doi.org/10.1016/S0014-5793(02)02635-2

Sokolova, I. A., Manukhina, E. B., Blinkov, S. M., Koshelev, V. B., Pinelis, V. G., & Rodionov, I. M. (1985). Rarefication of the arterioles and capillary network in the brain of rats with different forms of hypertension. *Microvascular Research*, *30*(1), 1–9. https://doi.org/10.1016/0026-2862(85)90032-9

Solano, M. E., & Arck, P. C. (2020). Steroids, Pregnancy and Fetal Development. *Frontiers in Immunology*, *10*, 3017. https://doi.org/10.3389/FIMMU.2019.03017/BIBTEX

Solloway, M. J., & Harvey, R. P. (2003). Molecular pathways in myocardial development: A stem cell perspective. *Cardiovascular Research*, *58*(2), 264–277. https://doi.org/10.1016/S0008-6363(03)00286-4/2/58-2-264-FIG5.GIF

Sriramula, S., Haque, M., Majid, D. S. A., & Francis, J. (2008). Involvement of tumor necrosis factor-α in angiotensin II-mediated effects on salt appetite, hypertension, and cardiac hypertrophy. *Hypertension*, *51*(5), 1345–1351. https://doi.org/10.1161/HYPERTENSIONAHA.107.102152

Srivastava, D., & Olson, E. N. (2000). A genetic blueprint for cardiac development. *Nature*, *407*(6801), 221–226. https://doi.org/10.1038/35025190

Staudt, D., & Stainier, D. (2012). Uncovering the molecular and cellular mechanisms of heart development using the zebrafish. *Annual Review of Genetics*, *46*, 397–418. https://doi.org/10.1146/annurev-genet-110711-155646

Steinke, J. W., & Borish, L. (2001). Th2 cytokines and asthma. Interleukin-4: Its role in the pathogenesis of asthma, and targeting it for asthma treatment with interleukin-4 receptor antagonists. In *Respiratory Research* (Vol. 2, Issue 2, pp. 66–70). https://doi.org/10.1186/rr40

Steptoe, A., Hamer, M., & Chida, Y. (2007). The effects of acute psychological stress on circulating inflammatory factors in humans: A review and meta-analysis. *Brain, Behavior, and Immunity*, *21*(7), 901–912. https://doi.org/10.1016/j.bbi.2007.03.011

Stocklin, E., Wissler, M., Gouilleux, F., & Groner, B. (1996). Functional interactions between Stat5 and the glucocorticoid receptor. *Nature*, *383*(6602), 726–728. https://doi.org/10.1038/383726a0

Streisinger, G., Walker, C., Dower, N., Knauber, D., & Singer, F. (1981). Production of clones of homozygous diploid zebra fish (Brachydanio rerio). *Nature*, *291*(5813), 293–296. https://doi.org/10.1038/291293a0

Struthers, A. D. (2013). A new approach to residual risk in treated hypertension-3P screening. *Hypertension*, *62*(2), 236–239. https://doi.org/10.1161/HYPERTENSIONAHA.113.01586

Su, S., Jimenez, M. P., Roberts, C. T. F., & Loucks, E. B. (2015). The Role of Adverse Childhood Experiences in Cardiovascular Disease Risk: a Review with Emphasis on Plausible Mechanisms. *Current Cardiology Reports*, *17*(10), 1–10. https://doi.org/10.1007/s11886-015-0645-1

Su, S., Wang, X., Kapuku, G. K., Treiber, F. A., Pollock, D. M., Harshfield, G. A., McCall, W. V., & Pollock, J. S. (2014). Adverse childhood experiences are associated with detrimental hemodynamics and elevated circulating endothelin-1 in adolescents and young adults. *Hypertension*, *64*(1), 201–207. https://doi.org/10.1161/HYPERTENSIONAHA.113.02755

Sugden, P. H., & Clerk, A. (1998). Cellular mechanisms of cardiac hypertrophy. *Journal of Molecular Medicine 1998 76:11*, *76*(11), 725–746. https://doi.org/10.1007/S001090050275

Suglia, S. F., Koenen, K. C., Boynton-Jarrett, R., Chan, P. S., Clark, C. J., Danese, A., Faith, M. S., Goldstein, B. I., Hayman, L. L., Isasi, C. R., Pratt, C. A., Slopen, N., Sumner, J. A., Turer, A., Turer, C. B., & Zachariah, J. P. (2018). Childhood and Adolescent Adversity and Cardiometabolic Outcomes: A Scientific Statement from the American Heart Association. *Circulation*, *137*(5), e15–e28. https://doi.org/10.1161/CIR.0000000000000536

Swirski, F. K., & Nahrendorf, M. (2018). Cardioimmunology: the immune system in cardiac homeostasis and disease. *Nature Reviews Immunology*, *18*(12), 733–744. https://doi.org/10.1038/s41577-018-0065-8

Szkodzinski, J., Hudzik, B., Osuch, M., Romanowski, W., Szygula-Jurkiewicz, B., Polonski, L., & Zubelewicz-Szkodzinska, B. (2011). Serum concentrations of interleukin-4 and interferon-gamma in relation to severe left ventricular dysfunction in patients with acute myocardial infarction undergoing percutaneous coronary intervention. *Heart and Vessels*, *26*(4), 399–407. https://doi.org/10.1007/s00380-010-0076-2

Tanai, E., & Frantz, S. (2016). Pathophysiology of Heart Failure. *Comprehensive Physiology*, *6*(1), 187–214. https://doi.org/10.1002/CPHY.C140055

Tang, C. H., Fu, X. J., Xu, X. L., Wei, X. J., & Pan, H. S. (2012). The anti-inflammatory and anti-apoptotic effects of nesfatin-1 in the traumatic rat brain. *Peptides*, *36*(1), 39–45. https://doi.org/10.1016/j.peptides.2012.04.014

Te Riet, L., Van Esch, J. H. M., Roks, A. J. M., Van Den Meiracker, A. H., & Danser, A. H. J. (2015a). Hypertension: Renin-Angiotensin-Aldosterone System Alterations. *Circulation Research*, *116*(6), 960–975. https://doi.org/10.1161/CIRCRESAHA.116.303587

Te Riet, L., Van Esch, J. H. M., Roks, A. J. M., Van Den Meiracker, A. H., & Danser, A. H. J. (2015b). Hypertension. *Circulation Research*, *116*(6), 960–975. https://doi.org/10.1161/CIRCRESAHA.116.303587

te Velde, A., Huijbens, R., Heije, K., de Vries, J., & Figdor, C. (1990). Interleukin-4 (IL-4) Inhibits Secretion of IL-1β, Tumor Necrosis Factor a, and IL-6 by Human Monocytes. *Blood*, *76*(7), 1392–1397. https://doi.org/10.1182/BLOOD.V76.7.1392.1392

Tilleman, H., Hakim, V., Novikov, O., Liser, K., Nashelsky, L., Di Salvio, M., Krauthammer,

M., Scheffner, O., Maor, I., Mayseless, O., Meir, I., Kayam, G., Sela-Donenfeld, D., Simeone, A., & Brodski, C. (2010). Bmp5/7 in concert with the mid-hindbrain organizer control development of noradrenergic locus coeruleus neurons. *Molecular and Cellular Neuroscience*, *45*(1), 1–11. https://doi.org/10.1016/j.mcn.2010.05.003

Timmermans, S., Souffriau, J., & Libert, C. (2019). A general introduction to glucocorticoid biology. *Frontiers in Immunology*, *10*(JULY), 1545. https://doi.org/10.3389/FIMMU.2019.01545/BIBTEX

Torres-Vázquez, J., Gitler, A. D., Fraser, S. D., Berk, J. D., Pham, V. N., Fishman, M. C., Childs, S., Epstein, J. A., & Weinstein, B. M. (2004). Semaphorin-plexin signaling guides patterning of the developing vasculature. *Developmental Cell*, *7*(1), 117–123. https://doi.org/10.1016/j.devcel.2004.06.008

Tracy, R. E. (2013). Eccentric may differ from concentric left ventricular hypertrophy because of variations in cardiomyocyte numbers. *Journal of Cardiac Failure*, *19*(7), 517–522. https://doi.org/10.1016/j.cardfail.2013.05.002

Ulrich-Lai, Y. M., & Herman, J. P. (2009). Neural regulation of endocrine and autonomic stress responses. *Nature Reviews Neuroscience 2009 10:6*, *10*(6), 397–409. https://doi.org/10.1038/nrn2647

Umland, S. P., Nahrebne, D. K., Razac, S., Beavis, A., Pennline, K. J., Egan, R. W., & Billah, M. M. (1997). The inhibitory effects of topically active glucocorticoids on IL-4, IL-5, and interferon-γ production by cultured primary CD4+ T cells. *Journal of Allergy and Clinical Immunology*, *100*(4), 511–519. https://doi.org/10.1016/S0091-6749(97)70144-1

Van Berlo, J. H., Maillet, M., & Molkentin, J. D. (2013). Signaling effectors underlying pathologic growth and remodeling of the heart. *Journal of Clinical Investigation*, *123*(1), 37–45. https://doi.org/10.1172/JCI62839

Van Varik, B. J., Rennenberg, R. J. M. W., Reutelingsperger, C. P., Kroon, A. A., De Leeuw, P. W., & Schurgers, L. J. (2012). Mechanisms of arterial remodeling: Lessons from genetic diseases. *Frontiers in Genetics*, *3*(DEC), 290. https://doi.org/10.3389/fgene.2012.00290

Vega, F., Panizo, A., Pardo-Mindan, J., & Diez, J. (1999). Susceptibility to apoptosis measured by MYC, BCL-2, and BAX expression in arterioles and capillaries of adult spontaneously hypertensive rats. *American Journal of Hypertension*, *12*(8 I), 815–820. https://doi.org/10.1016/S0895-7061(99)00045-X

Velagaleti, R. S., Gona, P., Pencina, M. J., Aragam, J., Wang, T. J., Levy, D., D'Agostino, R. B., Lee, D. S., Kannel, W. B., Benjamin, E. J., & Vasan, R. S. (2014). Left ventricular hypertrophy patterns and incidence of heart failure with preserved versus reduced ejection fraction. *American Journal of Cardiology*, *113*(1), 117–122. https://doi.org/10.1016/j.amjcard.2013.09.028

Viazzi, F., Leoncini, G., Derchi, L. E., & Pontremoli, R. (2014). Ultrasound Doppler renal resistive index: A useful tool for the management of the hypertensive patient. *Journal of Hypertension*, *32*(1), 149–153. https://doi.org/10.1097/HJH.0b013e328365b29c

Vitic, Z., Safory, H., Jovanovic, V. M., Sarusi, Y., Stavsky, A., Kahn, J., Kuzmina, A., Toker, L., Gitler, D., Taube, R., Friedel, R. H., Engelender, S., & Brodski, C. (2021). BMP5/7 protect dopaminergic neurons in an α-synuclein mouse model of Parkinson's disease. *Brain*, *144*(2), e15–e15. https://doi.org/10.1093/brain/awaa368

Vogt, C. J., SCHMID-SCHÖNBEIN, G. W., Schmid-Scho¨nbein, G. W., Scho¨nbein, S., & SCHMID-SCHÖNBEIN, G. W. (2001). Microvascular Endothelial Cell Death and Rarefaction in the Glucocorticoid-Induced Hypertensive Rat. *Microcirculation*, *8*(2), 129–139. https://doi.org/10.1111/J.1549-8719.2001.TB00163.X

Wang, T., & Secombes, C. J. (2015). The evolution of IL-4 and IL-13 and their receptor subunits. *Cytokine*, *75*(1), 8–13. https://doi.org/10.1016/j.cyto.2015.04.012

Wenzel, P., Knorr, M., Kossmann, S., Stratmann, J., Hausding, M., Schuhmacher, S., Karbach, S. H., Schwenk, M., Yogev, N., Schulz, E., Oelze, M., Grabbe, S., Jonuleit, H., Becker, C., Daiber, A., Waisman, A., Münzel, T., P, W., M, K., … T, M. (2011). Lysozyme M-positive monocytes mediate angiotensin II-induced arterial hypertension and vascular dysfunction. *Circulation*, *124*(12), 1370–1381. https://doi.org/10.1161/CIRCULATIONAHA.111.034470

Wiegers, G. J., & Reul, J. M. H. M. (1998). Induction of cytokine receptors by glucocorticoids: functional and pathological significance. *Trends in Pharmacological Sciences*, *19*(8), 317–321. https://doi.org/10.1016/S0165-6147(98)01229-2

Willenborg, S., Lucas, T., Van Loo, G., Knipper, J. A., Krieg, T., Haase, I., Brachvogel, B., Hammerschmidt, M., Nagy, A., Ferrara, N., Pasparakis, M., & Eming, S. A. (2012). CCR2 recruits an inflammatory macrophage subpopulation critical for angiogenesis in tissue repair. *Blood*, *120*(3), 613–625. https://doi.org/10.1182/blood-2012-01-403386

Wilson, K. S., Baily, J., Tucker, C. S., Matrone, G., Vass, S., Moran, C., Chapman, K. E., Mullins, J. J., Kenyon, C., Hadoke, P. W. F., & Denvir, M. A. (2015). Early-life perturbations in glucocorticoid activity impacts on the structure, function and molecular composition of the adult zebrafish (Danio rerio) heart. *Molecular and Cellular Endocrinology*, *414*, 120–131. https://doi.org/10.1016/j.mce.2015.07.025

Wlodaver, A., Pavlovsky, A., & Gustchina, A. (1992). Crystal structure of human recombinant interleukin-4 at 2.25 Å resolution. *FEBS Letters*, *309*(1), 59–64. https://doi.org/10.1016/0014-5793(92)80739-4

Wolf, G., Wenzel, U., Burns, K. D., Harris, R. C., Stahl, R. A. K., & Thaiss, F. (2002). Angiotensin II activates nuclear transcription factor-kappaB through AT1 and AT2 receptors. *Kidney International*, *61*(6), 1986–1995. https://doi.org/10.1046/J.1523-1755.2002.00365.X

Wolf, S., Arend, O., Schulte, K., Ittel, T. H., & Reim, M. (1994). Quantification of retinal capillary density and flow velocity in patients with essential hypertension. *Hypertension*, *23*(4), 464–467. https://doi.org/10.1161/01.HYP.23.4.464

Wu, J., & Bresnick, E. H. (2007). Glucocorticoid and Growth Factor Synergism Requirement for Notch4 Chromatin Domain Activation . *Molecular and Cellular Biology*, *27*(6), 2411–2422. https://doi.org/10.1128/mcb.02152-06

Wu, M. (2018). Mechanisms of trabecular formation and specification during cardiogenesis. *Pediatric Cardiology*, *39*(6), 1082. https://doi.org/10.1007/S00246-018-1868-X

Xia, J., Meng, Z., Ruan, H., Yin, W., Xu, Y., & Zhang, T. (2020). Heart Development and Regeneration in Non-mammalian Model Organisms. *Frontiers in Cell and Developmental Biology*, *8*, 1249. https://doi.org/10.3389/fcell.2020.595488

Xu, Y., Zhang, Y., & Ye, J. (2018). IL-6: A Potential Role in Cardiac Metabolic Homeostasis. *International Journal of Molecular Sciences*, *19*(9).

https://doi.org/10.3390/IJMS19092474

Yang, W.-J., Hu, J., Uemura, A., Tetzlaff, F., Augustin, H. G., & Fischer, A. (2015). Semaphorin-3C signals through Neuropilin-1 and PlexinD1 receptors to inhibit pathological angiogenesis. *EMBO Molecular Medicine*, *7*(10), 1267–1284. https://doi.org/https://doi.org/10.15252/emmm.201404922

Yu, R., Kim, N. S., Li, Y., Jeong, J. Y., Park, S. J., Zhou, B., & Oh, W. J. (2022). Vascular Sema3E-Plexin-D1 Signaling Reactivation Promotes Post-stroke Recovery through VEGF Downregulation in Mice. *Translational Stroke Research*, *13*(1), 142–159. https://doi.org/10.1007/s12975-021-00914-4

Zaffran, S., & Frasch, M. (2002). Early signals in cardiac development. *Circulation Research*, *91*(6), 457–469. https://doi.org/10.1161/01.RES.0000034152.74523.A8

Zajac, E., Schweighofer, B., Kupriyanova, T. A., Juncker-Jensen, A., Minder, P., Quigley, J. P., & Deryugina, E. I. (2013). Angiogenic capacity of M1- and M2-polarized macrophages is determined by the levels of TIMP-1 complexed with their secreted proMMP-9. *Blood*, *122*(25), 4054–4067. https://doi.org/10.1182/blood-2013-05-501494

Zanoli, L., Briet, M., Empana, J. P., Cunha, P. G., Maki-Petaja, K. M., Protogerou, A. D., Tedgui, A., Touyz, R. M., Schiffrin, E. L., Spronck, B., Bouchard, P., Vlachopoulos, C., Bruno, R. M., & Boutouyrie, P. (2020). Vascular consequences of inflammation: A position statement fromthe eshworking group onvascular structure and function and thearterysociety. *Journal of Hypertension*, *38*(9), 1682–1698. https://doi.org/10.1097/HJH.0000000000002508

Zaretsky, M. V., Alexander, J. M., Byrd, W., & Bawdon, R. E. (2004). Transfer of inflammatory cytokines across the placenta. *Obstetrics and Gynecology*, *103*(3), 546–550. https://doi.org/10.1097/01.AOG.0000114980.40445.83

Zhang, J. M., & An, J. (2007). Cytokines, inflammation, and pain. In *International Anesthesiology Clinics* (Vol. 45, Issue 2, pp. 27–37). https://doi.org/10.1097/AIA.0b013e318034194e

Zhang, J., Rudemiller, N. P., Patel, M. B., Karlovich, N. S., Wu, M., McDonough, A. A., Griffiths, R., Sparks, M. A., Jeffs, A. D., & Crowley, S. D. (2016). Interleukin-1 receptor activation potentiates salt reabsorption in angiotensin II-induced hypertension via the NKCC2 Co-transporter in the nephron. *Cell Metabolism*, *23*(2), 360–368. https://doi.org/10.1016/j.cmet.2015.11.013

Zhou, B., Carrillo-Larco, R. M., Danaei, G., Riley, L. M., Paciorek, C. J., Stevens, G. A., Gregg, E. W., Bennett, J. E., Solomon, B., Singleton, R. K., Sophiea, M. K., Iurilli, M. L., Lhoste, V. P., Cowan, M. J., Savin, S., Woodward, M., Balanova, Y., Cifkova, R., Damasceno, A., … Ezzati, M. (2021). Worldwide trends in hypertension prevalence and progress in treatment and control from 1990 to 2019: a pooled analysis of 1201 population-representative studies with 104 million participants. *The Lancet*, *398*(10304), 957–980. https://doi.org/10.1016/S0140-6736(21)01330-1/ATTACHMENT/F57BA96E-DFA3-4B0C-9FD5-188725B928ED/MMC1.PDF

Zhu, L., Pan, P., Fang, W., Shao, J., & Xiang, L. (2012). Essential Role of IL-4 and IL-4Rα Interaction in Adaptive Immunity of Zebrafish: Insight into the Origin of Th2-like Regulatory Mechanism in Ancient Vertebrates. *The Journal of Immunology*, *188*(11), 5571–5584. https://doi.org/10.4049/jimmunol.1102259

Publications

Apaydin DC, Zakarauskas-Seth BI, Carnevale L, Apaydin O, Perrotta M, Carnevale R, Kotini MP, Kotlar-Goldaper I, Belting HG, Carnevale D, Filosa A, Sawamiphak S. Interferon-γ drives macrophage reprogramming, cerebrovascular remodelling, and cognitive dysfunction in a zebrafish and a mouse model of ion imbalance and pressure overload. Cardiovasc Res. 2023. https://doi.org/10.1016/j.celrep.2020.108404.

Apaydin DC, Jaramillo PAM, Corradi L, Cosco F, Rathjen FG, Kammertoens T, Filosa A, Sawamiphak S. Early-Life Stress Regulates Cardiac Development through an IL-4-Glucocorticoid Signaling Balance. Cell Rep. 2020. https://doi.org/10.1093/cvr/cvac188.

Abbreviations

4-OHT	4-Hydroxytamoxifen
ACE	Angiotensinogen Converting Enzyme
ACTH	Adrenocorticotropic Hormone
AGT	Angiotensinogen
ANG	Angiotensin
AP-1	Activator Protein-1
AT1	Angiotensin II Type 1
AT2	Angiotensin II Type 2
BMP	Bone Morphogenic Protein
CBP	CREB- Binding Protein
cDNA	Complementary DNA
ChIP-seq	Chromatin Immunoprecipitation Sequencing
CNDP1	Carnosine Dipeptidase 1
CREB	Camp-Responsive Element-Binding Protein
CRF	Corticotropin-Releasing Factor
CSF	Colony-Stimulating Factor
DAMPs	Danger-Associated Molecular Patterns
DAPI	4′,6-Diamidin-2-Phenylindol
DC	Dendritic Cell
DMSO	Dimethylsulfoxide
DNStat3	Dominant Negative Form Of Stat3
DOCA	Deoxycorticosterone Acetate
dpf	Days Post Fertilization
ECM	Extracellular Matrix
EdU	5-Ethynyl-2´-Deoxyuridine
EF	Ejection Fraction
eNOS	Endothelial NO Synthase (Enos)
FACS	Fluorescence-Activated Cell Sorting
FBS	Fetal Bovine Serum
fps	Frame Per Second
FS	Fractional Shortening
GAPDH	Glyceraldehyde 3-Phosphate Dehydrogenase
GC	Glucocorticoid
GFP	Green Fluorescent Protein
GR	Glucocorticoid Receptor
GRa	Alpha Subunit of GR
GRb	Beta Subunit of GR
GRE	Glucocorticoid Response Elements
GRIP1	GR-Interacting Protein 1

h	Hour
HF	Heart Failure
HFpEF	Heart Failure With Preserved Ejection Fraction
HFrEF	Heart Failure With Reduced Ejection Fraction
HPA	Hypothalamic Pituitary Adrenal
hpf	Hour Post Fertilization
HPI	Hypothalamic Pituitary Interrenal
HSP	Heat Shock Protein
IFN	Interferon
Ig	Immunoglobulin
IL	Interleukin
IRS	Insulin Receptor Substrate Family
JAKs	Janus Kinases
MR	Mineralocorticoid Receptor
mRNA	Messenger RNA
NADPH	Nicotinamide Adenine Dinucleotide Phosphate
NF-κB	Nuclear Factor-Kb
nGRE	Negative Gres
NO	Nitric Oxide
NUCB2	Neucleobindin-2
PBS	Phosphate Buffered Saline
PCNA	Proliferating Cell Nuclear Antigen
PCR	Polymerase Chain Reaction
PTU	1-Phenyl-2-Thiourea
RAS	Renin Angiotensin System
REN	Renin
RNA	Ribonucleic Acid
RNase	Ribonuclease
ROS	Reactive Oxygen Species
RT-qPCR	Real Time Quantitative PCR
SEM	Standard Error Of The Mean
SRC1	Including Steroid Receptor Co-Activators 1
STAT	Signal Transducer And Activator Of Transcription
Th	T Helper
TNF	Tumor Necrosis Factor
Tnnt2	Troponin T2
TUNEL	Tdt-Mediated Dutp Nick-End Labeling
UAS	Upstream Activation Sequence

List of Figures

Acknowledgment

I would sincerely like to thank my supervisor, Dr. Suphansa Sawamiphak and Dr. Alessandro Filosa, for giving me the opportunity to be a part of the team and pursue my Ph.D. They provided me with consistent support, guidance, and feedback throughout this project. Their immense knowledge and plentiful experience have encouraged me all the time. I could not have undertaken this journey without their belief and encouragement.

I am extremely grateful to Prof. Dr. Holger Gerhardt and Prof. Dr. Sigmar Stricker for their participation in my committee meetings and for offering a different perspective on my work.

Many thanks to collaborators Dr. Thomas Kammertons, Prof. Dr. Fritz Rathjen, Prof. Dr. Daniela Carnevale, Dr. Heinz-Georg Belting, Dr. Maria Paraskevi Kotini, Marialuisa Perrotta, and Raimondo Carnevale, who have contributed in part to this thesis and manuscripts.

I would like to acknowledge the MDC Fish Facility, MDC Advanced Light Microscopy Facility, and MDC Flow Cytometry Facility for excellent support.

Thanks to all lab members, colleagues, and friends. I would like to express my appreciation to Bhakti and Paul for their participation in my projects, support, and patience. I am extremely thankful to Anne for all the support and excellent technical help.

I would like to thank all my friends. Huge thanks to Serkan and Aylin for all the cheerful weekends and for sharing happy and sad but unforgettable moments in Berlin.

From the bottom of my heart, I say big thanks to Laura Corradi for her energy, understanding, and help. There is no way I could express how much she means to me.

I owe my deepest gratitude to my dear parents, Bulent and Ozgul, and my sister Ilayda to whom I dedicate this dissertation. They were always there with endless support, love, and trust, wherever and whenever that was. Thank you for always making me smile, even when I am feeling down.

Finally, I would like to thank my beloved husband, Onur Apaydin. His constant, unwavering love and encouragement are what get me through the toughest of times. He always believed in me even when I didn’t. Thanks for being so wonderful!